PHARMACOKINETIC AND PHARMACODYNAMIC INVESTIGATIONS OF

SELECTED CHIRAL FLAVONOIDS

By

Karina R. Vega-Villa

A dissertation submitted in partial fulfillment of the requirements for the degree of

DOCTOR OF PHILOSOPHY

WASHINGTON STATE UNIVERSITY

College of Pharmacy

May 2009

To the faculty of Washington State University:

The members of the Committee appointed to examine the dissertation of Karina R. Vega-Villa find it satisfactory and recommend that it be accepted.
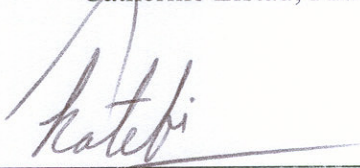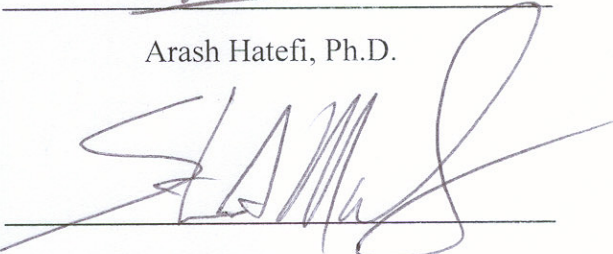
_____
Neal M. Davies, Ph.D., Chair

_____
Preston K. Andrews, Ph.D.

_____
Catherine Elstad, Ph.D.

_____
Arash Hatefi, Ph.D.

_____
Steve Martinez, D.V.M.

ACKNOWLEDGEMENTS

There have been many people who contributed to the research presented in this thesis. First and foremost, I would like to express my deepest gratitude to my thesis advisor, Dr. Neal M. Davies, for his exceptional guidance and scientific expertise during my time at Washington State University. Thanks for your support and encouragement, both scientifically and personally.

Special thanks to my Ph.D. Committee: Dr. Catherine Elstad, Dr. Arash Hatefi, Dr. Steve Martinez, and Dr. Preston Andrews for their support and guidance in the preparation of this thesis. I would also like to acknowledge Dr. Lisa Gloss and Traci Topping for assistance and use of their circular dichroism spectrometer.

I wish to thank all my colleagues in the laboratory: Connie M. Remsberg, Jody K. Takemoto, Nicole, D. Miranda and Dr. Yusuke Ohgami. Thanks for creating a great environment at work and for your friendship and moral support. Special thanks to past lab members, and especially to Dr. Jaime A. Yáñez F. for his time and patience in teaching me analytical and cell culture techniques. I would also like to acknowledge Marilyn Sánchez-Bonilla, whose support and friendship helped me through graduate life in Pullman.

Thanks to the staff and faculty in the Department of Pharmaceutical Sciences for always having their doors open and for helping me to find the answers I needed.

I acknowledge the support of my graduate research awards: the Dorothy Otto Kennedy Scholarship Fund, the Travel Award for Graduate Students from the Western Pharmacology Society, the Graduate School Travel Grant from Washington State University, the Ruben Loera Engineering and Science Award, and teaching assistantships from the Department of Pharmaceutical Sciences at Washington State University.

APPLICATIONS OF FLAVONOIDS ANALYSIS IN PHARMACEUTICAL AND HORTICULTURAL STUDIES

ABSTRACT

By Karina R. Vega-Villa, Ph.D.
Washington State University
May 2009

Chair: Dr. Neal M. Davies

High-performance liquid chromatographic (HPLC) methods were validated for the determination of homoeriodictyol, isosakuranetin, and taxifolin enantiomers in biological matrices. The quantification and racemization of these flavonoids in lemon, Yerba Santa, grapefruit, tu-fu-ling, tomato, and apple was accomplished.

The validated HPLC methods were applied in studying the pharmacokinetics of homoeriodictyol, isosakuranetin, and taxifolin in a rodent animal model. Their stereoisomers were detected in serum and urine of rats primarily as glucuro-conjugates. Different pharmacokinetic parameters were observed for each stereoisomeric form for all three xenobiotics including: half-life, total clearance, volume of distribution, and area under the curve.

To assess cytotoxicity, a variety of cancer cell lines were treated with racemic and stereoisomeric homoeriodictyol, isoskuranetin, and taxifolin. (+/-)-Isosakuranetin was most effective in cell growth inhibition of all cell lines studied. To assess amelioration of inflammation in an *in vitro* colitis model, colon adenocarcinoma cells were treated with the three flavonoids. Inflammation was induced and prostaglandin E_2 (PGE_2) release was measured. The flavonoids exhibited a concentration-dependent reduction in PGE_2 levels. The three flavonoids were also assessed for their antioxidant capacity; and cyclooxygenases and

histone deacetylase inhibitory activities. To evaluate experimental reduction of adipogenesis, pre-adipocytes were treated with the flavonoids. Differentiation was induced and triglyceride accumulation was assessed. The flavonoids showed concentration-dependent inhibition of triglyceride accumulation.

Using an alternative HPLC method of analysis, separation and quantification of various polyphenols in tomatoes and apples was achieved. Concentrations of polyphenols were measured with higher concentrations found in peel. The pharmacological activity of apple extracts was subsequently examined. Peel extracts demonstrated cell growth inhibition; reduction of inflammatory markers in experimental arthritis and colitis models; anti-oxidant activity; and inhibition of triglyceride accumulation in adipocytes.

In conclusion, the developed HPLC methods for the chiral flavonoids were sensitive, and stereospecific. Stereospecific assessment of the quantity of these flavonoids in selected fruit was also achieved. Stereoisomers of homoeriodictyol, isosakuranetin, and taxifolin were functionally distinct; enantio-specific pharmacokinetics and pharmacological activities were observed. Furthermore, analysis of polyphenol content was successfully achieved in tomatoes and apples; and the pharmacological activity of selected apple extracts demonstrated potential phytopreventive health benefits that require further experimental scrutiny.

TABLE OF CONTENTS

CHAPTER 1

CHAPTER 2

2. **STEREOSPECIFIC ASSAY DEVELOPMENT AND VALIDATION OF HOMOERIODICTYOL**

CHAPTER 3

CHAPTER 4

CHAPTER 6

CHAPTER 8

LIST OF TABLES

LIST OF FIGURES

PUBLICATIONS IN SUPPORT OF THIS THESIS

Vega-Villa KR, Yáñez JA, Remsberg CM, Ohgami Y, and Davies NM. Stereospecific High-Performance Liquid Chromatography Validation of Homoeriodictyol in Serum and Yerba Santa (*Eriodictyon glutinosum*). *J Pharm Biomed Anal.* 2008; **46**: 971-974.

Vega-Villa KR, Remsberg CM, Podelnyk KL, and Davies NM. Stereospecific High-Performance Liquid Chromatography Assay of Isosakuranetin in Rat Urine. *J Chromtogr B Analyt Technol Biomed Life Sci.* 2008; **875**: 142-147.

Vega-Villa KR, Remsberg CM, Ohgami Y, Yáñez JA, Takemoto JK, Andrews PK and Davies NM. Stereospecific High-Performance Liquid Chromatography of Taxifolin, Applications in Pharmacokinetics, and Determination in Tu Fu Ling (*Rhizoma smilacis glabrae*) and apple (*Malus* x *domestica*). *Biomed Chromatogr.* 2009; Mar 5 [Epub ahead of print].

Vega-Villa KR, Remsberg CM, Ohgami Y, Yáñez JA, Takemoto JK, and Davies NM. Pre-Clinical Pharmacokinetics of Racemic Homoeriodictyol, Isosakuranetin, and Taxifolin in Rats. Submitted to *Biopharmaceutics and Drug Disposition*, 2009

ABBREVIATIONS AND SYMBOLS

γ-CD	Gamma-cyclodextrin
β-CD	Beta-cyclodextrin
°C	Celsius
µg	Microgram
µl	Microliter
µM	Micromolar
ABTS	2,2'-Azino-bis(3-ethylbenzthiazoline-6-sulphonic acid
AIDS	Acquired immune deficiency syndrome
ADHD	Attention-deficit hyperactivity disorder
APX	Ascorbate peroxidase
AUC	Area under the curve
BAT	Brown adipose tissue
BW	Body weight
CAT	Catalase
CD	Circular dichroism
CE	Capillary electrophoresis
CHI	Chalcone isomerase
CHS	Chalcone synthase
C_{max}	Maximum concentration
CnC	Canine chondrocyte
CNS	Central nervous system
CL_H	Hepatic clearance

CL_M	Metabolite clearance
CL_R	Renal clearance
CL_T	Total clearance
COX	Cyclooxygenase
CrOMT6	*O*-methyltransferase
DAD-ESI-MS	Diodearray detection-electrospray ionization mass spectrometry
DMSO	Dimethyl sulfoxide
ER	Extraction ratio
F3H	Flavanone 3-hydroxylase
F3'H	Flavanone 3'-hydroxylase
FBS	Fetal bovine serum
f_e	Fraction excreted unchanged in urine
FLS	Flavonol synthase
f_{u-p}	Fraction unbound in plasma
FW	Fresh weight
g	Gram
GFR	Glomerular filtration rate
GR	Glutathione reductase
GC	Gas chromatography
h	Hour
Hc	Hematocrit
HDAC	Histone deacetylase
HEDT-Glu	Homoeriodictyol-7-O-β-D-glucopyranoside

HEPES	4-(2-Hydroxyethyl-1-piperazineethanesulphonic acid
HPLC	High performance liquid chromatography
HUVEC	Human umbilical vascular endothelial cells
IBMX	3-Isobutyl-1-methylxanthine
IC_{50}	Half maximal inhibitory concentration
I.D.	Inside diameter
IS	Internal standard
IV	Intravenous
k_E	Rate of elimination constant
LC	Liquid chromatography
LDL	Low-density lipoproteins
LOD	Limit of detection
LOQ	Limit of Quantification
M	Molar
m-HPPA	*m*-Hydroxyphenylpropionic acid
mM	Millimolar
MECK	Micellar electrokinetic chromatography
mg	Milligram
min	Minute
ml	Milliliter
MRP	Multidrug resistance associated protein
MS	Mass spectrometry
MW	Molecular weight

NO	Nitric oxide
n.d.	Not determined
ng	Nanogram
NMR	Nuclear magnetic resonance
O.D.	Outside diameter
OROSM	Oil red O stained material
PAR	Peak area ratio
PBS	Phosphate-buffered saline
PG	Prostaglandin
PGE_2	Prostaglandin E_2
Q	Blood flow
QC	Quality control
r^2	Coefficient of determination
RCB	Randomized complete block
r.p.m.	Revolutions per minute
RP-HPLC	Reversed-phase high performance liquid chromatography
R_s	Resolution
R.S.D.	Relative standard deviation
SC	Sodium cholate
S.D.	Standard deviation
S.E.M.	Standard error of the mean
$t_{\frac{1}{2}}$	Half-life
t_{max}	Time at C_{max}

TEAC	Trolox equivalent anti-oxidant capacity
TNF-α	Tumor necrosis factor alpha
UV	Ultraviolet
vs.	Versus
V_{SS}	Volume of distribution
WAT	White adipose tissue
XLogP	Partition coefficient

DEDICATION

This thesis is dedicated to my family; their support has been a tremendous part of my success.

Thanks to my husband Manuel Vega-Villa for his love, support, and encouragement; and

thanks to my family in Ecuador for their moral support and for always encouraging me to

follow my dreams.

1   Literature Review and Background

1.1   INTRODUCTION

This section reviews the chemical structures, biosynthetic pathway, and natural sources of three chiral flavonoids; two flavanones: homoeriodictyol and isosakuranetin, and one dihydroflavonol: taxifolin. In addition, a synopsis of the current knowledge of stereospecific methods of separation, the pharmacological activity, and pharmacokinetic studies of these three chiral flavonoids is also presented.

1.2 BACKGROUND

It has been reported that 5,000-10,000 compounds are screened before a single drug makes it to the market, and on average, it takes 10-15 years to develop a single drug [1]. Of the successfully developed drugs, 60% have a natural origin, either as modified or unmodified drug entities, or as a model for synthetic drugs – not all of them used for human diseases –, and it is estimated that 5-15% of the approximately 250,000-750,000 species of higher plants have been systematically screened for bioactive compounds [2]. Structure activity relationship (SAR) programs are generally employed to improve the chances of phytochemicals being developed as drug entities [3]. Further studies to develop more drugs of natural origin have been limited in part due to their structural complexity which is sometimes incompatible with high throughput formats of drug discovery and high extraction costs [1]. The potentially long resupply time and unforeseen political reasons such as warfare in developing nations also limits development of plant-based drugs [3]. As a result, plants remain and represent a virtually untouched reservoir of potential novel compounds. Nevertheless, the number of drugs developed each year based on natural products has remained constant over the last 22 years [3].

An understanding of the biosynthesis of natural compounds will enable researchers to further investigate possible therapeutic uses based on the activity of phytochemicals in plants. Plant chemicals are often given the moniker "phytochemicals", and can be classified either as primary or secondary metabolites [4]. Primary metabolites are widely distributed in nature, and are needed for physiological development in plants. On the other hand, secondary metabolites, are derived from the primary metabolites, are limited in distribution in the plant kingdom, and are restricted to a particular taxonomic group (**Fig. 1.1**). Secondary metabolites usually play an ecological role, for example, they act as pollinator attractants, are involved in

chemical defense, they often are end products from chemical adaptations to environmental stresses, or are synthesized in specialized cell types at different developmental stages of plant development or during disease or induced by sun-light [4].
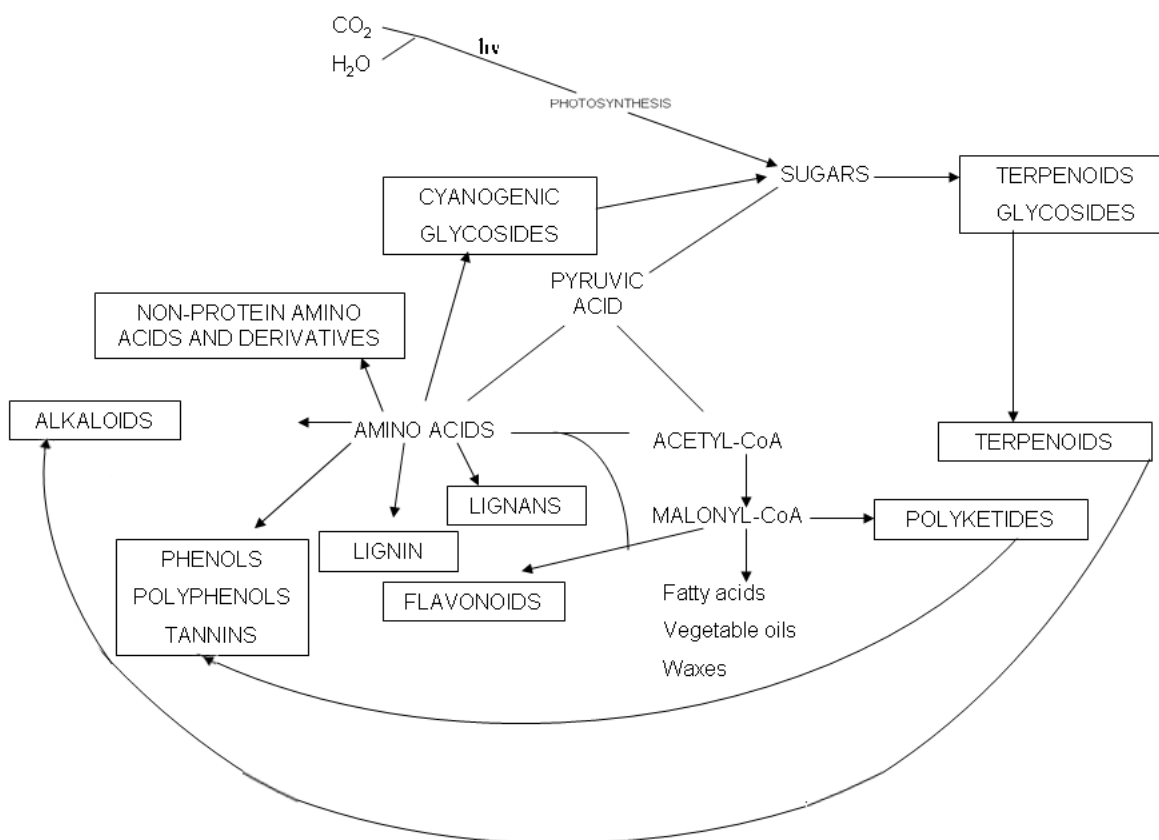
Figure 1.1. Biosynthetic origin of some plant derived compounds. Major groups of secondary metabolites are indicated by boxes. Adapted from Balandrin M and Klocke JA, 1985

Allelochemicals are phytotoxic compounds produced by higher plants that include flavonoids. Like other secondary metabolites, flavonoids have complex structures where multiple chiral centers are common [4]. A review of the basic chemistry of chiral compounds is necessary to facilitate the comprehensive understanding of future chapters in this thesis. Flavonoids consist of a C_{15} unit with two benzene rings A and B connected by a three carbon

chain (**Fig. 1.2**). This chain is closed in most flavonoids, forming the heterocyclic ring C; however, chalcones and dihydrochalcones present as an open ring system [5]. Depending on the oxidation state of the C-ring and on the connection of the B ring to the C ring [6], flavonoids can be classified into various subclasses. Flavonoids can undergo hydroxylation, methylation, glycosylation, acylation, prenylation, and sulfonation; these basic chemical metabolic substitutions generate the different subclasses: flavanols, flavanones, flavones, isoflavones, flavonols, dihydroflavonols, and anthocyanidins [5,6]. Flavonoids in nature are naturally most often found as glycosides and other conjugates; likewise, many flavonoids are polymerized by plants themselves or as a result of food processing [6].
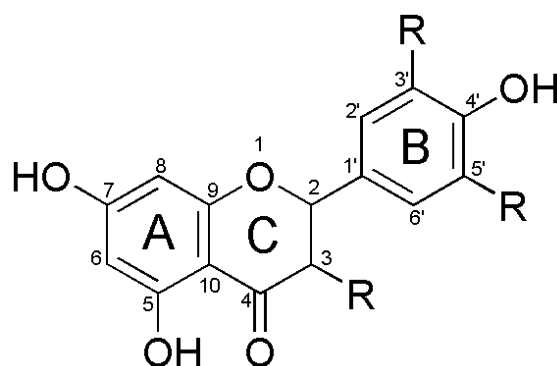
Figure 1.2. Basic chemical structure and numbering pattern of flavonoids. Adapted from Stafford HA, 1990.

Flavonoids are consumed in the human diet; the calculated flavonoid intake varies among countries since cultural dietary habits, available flora and weather influence what food is consumed; and therefore, the amount and subclasses of flavonoids ingested [6]. However, in the Western diet the overall amount of flavonoids consumed on a daily basis is likely in the milligram range. It has been determined that the consumption of selected subclasses of flavonoids may be more important in determining health benefits than the total flavonoid intake. The content of flavonoids is also potentially influenced by food processing and storage

conditions, which can result in transformation of flavonoids, and loss of flavonoid content [6].

The importance of considering the chiral nature of naturally occurring compounds and xenobiotics has been previously reviewed by Yáñez, *et al.* [7]. Chirality of flavonoids was first acknowledged by Krause and Galensa's studies in the early 1980's [8-10]. Chirality plays an important role in biological activity; disciplines like agriculture, nutrition, and pharmaceutical sciences have long recognized the existence of natural chiral compounds; however, developed methods of analysis have often failed to stereospecifically separate and discriminate compounds into their respective antipodes. The advantage of chiral separation methods includes a more thorough appreciation of the stereospecific disposition of natural compounds including flavonoids. Moreover, the lack of configurational stability is a common issue with chiral xenobiotics. Some chiral flavonoids have been reported to undergo non-enzymatic interconversion of one stereoisomer into another in isomerization processes such as racemization and enantiomerization [7]. Racemization refers to the conversion of an enantio-enriched substance into a mixture of enantiomers. Alternatively, enantiomerization refers to a reversible interconversion of enantiomers. The importance of isomerization in stereospecific chromatography as well as in the pharmaceutical manufacturing process has been described [7]. Therefore, the development of chiral methodology to analyze this kind of xenobiotics is necessary.

The study of the stereochemistry of flavonoids comprises mainly C-2 and C-3; nevertheless, the majority of natural flavonoids possess only one stereochemical isomer at the C-2 position. C-2 and C-3 act as chiral centers of dihydroxyflavonols and are important in flavonoid metabolism. Nomenclature of flavonoids with two chiral centers remains a topic of debate since the use of symbolism (+/-) or 2,3-*cis* or –*trans* seems to be inadequate to

describe four possible enantiomers [11]. It is also argued that the R, S nomenclature for absolute configuration is confusing for flavonoids because the designation of R or S changes at C-2 depend on the priority of neighboring groups, even though the stereochemistry remains the same [11]. An alternative nomenclature system was proposed by Hemingway *et al.* [12] based on that used for carbohydrate chemistry. In this system the prefix *ent-* has been used for the mirror images. However, scientific consensus has not been reached on stereochemical lexicon cognates and to date all these systems of nomenclature still remain being used and appearing in the biomedical, biochemical, agricultural, and food science literature.

1.3   HOMOERIODICTYOL

1.3.1 Natural Sources

Homoeriodictyol (+/- 3'-*O*-methyl-eriodictyol; +/- 5,7,4'-trihydroxy-3'methoxy-flavanone; $C_{16}H_{14}O_6$; MW=302.27 g/mol; XLogP=1.1) is a chiral flavanone consumed in citrus fruits and herbal products [7]. Homoeridictyol and its glycosides have been successfully identified or extracted from several plants in a variety of botanical families including Anacardiaceae (*Rhus* [13]); Asteraceae (*Lychnophora [14]*); Hydrophyllaceae (*Eriodictyon* [10,15]); Loranthaceae (*Viscum* [16-19]); Poaceae (*Zea* [20]); and Rutaceae (*Citrus* [21]).

1.3.2 Commercial Uses

Homoeriodictyol and its analogs have been commercially used as flavor modifiers [15]. Products made from Yerba Santa have been used in the pharmaceutical industry as bitter remedies for several years. However, these products may not be suitable for many food or pharmaceutical applications because they are too aromatic. Homoeriodictyol, a constituent of

Yerba Santa, and its sodium salt have been used in sensory studies and were shown to significantly decrease the bitter taste of caffeine without interfering with the desired intrinsic flavors or taste characteristics [15]. Moreover, homoeriodictyol sodium salt has been further investigated for its bitter masking properties in different chemical classes of bitter molecules [15].

Yerba Santa (*Eriodictyon glutinosum*) is also commercially available [22]. It has been used for the treatment of the common cold and asthma [15]. In the late 19th century alcoholic extracts of Yerba Santa were used as masking agents for quinine. Currently, Yerba Santa is being used to enhance moisturizing and lubricating properties of cosmetic, medical, and dental products [22].

1.3.3 Biosynthesis

Biosynthesis of homoeriodictyol has been previously studied [20,23,24]. McCormick first described homoeridictyol as a precursor of the anthocyanin peonidin, a pigment found in both immature and mature seeds in mutant maize aleurone tissue [20]. Subsequently, in 2003, Ibrahim *et al.* described the fungus *Cunninghamella elegans* as capable of converting 5,4'-dihydroxy-7,3'-dimethoxyflavanone into both homoeriodictyol and homoeriodictyol-7-sulfate [23]. The importance of this study was its contribution to the understanding of the possible similarities between mammalian and microbial systems in phase II conjugation reactions as a novel tool in metabolic drug investigations. *C. elegans* carried out C-7 demethylation, and sulfatation of 5,4'-dihydroxy-7,3'-dimethoxyflavanone to successfully produce the flavanone homoeriodictyol and its sulfo-conjugate [23]. In addition, methylation reactions have also been described to be a part of the biosynthesis of flavonoids [24]. For example, the flavonoids

detected in *Catharanthus roseus* have a simple methylation pattern; methyl groups in positions 3' and 5' are introduced by an unusual *O*-methyltransferase that performs two consecutive methylations in the B-ring. A recently identified *O*-methyltransferase (CrOMT6) was described to methylate the B-ring at 4' position, and in collaboration with dioxygenases facilitates the conversion of flavanones into flavones, dihydroflavonols, and flavonols [24]. Homoeriodictyol was reported to be the preferred substrate for CrOMT6, and depending on the acting dioxygenases, the corresponding flavone (flavone synthase), dihydroflavonol (flavanone 3β-hydroxylase), or flavonol (flavonol synthase, anthocyanidin synthase) resulted as a product.

1.3.4 Current Methods of Analysis

Homoeriodictyol exists in two enantiomeric forms: R(+)- and S(-)-configurations **(Fig. 1.3)** which were previously identified in Yerba Santa (*Eridictyon glutinosum*) [10]. In this study, Krause and Galensa reported that S(-)-homoeriodictyol was the predominant enantiomer in Yerba Santa; although its actual concentration was not reported, and lack of chromatographic baseline resolution and separation of enantiomers was observed [10].

Capillary electrophoresis, CE [25], micellar electrokinetic chromatography, MEKC [25,26], and high performance liquid chromatography, HPLC [10,27] have been previously used to separate homoeriodictyol enantiomers. Wistuba *et al.* reported improved resolution of enantiomer separation in racemic homoeriodictyol using CE (R_s= 1.23 – 6.47) and MEKC (R_s= 0.86 – 2.51) with different chiral selectors. Likewise, Asztemborska *et al.* reported enantioseparation of homoeriodictyol with poor resolution (R_s= 0.69) using MEKC. In comparison, Ficarra *et al.* attained enantioseparation of homoeriodictyol using HPLC, but did

not report a specific resolution value or publish any chromatographic data. In addition, the above mentioned analytical methods overlooked the possibility of racemization and did not validate nor evaluate the utility of these assays in biological matrices. Non-stereospecific assay methods cannot interpret the concentration-time relationship of the individual enantiomers. In addition, achiral analysis may be misleading in interpretation of the concentration dependence of each enantiomer in terms of concentration and toxicity, and anti-cancer relationships as well as the pharmacokinetic disposition.
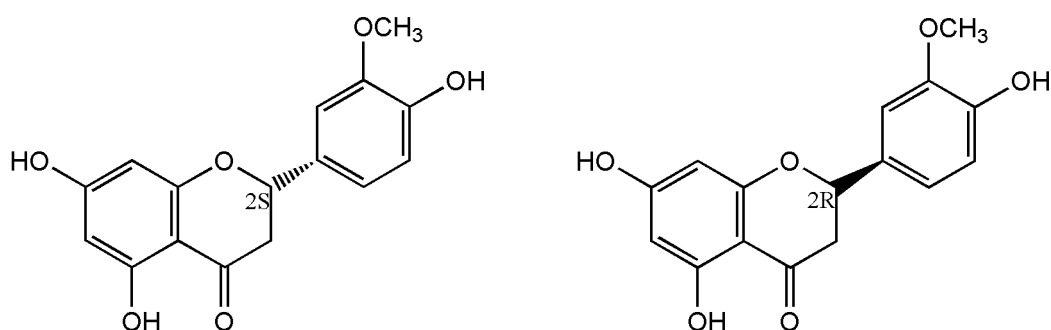
Figure 1.3. Chemical structure of homoeriodictyol enantiomers, S(-)- homoerioctyol (left) and R(+)-homoeriodictyol (right).

1.3.5 Pharmacokinetic Studies

Homoeridictyol and its glucuro- and sulfo-conjugates have been detected as metabolites in plasma and/or urine after the oral administration of flavanone [28], hesperidin [29], or eriocitrin [30] in rats and humans. Flavanone glycosides or aglycones were administered to healthy male humans, and plasma was analyzed for metabolites using HPLC; homoeriodictyol was detected only in samples of volunteers receiving flavanone glycosides, but not in those who received flavanone aglycones [28]. Similarly, hesperidin was orally administered to rats and plasma was analyzed using liquid chromatography – mass

spectrometry, LC-MS; homoeriodictyol was detected as a monoglucuronide and as a sulfate metabolite [29]. In another study, eriocitrin was orally administered to rats and plasma and urine were analyzed using HPLC and LC-MS; both homoeriodictyol and its glucuro-conjugate were detected [30].

To our knowledge, only one study has examined the pharmacokinetics of homoeriodictyol in rats. Booth *et al.* administered racemic homoeriodictyol at a dose of 150 mg/rat and used paper chromatography for the analysis of homoeriodictyol metabolites in urine [31]. Homoeriodictyol, its glucuro-conjugates, m-hydroxyphenylpropionic acid, m-coumaric acid, and dihydrofurelic acid were detected in urine after oral administration of homoeriodictyol. However, no stereospecific analysis or pharmacokinetic disposition parameters was reported. In another study, homoeriodictyol-7-*O*-β-D-glucopyranoside (HEDT-Glu) was administered to male and female rats via intravenous (IV) injection and urine and tissues were analyzed via HPLC [18] or LC-MS [32]. The previously developed analytical assays also detected homoeridictyol, but neither reported enantioseparation of homoeriodictyol enantiomers. Pharmacokinetic parameters and tissue distribution values were reported for HEDT-Glu and homoeriodictyol, but individual enantiomers were not analyzed. Plasma concentrations of HEDT-Glu in rat were detectable for at least 5 hours after IV administration; HEDT-Glu was cleared from the blood and distributed mainly to the liver and small intestine; at 0.083 hours post-dose the concentrations of HEDT-Glu in these tissues were 0.65 ± 0.24 µg/g and 0.51 ± 0.07 µg/g, respectively [18]. In comparison, homoeriodictyol was mainly detected in the kidney reaching 10.93 ± 2.92 µg/g at 0.083 hours post-dose [32].

1.3.6 Pharmacological Activity

Homoeriodictyol and its glycosides have been described to possess anti-microbial [13], anti-oxidant [30], anti-cancer [32-34], anti-inflammatory [18], anti-fungal [32], and anti-osteoporotic [17] activity. Homoeriodictyol was also described to increase coronary flow rate [32], decrease platelet aggregation [32], and act as a bitter masking or sweet enhancing agent [35].

1.4   ISOSAKURANETIN

1.4.1 Natural Sources

Isosakuranetin (+/- 4'-methylnaringenin; +/- 4'-methoxy-5,7-dihydroxyflavanone; +/-ponciretin; $C_{16}H_{14}O_5$; MW=286.28 g/mol; XLogP= 2.3) is a flavanone flavonoid with two enantiomeric forms: 2S- and 2R-isosakuranetin (**Fig. 1.4**). This flavanone has been identified as an important component of propolis [36-38], and several plants found in divergent botanical families including Asteraceae *(Baccharis* [39,40]); Combretaceae (*Terminalia* [41]); Eupatorieae (*Chromolaena* [42], *Eupatorium* [43]); and Rutaceae (*Citrus* [44]). Didymin (2S-isosakuranetin-7-rutinoside) and poncirin (2S-isosakuranetin-7-neohesperidoside), two main glycosides of isosakuranetin **(Fig. 1.5)**, have been described exclusively in Rutaceae (*Citrus* [44-48] and *Poncirus* [49-54]).
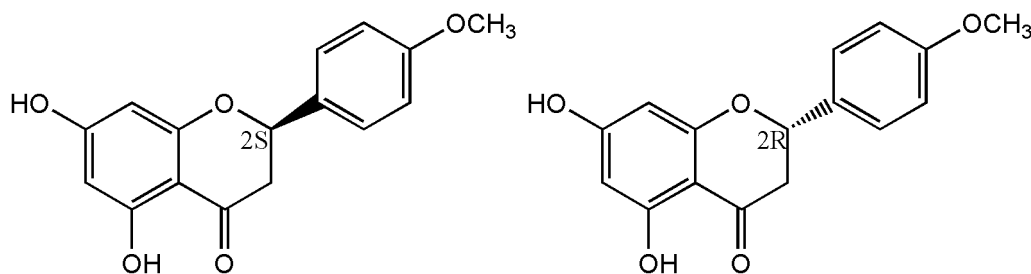
Figure 1.4. Chemical structure of isosakuranetin enantiomers, 2S-isosakuranetin (left) and 2R-isosakuranetin (right).

Flavanones in nature are found mostly as glycosides, attached to β-neohesperidose or β-rutinose sugars through the C-7 hydroxyl group [47,55]. The flavanone neohesperidosides and rutinosides can be easily distinguished by their taste properties: the neohesperidosides are bitter, whereas the rutinosides are tasteless [55]. Hot alkali on 7- β-neohesperidosides splits off the B-ring and carbon-2 to yield phloracetophenone 4'- β-neohesperidoside; however, 7-β-rutinosides do not display phloracetophenone 4' β-rutinoside formation when exposed to hot alkali but instead generate a sugar-aglycone bond split [55].
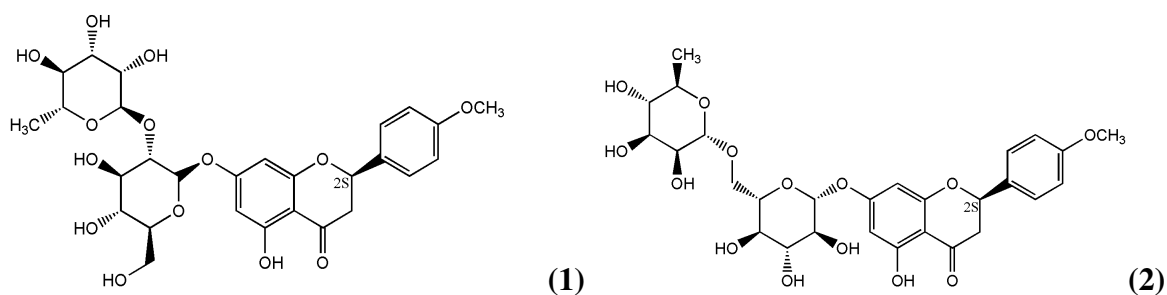
Figure 1.5. Isosakuranetin glycosides **(1)** poncirin (2S-isosakuranetin-7-neohesperidoside) and **(2)** didymin (2S-isosakuranetin-7-rutinoside)

1.4.2 Commercial Uses

Isosakuranetin has been included in its glycosylated form (isosakuranetin-7-β-rutinoside) in dietary supplements, vitamins, skin care products, energy drinks and so forth [22]. Isosakuranetin is a major component of propolis. Propolis is a natural resinous substance made by honeybees from plant exudates and used to protect honeycombs against intruders [39]. The composition of propolis depends on the plants in the region and the season in which it is collected by the bees. Propolis has been used in folk medicine and is currently studied for its biological activities. Currently, propolis is extensively incorporated in food and beverages as a dietary supplement [39].

1.4.3 Biosynthesis

Biosynthesis of isosakuranetin has been poorly studied [56,57]. Preliminary evidence of the existence of a "flavanone synthase" which converts chalcone glycosides into flavanone glycosides was presented in 1956. The enzymatic activity of "flavanone synthase" responsible for poncirin chalcone's conversion into poncirin was studied using various sources including *Citrus*, *Poncirus*, *Cosmos* and *Dahlia*. Peel tissue from *Citrus aurantium* showed the highest flavanone synthase activity [57]. Subsequently, Kim *et al.* demonstrated the existence of SOMT-2, a soybean (*Glycine max*, Fabaceae) *O*-methyltransferase expressed in *Escherichia coli* capable of converting naringenin into isosakuranetin by methylation at the 4'-hydroxyl position [56]. *O*-Methylation of flavonoids has been described to alter the chemical reactivity of their phenolic hydroxyl groups and enhance their lipophilicity.

1.4.4 Current Methods of Analysis

Isosakuranetin has a chiral carbon center and thus exists in two enantiomeric forms. The stereochemistry of flavanones has been widely studied; carbon-2 acts as the chiral center that can occur in either the S or R configurations [57,58]; with the 2S configuration being predominant in nature [59]. Methods used to identify isosakuranetin or its glycosides include paper chromatography [57], mass spectrometry, MS [42], micellar electrokinetic chromatography, MEKC [26,60,61], capillary electrophoresis, CE [61-63], high performance liquid chromatography, HPLC [8,36,37,39,44-47,49,51,58,64], HPLC-diodearray detection-electrospray ionization mass spectrometry, DAD-ESI-MS [45,65,66], and nuclear magnetic resonance, NMR spectrometry [42,50].

Nevertheless, enantiomeric separation of isosakuranetin has only been attempted by a few groups [8,26,60-62] by means of MEKC [26,60,61], CE [61,62], and HPLC [8]. Using sodium cholate (SC) and γ-cyclodextrin (γ-CD) as chiral modifiers with MEKC, Asztemborska *et al.* described enantioseparation of isosakuranetin; however, resolution was poor (R_s= 0.84) and complete separation was not accomplished. Wistuba *et al.* instead used sodium dodecyl sulphate (SDS) and γ-CD with MEKC, obtaining higher resolution (R_s= 1.78) [61]. Park and Jung applied highly sulphated cyclosophoraoses to MEKC and also obtained good resolution (R_s = 1.483) but the lack of commercial availability of this chiral selector limits the utility of this method. Furthermore, enantioseparation of isosakuranetin was reported by Kwon *et al.* using cyclic β-(1→3), (1→6)-glucans from *Bradyrhyzobium japonicum* with CE, fair resolution was achieved (R_s= 1.41), but the lack of commercial sources for this chiral selector also restricts the utility of this method. Likewise, Wistuba *et al.* developed a method using CE and anionic cyclodextrin derivates as buffer additives. High resolution (R_s= 3.43) was obtained with this method using sulfato-β-CD at pH 7. Finally, Krause and Galensa reported enantiomeric separation of isosakuranetin using cellulose triacetate as stationary phase in HPLC; baseline resolution is stated but no chromatographic data or R_s value is provided and validation in biological fluids was not accomplished. Nevertheless, the authors concluded that the selectivity between enantiomers is not sufficient since enantiomers appear in a relatively narrow retention zone [8].

1.4.5 Pharmacokinetic Studies

Isosakuranetin and its glucoro-conjugates have been previously detected as metabolites in rats administered the flavonoid naringin [65]. According to Silberberg *et al.*,

the methylation of 4'-hydroxyl in naringin produced isosakuranetin, since aromatic flavonoid compounds can undergo methylation, hydroxylation, and demethylation reactions via bacterial metabolism in the large intestine. Both healthy rats and rats bearing Yoshida's sarcoma cells produces isosakuranetin and its glucuronides in plasma, urine, liver, and kidney; however, lower concentrations were detected in tumor bearing rats. A reduction in tumor concentration of flavonoids could be the result of multi-drug resistance associated protein (MRP) activity, for which flavonoids may act as substrates [65].

Metabolism of flavonoids has been described to occur in intestinal microflora. Poncirin, for example, is converted to isosakuranetin [67], 4-hydroxybenzoic acid; 2,4-dihydroxyacetophenone; phloroglucinol; and pyrogallol by human intestinal microflora *in vitro*, in particular: *Fusobacterium* K-60, *Eubacterium* YK-4, and *Bacteroides* JY-6 [68]. Isosakuranetin was further converted to phenolic acid by *Streptococcus* S-1, *Lactobacillus* L-2, *Bifidobacterium* B-9, and *Bacteroides* JY-6 [68]. Shimuzu *et al.* demonstrated that isosakuranetin in propolis extracts can be incorporated into intestinal Caco-2 cells and transported from the apical to the basolateral side *in vitro* [36]. These findings are valuable for studies related to intestinal cell function involved in absorption from the gastrointestinal tract. To our knowledge, there are no pharmacokinetic studies of isosakuranetin that acknowledge the importance of its chiral nature and disposition.

1.4.6 Pharmacological Activity

Isosakuranetin has been previously described to have anti-mycobacterial [42], anti-fungal [69], anti-oxidant [37,70], anti-bacterial [52], neuroprotective [71], enteroprotective [52,72], anti-cancer [41,52,68], and anti-allergic [54] properties. Poncirin and didymin were

found to have numerous biological activities such as anti-inflammatory [49,50,53], anti-oxidant [70], anti-cancer [68], anti-platelet [68], anti-atherogenic [66] and immunomodulatory [73], properties. However, there is a lack of information regarding the stereospecific activity or disposition of isosakuranetin enantiomers in biological matrices like urine and serum. Achiral analysis of isosakuranetin may be misleading in that absorption, distribution, metabolism and elimination may all be stereoselective processes. Measuring enantiomers may facilitate establishment of more meaningful concentration effect relationships of chiral drugs. Separation of enantiomers in biological matrices is thus important to comprehensively understand the stereospecificity of action and disposition of isosakuranetin.

1.5 TAXIFOLIN

1.5.1 Natural Sources

Racemic taxifolin (+/- 3,5,7,3',4'-pentahydroxyflavanone; +/- dihydroquercetin; $C_{15}H_{12}O_7$; MW = 304.25 g/mol; XLogP = 0.79-3.73 [74]), a dihydroflavonol, and its glycosides have been previously identified in plants included in a variety of botanical families including: Alliaceae (*Allium* [75]); Annonaceae (*Cleistopholis* [76]); Apocynaceae (*Trachelospermum* [77]); Asteraceae (*Silybum* [78,79], *Tessaria* [80], *Centaurea* [81], *Proustia* [82]); Cactaceae (*Opuntia* [83]); Clusiaceae (*Garcinia* [84], *Hypericum* [85]); Cupressaceae (*Chamaecyparis* [86], *Thujopsis* [87]); Ericaceae (*Rhododendron* [88]); Fabaceae (*Acacia* [89], *Genista* [90], *Trifolium* [91]); Juglandaceae (*Englehardtia* [92]); Lamiaceae (*Origanum* [93], *Thymus* [94]); Liliaceae (*Rhyzoma* [95-99]); Loranthaceae (*Taxillus* [100]); Ochnaceae (*Ochna* [101]); Oleaceae (*Olea* [102]); Pinaceae (*Picea* [103],

Pinus [104-106], *Larix* [107,108], *Pseudotsuga* [108]); Poaceae (*Fussia* [109]); Polygonaceae (*Polygonum* [110]); Proteaceae (*Helicia* [111]); Smilacaceae (*Smilax* [99,112,113]); Solanaceae (*Petunia* [114]); and Vitaceae (*Ampelopsis* [115], *Vitis* [116]). Likewise, several cultivars of wine have been analyzed for their taxifolin content [117,118]. The most widely studied of these plants is *Rhizoma smilacis glabrae* or tu fu ling, which has been used in traditional Chinese medicine to treat cancer and acquired immune deficiency syndrome (AIDS) patients [96]. Clinically, taxifolin has been used to treat several illnesses including infection of the urinary system, leptopirosis, dermatitis, brucellosis, eczema, acute bacterial dysentery, acute and chronic nephritis, syphilis, arthritis, and folliculitis [95-99]. Taxifolin has been successfully isolated from *Rhizoma smilacis glabrae* showing high extraction efficiency by sonication and use of hot solvents. Chen *et al.* did not accomplish total enantiomeric separation of the four taxifolin enantiomers using an HPLC method [96]. Nevertheless, the separation and identification of the four glycosylated taxifolin enantiomers (neoastilbin, astilbin, neoisoastilbin, and isoastilbin; **Fig. 1.6**) and racemic taxifolin was attained in this study [96].
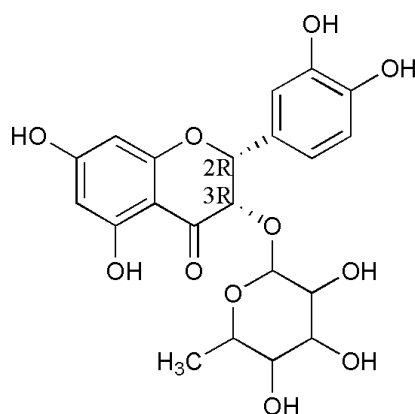
Figure 1.6. Chemical structures of a taxifolin rhamnoside, astilbin

1.5.2 Commercial Uses

Taxifolin has been reported to be a potent anti-oxidant and has been used as a biological active supplement in the food industry [119]. Taxifolin is commercially available as a food additive and is used in vegetable oils, milk powder, pastry, and so forth.

Plants like French maritime pine bark (*Pinus pinaster*) and katsura (*Cercidiphyllum japonicum*) in which taxifolin is a major component are currently being investigated. An extract of French maritime pine bark (*Pinus pinaster*), Pycnogenol®, is being used in the treatment of attention-deficit hyperactivity disorder (ADHD) in Europe with positive results [106]. Pycnogenol® has been demonstrated to stimulate endothelial nitric oxide synthase. Increased production of nitric oxide (NO) may improve brain functions such as memory, learning, and modulation of wakefulness [106]. Likewise, katsura (*Cercidiphyllum japonicum*) has been reported as an effective hair growth control agent [120]. Polyphenolic compounds in katsura showed proliferation of mouse epithelial cells *in vitro* that are currently being investigated as accelerators of hair regrowth [106].

1.5.3 Biosynthesis

Biosynthesis of taxifolin has been previously studied. Brignolas *et al.* reported the synthesis of taxifolin glycoside in a fungus-resistant clone of Norway spruce (*Picea abies* Karst) after inoculation with *Ophiostoma polinicum* Siem, a pathogenic fungus associated with a bark beetle, *Ips typographus* L., but not after sterile inoculation or in an unwounded clone. These findings suggest the flavonoid pathway may be involved in resistance to pathogenic fungi. In this report, chalcone synthase (CHS) activity was described to be higher in the resistant clone that in a clone susceptible to the pathogenic fungus [103]. Enzymes like CHS have been described to play a role in the biosynthesis of flavonoids. For example,

production of rutin was described following administration of exogenous taxifolin **(Fig. 1.7)** in Satsuma mandarin (*Citrus unshiu*) peel tissues, which demonstrated the ability of peel tissue to convert dihydroflavonols into flavonol glycosides. Flavonol synthase (FLS) increased in peel during maturation, unlike other enzymes involved in flavonoid biosynthesis including CHS, chalcone isomerase (CHI), and flavanone 3-hydroxylase (F3H) [121].
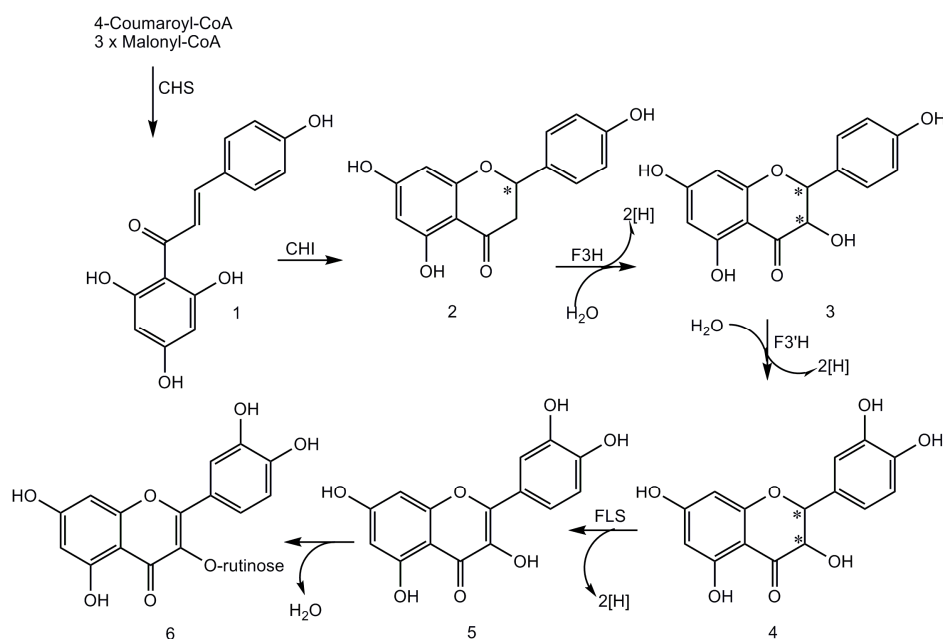
Figure 1.7. Biotransformation pathway of flavonoids in *Citrus unshiu*. 1, naringenin chalcone; 2, (+/-)-naringenin; 3, (+/-)-dihydrokaempferol; 4, (+/-)-taxifolin; 5, quercetin; 6, rutin; CHS, chalcone synthase; CHI, chalcone isomerase; F3H, flavanone 3-hydroxylase; F3'H, flavanone 3'-hydroxylase; FLS, flavonol synthase. The asterisks denote chiral centers. Adapted from Moriguchi *et al.*, 2002.

Taxifolin has been described as an intermediate in the biosynthesis of other flavonoids. In this matter, it has been reported that of the four phenolic hydroxyl groups, 7-OH is most and 5-OH least acidic [80]. These findings are important for determination of the methylation pattern and the possible metabolic products of taxifolin methylation. In *Centaurea maculosa*

roots, for example, kaempferol was converted into taxifolin, which in turn was converted into catechin. These three flavonoids were described as phytotoxic root exudates produced by *C. maculosa* [81]. In comparison, Matsuda *et al.* described the biotransformation of catechin into taxifolin by *Burkholderia* sp KTC-1. This biotransformation occurred in two steps: 4-hydroxylation, and dehydrogenation with the formation of leucocyanidin as an intermediate [122]. (±)-Catechin 4-hydroxylase and leucocyanidin 4-dehydrogenase were described to accumulate in the cytosol of the aerobic bacteria used in this study.

Only one study considers the isomerization of taxifolin [123]. (2R3R)-Taxifolin was converted into (2S3R)-taxifolin with the opening of the heterocyclic ring and the formation of an intermediate quinine methide with heat < 100°C. When acidic or basic methylation was used under heat > 100°C, isomerization did not occur; and alphitonin was formed. Alphitonin (2-benzyl-2,3',4,4',6-pentahydroxy-3-coumaranone) is a by-product of taxifolin methylation [123].

1.5.4 Current Methods of Analysis

Taxifolin has two carbon chiral centers, and thus exists in four enantiomeric forms; therefore, stereospecific analytical methods are needed to address its chiral disposition [11,124]. Using the RS nomenclature (Chapter I), four taxifolin enantiomers can be identified: 2S3S, 2R3R, 2R3S, and 2S3R **(Fig. 1.8)**.
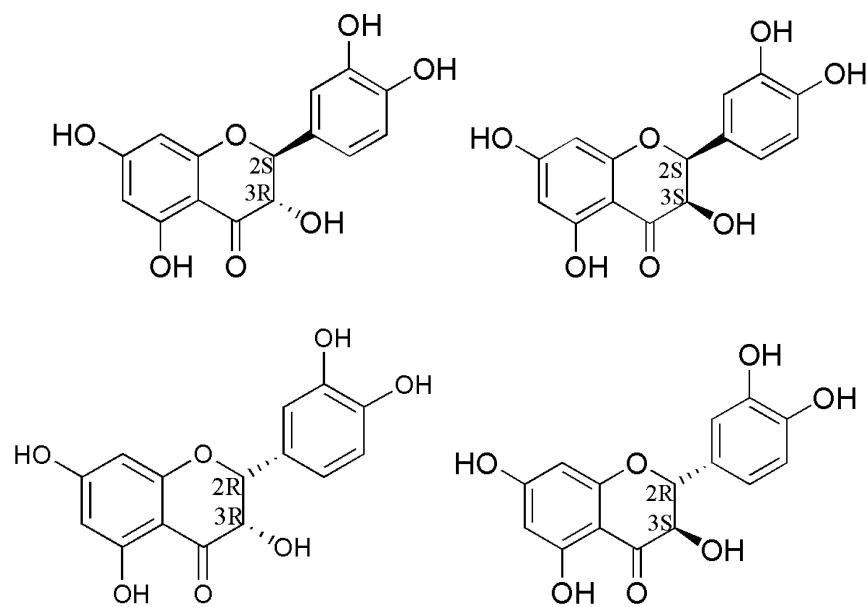
Figure 1.8. Chemical structure of taxifolin enantiomers, (2S3R)-(+)-taxifolin (upper left), (2S3S)-(-)-taxifolin (upper right), (2R3R)-(+)-taxifolin (lower left), and (2R3S)-(-)-taxifolin (lower right).

Racemic taxifolin has been previously identified in several plants using an array of analytical methods including liquid chromatography, LC [88,91-93,96,97,109,115,118,125-129], gas chromatography [108], nuclear magnetic resonance, NMR spectrometry [75,76,78,80,83,87,93,111,113], circular dichroism, CD [87], and mass spectrometry, MS [78,90,91,93,108,110,115,116,128,130]. Few studies have examined the chiral nature of taxifolin using LC [102,107,127,131], and NMR spectrometry [104,130,132]. Ng *et al.* acknowledged the importance of developing methods to discriminate and recognize taxifolin enantiomers in natural products, but failed to achieve total separation of taxifolin enantiomers using a methylated β-cyclodextrin chiral stationary phase using LC [7,127]. The available studies that have considered enantio-separation of taxifolin did not separate all four enantiomers, but only two enantiomers [102,104,107,123,130,131]. Studies with taxifolin glycosides have accomplished the enantio-separation or identification of one [104,113], two

[77,96], or four [87] of its enantiomers via HPLC [96], NMR spectrometry [77,87,104,113], CD [87], and MS [98].

1.5.5 Pharmacokinetic Studies

There are a paucity of studies on the pharmacokinetics of taxifolin [133,134]. A pharmacokinetic analysis of maritime pine bark extract demonstrated the presence of taxifolin in human plasma after single and multiple doses of the extract were administered orally ($AUC_{[0-t]}$ = 2311.11±85.98 ng/ml × h; C_{max} = 33.34±12.54 ng/ml; t_{max} = 8.2±2.5 h) [134]. Likewise, after oral administration of Pycnogenol, the active constituent of maritime pine bark, taxifolin was detected in human urine [133]. Flavonoid metabolism in humans is known to involve the intestinal microflora [128,135], as well as liver enzymes [136]. Among the microflora shown to participate in the metabolism of taxifolin, *Eubacterium ramulus* and *Clostridium orbiscindens* have been described to convert taxifolin into phenolic acids. *E. ramulus* is found in human feces and has been described to convert quercetin into taxifolin, which in turn is converted into its chalcone; following a series of additional conversions taxifolin is finally converted into 3,4-dihydroxyphenylacetic acid [128] **(Fig 1.9)**. Likewise, *C. orbiscindens* is found in human feces and has also been described to have the ability to convert taxifolin into 3,4-dihydroxyphenylacetic acid [135] **(Fig. 1.10)**. However, *C. orbiscindens* is an asaccharolytic organism, which relies on the deglycosilation performed by human tissues (small intestine, liver) and bacteria such as *E. ramulus*, *Enterococcus casseliflavus*, and *Bacteroides* sp. for flavonoid degradation [135]. Flavonoid metabolism by liver enzymes has been studied by Nielsen *et al.*; in their study, cytochrome P450 activity did not appear to be involved in taxifolin metabolism in rat liver microsomes [136]. Nielsen *et al.*

described the structural characteristics and the tentative products of flavonoids metabolized by liver enzymes: 1) flavonoids without a 4'-hydroxyl group in B ring undergo hydroxylation by microsomal enzymes to catechol (3',4'-dihydroxyl) structures; 2) flavonoids with a 4'-methoxyl group, but not those with a methoxyl in the 3'-position, undergo demethylation into the hydroxyl compound (i.e. isosakuranetin); and 3) flavonoids with two or more hydroxyl groups in the B ring or a 3'-methoxyl group are not metabolized by microsomal enzymes (i.e. homoeriodictyol, taxifolin). In addition, cytochrome P450s involved in flavonoid metabolism have been described to exhibit stereoselectivity. [136].
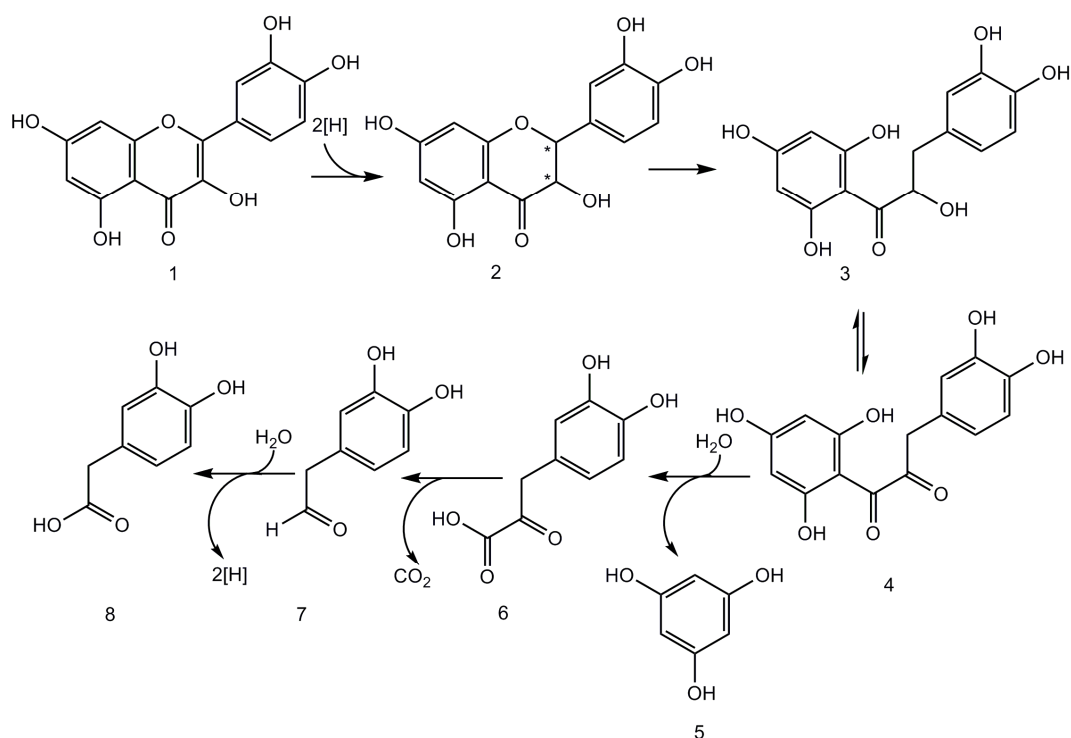
Figure 1.9. Metabolism of taxifolin by *Eubacterium ramulus*. 1, quercetin; 2, (+/-)-taxifolin; 3, taxifolin chalcone; 4, hydrokaempferol chalcone; 5, phloroglucinol; 6, 2-keto-3-(3,4-dihydroxyphenyl)propionic acid; 7, 3,4-dihydroxyphenylacetaldehyde; 8, 3,4-dihydroxyphenylacetic acid. The asterisks denote chiral centers. Adapted from Schneider H and Blaut M, 2000.
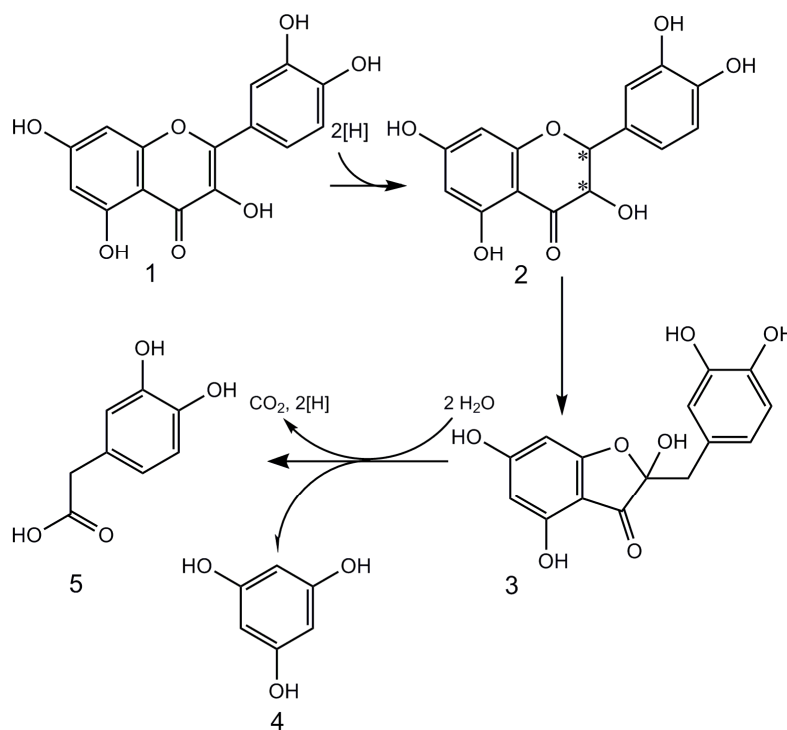
Figure 1.10. Metabolism of taxifolin by *Clostridium orbiscindens*. 1, quercetin; 2, (+/-)-taxifolin; 3, alphitonin; 4, phloroglucinol; 5, 3,4-dihydroxyphenylacetic acid. The asterisks denote chiral centers. Adapted from Schoefer L *et al.*, 2003.

1.5.6 Pharmacological Activity

Several of the plants described to possess taxifolin are used in traditional and clinical medicine [76,79,82-84,92,94-97,105,108,110,111,137]; some are ingested in the human diet [75,91,94,110,116-118,121,138]; and others are being studied for their potential use in drug development [90,101].

Racemic taxifolin and its glycosides have been previously studied for their potent anti-oxidant properties [82,92,105,108,137,139]. Taxifolin is a very common anti-oxidant additive in the food industry [94], and has also been described to have anti-inflammatory and analgesic properties [82], hepato-protective capacity [140], free radical scavenger activity

[92,94,108,141], and also demonstrates a protective role in plants against pathogens [81,103]. (2R3R)-(2R3R)-(+)-Taxifolin, one of its four enantiomers, has been described to possess tyrosinase inhibitory capacity; and thus it is used in depigmentation drugs and whitening cosmetics, as well as a food additive and an insect control agent [110].

1.6   OBJECTIVES

The stereochemistry of flavonoids has been poorly studied; even though flavonoids are one of the largest groups of phytochemicals, few studies have acknowledged the importance of their stereochemistry in the biological activity of these phytochemicals. Homoeriodictyol, isosakuranetin and taxifolin are chiral flavonoids ingested in the human diet as food components or as ingredients in dietary supplements. Preliminary work has been undertaken to analyze the pharmacological activity of homoeriodictyol, isosakuranetin, and taxifolin; however, studies acknowledging the effect of their chiral stereochemistry are limited or non-existent. Likewise, the pharmacokinetic analysis of homoeriodictyol, isosakuranetin and taxifolin needs to be considered with respect to the chiral nature of these compounds to better understand their biological disposition and activity. It has been reported that the consumption of selected flavonoids is important from a health perspective [4], so analyzing particular flavonoids in tomatoes and apples may contribute to a more comprehensive understanding of flavonoid benefits after human consumption. Therefore, the specific objectives of this project were:

1. To develop and validate novel, sensitive, and stereospecific RP-HPLC assays in biological fluids for homoeriodictyol, isosakuranetin, and taxifolin (Chapters II-IV).

2. To characterize the stereospecific pharmacokinetic parameters of homoeriodictyol, isosakuranetin, and taxifolin in a rat model as well as the stereospecific quantification of homoeriodictyol, isosakuranetin, and taxifolin in fruits and herbs (Chapter V).

3. To evaluate the pharmacological activity of homoeriodictyol, isosakuranetin, and taxifolin in *in vitro* cancer, inflammation, oxidation, and adipogenesis models (Chapter VI).

4. To delineate the selected polyphenol content of hybrid tomato cultivars using two distinct fertility management alternatives (Chapter VII).

5. To analyze the selected polyphenol content of several apple cultivars at various harvest maturities, harvest years, and fertility management alternatives; and under commercial storage and shelf-life conditions; and to characterize the pharmacological activity of apple extracts in *in vitro* cancer, inflammation, oxidation, and adipogenesis models (Chapter VIII).

2 Stereospecific Assay Development and Validation of Homoeriodictyol

2.1 INTRODUCTION

This section describes the development of a selective, accurate, reproducible, and stereospecific assay using reverse phase high performance liquid chromatography, RP-HPLC for simultaneous separation of homoeriodictyol enantiomers in biological matrices. Furthermore, the validation of the RP-HPLC assay in rat serum is reported in this chapter.

2.2   BACKGROUND

Enantioseparation of homoeriodictyol has been previously attained using CE, and MEKC (Chapter I). However, there are no HPLC methods that have successfully attained separation of homoeriodictyol enantiomers in biological matrices in the literature.

2.3   METHODS

2.3.1 HPLC Apparatus and Conditions

The HPLC system used was a Shimadzu HPLC (Kyoto, Japan), consisting of an LC-10ATVP pump, a SIL-10AF auto injector, a SPD-M10A VP spectrophotometric diodearray detector, and a SCL-10A VP system controller. Data collection and integration were accomplished using Shimadzu EZ Start 7.1.1 SP1 software. The analytical column used was Chiralcel® OJ-RH column (150mm × 4.6mm i.d., 5-µm particle size, Chiral Technologies Inc., PA, USA) protected by a Chiralcel OJ-RH guard column (0.4cm x 1cm, 5-µm particle size). The mobile phase consisted of acetonitrile, water and phosphoric acid (22:78:0.1, v/v/v), filtered and degassed. Separation was carried out isocratically at 25 ± 1°C, a flow rate of 1.0 ml/min, with ultraviolet (UV) detection at 288 nm.

2.3.2 Chemicals and Reagents

Racemic homoeriodictyol was purchased from Indofine Chemical Company (Hillsborough, NJ, USA). Racemic indoprofen, β-glucuronidase from *Escherichia coli* Type IX A, β-glucuronidase from *Helix pomatia* type-HP-2, and halothane were purchased from Sigma Chemicals (MO, USA). HPLC grade acetonitrile and water were purchased from J. T. Baker (Phillipsburg, NJ, USA). Phosphoric acid was purchased from Aldrich Chemical Co.

Inc. (WI, USA). Rats were obtained from Charles River Laboratories. Ethics approval for animal experiments was obtained from Washington State University.

2.3.3 Stock and Working Standard Solutions

Racemic homoeriodictyol and racemic indoprofen (internal standard) solutions of 100.0 μg/ml were dissolved in methanol. Calibration standard curves were prepared yielding concentrations of 0.5, 1.0, 5.0, 10.0, 50.0 and 100.0 μg/ml of each homoeriodictyol enantiomer.

2.3.4 Sample Preparation

Rats were humanely sacrificed using an overdose of halothane, blank serum was obtained from untreated rats, and stored at -20°C to be used as the biological matrix; water was used in the case of botanical analysis. To the working standards or samples (0.1 ml), 25 μl of racemic indoprofen (internal standard) was added into 2.0 ml Eppendorf tubes. The mixture was vortexed for 1 minute and 1 ml of cold acetonitrile was added to precipitate proteins. The samples were centrifuged at 5,000 r.p.m. for 5 minutes. The supernatant was collected and evaporated to dryness under compressed nitrogen gas. The residue was reconstituted with 200.0 μl of mobile phase, vortexed and centrifuged, the supernatant was transferred to HPLC vials and 150.0 μl of it was injected into the HPLC system.

2.3.5 Precision and Accuracy

The within-run and between-run precision and accuracy of the replicate assays (n = 6) were tested over a range of 0.5 to 100.0 μg/ml on the same day and on six different days within one week. The precision was evaluated by the relative standard deviation (R.S.D.). The accuracy was estimated based on the mean percentage error of measured concentration to the actual concentration [142].

2.3.6 Limit of Quantification (LOQ) and Limit of Detection (LOD)

The limit of quantification (LOQ) refers to the highest and lowest concentrations that can be reliably quantified. The LOQ was determined by repeated analysis of spiked rat serum samples in six replicates. An acceptance criteria of 15% was used to determine precision and accuracy at the LOQ.

The limit of detection (LOD) refers to the lowest concentration different from the negative control or blank that can be distinguished from background noise. A signal to noise ratio ≥ 3:1 was used to determine the LOD by means of UV detection of serum samples.

2.3.7 Recovery

Recovery of homoeriodictyol enantiomers was performed in the same concentration range (0.5-100.0 μg/ml). The samples were prepared as described in the sample preparation section. The extraction efficiency was determined by comparing the peak area ratio (PAR) of enantiomeric homoeriodictyol and R(-)-indoprofen to the PAR of corresponding concentration injected directly in the HPLC without extraction.

2.3.8 Stability of Homoeriodictyol Samples in Rat Serum

The freeze-thaw stability of homoeriodictyol enantiomers (0.5-100.0 µg/ml) was evaluated in triplicate without being frozen at first, and then stored at -70°C and thawed at room temperature (25 ± 1°C) for three cycles. The stability of homoeriodictyol in reconstituted extracts was investigated using pooled extracts from quality control (QC) samples of one concentration level 10.0 µg/ml. The sample was kept in the sample rack of the auto-injector and injected into HPLC system every 4 hours, from 0 to 24 hours.

2.3.9 Quantification of Homoeriodictyol in Lemon (Citrus limonia) and Lemonade

Samples of conventionally grown and organically grown lemons as well as conventional and organic lemonade were purchased from grocery stores in the area. One milliliter of fresh lemon juice obtained from the fruit or one milliliter of lemonade was added into 15 ml conical tubes corresponding to free and total duplicates. Three milliliters of HPLC-grade water were added to all samples, followed by 25.0 µl of IS to the free samples only. Free samples were dried to completion using a nitrogen evaporator, and stored at 4°C until processing. To the total samples, 330.0 µl 0.78 M sodium acetate-acetic acid buffer (pH 4.8), and 300.0 µl 0.1 M ascorbic acid were added, samples were vortexed for 30 seconds, and 600.0 µl crude preparation of *Helix pomatia* glucuronidase type H-2 was added and gently mixed. Total samples were incubated in a water bath at 37°C for 17-24 hours; 25 µl of IS were added, followed by 3.0 ml of cold acetonitrile. Samples were vortexed for 30 seconds, centrifuged for 5 minutes at 5,000 r.p.m. and the supernatant was collected into new eppendorf tubes, and dried until completion under compressed nitrogen gas. The stored free samples were removed from the refrigerator (4°C), and left at room temperature for 5 minutes.

Free and total samples were reconstituted at the same time, 400.0 µl of mobile phase was added to each sample, samples were vortexed for 30 seconds, centrifuged for 5 minutes at 5,000 r.p.m. and the supernatant was carefully transferred to HPLC vials; 150.0 µl of sample was injected into the HPLC system for analysis.

2.3.10   *Quantification and Racemization in Yerba Santa (Eriodictyon glutinosum)*

One gram of Yerba Santa powder (American Health and Herbs, OR, USA) was extracted with 20 ml HPLC-grade methanol [10]. The extracts were evaporated to dryness using a rotary evaporator, and the dried samples were dissolved in 1 ml of mobile phase, vortexed and centrifuged. The supernatant was filtered through a 13 mm syringe filter. The solution was further diluted 10-fold, and 150 µl injected into the HPLC system. For racemization, the extracts were evaporated to dryness using a rotary evaporator and later reconstituted in 25% methanol in water [10]. The sample was heated for 1 h at 70°C and filtered through a 13 mm syringe filter; 150.0 µl of sample was injected into the HPLC system for analysis.

2.3.11   *Data Analysis*

Quantification was based on calibration curves constructed using PAR of homoeriodictyol enantiomers to internal standard R(-)-indoprofen, against homoeriodictyol concentrations using unweighted least squares linear regression.

2.4   RESULTS AND DISCUSSION

2.4.1 Chromatography

Separation of homoeriodictyol enantiomers and the internal standard in biological fluids was achieved successfully **(Figure 2.1).** No interfering peaks co-eluting with the compounds of interest **(Figs. 2.1.1)**. Under reverse-phase conditions R(+)-homoeriodictyol eluted first [10]; the retention times of R(+)- and S(-)- homoeriodictyol were approximately 69 and 78 minutes, respectively. The internal standard (R-(-)-indoprofen) eluted at approximately 55 minutes **(Fig. 2.1.2)**. Optimal separation was achieved when the combination of acetonitrile, water and phosphoric acid was 22:78:0.1 (v/v/v) with a flow rate of 1.0 ml/min.
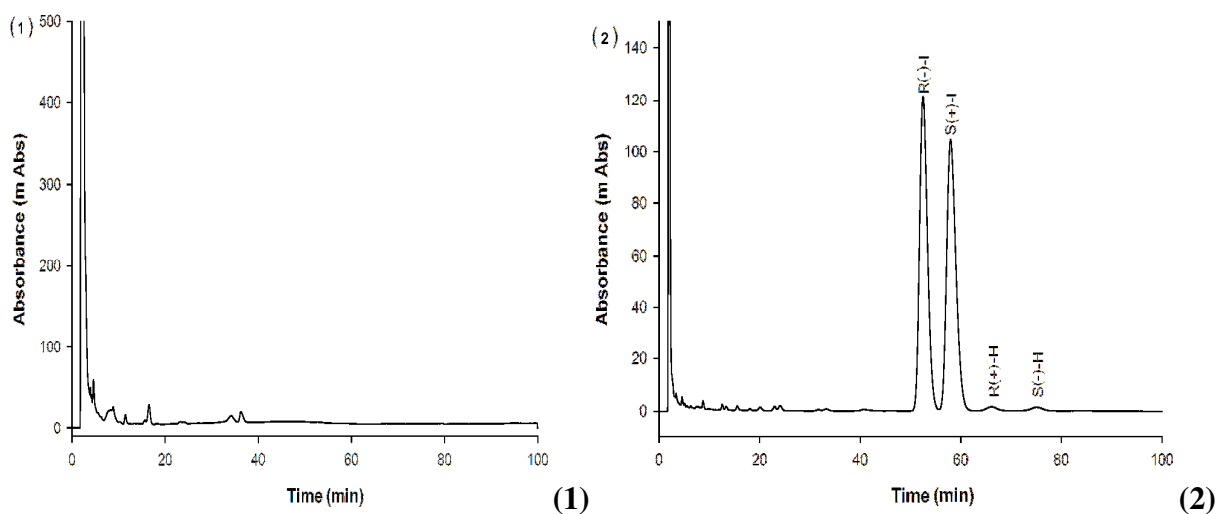
Figure 2.1. Representative chromatograms, of **(1)** drug-free serum demonstrating no interfering peaks co-eluted with the compounds of interest; and **(2)** serum containing homoeriodictyol (H) enantiomers (R(+)-H, S(-)-H) each with concentration of 10.0 µg/ml and the internal standard, R(-)-indoprofen (R(-)-I); with this method, separation of racemic indoprofen is also achieved (R(-)-I, S(+)-I).

2.4.2 Linearity, LOQ and LOD

Excellent linear relationships (r^2 = 0.995) were demonstrated between PAR of R(+)- and S(-)-homoeriodictyol to the internal standard and the corresponding serum concentrations of homoeriodictyol enantiomers over a range of 0.5 to 100.0 μg/ml. Mean regression lines from the validation runs were described by R(+)-homoeriodictyol (μg/ml) = 0.01880x – 0.0012 and S(-)-homoeriodictyol (μg/ml) = 0.0178x - 0.0006. LOQ of this assay was 0.5 μg/ml with the corresponding between day R.S.D. of 6.55 and 5.94% for R(+)- and S(-)-homoeriodictyol, respectively and bias of -10.80 and -14.97% for R(+)- and S(-)-homoeriodictyol, respectively. The back-calculated concentration of QC samples was within the acceptance criteria **(Table 2.1).**

Table 2.1. Within- and between-day precision and accuracy of the assay for homoeriodictyol (H) enantiomers in rat serum (n = 6, mean, R.S.D., and Bias)

	Homoeriodictyol concentration (μg/ml)											
	Observed				R.S.D. (%)				Bias (%)			
Added	Within-day		Between-day		Within-day		Between-day		Within-day		Between-day	
	R(+)-H	S(-)-H	R(+)-H	S(-)-H	R(+)-H	S(-)-H	R(+)-H	S(-)-H	R(+)-H	S(-)-H	R(+)-H	S(-)-H
0.5	0.57	0.57	0.45	0.43	14.84	14.94	6.55	5.94	13.52	14.53	-10.80	-14.97
1	1.04	1.03	1.11	0.86	5.46	4.71	10.63	9.37	4.02	3.45	10.62	-13.51
5	4.68	4.82	4.46	4.40	5.73	1.73	5.12	6.48	-6.34	-3.62	-10.79	-12.03
10	9.69	9.77	8.88	8.87	4.00	7.10	14.96	12.23	-3.11	-2.30	-11.23	-11.33
50	52.36	53.09	48.14	48.04	1.15	8.44	5.39	5.28	4.73	6.18	-3.72	-3.91
100	98.92	99.86	101.19	101.28	4.73	4.04	1.28	1.28	-1.08	-0.14	1.19	1.28

2.4.3 Precision, Accuracy and Recovery

Within- and between-run precision (R.S.D.) calculated during replicate assays (n = 6) of homoeriodictyol enantiomers was <15% over a wide range of concentrations **(Table 2.1)**. The intra- and inter-run bias assessed during the replicate assays for homoeriodictyol enantiomers varied between -14.97 and 14.53% **(Table 2.1).** These data indicated that the developed HPLC method is reproducible and accurate. The mean extraction efficiency for homoeriodictyol enantiomers from biological fluids varied from 88.54 to 112.17% **(Table 2.2).**

Table 2.2. Recovery of homoeriodictyol enantiomers from rat serum (n = 6, mean ± S.D.).

Concentration (µg/ml)	Recovery (%) (Mean ± S.D.)	
	R(+)-homoeriodictyol	S(-)-homoeriodictyol
0.5	96.39 ± 5.66	103.98 ± 4.23
1	102.63 ± 10.91	112.17 ± 5.62
5	100.66 ± 5.32	97.81 ± 6.34
10	101.91 ± 5.40	96.66 ± 5.09
50	92.07 ± 4.96	88.54 ± 4.67
100	102.46 ± 1.32	103.40 ± 1.32

2.4.4 Stability of Homoeriodictyol Samples

No significant degradation was detected after the samples of racemic homoeriodictyol in biological fluids following three freeze-thaw cycles. Recoveries of R(+)- and S(-)-homoeriodictyol were respectively from 85.35 to 107.37% and 85.53 to 103.86% following three freeze-thaw cycles for homoeriodictyol QC samples of homoeriodictyol or R(-)-indoprofen. There was no significant decomposition observed after the reconstituted extract of racemic homoeriodictyol was stored in the auto-injector at room temperature for 24 hours; the

measurements were from 97.87 to 98.90% of the initial value for extracts of racemic homoeriodictyol in biological fluids of 0.5 to 100.0 µg/ml.

2.4.5 Quantification of Homoeridictyol in Lemon (Citrus limonia) and Lemonade

The HPLC method was applied to the quantification of homoeriodictyol enantiomers in organic and conventional lemon (*Citrus limonia*) and lemonade. The fruit of lemon is classified as a modified berry called hesperidium. In citrus fruits, the terms *albedo* and *flavedo* are used to describe the components of the *pericarp*, the peripheral surface; and *carpels* to describe the juicy vesicles that form the edible part of the fruit. The juice extracted from carpels in lemon was used to analyze the homoeriodictyol content (**Fig. 2.2.**).
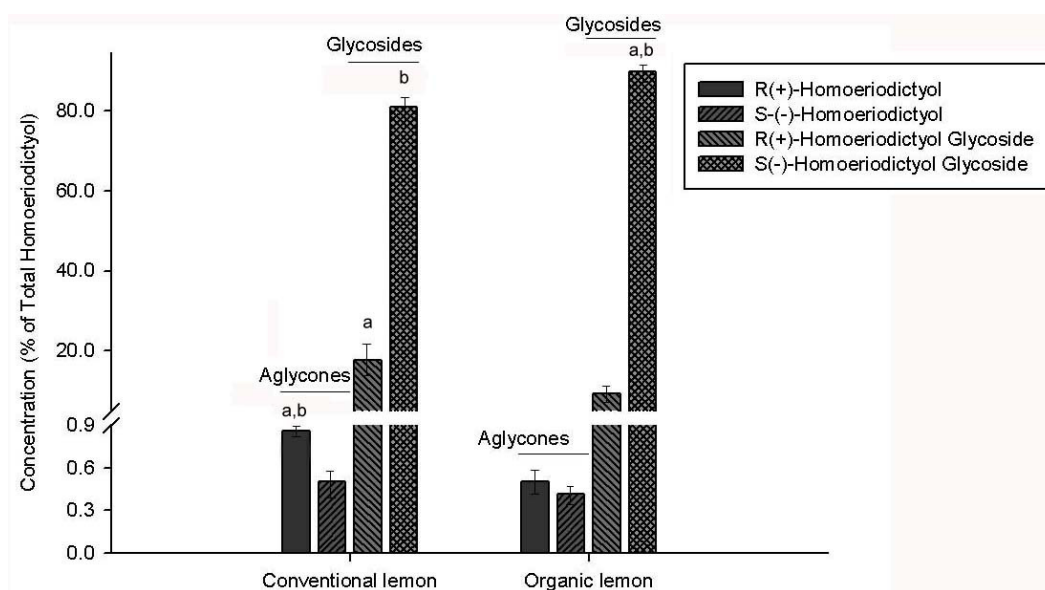
Figure 2.2. Comparison of enantiomeric content of homoeriodictyol in conventional and organic lemon (*Citrus limonia,* n = 4, mean ± S.E.M). a, P < 0.05, organic vs. conventional; b, P < 0.05, R(+) vs. S(-).

Homoeriodictyol is mostly determined as glycosides in plants; of these, the S(-)-enantiomer glycoside was demonstrated to be the predominant form for both conventional and organic lemons. Moreover, organic lemon contained the highest concentration of S-(-)-homoeriodictyol glycoside (619.62 ± 92.94 mg/100 g FW). A summary of the content of homoeriodictyol and its glycosides in conventional and organic lemon is presented in **Table 2.3**.

Table 2.3. Content of homoeriodictyol enantiomers and its glycosides in conventional and organic lemon (*Citrus limonia*, n = 4, mean ± S.E.M.). a, P < 0.05, organic vs. conventional; b, P < 0.05, R(+) vs. S(-).

% of Total Homoeriodictyol	Conventional		Organic	
	R(+)-Homoeriodictyol	S-(-)-Homoeriodictyol	R(+)-Homoeriodictyol	S-(-)-Homoeriodictyol
Glycoside	17.65 ± 3.11^a	80.98 ± 2.01^b	9.27 ± 0.19	89.81 ± 1.80^{ab}
Aglycone	0.86 ± 0.11^{ab}	0.51 ± 0.15	0.50 ± 0.15	0.42 ± 0.09
Total Enantiomer	18.51 ± 3.22^a	81.49 ± 2.16^b	9.77 ± 0.34	90.23 ± 1.89^{ab}
Total Gycosides	98.63 ± 5.12		99.08 ± 1.99	
Total Aglycones	1.37 ± 0.26		0.92 ± 0.24	

The developed assay was also used to measure the amount of homoeriodicytol enantiomers in commercially available conventional and organic lemonade. Similar to the results with lemons, lemonades were also demonstrated to contain high amounts of glycosides. The R-(+)-homoeriodictyol glycoside was predominant in conventional lemonade; whereas organic lemonade contained glycosides mainly in the S(-)-form (**Fig. 2.3**). A summary of the content of homoeriodictyol enantiomers and its glycosides in lemonade is presented in **Table 2.4.**
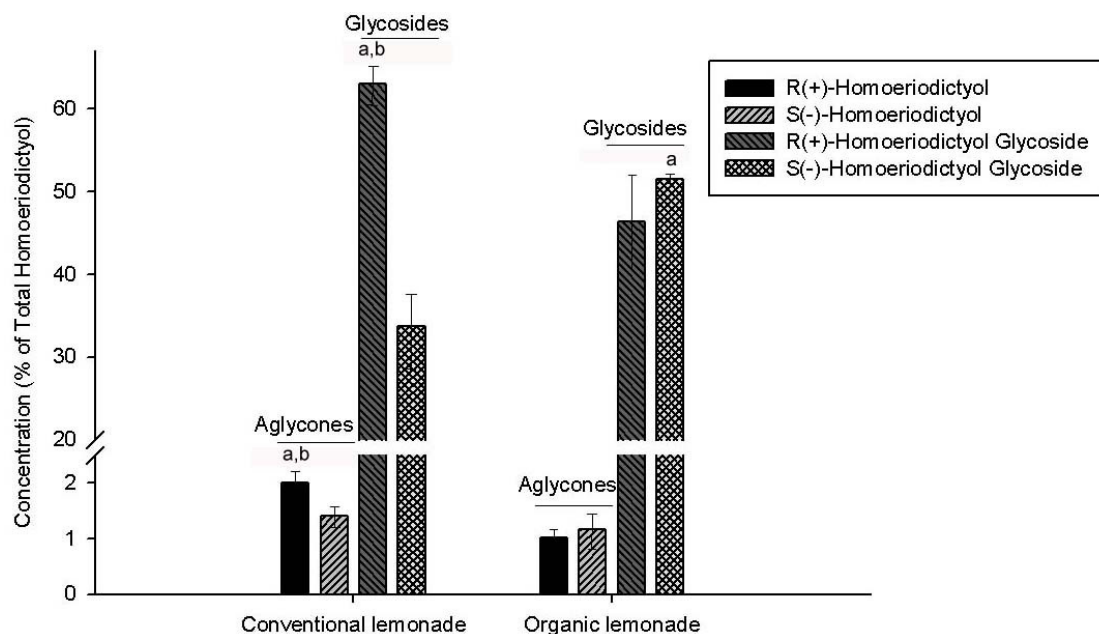
Figure 2.3. Comparison of enantiomeric content of homoeriodictyol in conventional and organic lemonade (n = 3, mean ± S.E.M). a, P < 0.05, organic vs. conventional; b, P < 0.05, R(+) vs. S(-).

Table 2.4. Content of homoeriodictyol enantiomers and its glycosides in conventional and organic lemonade (n = 3, mean ± S.E.M). a, P < 0.05, organic vs. conventional; b, P < 0.05, R(+) vs. S(-).

% of Total Homoeriodictyol	Conventional		Organic	
	R(+)-Homoeriodictyol	S-(-)-Homoeriodictyol	R(+)-Homoeriodictyol	S-(-)-Homoeriodictyol
Glycoside	62.93 ± 5.11[a,b]	33.66 ± 6.12	46.38 ± 7.12	51.44 ± 0.51[a]
Aglycone	2.01 ± 0.49[a,b]	1.40 ± 0.45	1.01 ± 0.43	1.17 ± 0.51
Total Enantiomer	64.94 ± 5.60[b]	35.06 ± 6.57	47.39 ± 7.55	52.61 ± 1.02[a]
Total Gycosides	96.59 ± 11.23		97.82 ± 7.63	
Total Aglycones	3.41 ± 0.94		2.18 ± 0.94	

2.4.6 Quantification and Racemization in Yerba Santa (Eridictyon glutinosum)

The HPLC method was applied to the quantification of homoeriodictyol enantiomers in Yerba Santa **(Figure 2.4).** Yerba Santa has been reported to contain stereochemically enriched S(-)-homoeriodictyol [10]. As shown in **Fig.2.4.1**, Yerba Santa contains predominantly S(-)-homoeriodictyol (99.91%). The racemization process of homoeriodictyol under 25% methanol heated to 70°C for 1 hour was examined. After racemization, the content of S(-)-homoeriodictyol decreased from 99.91% to 61.71% and the content of R(+)-homoeriodictyol increased to 30.29% **(Fig. 2.5)**.

(1)　　　　**(2)**
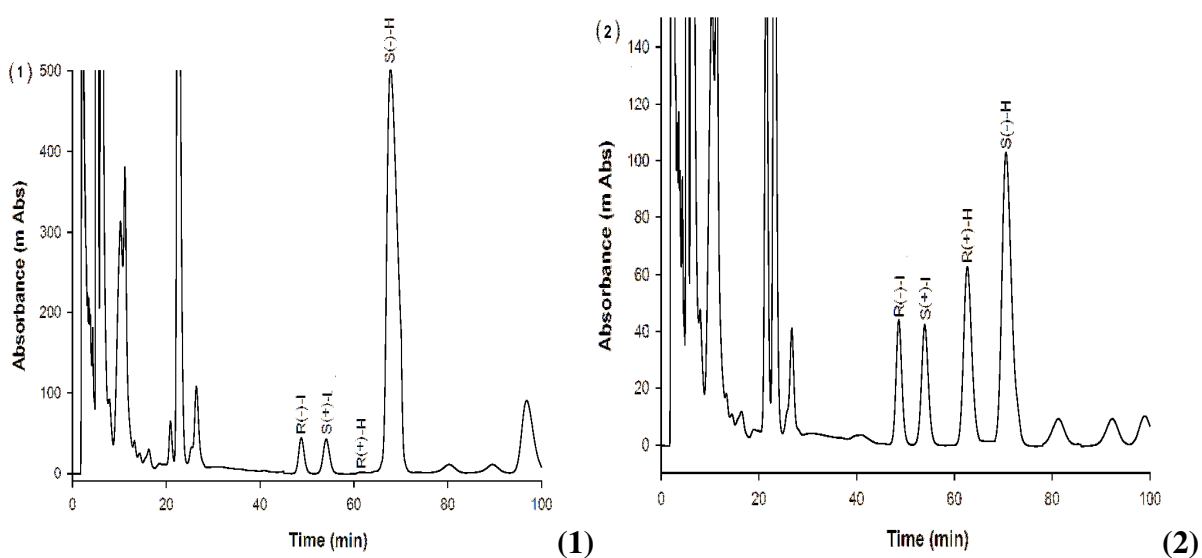
Figure 2.4. Representative chromatographs of **(1)** Yerba Santa (*E. glutinosum*) sample containing homoeriodictyol (H) enantiomers predominantly in the S(-)-form (S(-)-H) and the internal standard, R(-)-indoprofen (R(-)-I), and **(2)** Yerba Santa (*E. glutinosum*) after racemization (1 h heat treatment at 70°C in 25% methanol). With this method, separation of racemic indoprofen is also achieved (R(-)-I, S(+)-I).
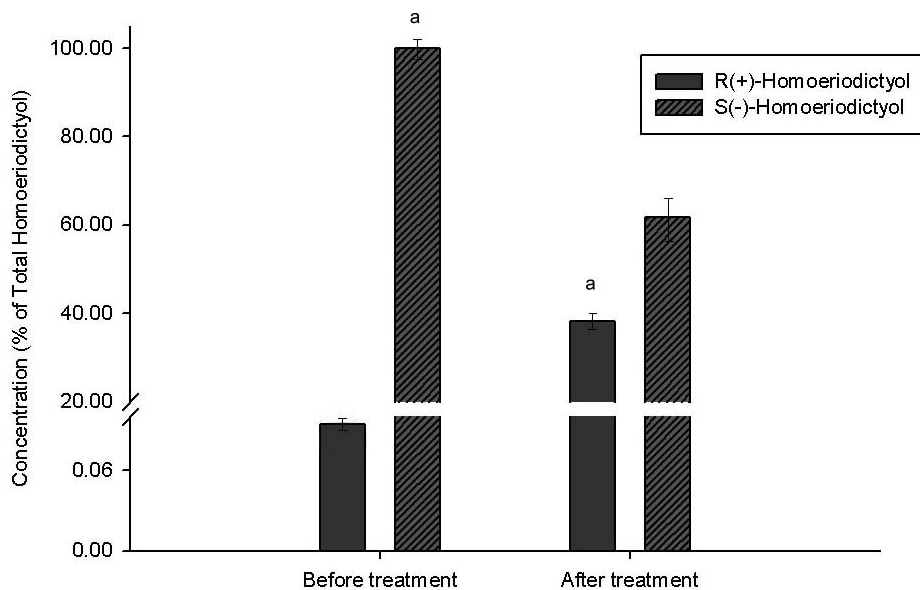
Figure 2.5. Comparison of enantiomeric content in Yerba Santa before and after racemization of homoeriodictyol (n = 3, mean ± S.E.M). a, $P < 0.05$, R(+) vs. S(-).

2.5 CONCLUSIONS

In summary, the developed stereospecific HPLC method for homoeriodictyol is sensitive, reproducible, and accurate. It has been applied to study the stereospecificity of homoeriodictyol in Yerba Santa, lemons, and lemonade and to examine racemization. The HPLC method was for the first time used to examine the stereospecific concentrations of homoeriodictyol in organic and conventional lemonade products.

3 <u>Stereospecific Assay Development and Validation of Isosakuranetin</u>

3.1 INTRODUCTION

This section describes the development of a selective, accurate, reproducible, and stereospecific assay using reverse phase high performance liquid chromatography, RP-HPLC for simultaneous separation of isosakuranetin enantiomers in biological matrices. Moreover, the validation of the RP-HPLC assay in rat serum is reported in this chapter.

3.2   BACKGROUND

Several method of isosakuranetin analysis have been previously attempted to separate its enantiomers using MEKC, CE, and HPLC (Chapter I). However, no validated method capable of baseline separation of isosakuranetin in biological matrices exists in the literature to date.

3.3   METHODS

3.3.1 HPLC Apparatus and Conditions

The HPLC system used was a Shimadzu HPLC (Kyoto, Japan), consisting of an LC-10AT-VP pump, a SIL-10AF auto injector, a SPD-M10A VP spectrophotometric diodearray detector, and a SCL-10A VP system controller. Data collection and integration were accomplished using Shimadzu EZ Start 7.1.1 SP1 software. The analytical column used was Chiralpak® AD™-RH column (150mm × 4.6mm i.d., 5-µm particle size, Chiral Technologies Inc., Exton, PA, USA). The mobile phase consisted of 100% HPLC-grade methanol filtered and degassed. Separation was carried out isocratically at 25 ± 1°C, a flow rate of 0.40 ml/min, with ultraviolet (UV) detection at 286 nm.

3.3.2 Chemicals and Reagents

Racemic isosakuranetin was purchased from Indofine Chemical Company (Hillsborough, NJ, USA). Didymin (2S-isosakuranetin 7-rutinoside) was purchased from Extrasynthèse (Genay, France). 7-Ethoxycoumarin, β-glucuronidase from *Escherichia coli* Type IX A, and halothane were purchased from Sigma Chemicals (St Louis, MO, USA). HPLC grade methanol was purchased from J. T. Baker (Phillipsburg, NJ, USA). Rats were

obtained from Charles River Laboratories. Ethics approval for animal experiments was obtained from Washington State University.

3.3.3 Stock and Working Standard Solutions

Racemic isosakuranetin and 7-ethoxycoumarin (internal standard) solutions of 100.0 µg/ml were dissolved in methanol. Calibration standard curves were prepared yielding concentrations of 0.5, 1.0, 5.0, 10.0, 50.0 and 100.0 µg/ml of each isosakuranetin enantiomer.

3.3.4 Sample Preparation

Urine from untreated rats was collected and used as the biological matrix; water was used in the case of botanical analysis. To the working standards or urine samples (0.1 ml), 100.0 µl of 7-ethoxycoumarin (internal standard) was added into 2.0 ml Eppendorf tubes. The mixture was vortexed (Vortex Genie-2, VWR Scientific, West Chester, PA, USA) for 1 minute and centrifuged at 5,000 r.p.m. for 5 minutes (Beckman Microfuge centrifuge, Beckman Coulter Inc., Fullerton, CA, USA). The supernatant was collected and evaporated to dryness under compressed nitrogen gas using an N-Evap analytical evaporator (Organomation Associates, Inc., Berlin, MA, USA). The residue was reconstituted with 200.0 µl of mobile phase, vortexed for 1 minute and centrifuged at 5,000 r.p.m. for 5 minutes, the supernatant was then transferred to HPLC vials and 150.0 µl of it was injected into the HPLC system.

Serum from untreated rats was collected and also used as a biological matrix. A solid phase extraction method was developed to prepare serum samples as follows: To 0.1 ml serum, an equal volume of glycol/water buffer (pH 2.0) was added. Strata x 60 mg/3 mL cartridge tubes (Phenomenex, Inc., Torrance, CA, USA) were conditioned and equilibrated

with 2.0 ml methanol, and 2.0 ml HPLC grade water, respectively using a vaccum manifold (Phenomenex, Inc., Torrance, CA, USA). After loading the buffer-treated samples at a flow rate of 1-2 ml/min, cartridges were washed with 2.0 ml of water and 20:80 methanol/water solution each. Cartridges were dry to completion for 30 - 60 seconds to ensure that all traces of wash solvents were removed. Finally, elution of the samples from the cartridge was accomplished using 4.0 ml 1:1 methanol/acetonitrile solution at a flow rate of 1 - 2 ml/min; samples were collected in 15 ml conical tubes and dried to completion using a nitrogen evaporator and stored at 4°C for future analysis. When all samples were ready for analysis, 0.3 ml of the mobile phase was used to reconstituted the samples, and 0.1 ml of 7-ethoxycoumarin (IS) was added. Samples were centrifuged at 5,000 r.p.m. for 5 minutes. The supernatant was collected and 150.0 µl transferred into HPLC vials for analysis.

3.3.5 Precision and Accuracy

The within-run and between-run precision and accuracy of the replicate assays (n = 6) were tested at 0.5, 1.0, 5.0, 10.0, 50.0 and 100.0 µg/ml on the same day and on six different days within one week, respectively. The precision was evaluated by the relative standard deviation (R.S.D.). The accuracy was estimated based on the mean percentage error of measured concentration to the actual concentration [142].

3.3.6 Limit of Quantification (LOQ) and Limit of Detection (LOD)

The LOQ was determined by repeated analysis of spiked rat urine samples in six replicates. An acceptance criteria of 15% was used to determine precision and accuracy at the

LOQ. A signal to noise ratio $\geq$ 3:1 was used to determine the LOD by means of UV detection of urine samples.

3.3.7 Recovery

The relative and absolute recovery for isosakuranetin enantiomers from biological fluids were assessed at 0.5, 1.0, 5.0, 10.0, 50.0 and 100.0 µg/ml and the recovery of the internal standard was evaluated at the concentration used in sample analysis (100.0 µg/ml). The samples were prepared as described in the sample preparation section. Urine was used as the matrix for the relative recovery studies, whereas water was used for the absolute recovery studies. A known amount of racemic isosakuranetin or 7-ethoxycoumarin was spiked into 0.1 ml blank rat urine or water to give the above concentrations. The extraction efficiency was determined by comparing the peak area ratio (PAR) of enantiomeric isosakuranetin and 7-ethoxycoumarin to the PAR of corresponding concentration injected directly in the HPLC without extraction.

3.3.8 Stability of Isosakuranetin Samples in Rat Urine

The freeze-thaw stability of isosakuranetin enantiomers was evaluated in triplicate at 0.5 and 100.0 µg/ml using quality control (QC) samples [143]. These samples were analyzed without being frozen at first, and then stored at -70°C and thawed at room temperature (25 ± 1°C) for three freeze-thaw cycles.

The stability of isosakuranetin in reconstituted extracts during run-time in the HPLC auto-injector was investigated using pooled extracts from QC samples of two concentration levels, 0.5 and 100.0 µg/ml [143]. Samples were kept in the sample rack of the auto-injector

and injected into HPLC system every 4 hours, from 0 to 24 hours at the temperature of the auto-injector (25 ± 1 °C).

3.3.9 Quantification in Grapefruit (Citrus paradisi)

Samples of grapefruit were purchased from grocery stores in the area. One milliliter of fresh grapefruit juice obtained from the fruit was added into 15 ml conical tubes corresponding to free and total duplicates. Three milliliters of HPLC-grade water was added to all samples, followed by 25.0 µl of IS to the free samples only. One set of samples were dried to completion using a nitrogen evaporator, and stored at 4°C until process. Another set of samples was added 330.0 µl 0.78 M sodium acetate-acetic acid buffer (pH 4.8), and 300.0 µl 0.1 M ascorbic acid, samples were vortexed for 30 seconds, and 600.0 µl crude preparation of *Helix pomatia* glucuronidase type H-2 was added and gently mixed. These samples incubation in a water bath at 37°C was undertaken for 17-24 hours; 25 µl of IS were added, followed by 3.0 ml of cold acetonitrile. Samples were vortexed for 30 seconds, centrifuged for 5 minutes at 5,000 r.p.m. and the supernatant was collected into new Eppendorf tubes, and dried until completion under compressed nitrogen gas. The stored untreated samples were removed from the refrigerator (4°C), and left at room temperature for 5 minutes Both sets of samples were reconstituted at the same time, 400.0 µl of mobile phase was added to each sample, samples were vortexed for 30 seconds, centrifuged for 5 minutes at 5,000 r.p.m. and the supernatant was carefully transferred to HPLC vials; 150.0 µl of sample was injected into the HPLC system for analysis.

3.3.10   Data Analysis

Analyte quantification was based on calibration curves constructed using PAR of isosakuranetin enantiomers to internal standard 7-ethoxycoumarin, against isosakuranetin concentrations using unweighted least squares linear regression.

3.4 RESULTS AND DISCUSSION

3.4.1 Chromatography

Separation of isosakuranetin enantiomers and the internal standard in urine was successfully achieved **(Fig. 3.1).** No interfering peaks co-elute with the compounds of interest **(Figs. 3.1.1).** Didymin, the 7-rutinoside of isosakuranetin is described to be in the 2S configurational state and is sold as S configuration by Extrasynthèse [55,58,144]. When didymin was cleaved to its aglycone using β-glucuronidase and analyzed under our chromatographic conditions, the 2S aglycone isosakuranetin eluted at 38 minutes. The retention times of 2S- and 2R-isosakuranetin were approximately 38 and 51 minutes, respectively. Separation of enantiomers is also possible at different flow rates as high as 1.0 ml/min with 4 minute separation of enantiomers and higher sensitivity due to decreased signal to noise ratio. However, stereochemically pure enantiomers are more easily attained at a flow rate of 0.40 ml/min due to a peak-to-peak separation of 14 minutes; optimized for our isolation purposes for future pharmacological investigations of isosakuranetin enantiomers. The internal standard eluted at approximately 10 minutes **(Fig. 3.1.2)**. Optimal separation was achieved with 100% HPLC-grade methanol and a flow rate of 0.40 ml/min.
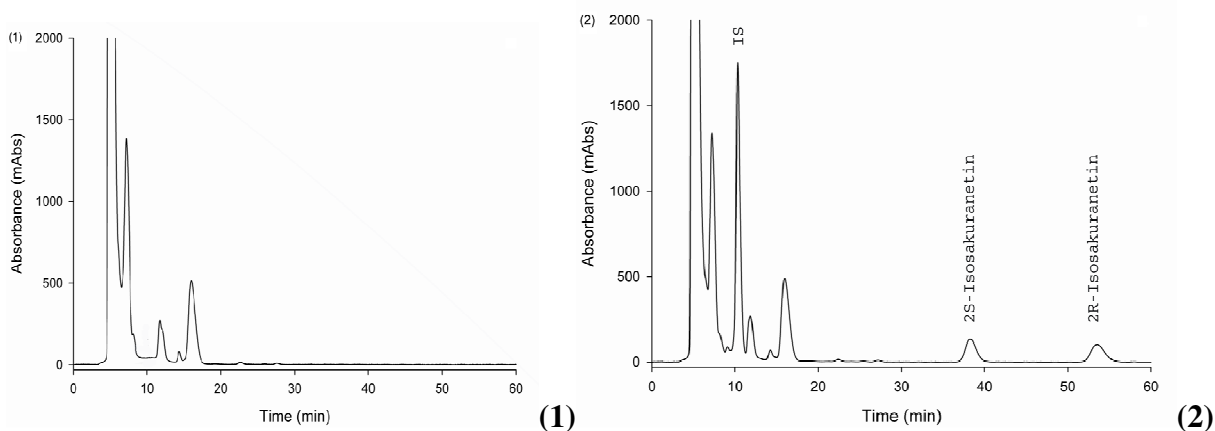
Figure 3.1. Representative chromatograms, of (**1**) drug-free rat urine demonstrating no interfering peaks co-eluted with the compounds of interest; and (**2**) rat urine containing isosakuranetin enantiomers each with concentration of 10.0 µg/ml and the internal standard (IS), 7-ethoxycoumarin.

Enantioseparation of isosakuranetin was also successfully accomplished in rat serum (**Fig. 3.2**). Optimal separation was achieved with 100% HPLC-grade methanol and a flow rate of 0.40 ml/min.
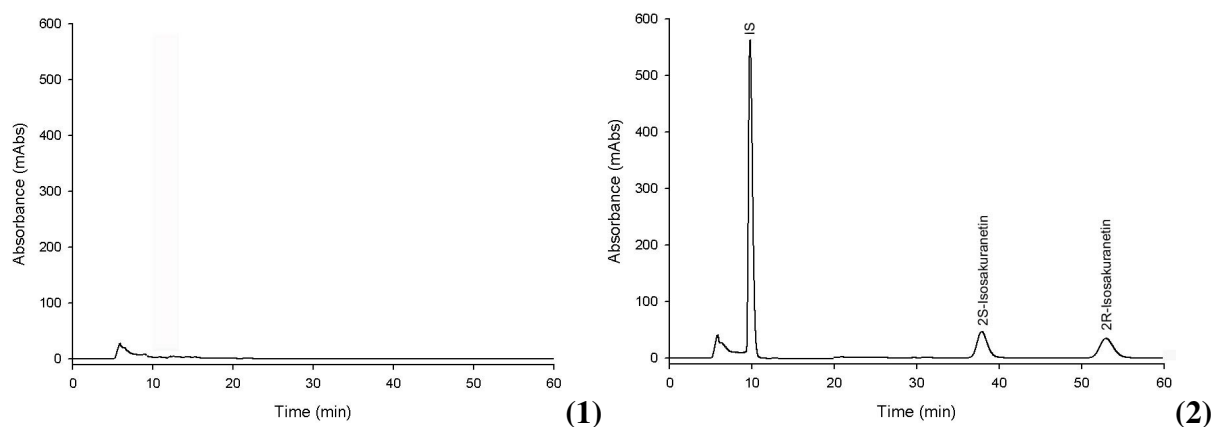
Figure 3.2. Representative chromatograms, of (**1**) drug-free rat serum demonstrating no interfering peaks co-eluted with the compounds of interest; and (**2**) rat serum containing isosakuranetin enantiomers each with concentration of 10.0 µg/ml and the internal standard (IS), 7-ethoxycoumarin.

3.4.2 Linearity, LOQ and LOD

Excellent linear relationships (r^2 = 0.999) were demonstrated between PAR of isosakuranetin enantiomers to the internal standard and the corresponding urine concentrations of isosakuranetin enantiomers over a range of 0.5 to 100.0 µg/ml. Mean regression lines from the validation runs were described by 2S-isosakuranetin (µg/ml) = $0.0304x$ – 0.0081 and 2R-isosakuranetin (µg/ml) = $0.0302x$ - 0.0068. LOQ of this assay was 0.5 µg/ml with the corresponding between-day R.S.D. of 7.97 and 10.90% for 2S- and 2R-isosakuranetin, respectively and bias of 3.26 and 2.11% for 2S- and 2R-isosakuranetin, respectively. The back-calculated concentration of QC samples was within the acceptance criteria **(Table 3.1).**

Table 3.1. Within- and between-day precision and accuracy of the assay for isosakuranetin (ISK) enantiomers in rat urine (n = 6, mean, R.S.D., and Bias).

Added	Isosakuranetin concentration (µg/ml)											
	Observed				R.S.D. (%)				Bias (%)			
	Within-day		Between-day		Within-day		Between-day		Within-day		Between-day	
	2S-ISK	2R-ISK	2S-ISK	2R-ISK	2S-ISK	2R-ISK	2S-ISK	2R-ISK	2S-ISK	2R-ISK	2S-ISK	2R-ISK
0.5	0.52	0.51	0.52	0.52	8.58	14.49	7.97	10.90	3.26	2.11	3.53	3.87
1	0.97	0.97	1.01	1.14	8.05	0.22	11.77	5.55	-2.53	-3.29	1.42	13.82
5	5.36	5.30	4.90	4.77	3.24	4.23	10.67	9.60	7.20	5.96	-2.06	-4.68
10	10.90	10.96	10.43	10.17	1.34	2.08	10.32	10.54	8.97	9.57	4.27	1.74
50	51.85	52.02	51.95	52.51	1.18	1.77	5.62	3.41	3.71	4.04	3.91	5.03
100	99.89	99.85	99.27	99.28	0.36	0.14	1.54	0.97	-0.11	-0.15	-0.73	-0.72

3.4.3 Precision, Accuracy and Recovery

Within- and between-run precision (R.S.D.) calculated during replicate assays (n = 6) of isosakuranetin enantiomers was <15% over a wide range of concentrations **(Table 3.1).** The intra- and inter-run bias assessed during the replicate assays for isosakuranetin enantiomers varied between -0.72 and 13.82% **(Table 3.1).** These data indicated that the developed HPLC method is reproducible and accurate. The mean extraction efficiency for isosakuranetin enantiomers from biological fluids varied from 86.93 to 104.05% **(Table 3.2).** Absolute recovery, in comparison, varied from 93.39 to 109.97%.

Table 3.2. Recovery of isosakuranetin enantiomers from rat urine (n = 6, mean ± S.D.).

Concentration (µg/ml)	Recovery (%) (Mean ± S.D.)	
	2S-Isosakuranetin	2R-Isosakuranetin
0.5	100.25±7.99	101.72±11.08
1	104.05±12.25	96.97±12.54
5	91.36±9.75	86.93±8.71
10	95.69±9.87	94.03±8.49
50	102.22±3.87	98.98±5.35
100	99.46±1.05	99.78±1.23

3.4.4 Stability of Isosakuranetin Samples

No significant degradation was detected in the samples of racemic isosakuranetin in biological fluids following three freeze-thaw cycles. Recoveries of 2S- and 2R-isosakuranetin were respectively from 91.36 to 104.05% and 86.93 to 101.72% following three freeze-thaw cycles for QC samples of isosakuranetin or 7-ethoxycoumarin. There was no significant decomposition observed after the reconstituted extract of racemic isosakuranetin was stored in

the auto-injector at room temperature for 24 h; measured values were 90.06 to 98.52% of the initial value for extracts of racemic isosakuranetin in biological fluids (0.5-100.0 µg/ml). The use of β-glucuronidase has previously been shown to have no effect on the stability and selectivity of enantioseparation assays of similar chiral flavanones [145].

3.4.5 Quantification in Grapefruit (Citrus paradisi)

Isosakuranetin has been previously reported in *Citrus* (Chapter I); however enantiomeric separation has not been previously published. The fruit of *Citrus paradisi* is classified as a modified berry called hesperidium. Carpels contain juicy vesicles that form the edible part of the fruit (Chapter II). The juice extracted from carpels in grapefruit was used to analyze the isosakuranetin content (**Fig. 3.3**).
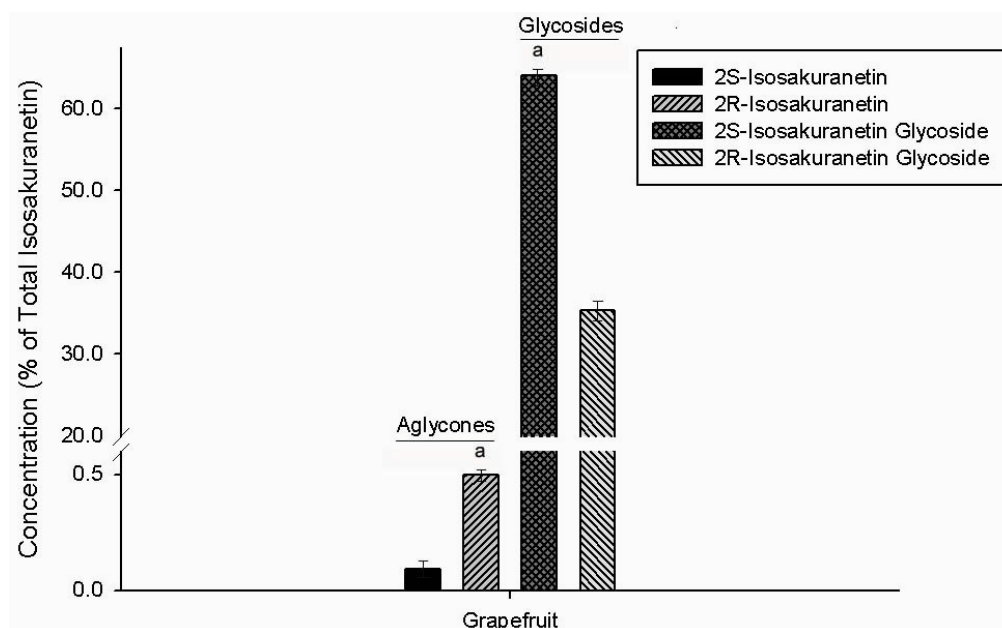
Figure 3.3. Content of isosakuranetin enantiomers and its glycosides in samples of grapefruit (*Citrus paradisi*, n = 3, mean ± S.E.M.). a, P < 0.05, 2S vs. 2R.

The highest concentrations of isosakuranetin enantiomers corresponded to the glycosides. The 2S glycoside and the 2R aglycone (25.58% and 0.20% of total isosakuranetin, respectively) presented the highest concentrations for glycosides and aglycones, respectively. A summary of the isosakuranetin content in grapefruit is presented in **Table 3.3.**

Table 3.3. Content of Isosakuranetin enantiomers and its glycosides in grapefruit (*Citrus paradisi*, n = 3, mean ± S.E.M.) a, P < 0.05, 2S vs. 2R.

% of Total Isosakuranetin	2S-Isosakuranetin	2R-Isosakuranetin
Glycoside	64.02 ± 0.02[a]	35.39 ± 0.03
Aglycone	0.09 ± 0.03	0.50 ± 0.03[a]
Total Enantiomer	64.11 ± 0.05[a]	35.89 ± 0.06
Total Glycosides	99.41 ± 0.05	
Total Aglycones	0.59 ± 0.06	

3.5 CONCLUSIONS

In summary, the developed stereospecific HPLC method for isosakuranetin is sensitive, reproducible, and accurate. It has been applied for the first time to examine the enantiomeric content of isosakuranetin in grapefruit.

4 <u>Stereospecific Assay Development and Validation of Taxifolin</u>

4.1 INTRODUCTION

This section describes the development of a selective, accurate, reproducible, and stereospecific assay using reverse phase high performance liquid chromatography, RP-HPLC for simultaneous separation of taxifolin enantiomers in biological matrices. The validation of the RP-HPLC assay in rat serum is reported in this chapter.

4.2 BACKGROUND

Preliminary enantioseparation of taxifolin has been previously attained using LC, and NMR spectrometry although separation of all four enantiomers has not been previously achieved in the biomedical literature (Chapter I).

4.3 METHODS

4.3.1 HPLC Apparatus and Conditions

The HPLC system used was a Shimadzu HPLC (Kyoto, Japan), consisting of an LC-10ATVP pump, a SIL-10AF auto injector, a SPD-M10A VP UV/VIS spectrophotometric diodearray detector, and a SCL-10A VP system controller. Injection volume was 150.0 µl. Data collection and integration were accomplished using Shimadzu EZ Start 7.1.1 SP1 software. The analytical column used was a Chiralcel® OJ-RH column (150mm × 4.6mm i.d., 5-µm particle size, Chiral Technologies Inc., Exton, PA, USA) protected by a Chiralcel® OJ-RH guard column (0.4cm x 1cm, 5-µm particle size, Chiral Technologies Inc., Exton, PA, USA). The mobile phase consisted of acetonitrile, water, and phosphoric acid (15:85:0.5, v/v/v), filtered and degassed under reduced pressure prior to use. Separation was carried out isocratically at 25 ± 1°C, a flow rate of 0.35 ml/min, with ultraviolet (UV) detection at 288 nm.

4.3.2 Chemicals and Reagents

Racemic taxifolin was purchased from Indofine Chemical Company (Hillsborough, NJ, USA), (2R3R)-(+)-taxifolin from Extrasynthèse (Genay, France), and (2R3R)-(+)-taxifolin-3-O-rhamnoside from Apin Chemicals Ltd. (Oxon, United Kingdom). 2-

Thiobarbituric acid was purchased from Fluka (St Louis, MO, USA). β-Glucuronidase from *Escherichia coli* Type IX A, formic acid, halothane and β-glucuronidase from *Helix pomatia* Type-HP-2 were purchased from Sigma Chemicals (St Louis, MO, USA). HPLC grade acetonitrile and water were purchased from J. T. Baker (Phillipsburg, NJ, USA). Phosphoric acid was purchased from Aldrich Chemical Co. Inc. (Milwaukee, WI, USA). Rats were obtained from Charles River Laboratories. Ethics approval for animal experiments was obtained from Washington State University IACUC, Institutional Animal Care and Use Committee.

4.3.3 Stock and Working Standard Solutions

Racemic taxifolin and 2-thiobarbituric acid (2-TBA) solutions of 100.0 μg/ml were dissolved in methanol. These solutions were protected from light and stored at -20°C between uses, for no longer than three months. Calibration standard curves in serum were prepared daily from the stock solutions by sequential dilution with blank rat serum, yielding concentrations of 0.5, 1.0, 5.0, 10.0, 50.0 and 100.0 μg/ml of each taxifolin enantiomer.

Quality control (QC) samples were prepared from the stock solution of racemic taxifolin by dilution with blank rat serum to yield concentrations of 0.5, 1.0, 5.0, 10.0, 50.0 and 100.0 µg/ml. The QC samples were divided into 0.5 ml aliquots in screw-capped test tubes and stored at -20°C before use.

4.3.4 Sample Preparation

Rats were humanely sacrificed using halothane, blank serum was obtained from untreated rats, and stored at -20°C to be used as the biological matrix; water was used in the

case of botanical analysis. To the working standards or samples (0.1 ml), 25.0 μl of 2-thiobarbituric acid (internal standard, IS) was added into 2.0 ml Eppendorf tubes. The mixture was vortexed for 1 minute and 1.0 ml of ice-cold acetonitrile was added to precipitate proteins. The samples were centrifuged at 5,000 r.p.m. for 5 minutes using Beckman Microfuge (Beckman Coulter, Inc., CA, USA). The supernatant was transferred to new vials and evaporated to dryness under compressed nitrogen gas using an analytical evaporator (Organomation Associates Inc., Berlin, MA, USA). The residue was reconstituted with 200.0 μl of mobile phase, vortexed and centrifuged, the supernatant was transferred to HPLC vials, and 150.0 μl was injected into the HPLC system.

4.3.5 Precision and Accuracy

The within-run and between-run precision and accuracy of the replicate assays (n = 6) were tested by using six different concentrations, namely 0.5, 1.0, 5.0, 10.0, 50.0 and 100.0 μg/ml, on the same day and on six different days within one week, respectively. The precision was evaluated by the relative standard deviation (R.S.D.). The accuracy was estimated based on the mean percentage error of measured concentration to the actual concentration [142]. The values of R.S.D. and bias should be within 15%, at all concentrations tested [146].

4.3.6 Limit of Quantification (LOQ) and Limit of Detection (LOD)

The LOQ and LOD were defined in Chapter II. The LOQ was determined by repeated analysis of spiked rat serum samples in six replicates. An acceptance criteria of 15% was used to determine precision and accuracy at the LOQ. A signal to noise ratio $\geq$ 3:1 was used to determine the LOD by means of UV detection of serum samples.

4.3.7 Recovery

Relative recovery of taxifolin enantiomers was accomplished over the same concentration range (0.5-100.0 μg/ml, n = 6). A known amount of racemic taxifolin was combined with 0.1 ml of rat serum to give the above concentrations, and 1.0 ml of ice-cold acetonitrile was added to denature and precipitate proteins. The mixture was centrifuged at 5,000 r.p.m. for 5 minutes and the resulting supernatant was analyzed by HPLC. The extraction efficiency was determined by comparing the peak area ratio (PAR) of enantiomeric taxifolin and 2-thiobarbituric acid to the PAR of corresponding concentration injected directly in the HPLC without protein precipitation.

4.3.8 Stability of Taxifolin Samples in Rat Serum and Urine

The freeze-thaw stability of taxifolin enantiomers (0.5-100.0 μg/ml) was evaluated in triplicate without being frozen at first, and then stored at -70°C and thawed at room temperature (25 ± 1°C) for three cycles. The stability of taxifolin in reconstituted extracts was investigated using pooled extracts from QC samples of one concentration level, 10.0 μg/ml. The sample was kept in the sample rack of the auto-injector and injected into HPLC system every 4 hours, from 0 to 24 hours.

4.3.9 Circular Dichroism Procedures

Circular Dichroism (CD) data were recorded on an AVIV stopped flow CD spectrometer (Model 202 SF, AVIV Instruments Inc., Lakewood, New Jersey, USA) connected to a refrigerated recirculator (CFT-75, Neslab).

4.3.10   LC-ESI-MS System and Conditions

To further verify the separation of taxifolin enantiomers, a LC-ESI-MS was employed. The LC-ESI-MS system used was a Shimadzu LCMS-2010 EV liquid chromatograph mass spectrometer system (Kyoto, Japan) connected to the LC portion consisting of two LC-10AD pumps, a SIL-10AD VP auto injector, a SPD-10A VP UV detector, and a SCL-10A VP system controller. Data analysis was accomplished using Shimadzu LCMS Solutions Version 3 software (Kyoto, Japan). The chromatographic methods were only slightly modified from the above HPLC system conditions. The same Chiralcel® OJ-RH analytical column and guard column were used, UV detection was set at 288 nm, and the flow rate was 0.35 ml/min. The mobile phase was altered to consist of acetonitrile, water, and formic acid (15:85:0.5, v/v/v). Formic acid is preferred in electrospray ionization due to improved ionization compared to phosphoric acid which was employed in the HPLC method. The mass spectrometer conditions consisted of a curved desolvation line (CDL) temperature of 200ºC and a block temperature of 200ºC. The CDL, interface, and detector voltages were -20.0 V, 4.5 kV, and 1.2 kV, respectively. Vacuum was maintained by an Edwards® E2M30 rotary vacuum pump (Edwards, UK). Liquid nitrogen (Washington State University Central Stores) was used as a source of nebulizer gas (1.5 L/min) and as a source of drying gas (0.1 L/min). Taxifolin was monitored in selected ion monitoring (SIM) negative and positive mode with the single plot transition at m/z 303 and 305, respectively.

4.3.11   Extraction of Taxifolin from Rhizoma smilacis glabrae

Taxifolin was extracted from *Rhizoma smilacis glabrae* following the procedure described by Prati, *et al.* [91] with minor modifications. Briefly, 1.0 g of tu fu ling herb

extract powder was extracted with 3 x 30.0 ml of 70% ethanol, adjusted to pH 2.0 with formic acid. Each step involved an extraction for 3 hours at room temperature. The extracts were combined and defatted with 3 x 30.0 ml of petroleum ether. The defatted extracts were dried under nitrogen gas using an analytical evaporator, reconstituted in mobile phase, and injected into the HPLC system at a volume of 150.0 µl for analysis.

4.3.12   *Extraction of Taxifolin from Malus x domestica*

Extraction of taxifolin from *Malus* x *domestica* was accomplished as follows: 0.1 g of sample (peel or flesh, organic growth) was measured and frozen under liquid nitrogen. Each sample was prepared in duplicate; the frozen samples were placed into the extraction glass tube and 1.0 ml of methanol was added. Extraction was performed for 1 minute using a Thomas tissue grinder (Thomas Scientific, Swedesboro, NJ, USA). The extraction was mixed and the fruit tissue was placed into a 2.0 ml Eppendorf tube, 0.5 ml of methanol was added to the extraction glass for rinsing and combined with the extraction mix. A total volume of 1.5 ml was obtained per extraction; the samples were vortexed for 30 seconds and centrifuged at 5,000 r.p.m. for 5 minutes One of the duplicates was treated to extract only aglycones (free) and the second of the duplicates was treated to cleave any glycosides to aglycones (total) by using β-glucuronidase from *Helix pomatia* Type HP-2 [147]. The supernatant of the free untreated samples was transferred into 2.0 ml Eppendorf tubes, and 25 µl of IS was added, samples were vortexed for 10 seconds, dried to completion under nitrogen gas using an analytical evaporator, and stored at 4°C before analysis. The supernatant of the total samples was transferred into 15.0 ml conical tubes. The total samples were dried to completion under nitrogen gas, then 1.0 ml of HPLC-grade water, 110.0 µl 0.78 M sodium acetate-acetic acid

buffer (pH 4.8), and 100.0 µl 0.1 M ascorbic acid were added. The samples were vortexed for 30 seconds, and incubated for 17-24 hours at 37°C in a shaking incubator following the addition of 200.0 µl of crude preparation of β-glucuronidase from *Helix pomatia* Type HP-2. After incubation, 1.0 ml of ice-cold acetonitrile was added to stop the enzymatic activity of β-glucuronidase, the samples were vortexed for 10 seconds, and centrifuged at 5,000 r.p.m. for 5 minutes The supernatant was collected into 15.0 ml conical tubes and dried to completion under nitrogen gas using an analytical evaporator after 25.0 µl of IS was added; then were stored at 4°C before analysis. When all samples were ready for analysis, they were reconstituted in 200.0 µl of mobile phase, vortexed for 30 seconds, and centrifuged at 5,000 r.p.m. for 5 minutes; 150.0 µl of sample was injected into the HPLC system for analysis. Glycoside content was calculated by subtracting the concentration of the free samples from the total samples incubated with β-glucuronidase.

4.3.13 Data Analysis

Quantification was based on calibration curves constructed using PAR of taxifolin enantiomers to IS, against taxifolin concentrations using unweighted least squares linear regression.

4.4 RESULTS AND DISCUSSION

4.4.1 Chromatography

Baseline separation of taxifolin enantiomers and the IS in biological fluids was successfully achieved **(Fig. 4.1).** No interfering peaks co-eluting with the compounds of interest were evident **(Fig. 4.1.1).** Taxifolin-3-*O*-rhamnoside (astilbin, **Fig. 1.5**), is described

to be in the (2R3R)-(+) configurational state and is sold as (2R3R)-(+) configuration by Apin Chemicals Ltd. (2R3R)-(+)-Taxifolin is sold as by Extrasynthèse as the pure enantiomer. When taxifolin-3-*O*-rhamnoside was cleaved to its aglycone using *β*-glucuronidase and analyzed under our chromatographic conditions, the (2R3R)-(+)-taxifolin configuration eluted at approximately 82 minutes. When the pure (2R3R)-(+) enantiomer was analyzed, it also eluted around 82 minutes, confirming that the taxifolin-3-*O*-rhamnoside has this configurational state. Based on literature information [130], and comparing our CD data obtained with published work [83,86,111,117,148], we were able to distinguish the enantiomers of taxifolin which eluted in the following order: (2S3R)-(+) ~68 min, (2S3S)-(-) 73 min, (2R3R)-(+) 82 min, and (2R3S)-(-) 126 min **(Fig 4.2).** Mass spectrometry was used to confirm the m/z ratio of each eluted peak for identification of the taxifolin enantiomers **(Fig. 4.3).** The IS eluted at approximately 10 minutes **(Fig. 4.1.2).** Several HPLC conditions were tested before optimal separation was achieved; the best resolution was attained when the combination of acetonitrile, water, and phosphoric acid was 15:85:0.5 (v/v/v) and the flow rate of 0.35 ml/min. Identification of enantiomers of taxifolin has been previously reported; however, these studies only addressed the identification or separation of only two enantiomers of taxifolin [104,107,123,131] or its glycosides [77,98]. Identification or separation of the four taxifolin enantiomers has only been previously attained when taxifolin is glycosylated [87,96]. Identification of the four taxifolin enantiomers was reported by Kielhmann and Slade, and Kolesnik *et al.*, but enantio-isolation was not accomplished by Kielhmann and Slade [80] and no chromatographic or stereospecific data has been made available by Kolesnik *et al.* [130].
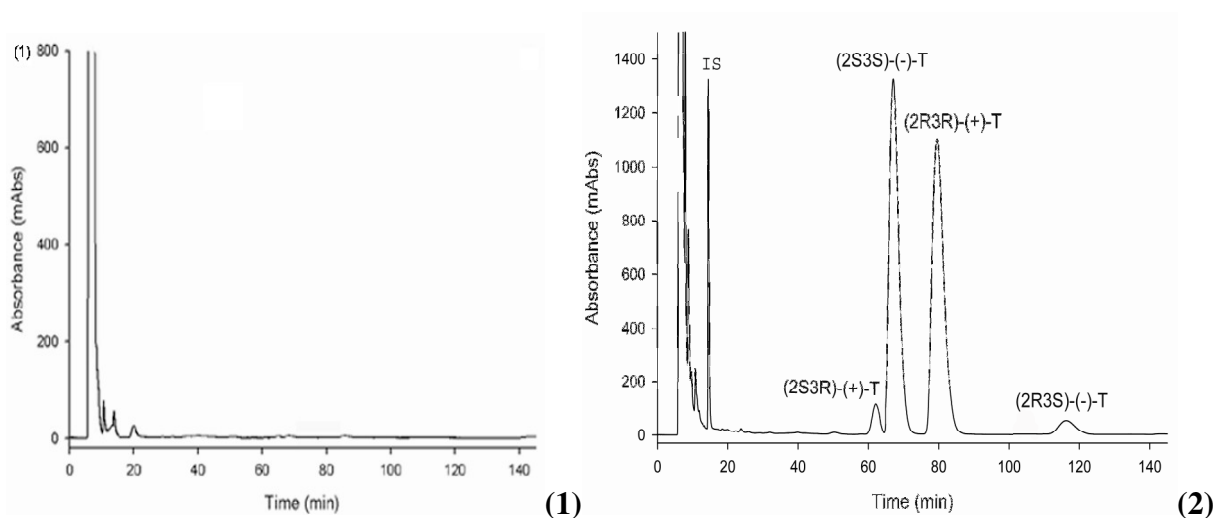
Figure 4.1. Representative chromatograms of **(1)** drug-free serum demonstrating no interfering peaks co-eluted with the compounds of interest; and **(2)** serum containing enantiomers – (2S3R)-(+)-, (2S3S)-(-)-, (2R3R)-(+)-, and (2R-3S)-(-)-taxifolin (T) – after 100 µg/ml taxifolin injection.
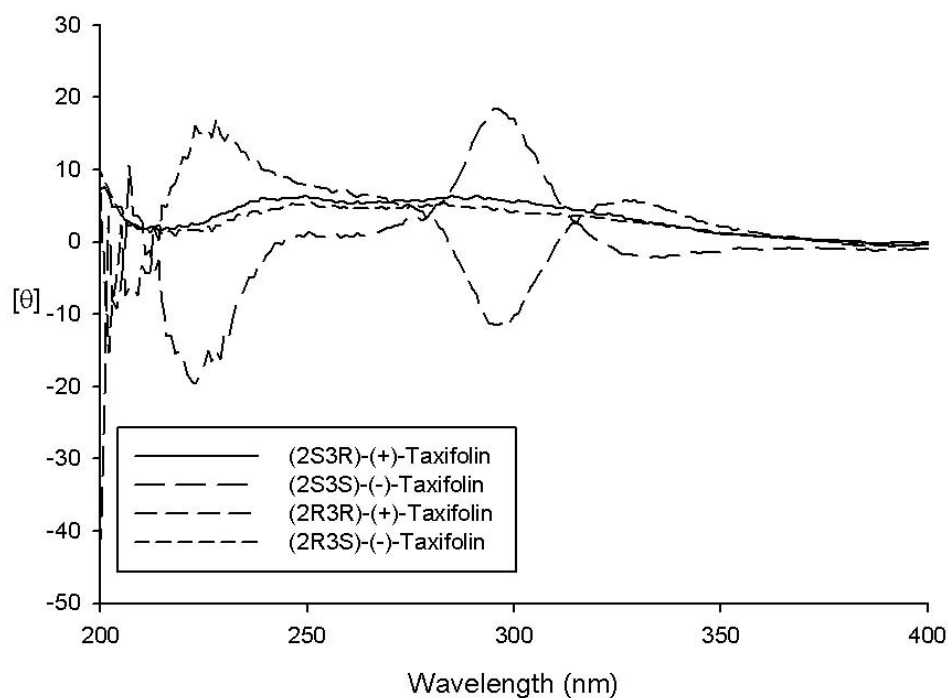
Figure 4.2. Representative circular dichroism data of each isolated taxifolin enantiomer: (2S3R)-(+), (2S3S)-(-), (2R3R)-(+), and (2R3S)-(-).
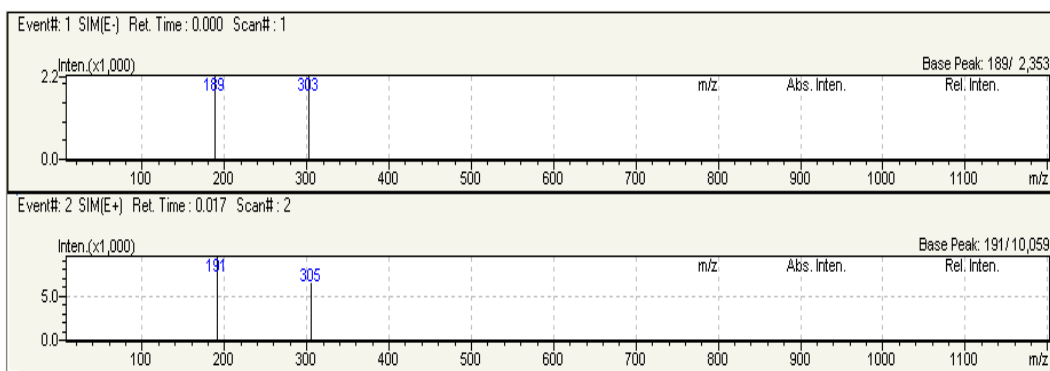
Figure 4.3. Representative liquid chromatography-mass spectrometry data of taxifolin (MW = 304.25 g/mol) monitored in selected ion monitoring (SIM) negative (top) and positive (bottom) mode.

4.4.2 Linearity, LOQ and LOD

Excellent linear relationships (r^2 = 0.995) were demonstrated between PAR of taxifolin enantiomers to the IS and the corresponding serum concentrations of taxifolin enantiomers over a range of 0.5 to 100.0 µg/ml. Mean regression lines from the validation runs were described by the four taxifolin enantiomers as follows: (2S3R)-(+)-taxifolin (µg/ml) = 0.0024x – 0.0014, (2S3S)-(-)-taxifolin (µg/ml) = 0.0550x + 0.0066, (2R3R)-(+)-taxifolin (µg/ml) = 0.0608x + 0.0067, and (2R3S)-(-)-taxifolin (µg/ml) = 0.0030*x* - 0.0002. LOQ of this assay was 0.5 µg/ml with the corresponding between day R.S.D. of 12.50, 6.51, 8.15, and 7.53% for (2S3R)-(+)-, (2S3S)-(-)-, (2R3R)-(+)-, and (2R3S)-(-)-taxifolin, respectively and bias of 6.14, 14.04, -0.96, and 6.75% for (2S3R)-(+)-, (2S3S)-(-)-, (2R3R)-(+)-, and (2R3S)-(-)-taxifolin, respectively **(Table 4.2).** Table 4.1 demonstrates that the back-calculated concentration of QC samples was within the acceptance criteria**.**

Table 4.1. Within-day precision and accuracy of the assay for taxifolin enantiomers in rat serum (n = 6, mean, R.S.D., and Bias).

	Taxifolin concentration (µg/ml) – Within-day											
Added	Observed				R.S.D. (%)				Bias (%)			
	2S3R (+)	2S3S (-)	2R3R (+)	2R3S (-)	2S3R (+)	2S3S (-)	2R3R (+)	2R3S (-)	2S3R (+)	2S3S (-)	2R3R (+)	2R3S (-)
0.5	0.49	0.53	0.54	0.55	1.11	11.64	9.76	0.50	-2.87	5.16	7.37	9.60
1	0.89	0.93	1.00	0.97	4.48	3.11	14.87	12.00	-10.81	-6.57	0.05	-3.43
5	5.02	5.07	4.95	5.43	13.34	14.08	9.39	11.04	0.47	1.43	-1.01	8.57
10	10.87	10.48	10.65	10.74	10.26	6.06	4.58	6.83	8.68	4.79	6.48	7.43
50	49.73	48.23	46.62	46.43	10.69	11.58	8.61	8.24	-0.53	-3.53	-6.76	-7.14
100	100.65	100.76	101.46	100.78	3.52	2.67	1.75	3.84	0.65	0.76	1.46	0.78

Table 4.2. Between-day precision and accuracy of the assay for taxifolin enantiomers in rat serum (n = 6, mean, R.S.D., and Bias).

	Taxifolin concentration (µg/ml – Between-day											
Added	Observed				R.S.D. (%)				Bias (%)			
	2S3R (+)	2S3S (-)	2R3R (+)	2R3S (-)	2S3R (+)	2S3S (-)	2R3R (+)	2R3S (-)	2S3R (+)	2S3S (-)	2R3R (+)	2R3S (-)
0.5	0.53	0.57	0.50	0.53	12.50	6.51	8.15	7.53	6.14	14.04	-0.96	6.75
1	1.10	1.02	0.96	1.06	6.40	12.85	13.67	10.39	9.58	1.84	-3.76	5.76
5	4.41	4.55	4.74	4.36	4.18	8.48	4.11	10.61	-11.85	-8.99	-5.23	-12.71
10	11.02	10.80	9.78	11.21	10.35	14.95	5.22	3.41	10.16	2.37	7.96	12.07
50	48.72	47.35	46.64	49.06	3.80	5.43	2.29	4.36	-2.55	-5.30	-6.73	-1.87
100	100.47	101.32	101.71	100.78	2.42	1.23	0.71	1.49	0.47	1.32	1.71	0.78

4.4.3 Precision, Accuracy and Recovery

Within- and between-run precision (R.S.D.) was calculated during replicate assays (n = 6) of taxifolin enantiomers was <15% over a wide range of concentrations (**Tables 4.1** and **4.2).** The intra- and inter-run bias assessed during the replicate assays for taxifolin

enantiomers varied between -12.71 and 14.04% **(Tables 4.1** and **4.2).** These data indicated that the developed HPLC method is reproducible and accurate. The mean extraction efficiency for taxifolin enantiomers from biological fluids varied from 91.50 to 111.10% **(Table 4.3).**

Table 4.3. Recovery of taxifolin enantiomers from rat serum (n = 6, mean ± S.D.).

Concentration (µg/ml)	Recovery (%) (Mean ± S.D.)			
	2S3R (+)	2S3S (-)	2R3R (+)	2R3S (-)
0.5	101.80 ± 1.13	98.30 ± 11.44	100.33 ± 9.79	103.92 ± 0.52
1	93.63 ± 2.96	103.53 ± 3.22	103.63 ± 7.06	98.91 ± 11.87
5	97.54 ± 13.01	104.58 ± 12.94	96.80 ± 6.13	111.10 ± 12.27
10	105.70 ± 9.15	110.95 ± 6.72	99.34 ± 4.55	99.75 ± 6.81
50	104.88 ± 0.02	101.07 ± 11.70	91.50 ± 7.87	96.38 ± 7.96
100	96.19 ± 3.38	98.55 ± 2.64	93.42 ± 1.64	95.09 ± 3.65

4.4.4 Quantification of Taxifolin in Tu fu ling (Smilax glabra rhizome) and Apple (Malus x domestica)

The HPLC method was applied to the quantification of taxifolin enantiomers in *Rhizoma smilacis glabrae* and *Malus* x *domestica* **(Fig. 4.4 - 4.6)**. *Rhizoma smilacis glabrae* contained predominantly (2R3R)-(+)-taxifolin (99.97 %) while (2S3R)-(+)-, (2S3S)-(-)-, and (2R3S)-(-)-taxifolin are found in minor quantities (0.008-0.01 %).

The fruit of *Malus* x *domestica* has been classified as a pome fruit, and also as an accessory fruit because the edible portion originates from the non-ovarian, fused floral tube. The fruit is usually composed of five carpels, with the pericarp forming the core. The edible portion is called the cortex and is formed by the fusion of the floral tube (hypanthium). Samples of the cortical tissue were taken and labeled "peel".

The content of taxifolin enantiomers was evaluated in conventional and organic apples (**Fig. 4.5** and **Fig. 4.6**). Overall, peel samples contained higher quantities of taxifolin enantiomers when compared to flesh in both conventional and organic apples.
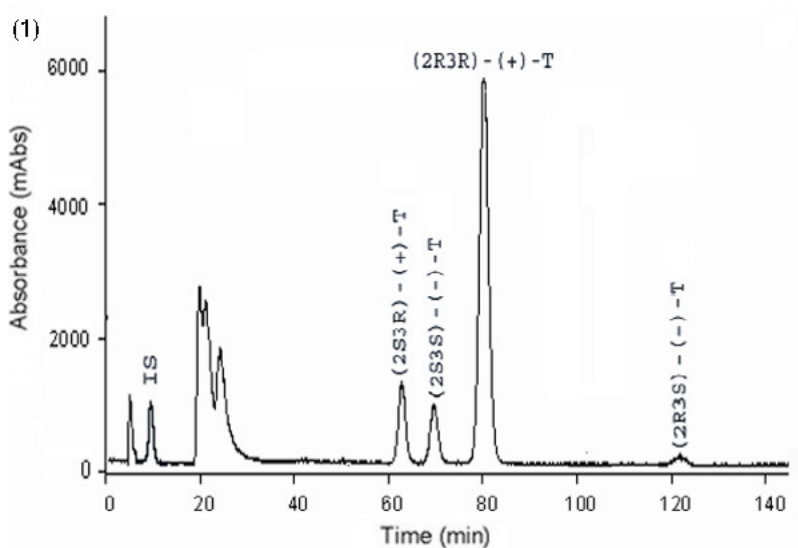
Figure 4.4. Representative chromatograph of tu fu ling (*Rhizoma smilacis glabrae*) sample containing taxifolin (T) enantiomers predominantly in the (2R3R)-(+)-form. The internal standard (IS) used was 2-thiobarbituric acid (2-TBA).

In conventionally grown apples, the highest concentrations of taxifolin enantiomers in peel corresponded to taxifolin glycosides. The (2R3S)-(-)-taxifolin glycoside (41.12% of total taxifolin) and the (2S3R)-(+)-taxifolin aglycone (16.99% of total taxifolin) presented the highest concentrations for glycosides and aglycones, respectively **(Fig. 4.5).**
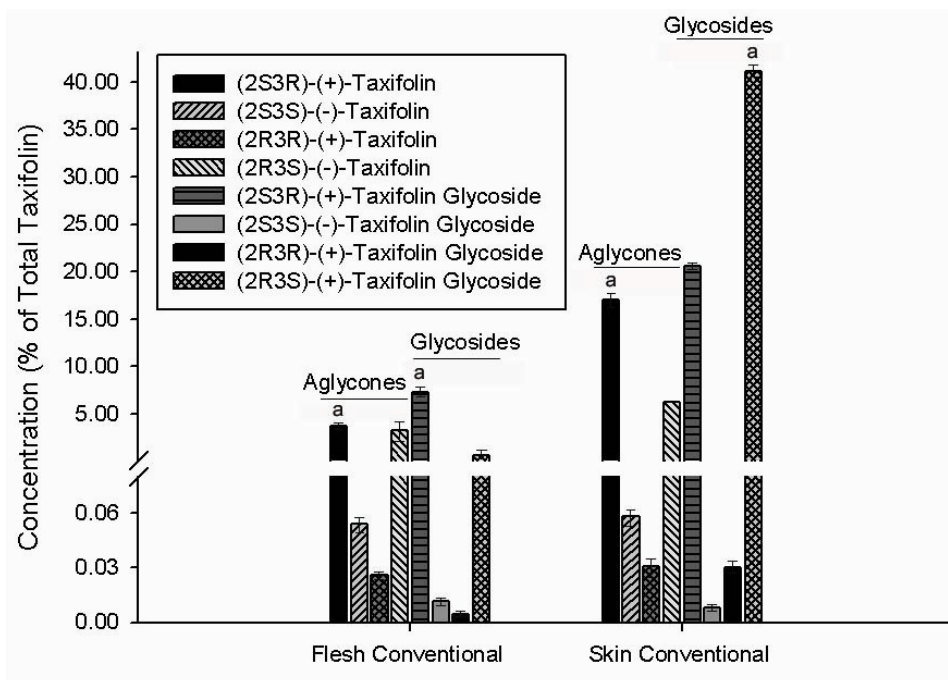
Figure 4.5. Content of taxifolin enantiomers and its glycosides in flesh and peel samples of conventionally grown 'Red Delicious' apple (*Malus* x *domestica*, n = 3, mean ± S.E.M.). a, P < 0.05, conventional vs. organic.

Peel samples of organically grown apples contained higher quantities of taxifolin enantiomers when compared to flesh, 509.91 ± 5.60 mg/100 g FW and 112.65 ± 2.49 mg/100 g FW, respectively. The aglycone and glycoside forms of (2R3S)-(-)-taxifolin corresponded to the highest concentrations of each taxifolin form, respectively. The highest concentrations of taxifolin enantiomers in the peel of organic apples corresponded to glycosides, similar to the findings observed in conventional apples. Nevertheless, most of the taxifolin enantiomers demonstrated higher concentrations in organic apples compared to conventional apples. A summary of the taxifolin content in both conventional and organic apples is presented in **Table 4.4.**
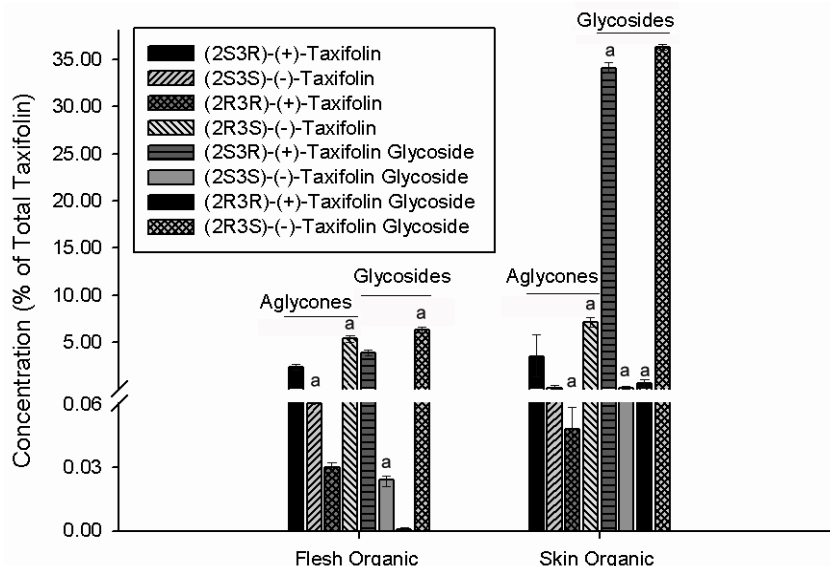
Figure 4.6. Content of taxifolin enantiomers and its glycosides in flesh and peel samples of organically grown 'Red Delicious' apple (*Malus* x *domestica*, n = 3, mean ± S.E.M.). a, P < 0.05, conventional vs. organic.

Table 4.4. Content of taxifolin enantiomers and its glycosides in conventional and organic apple (*Malus* x *domestica*, n = 3, mean ± S.E.M.). a, P < 0.05, conventional vs. organic.

% of Total Taxifolin		Conventional		Organic	
		Flesh	**Peel**	**Flesh**	**Peel**
(2S3R)-(+)-Taxifolin	Glycoside	7.22 ± 0.11[a]	20.62 ± 0.11	3.92 ± 0.10	34.12 ± 0.15 [a]
	Aglycone	3.75 ± 0.10 [a]	16.99 ± 0.60 [a]	2.38 ± 0.10	3.45 ± 0.11
	Total	**10.97 ± 0.22[a]**	**37.61 ± 0.71**	**6.30 ± 0.20**	**37.57 ± 0.26**
(2S3S)-(-)-Taxifolin	Glycoside	0.01 ± 4E-03	0.008 ± 2E-04	0.02 ± 1E-03[a]	0.09 ± 0.01 [a]
	Aglycone	0.05 ± 7E-03	0.06 ± 6E-03	0.06 ± 1E-03[a]	0.15 ± 1E-03[a]
	Total	**0.06 ± 1E-01**	**0.07 ±6E-04**	**0.08 ± 4E-03[a]**	**0.24 ± 0.01 [a]**
(2R3R)-(+)-Taxifolin	Glycoside	0.004 ± 1E-04	0.03 ± 1E-03	0.001 ± 1E-04	0.62 ± 0.02 [a]
	Aglycone	0.03 ± 5E-03	0.03 ± 2E-03	0.03 ± 5E-03	0.04 ± 0.01
	Total	**0.03 ±1E-04**	**0.06 ± 3E-03**	**0.03 ± 5E-03**	**0.66 ± 0.03[a]**
(2R3S)-(-)-Taxifolin	Glycoside	0.57 ± 0.11	41.12 ± 0.11 [a]	6.29 ± 0.10 [a]	36.32 ± 0.15
	Aglycone	3.30 ± 0.13	6.20 ± 0.15	5.39 ± 0.10 [a]	7.10 ± 0.50 [a]
	Total	**3.87 ± 0.24**	**47.32 ± 0.26**	**11.68 ± 0.20[a]**	**43.42 ± 0.65**
Total Glycosides		**7.81 ± 0.22**	**61.77 ± 0.22**	**10.23 ± 0.20 [a]**	**71.16 ± 0.28[a]**
Total Aglycones		**7.13 ± 0.24**	**23.28 ± 0.76[a]**	**7.86 ± 0.21 [a]**	**10.74 ± 0.62**

4.4.5 Stability of Taxifolin Samples

No significant degradation was detected after the samples of racemic taxifolin in biological fluids following three freeze-thaw cycles. Recovery of the taxifolin enantiomers were from 79.96 to 109.79%, 92.09 to 103.60, 92.47 to 117.28, and 91.07 to 107.14% for (2S3R)-(+)-, (2S3S)-(-)-, (2R3R)-(+)-, and (2R3S)-(-)-taxifolin, respectively; following three freeze-thaw cycles for QC samples of taxifolin. There was no significant decomposition observed after the reconstituted extract of racemic taxifolin was stored in the auto-injector at room temperature for 24 h; the measurements were from 97.87 to 98.90% of the initial value for extracts of racemic taxifolin in biological fluids of 0.5 to 100.0 µg/ml.

4.5   CONCLUSIONS

In summary, the developed stereospecific HPLC method for taxifolin is sensitive, reproducible, and accurate. It has been applied for the first time to examine the concentrations of enantiomeric taxifolin in *Rhizoma smilacis glabrae* and organic and conventional *Malus* x *domestica*. Further studies are ongoing in our laboratory to further characterize taxifolin and other flavonoid enantiomers as well as their pharmacological and toxicological activity.

5 Pre-Clinical Pharmacokinetics of Racemic Homoeriodictyol, Isosakuranetin, and Taxifolin in Rats

5.1 INTRODUCTION

This chapter describes the stereospecific pharmacokinetic disposition of homoeriodicytol, isosakuranetin, and taxifolin in Sprague-Dawley male rats as modeled using WinNonlin® pharmacokinetic software. The validated HPLC methods are used to analyze serum and urine samples of rats following intravenous administration of each flavonoid via jugular vein administration. The characterization and interpretation of the pharmacokinetic disposition profiles of homoeriodicytol, isosakuranetin, and taxifolin are described.

5.2 BACKGROUND

Humans ingest flavonoids including homoeriodicytol, isosakuranetin, and taxifolin from a variety of dietary sources on a daily basis. In addition, these compounds are all available in a plethora of nutraceutical products. Moreover, some of these compounds are being scrutinized and developed into therapeutic agents due to their pharmacological activities (Chapter I).

Small structural differences – like those produced by chirality – in the chemical structures of homoeriodicytol, isosakuranetin, and taxifolin may yield significant differences in their pharmacokinetic disposition. Previous pharmacokinetic studies of these compounds have not taken into consideration the chemical stereospecificity of homoeriodicytol, isosakuranetin, and taxifolin (Chapter I).

Therefore, it is fundamental to characterize the distribution, metabolism and elimination of these compounds. The area under the curve (AUC); serum half-life ($t\frac{1}{2}_s$); urine half-life ($t\frac{1}{2}_u$); total, hepatic and renal clearance (CL_T, CL_H, CL_R); volume of distribution (V_{SS}); and extraction ratio (ER) of the stereoisomers of homoeriodicytol, isosakuranetin, and taxifolin were determined in a rat model.

5.3 METHODS

5.3.1 Chemicals and Reagents

Racemic homoeriodictyol, isosakuranetin, and taxifolin were purchased from Indofine Chemical Company (Hillsborough, NJ, USA); (2R3R)-(+)-taxifolin from Extrasynthèse (Genay, France). Dimethyl sulfoxide (DMSO), indoprofen, 7-ethoxycoumarin, 2-thiobarbituric acid, β-glucuronidase from *E. coli* Type IX-A, and halothane were purchased

from Sigma Chemicals (St Louis, MO, USA); HPLC grade acetonitrile, methanol and water were purchased from J. T. Baker (Phillipsburg, NJ, USA). Phosphoric acid was purchased from Aldrich Chemical Co. Inc. (WI, USA). PDI sterile alcohol prep pads were purchased from Professional Disposables International (Orangeburg, NJ, USA). Dr. Bond™ super glue was purchased from Permatex, Inc. (Solon, OH, USA). 0.9% Sodium chloride irrigation, USP was purchased from Baxter Healthcare Corporation (Deerfield, IL, USA). Rats were obtained from Charles River Laboratories. Ethics approval for animal experiments was obtained from the Institutional Animal Care and Use Committee of Washington State University (approval number 3204).

5.3.2 Surgical Equipment

Silastic® laboratory tubing (0.64 mm I.D. × 1.19 mm O.D.) was purchased from Dow Corning Corporation (Midland, MI, USA). Intramedic™ polyethylene (PE) 50 (0.56 mm I.D. × 0.93 mm O.D.), 90 (0.83 mm I.D. × 1.23 mm O.D.), and 190 (1.15 mm I.D. × 1.64 mm O.D.) tubing was purchased from Becton Dickinson and Company (Sparks, MD, USA). Tygon® R-3603 flexible plastic tubing (0.76 mm I.D. × 2.30 mm O.D.) was purchased from Saint-Gobain Performance Plastics (Akron, OH, USA). Monoject® 23 gauge (0.6 mm × 25.0 mm) and 18 gauge (1.2 mm × 38.1 mm) polypropylene hub hypodermic needles were purchased from Sherwood Medical (St Louis, MO, USA). Ethicon reverse cutting PDS[*]II monofilament (polydioxanone) clear surgical sutures (size 4-0, needle FS-2) were purchased from Ethicon, a division of Johnson & Johnson Medical Limited (Livingston, UK). Look® black braided silk non-absorbable, non-sterile surgical suture (size 3-0) was purchased from Surgical Specialties Corporation (Reading, PA, USA). The FluTec Mk III, a precision

temperature-compensated anesthetic vaporizer from Cyprane (Keighley, Yorkshire, UK; distributed by Fraser Harlake, Orchard Park, NY, USA) was utilized along with an MXR anesthetic regulator from Porter Instruments Co., Inc. (Hatflied, PA, USA) during the surgical procedures.

5.3.3 Chromatographic Systems and Conditions

The HPLC system used in the analysis of homoeriodicytol was a Shimadzu HPLC (Kyoto, Japan), consisting of an LC-10ATVP pump, a SIL-10AF auto injector, a SPD-M10A VP spectrophotometric diodearray detector, and a SCL-10A VP system controller. Data collection and integration were accomplished using Shimadzu EZ Start 7.1.1 SP1 software. The analytical column used was Chiralcel® OJ-RH column (150mm × 4.6mm i.d., 5-µm particle size, Chiral Technologies Inc., PA, USA) protected by a Chiralcel® OJ-RH guard column (0.4cm x 1cm, 5-µm particle size). The mobile phase consisted of acetonitrile, water and phosphoric acid (22:78:0.1, v/v/v), filtered and degassed. Separation was carried out isocratically at 25 ± 1°C and a flow rate of 1.0 ml/min with ultraviolet (UV) detection at 288 nm as validated and described in detail in Chapter II.

The HPLC system used in the analysis of isosakuranetin was a Shimadzu HPLC (Kyoto, Japan), consisting of an LC-10AT-VP pump, a SIL-10AF auto injector, a SPD-M10A VP spectrophotometric diodearray detector, and a SCL-10A VP system controller. Data collection and integration were accomplished using Shimadzu EZ Start 7.1.1 SP1 software. The analytical column used was Chiralpak® AD™-RH column (150mm × 4.6mm i.d., 5-µm particle size, Chiral Technologies Inc., Exton, PA, USA). The mobile phase consisted of 100% HPLC-grade methanol filtered and degassed. Separation was carried out isocratically at

25 ± 1°C and a flow rate of 0.40 ml/min with ultraviolet (UV) detection at 286 nm as validated and described in Chapter III.

The HPLC system used in the analysis of taxifolin was a Shimadzu HPLC (Kyoto, Japan), consisting of an LC-10ATVP pump, a SIL-10AF auto injector, a SPD-M10A VP UV/VIS spectrophotometric diodearray detector, and a SCL-10A VP system controller. Data collection and integration were accomplished using Shimadzu EZ Start 7.1.1 SP1 software. The analytical column used was a Chiralcel® OJ-RH column (150mm × 4.6mm i.d., 5-µm particle size, Chiral Technologies Inc., Exton, PA, USA) protected by a Chiralcel® OJ-RH guard column (0.4cm x 1cm, 5-µm particle size, Chiral Technologies Inc., Exton, PA, USA). The mobile phase consisted of acetonitrile, water, and phosphoric acid (15:85:0.5, v/v/v), filtered and degassed under reduced pressure prior to use. Separation was carried out isocratically at 25 ± 1°C and a flow rate of 0.35 ml/min with ultraviolet (UV) detection at 288 nm as validated and described in Chapter IV.

5.3.4 Jugular Vein Cannulation Surgery

Cannulas were prepared by immersing a 2 cm segment of Silastic® tubing in halothane for about 30 seconds to expand the tubing. A 25 cm length of single lumen PE 50 tubing was then inserted into the internal diameter of the Silastic® tubing. A 10 cm black silk surgical suture was tied at the conjunction of the two tubings and fixed in place with super glue.

Each rat (average body weight = 0.25 kg) was anaesthetized using halothane, secured to the bench in dorsal recumbency with adhesive medical tape, and positioned as straight as possible with the forelimbs at 90° angles to the spine; administration of the anesthetic plus

oxygen continued throughout the surgical procedure using an anesthetic vaporizer and a regulator. The front limbs were fully extended which caused the anterior border of the pectoral muscle to restrict venous return in the jugular vein, facilitated visualization, and produced jugular vein distention. To ensure that surgical plane of anesthesia was maintained rats were constantly monitored by toe pinch (pedal) reflex, respiratory rate, and color of mucous membranes. The inferred area of the jugular vein was shaved clean to the skin and sanitized thoroughly with sterile alcohol pads. A small incision was made in the skin above the vein with operating scissors. The subcutaneous fat was teased open using two microdissecting forceps to expose the jugular vein. Two segments of silk surgical suture were pulled underneath the vein by #7 Dumont tweezers, one close to the cephalic region, and the other one close to the cardiac region. The silk surgical suture close to the cephalic region was advanced towards the head, tied off, fastened, and the two ends were taped against the bench in order to minimize blood flow from the head. The silk surgical suture close to the cardiac region was pulled towards the abdomen and anchored using a hemostat to ensure patency of the vein; a small nick in the jugular vein was carefully made using a pair of long vannas scissors (8 cm) and two ends of a pair of Dumont tweezers were inserted into the vein through the nick. Another pair of #7 Dumont tweezers was used to hold the cannula; the Silastic® tubing end of the cannula was then inserted into the vein through the opening of the two ends of the inserted tweezers and was advanced gently into the vein towards the heart; once the cannula reached the trunk of the vein a small drop of blood usually appeared in the hub of the cannula. Saline solution was used to keep the incision moist during the insertion. After the insertion of the cannula, the jugular blood flow was evaluated using saline solution to verify it was properly positioned in the vein. Once the cannula was positioned, the silk surgical suture

held by the hemostat was used to tie up the cannula to the jugular vein. Excess silk surgical suture was cut from both segments. Next, a small incision was made in the dorsal epidermis of the rat; an 18-gauge needle was advanced under the skin and out of the incision area on the anterior scapula of the animal. The PE 50 end of the cannula was externalized through the internal diameter of the needle and out from the dorsal skin. Small sections of modified PE 190 and PE 90 were used to anchor the cannula to the dorsal skin using super glue to hold them in place. The cannula was then shortened (~20 cm); flexible plastic tubing was attached to the external end of the cannula with super glue and blocked by a 23-gauge needle with saline to prevent bleeding (**Fig. 5.1**). The incision area was then closed using clear surgical sutures and the rat was placed in the metabolic cage to recover overnight. Rats were given free access to water; but food was removed during recovery.
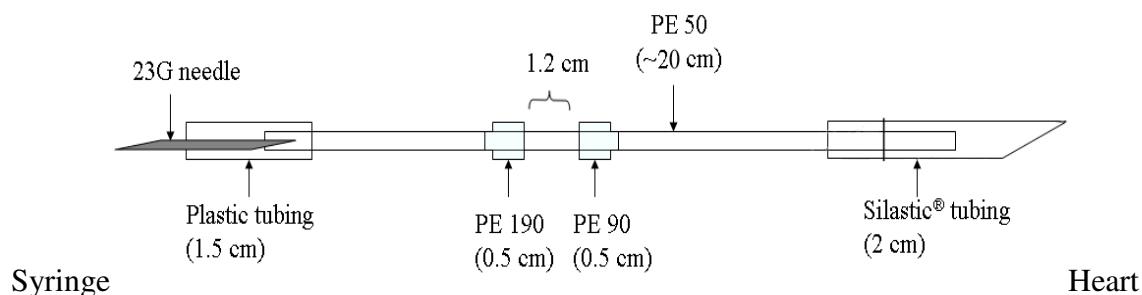
Figure 5.1. Scheme of a cannula. The Silastic® tubing is inserted through the jugular vein into the heart. The cannula is fixed to the dorsal skin of the rat with PE 190 (external anchor) and PE 90 (internal anchor) segments. The plastic tubing in the external end protects the cannula from rupture caused by the needle used to close it.

5.3.5 Pharmacokinetic Experimental Design

Twelve (12) male Sprague-Dawley rats (average weight: 300 g) were cannulated as described in Section 5.3.4. Each animal was placed in separate metabolic cages, allowed to recover overnight, and fasted for 12 hours before dosing. On the first day of the experiment,

the animal was dosed intravenously with racemic homoeriodicytol (10 mg/kg), racemic isosakuranetin (10 mg/kg) or racemic taxifolin (40 mg/kg) dissolved in PEG 600 and 2% DMSO.

Serial blood samples (0.50 ml) were collected in 2 ml eppendorf tubes after homoeriodicytol, isosakuranetin, and taxifolin administration at 0, 1, and 30 minutes, and 1, 2, 4, 6, 24, 48, 72, and 96 hours. Whole blood samples were centrifuged to obtain serum (0.1 ml duplicates) at each time point and serum was stored at –20°C. After each sample collection, the cannula was flushed with 0.50 ml of saline solution.

Similarly, urine samples were collected in 15 ml conical tubes after homoeriodicytol, isosakuranetin, and taxifolin administration at 0, 2, 4, 6, 12, 24, 48, 72, and 96 hours. 0.1 ml duplicate samples of urine were collected in 2 ml eppendorf tubes and stored at –20°C.

Serum and urine samples (0.1 ml) were prepared as described in Chapters II – IV. Subsequently, one sample from each of the duplicates at all time points for serum and urine was treated with or without 40.0 µl of 500 U/ml β-glucuronidase from *E. coli* Type IX-A. The serum and urine duplicates treated with β-glucuronidase were then incubated at 37°C for 2 hours to liberate glucuronide conjugates [149]. These samples were evaporated under compressed nitrogen gas using an analytical evaporator after the addition of the respective internal standard: indoprofen for homoeriodicytol samples, 7-ethoxycoumarin for isosakuranetin samples, and 2-thiobarbituric acid for taxifolin samples. The residue was reconstituted with 200.0 µl of the corresponding mobile phase, vortexed for 30 seconds and centrifuged at 5,000 rpm for 5 minutes. The supernatant was transferred to HPLC vials and 150.0 µl of sample was injected into the respective HPLC system.

5.3.6 Data Analysis

Pharmacokinetic analysis was performed using data from individual rats for which the mean and standard error of the mean (S.E.M.) were calculated for each group. The elimination rate constant (k_E) was estimated by linear regression of the serum concentrations in the log-linear terminal phase. In order to estimate the serum concentrations (C_0) immediately after racemic homoeriodicytol, isosakuranetin, and taxifolin IV dosing, a two-compartmental model was fitted to the serum concentration versus time data using WinNonlin® software (Version 5.2). The estimated C_0 was then used with the actual measured serum concentrations to determine the area under the serum concentration-time curve (AUC). The AUC_{0-INF} was calculated using the combined log-linear trapezoidal data from time of dosing to the last measured concentration, plus the quotient of the last measured concentration divided by the rate constant (K_E). Non-compartmental pharmacokinetic methods were used to calculate mean residence time (MRT, by dividing $AUMC_{0-INF}$ by AUC_{0-INF}), total clearance (CL_T, by dividing dose by AUC_{0-INF}) and volume of distribution (V_{SS} by dividing CL_T by K_E). The half-lives ($t\frac{1}{2}$) for serum and urine were calculated using the following equation: $t\frac{1}{2} = 0.963/K_E$. Data were expressed as the mean ± S.E.M. of replicate determinations.

5.4   RESULTS AND DISCUSSION

Linearity in the standard curves was demonstrated in serum and urine samples from homoeriodictyol, isosakuranetin, and taxifolin over the concentration range studied. In addition, chromatographs were free of interference from endogenous components. Samples incubated with β-glucuronidase from *Escherichia coli* type IX-A demonstrated the presence of at least one glucuronidated metabolite based on the increase in the concentrations of homoeriodictyol, isosakuranetin and taxifolin in the aglycone form following enzymatic

hydrolysis. This was assessed using the validated HPLC methods described in Chapter II through IV.

Serum was analyzed because the concentrations in the blood compartment of homoeriodictyol, isosakuranetin, and taxifolin are reflective of the concentrations at the sites where these compounds may show pharmacological activity. The non-invasiveness of blood sampling compared to sampling at the effect site makes it a preferred method of pharmacokinetic analysis. Urine was also analyzed since it can be easily collected and can provide important pharmacokinetic information such as rate of elimination constant (k_E), half-life ($t\frac{1}{2}$), and fraction excreted unchanged in urine (f_e).

5.4.1 Homoeriodictyol Serum Disposition

The HPLC method described in Chapter II has been applied to the determination of homoeriodicytol enantiomers in pharmacokinetic studies in rats (n = 4). Homoeriodictyol has previously been demonstrated to be detectable in serum after administration to animals [32]; however, no stereospecific analysis data has previously been reported.

Following administration of homoeriodicytol intravenously (10 mg/kg), the serum disposition was examined (**Fig. 5.2**). Homoeriodictyol enantiomers were detected in serum primarily as glucuro-conjugates, and the R(+)-homoeriodicytol conjugated and non-conjugated forms were predominant in serum at all time points examined. The serum concentration vs. time profile observed for the non-conjugated forms of homoeriodicytol enantiomers demonstrated stereoselective disposition since R(+)-homoeriodicytol was found in slightly higher concentrations than S(-)-homoeriodicytol. The serum concentration-time profiles for the two enantiomers of homoeriodicytol were characterized by a rapid decline in

concentrations, representing a distribution phase within the first 30 minutes followed by an increase at 1 hour and a rapid elimination phase up to 4 hours. Even though serum samples were collected and analyzed up to 120 hours, detection in serum was possible only up to 4 hours post-dose.

The serum concentration-time profiles of both homoeriodicytol enantiomers follow a biexponential pattern which suggests that the compounds follow a multi-compartment model. A two-compartment open model presents a serum concentration-time curve with two distinct phases: a distribution phase and an elimination phase. The distribution phase represents an initial, more rapid decline of drug from the central compartment into the tissue compartment. Conversely, the elimination phase represents the decline in parallel of serum and tissue concentrations [150]. In addition, a visible secondary peak in the serum drug-concentration time curve suggests the possibility of enterohepatic recirculation as has been demonstrated for other xenobiotics such as morphine, indomethacin, etc [150].

After systemic administration a drug or its metabolite may be secreted into bile and excreted into the duodenum. Subsequently, the drug/metabolite may be excreted in the feces or the drug may be enterically reabsorbed in the ileum and become systematically available [150]. When reabsorbed, the drug is said to enter enterohepatic recirculation. Hydrolysis in the intestine may convert the drug excreted as a metabolite, i.e. glucuronide conjugates, back into the parent drug in the gastrointestinal tract by the action of β-glucuronidases which are naturally present in intestinal bacteria such as *E. coli*. As a consequence, the parent drug becomes available for reabsorption and this futile cycle is referred to as entero-hepatic circulation. Drugs with molecular weights of 300 – 500 g /mol, like homoeriodicytol (MW 302.27 g/mol), can be excreted both in urine and bile. These drugs because of there free

hydroxyl moieties are often conjugated by phase II metabolism and subsequently excreted as glucuronide metabolites which increase their polarity and molecular weight by nearly 200 g /mol. Biliary excreted-drug is then reabsorbed systematically from the gastrointestinal (GI) tract producing a secondary peak in the serum concentration versus time profile.

Metabolites may have pharmacological and/or adverse activities; therefore, it is important to study metabolite disposition. The glucuronidated metabolites of homoeriodicytol exhibit serum concentration-time profiles that suggest stereospecific differences since R(+)-homoeriodicytol demonstrates higher concentrations than S(-)-homoeriodicytol. Similar to the parent compounds, the glucuronidated metabolites also appear to experience entero-hepatic recirculation due to a peak in the serum concentration-time profile at 1 hour (**Fig. 5.2**).
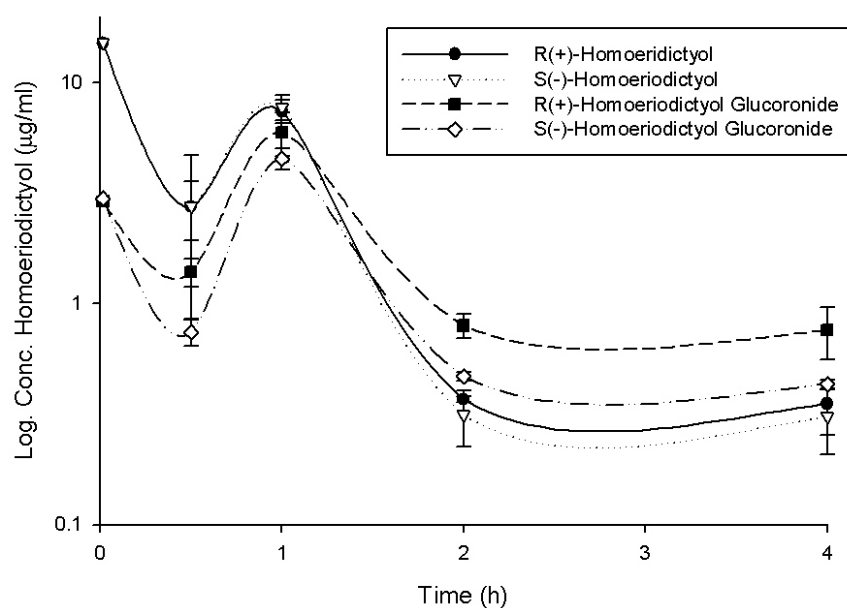
Figure 5.2. Disposition in serum of R(+)- and S(-)-homoeriodicytol and the corresponding glucuro-conjugates following administration of (+/-)-homoeriodicytol (10 mg/kg) to rats (n = 4, mean ± S.E.M.).

5.4.2 Homoeriodictyol Urinary Excretion

The HPLC method described in Chapter II was also applied to the stereospecific determination of homoeriodicytol in the urinary excretion study in rats (n = 4). Following IV administration of racemic homoeriodicytol (10 mg/kg), the R(+)- and S(-)- enantiomeric forms were detected in urine primarily as glucuro-conjugates, and R(+)-homoeriodicytol (conjugated and non-conjugated) was predominant in urine as it was in serum (**Fig 5.3**). The total amount excreted in urine over time profiles for R(+)- and S(-)-homoeriodicytol suggest stereospecific differences and were characterized by a rapid increase in concentrations. R(+)-homoeriodicytol was detected at significantly higher concentrations than S(-)-homoeriodicytol.

The cumulative total amount excreted in urine versus time plot demonstrated the predominance of homoeriodicytol glucuronides for both enantiomeric forms over the non-conjugated forms suggesting extensive phase II metabolism. During metabolism, lipophilic compounds may be converted into more readily excreted polar metabolites. During phase I metabolism, polar metabolites are formed by oxidation, reduction, hydrolysis, cyclization, and decyclization. Usually phase II metabolism follows phase I metabolism and is characterized by conjugation reactions that result in products of higher molecular weight that are more easily excreted from the body.

R(+)-homoeriodicytol glucuronide has higher concentrations that S(-)-homoeriodicytol glucuronide in urine at all point times examined. This suggests that the homoeriodicytol glucuronidated metabolites in urine demonstrate stereoselective excretion similar to the non-conjugated forms.
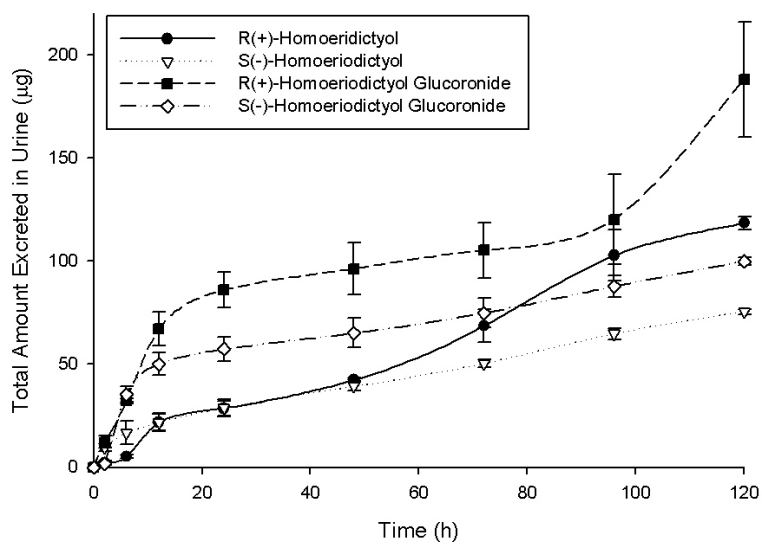
Figure 5.3. Total amount excreted in urine of R(+)- and S(-)-homoeriodicytol and its glucuro-conjugates following administration of (+/-)-homoeriodicytol (10 mg/kg) to rats (n = 4, mean ± S.E.M.).

The rate of urinary excretion-time plot was also obtained from urine, and R(+)-homoeriodicytol in the conjugated and non-conjugated forms were predominant as previously demonstrated in the serum concentration-time plot and the total amount excreted in urine-time plot (**Fig. 5.4**). The rate of urinary excretion-time plot demonstrated stereospecific differences between R(+)-homoeriodicytol and S(-)-homoeriodicytol since R(+)-homoeriodicytol exhibited a higher rate of excretion. The rate of urinary excretion-time profiles of R(+)- and S(-)-homoeriodicytol were characterized by an increase in the rate of excretion at 4 hours followed by a rapid decline up to 108 hours.

The glucuronidated metabolites of homoeriodicytol exhibit a rate of urinary excretion-time profile that suggest stereoselective excretion similar to the non-conjugated forms since R(+)-homoeriodicytol glucuronide exhibits higher concentrations than S(-)-homoeriodicytol glucuronide at all time points. Despite the differences in solubility and lipophilicity of

homoeriodicytol enantiomers and their glucuronidated metabolites, it can be observed that both of these compounds have similar rates of excretion (**Fig. 5.4**). This similarity indicates that homoeriodicytol enantiomers and the respective glucuronides undergo similar apparent elimination (parallel lines) and suggest that the metabolites are formation-rate limited.
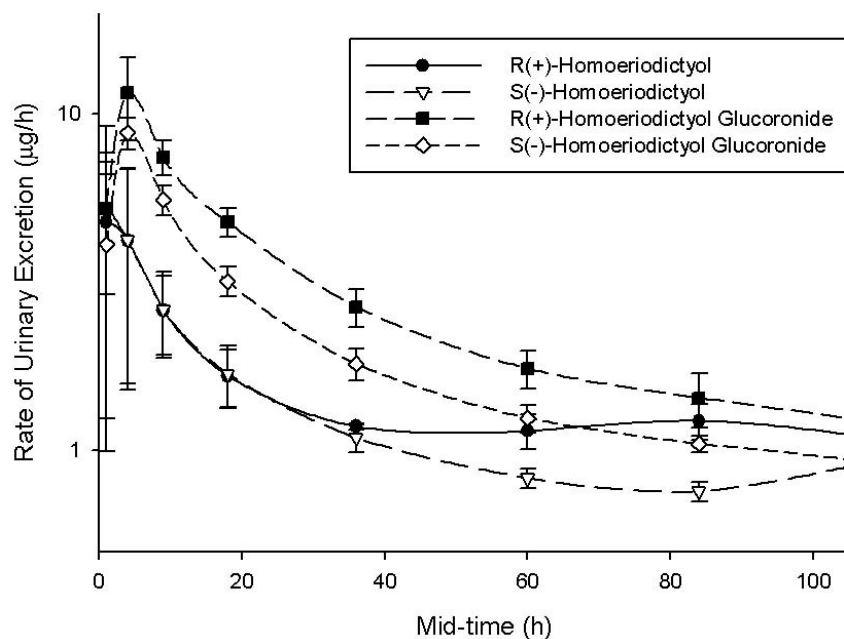
Figure 5.4. Rate of urinary excretion plot of R(+)-homoeriodicytol, S(-)-homoeriodicytol and their respective glucuronides after i.v. administration of (+/-)-homoeriodicytol (10 mg/kg) to rats (n = 4, mean ± S.E.M.)

5.4.3 Homoeriodictyol Pharmacokinetics

After serum and urine were analyzed using the validated HPLC method for homoeriodicytol described in Chapter II, the pharmacokinetic parameters were determined using a pharmacokinetic software (WinNonlin software Version 5.2). The area under the curve (AUC_{0-INF}), volume of distribution (V_{SS}), total clearance (CL_T), serum half-life ($t\frac{1}{2}$), and rate of elimination constant (k_E) were obtained from serum, whereas, the urine half-life

(t½), rate of elimination constant (k_E) and fraction excreted unchanged in urine (f_e) were obtained from urine. Differences were observed for the t½ values obtained from serum and urine; therefore, discrepancies in the k_E values ($k_E = 0.693/t½$) were also observed. This discrepancy in half-life values for serum and urine suggest that half-life is likely significantly underestimated in serum and this may be related to assay sensitivity limits of homoeriodicytol in serum and thus poor approximation of the true terminal half-life in serum. Previous studies have demonstrated underestimation of plasma half-life due to assay sensitivity limits of procainamide [151]. Furthermore, homoeriodicytol was measured up to only 4 hours in serum; whereas, in urine it was measured up to 120 hours. Thus, it is evident that urine is a far better biological fluid to utilize in the determination of homoeriodicytol pharmacokinetic parameters because of the limit of assay sensitivity in serum of our HPLC method. Similar findings have been reported for other flavonoids and stilbenes including naringenin [152], pterostilbene [153] and sakuranetin [154].

Therefore, the pharmacokinetic parameters of homoeriodicytol enantiomers determined by employing the k_E from urine were calculated (**Table 5.1**). Non-compartmental analysis demonstrated differences in some pharmacokinetic parameters between R(+)-homoeriodicytol and S(-)-homoeriodicytol. Compared to the values obtained using the k_E from urine, the use of serum k_E in calculating pharmacokinetic parameters produces a significant underestimation of AUC_{0-INF}, and half-life; whereas, clearance, extraction ratio, and k_E were overestimated. For that reason, the pharmacokinetic parameters obtained using k_E from urine are suggested to be more reliable for homoeriodicytol than the serum values. Thus, R(+)-homoeriodicytol and S(-)-homoeriodicytol have long half-lives (t½ = $0.693/k_E$, 42.25 ± 6.57 h, and 47.62 ± 6.14 h, respectively) which represent the time they remain in the body.

The average blood volume and total body water volume of a 0.25 kg rat are 13.5 ml and 167 ml, respectively. This translates into a blood volume of 0.054 L/kg and a total water volume of 0.668 L/kg. These values are important in the interpretation of volume of distribution ($V_{SS} = CL_T/k_E$). The extent of distribution of xenobiotics is determined by the partitioning across various membranes, and the binding to tissue and blood components. Physiological volumes of different compartments relative to the body weight (BW) are important in the understanding of the extent of distribution. If a xenobiotic has a V_{SS} close to 4% BW, it is said to remain in the vascular tissue, if the V_{SS} is close to 13% BW, it is said to be in the extracellular compartment, and if the V_{SS} is close to 41%, then it has reached the intracellular compartment. Thus, higher values of V_{SS} would represent greater penetration into tissues.

Table 5.1. Stereospecific pharmacokinetics of homoeriodicytol after IV administration in rats (10 mg/kg). k_E and t½ values from urine are included for comparison (n = 4, mean ± S.E.M.). a, $P < 0.05$, R(+) vs. S(-).

Pharmaceutical Parameter	Units	R(+)-Homoeriodictyol	S(-)-Homoeriodictyol
k_E urine	h^{-1}	1.64E-02 ± 2.34E-03	1.46E-02 ± 1.34E-03
(k_E serum)	(h^{-1})	(6.23E-02 ± 0.01)	(6.52E-02 ± 0.01)
AUC_{0-INF}	µg×h/ml	941.89 ± 100.11	1140.83 ± 117.12
f_{e-u}	%	6.30E-03 ± 6.34E-04	5.31 ± 0.45[a]
f_{e-g}	%	0.57 ± 0.07	0.79 ± 0.11[a]
CL_T	L/h/kg	5.31E-03 ± 1.93E-04[a]	4.38E-03 ± 6.12E-04
CL_R	L/h/kg	3.34E-07 ± 5.00E-08	2.33E-04 ± 3.21E-05[a]
CL_H	L/h/kg	5.31E-03 ± 1.38E-04[a]	4.15E-03 ± 1.46E-04
V_{SS}	L/kg	0.32 ± 0.03	0.30 ± 0.04
t½ urine	h	42.25 ± 6.57	47.62 ± 6.14
(t½ serum)	(h)	(11.12 ± 1.57)	(10.63 ± 1.45)
ER	-	2.97E-02 ± 4.40E-03	2.32E-02 ± 3.40E-03

The V_{SS} values reported for R(+)-homoeriodicytol and S(-)-homoeriodicytol are 0.32 ± 0.03 L/kg and 0.30 ± 0.04, respectively. These values are 5.9-fold and 5.5-fold higher than the blood volume (0.054 L/kg) and lower than the total water volume (0.668 L/kg), representing 47% and 45% of the total water volume, respectively. This findings suggest that R(+)- and S(-)-homoeriodicytol exit the vascular circulation and are extensively distributed into tissues. This preferential distribution into tissues may be due to the relative lipophilicity of homoeriodicytol (XLogP = 1.1).

The area under the curve, ($AUC_{0\text{-}INF}$ = (C_0/k_E)/(C_{last}/k_E), where C0: initial concentration, Clast: concentration at last time point) which represents the overall amount of drug in the blood compartment, is higher for S(-)-homoeriodicytol compared to R(+)-homoeridictyol (941.89 ± 100.11 µg×h/ml and 1140.83 ± 117.12 µg×h/ml, respectively). Conversely, the total clearance (CL_T = Dose/$AUC_{0\text{-}INF}$) was higher for R(+)-homoeriodicytol (CL_T = 5.31E-03 ± 1.93E-04 L/h/kg) compared to S(-)-homoeriodicytol (4.38E-03 ± 6.12E-04 L/h/kg).

The fraction excreted unchanged in urine ($f_{e\text{-}u}$) represents the percentage of R(+)- or S(-)-homoeriodicytol excreted in urine in the non-conjugated form. The fraction of glucuro-conjugate excreted in urine ($f_{e\text{-}g}$) represents the percentage of glucuronidated metabolites excreted in urine. S(-)-homoeriodicytol and its glucuronidated form are excreted more readily in urine (5.31% ± 0.45, and 0.79% ± 0.11, respectively) than R(+)-homoeridictyol and its glucuro-conjugate. Nevertheless, the renal clearance (CL_R = CL_T × f_e) is lower than the hepatic clearance (CL_H = CL_T – CL_R, assuming that non-renal = hepatic) for both R(+)- and S(-)-homoeridictyol.

The glomerular filtration rate (GFR) of a 0.25 kg rat was reported to be 0.31 L/h/kg [155]. The GFR is an important facet in renal clearance. The fraction unbound in plasma (f_{u-p} = $C_{unbound}/C_{total}$) represents the percentage of xenobiotics in the blood that are not bound to plasma proteins. When renal clearance (CL_R) is equal to GFR $\times$ f_{u-p}, CL_R occurs mainly by filtration. If CL_R is greater than GFR $\times$ f_{u-p}, tubular secretion is mostly responsible for clearance by the kidneys. Finally if CL_R is lower than GFR $\times$ f_{u-p}, tubular reabsorption is said to occur [150]. If f_{u-p} values were available for any homoeriodicytol, isosakuranetin or taxifolin stereoisomers, more information about the pathway of CL_R may be obtainable [156,157].

Davies and Morris reported the mean hepatic blood flow (Q) for 0.25 kg rats to be 3.31 L/h/kg and an hematocrit (Hc) of 0.46 [155] which yields a mean hepatic plasma flow of 1.79 L/h/kg (Plasma flow = Q $\times$ (1 – Hc) [158]). This value is important in order to understand hepatic clearance. The extraction ratio (ER = CL_H/Q_H) is a rough estimation of liver extraction and can be low (0 – 0.3), intermediate (0.3 – 0.7), or high (0.7 – 1.0). Hepatic clearance (CL_H) for R(+)-homoeriodicytol and S(-)-homoeriodicytol correspond to 5.31E-03 ± 1.38E-04 L/h/kg and 4.15E-03 ± 1.46E-04 L/h/kg, respectively (**Table 5.1**) each representing 0.2% of the hepatic plasma flow (1.79 L/h/kg). The ER for both R(+)- and S(-)-homoeridictyol are <0.3. Therefore, these findings suggest that R(+)-homoeriodicytol and S(-)-homoeriodicytol are low hepatic extraction compounds.

Previous studies have reported homoeriodicytol mainly as a metabolite of other flavonoids administered to rats. Booth *et. al.* reported the formation of homoeriodicytol as a metabolite after administration of eriodictyol through a stomach tube [31]. After administration of 300 mg/rat of eriodictyol, *m*-hydroxyphenylpropionic acid (*m*-HPPA), *m*-

coumaric acid, eriodictyol glucuronide and homoeriodicytol were detected in urine. It was suggested that methylation of the 3'-hydroxyl group in eriodictyol resulted in the formation of homoeriodicytol by the rat liver. Then, homoeriodicytol (150 mg/rat) was also administered through a stomach tube, and *m*-HPPA, homoeriodicytol glucuronide, homoeriodicytol, *m*-coumaric acid and hydroferulic acid were detected in urine [31]. These findings confirmed that homoeriodicytol is absorbed from the intestinal tract and that cleavage of ring C in the flavonoid structure was responsible for the formation of *m*-HPPA after administration of homoeriodicytol and eriodictyol.

Homoeriodictyol was also reported as a metabolite after the administration of eriocitrin to rats [30]. Eriocitrin (75 µmol/kg) was administered through gastric intubation; and eriodictyol, homoeriodicytol and hesperetin in their conjugated forms were detected in plasma up to 4 hours. Detection of the non-conjugated forms was not possible in plasma. In contrast, the non-conjugated and conjugated forms of eriodictyol, homoeriodicytol and hesperetin were detected in urine after the administration of eriocitrin (50 µmol/kg) up to 24 hours [30]. These findings support the results presented in this thesis that urine is a better matrix for pharmacokinetic studies of homoeriodicytol. It was suggested that eriocitrin is transformed by the liver into eriodictyol, which in turn is converted into homoeriodicytol by methylation of its 3'-hydroxyl group.

Matsumoto *et. al.* also reported homoeriodicytol as a metabolite after the administration of hesperidin to rats [29]. After oral administration of hesperidin (100 mg/kg) mainly glucuronides of hesperetin were detected (hesperetin-7-O-β-glucuronide and hesperetin-3'-O-β-glucuronide), but homoeriodicytol conjugates were also found in plasma up to 24 hours. Homoeriodictyol conjugates were mainly in the glucuronidated form; even

though homoeriodicytol-sulfates were also found. Homoeriodictyol in the conjugated form reached a peak at 6 hours in plasma after oral administration of hesperidin. This discrepancy in the time at which a peak concentration is attained in plasma (6 h vs. 1h) may be due to the fact that hesperidin undergoes deglycosilation, demethylation, remethylation, and glucuronidation in the liver to form homoeriodicytol conjugates. Hesperidin is demethylated into eriodictyol which in turn is methylated to form homoeriodicytol.

Previous studies of the pharmacokinetics of homoeriodicytol in rats have not considered the stereochemistry of this compound. Homoeriodictyol has been reported to distribute mainly to the kidneys (10.93 ± 2.92 µg/g) and liver (1.98 ± µg/g) in rats [32] immediately after (0.083 h) the administration of homoeriodicytol (13.2 mg/kg) to rats. After 1h, however, homoeriodicytol was preferentially distributed in kidney and stomach (1.03 ± 0.87 µg/ml, and 0.42 ± 0.20 µg/g, respectively). These findings support the assertion of enterohepatic recycling proposed for homoeriodicytol. Hydrolysis may convert the homoeriodicytol glucuronide back into the parent compound in the GI tract by the action of β-glucuronidases in intestinal bacteria [150]. Zhao *et. al.* also reported better recovery (92.8%) from urine compared to tissues [18,32] and plasma [18] which support the findings in this thesis that propose urine as the most appropriate matrices for quantitative analysis.

The amount of administered dose of drug that is converted into metabolites can be calculated if the metabolite clearance (CL_M) is known. In order to estimate CL_M, the administration of the metabolite orally is necessary. Homoeriodictyol-7-O-β-D-glucopyranoside (HEDT-Glu), a metabolite of homoeriodicytol, was administered to rats (13.2 mg/kg) and was reported to distribute to the liver and the small intestine [18]. The chemical structure of glucopyranoside and glucuronide conjugates of homoeriodicytol differ

only in the substitution attached to C-2' (–CH$_2$OH and –COOH, respectively). After I.V. administration of HEDT-Glu (13.2 mg/kg) a biexponential pattern was observed [18], similar to what was reported for homoeriodicytol. The half-life was reported to be 1.27 ± 0.31 hours, the AUC was 16.04 ± 3.19 µg×h/ml, and the CL$_T$ was 0.85 ± 0.17 L/h/kg. From this it can be derived that the amount of metabolite formed following a 13.2 mg/kg I.V. dose of homoeriodicytol [32] (CL$_M$ × AUC$_M$) is 13.63 mg/kg (uncorrected for molecular weight differences [159]). This indicates that HEDT-Glu is a major route of elimination of homoeriodicytol. Compared to homoeridictyol (MW = 302.27 g/mol, XLogP = 1.1), HEDT-Glu is a larger molecule (MW = 596.53 g/mol), which is more hydrophilic (XLogP = - 0.7); therefore, differences in pharmacokinetic disposition are expected. Similar studies with the glucuro-conjugates of homoeriodicytol may allow the estimation of homoeriodicytol eliminated in this form.

In summary, the pharmacokinetics of homoeriodicytol reveals distribution, metabolism, and elimination that are dependent on the stereochemistry of the enantiomers. Both R(+)- and S(-)-homoeriodicytol have long half-lives, they distribute from the central compartment and penetrate into tissues. R(+)-homoeriodicytol and S(-)-homoeriodicytol are metabolized in the liver into glucuro-conjugates and are mainly cleared by non-renal routes. S(-)-homoeriodicytol excretion in the urine is stereospecific and higher than the R(+)-homoeriodicytol enantiomer.

5.4.4 Isosakuranetin Serum Disposition

The HPLC method described in Chapter III was applied to the study of isosakuranetin disposition in Sprague-Dawley rats (n = 4). Isosakuranetin has been previously detected in rat

serum after administration of naringin [65], but its stereospecific disposition has not been previously studied.

Following the IV administration of racemic isosakuranetin (10 mg/kg), serum disposition of 2S- and 2R-isosakuranetin was examined (**Fig. 5.5**). Isosakuranetin enantiomers were detectable in serum primarily as glucuroconjugates and 2S-isosakuranetin concentrations in the conjugated and non-conjugated forms were slightly higher in serum when compared to the 2R-enantiomer. The serum concentration vs. time profile observed for isosakuranetin does not demonstrate stereoselective disposition. Even though there are differences between the concentrations of 2S- and 2R-isosakuranetin in serum, the differences are not significant. The serum concentration-time profiles for both enantiomers of isosakuranetin show a steep decline in concentrations, representing a rapid distribution phase within the first half an hour post-dose.

The glucuronidated metabolites of isosakuranetin exhibit similar serum concentration-time profiles, which indicate lack of stereoselectivity. The serum concentration-time profiles of the glucuro-conjugates were characterized by a rapid decline in concentration within the first 30 minutes, representing a distribution phase, followed by an elimination phase up to 2 hours. Similar to the observation with homoeriodicytol, detection of isosakuranetin was possible only up to 0.5 hours for aglycones and 2 hours for glucuro-conjugates even though serum was collected and analyzed up to 120 hours. 2S-Isosakuranetin glucuronide showed slightly higher concentrations than the glucuronidated metabolite of the 2R-enantiomer although not statistically significant. The serum concentration-time profile of the glucuro-conjugates of isosakuranetin enantiomers follows a biexponential pattern which is not seen in the non-conjugated isosakuranetin profiles possibly due to the limit of assay sensitivity in

serum at low concentrations. Therefore, the analysis of the glucuro-conjugated metabolites was important to demonstrate that isosakuranetin follows a multicompartment model.
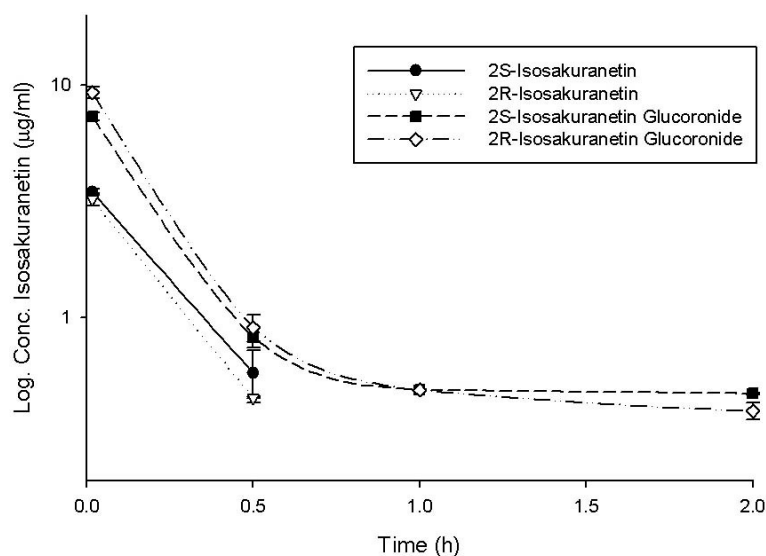
Figure 5.5. Disposition in serum of 2S- and 2R-isosakuranetin and the corresponding glucuro-conjugates following administration of (+/-)-isosakuranetin (10 mg/kg) to rats (n = 4, mean ± S.E.M.).

5.4.5 Isosakuranetin Urinary Excretion

The HPLC method was applied to the stereospecific determination of isosakuranetin in the urinary excretion study in rats (n = 4). Isosakuranetin enantiomers were detected in urine primarily as glucuro-conjugates following IV administration of racemic isosakuranetin (10 mg/kg). The cumulative total amount excreted in urine versus time plot demonstrated the predominance of isosakuranetin glucuronides for both enantiomeric forms over the aglycone form (**Fig. 5.6**) and 2S-isosakuranetin had higher concentrations in the conjugated and non-conjugated forms compared to 2R-isosakuranetin. The total amount excreted in urine-time profiles for 2S- and 2R-isosakuranetin suggest stereospecific differences and demonstrated a rapid increase in concentrations in urine over time. 2S-isosakuranetin showed slightly higher concentrations in urine compared to the 2R-enantiomer.
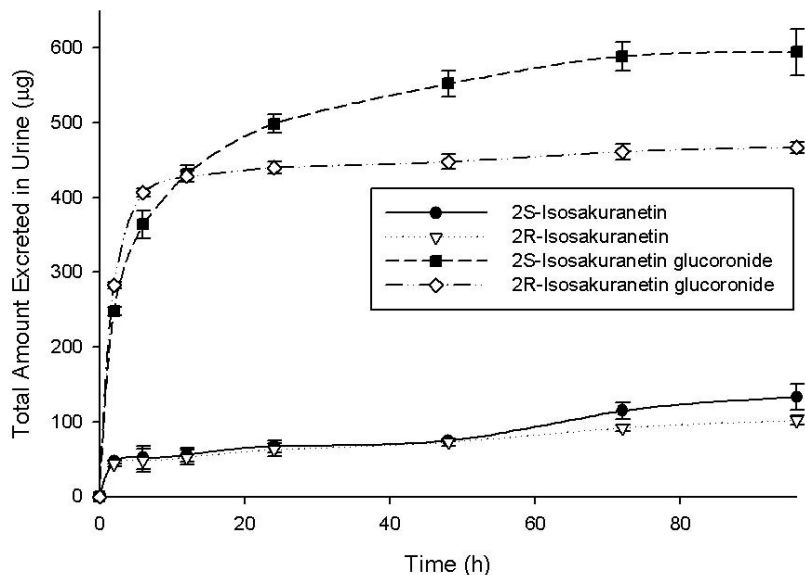
Figure 5.6. Total amount excreted in urine of 2S- and 2R-isosakuranetin and its glucuro-conjugates following administration of (+/-)-isosakuranetin (10 mg/kg) to rats (n = 4, mean ± S.E.M.).

In addition, the cumulative urinary excretion-time plot demonstrated the predominance of isosakuranetin glucuronides for the two enantiomeric forms, 2S and 2R, which indicates extensive phase II metabolism. 2S-isosakuranetin glucuronide was predominant in urine at all point times examined compared to 2R-isosakuranetin glucuronide suggesting that isosakuranetin glucuronides in urine are stereoselectively excreted. Conversely, differences in the rate of excretion in urine of the conjugated forms showed enantiospecific differences at 72 h and 96 h, but not earlier.

The rate of urinary excretion rate vs. time plot of the 2S and 2R enantiomers of isosakuranetin was also obtained from urine (**Fig. 5.7**). The rate of urinary excretion-time plots demonstrated stereospecific differences between 2S- and 2R-isosakuranetin after 36 h

that were not significantly significant. Likewise, in the case of the glucuro-conjugates, differences were not significant. However, the glucuronidated forms of 2S-isosakuranetin and 2R-isosakuranetin showed higher rate of excretion compared to the non-conjugated counterparts.
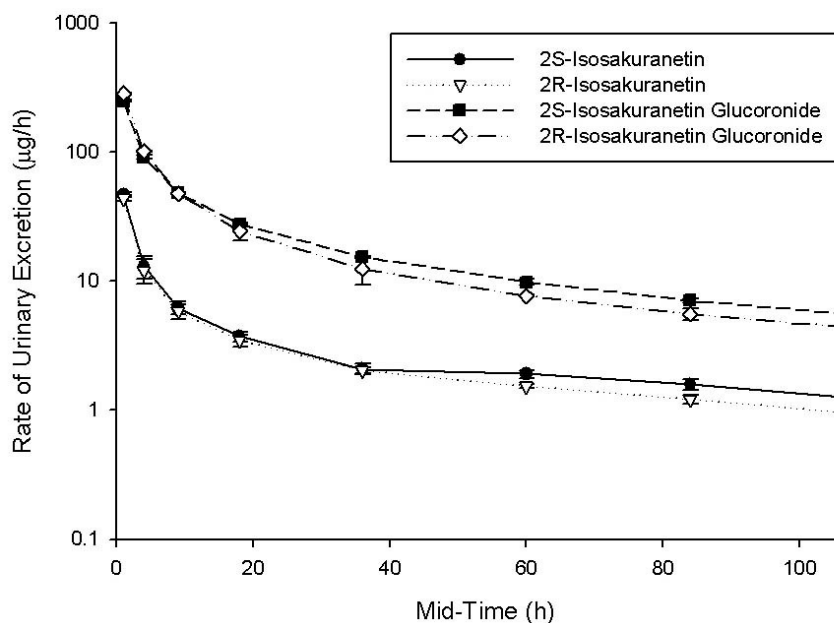
Figure 5.7. Rate of urinary excretion plot of 2R-isosakuranetin, 2S-isosakuranetin and their respective glucuronides after i.v. administration of (+/-)-isosakuranetin (10 mg/kg) to rats (n = 4, mean ± S.E.M.)

5.4.6 Isosakuranetin Pharmacokinetics

After serum and urine were analyzed, the pharmacokinetic parameters were determined. The $AUC_{0\text{-INF}}$, V_{SS}, CL_T, $t\frac{1}{2}$, and k_E were obtained from serum, and $t\frac{1}{2}$, k_E, and f_e were attained from urine. Similar to what was described for homoeriodicytol; differences were observed for the $t\frac{1}{2}$ of serum and urine, as well as for k_E values ($0.693/t\frac{1}{2}$). This might be due to assay sensitivity limits in serum as in the case of homoeriodicytol and other

flavonoids. In addition, isosakuranetin is detectable in serum up to 2 hours; while in urine, detection of isosakuranetin is possible up to 96 hours. These findings suggest that urine might be a better biological matrix for determining isosakuranetin pharmacokinetics.

Consequently, the pharmacokinetic parameters of isosakuranetin were calculated using the k_E from urine and are presented in **Table 5.2**. The non-compartmental analysis of 2S-isosakuranetin and 2R-isosakuranetin showed differences in some pharmacokinetic parameters. Compared to the pharmacokinetic parameters obtained from using the true k_E from urine, the use of serum in the estimation of pharmacokinetic parameters results in a considerable underestimation of $AUC_{0\text{-}INF}$, V_{SS}, and t½. Alternatively, clearance and ER were overestimated in serum.

Therefore, the pharmacokinetic parameters obtained from urine are believed to be more reliable than the serum values. Accordingly, 2S-isosakuranetin and 2R-isosakuranetin have long half-lives (43.29 ± 6.01 h and 29.07 ± 4.02 h, respectively) and high V_{SS} (**Table 5.2**). The V_{SS} of 2S-isosakuranetin (1.23 ± 0.17 L/kg) and 2R-isosakuranetin (1.27 ± 0.18 L/kg) are much higher than the total blood volume (0.054 L/kg) and total water volume (0.668 L/kg) [155], corresponding to 184% and 190% of the total water volume. This indicates that 2S and 2R-isosakuranetin exit the central compartment and are widely distributed into tissues. Like homoeriodicytol, isosakuranetin is also highly lipophilic (XLogP = 2.3) which might explain the preferential distribution into tissues and greater V_{SS} compared to homoeriodicytol.

The $AUC_{0\text{-}INF}$ was higher for 2S-isosakuranetin (253.06 ± 37.15 µg × h/ml) compared to 2R-isosakuranetin (165.71 ± 23.12 µg × h/ml); whereas CL_T was stereoselective form 2R-isosakuranetin. The $f_{e\text{-}u}$ values for 2S-isosakuranetin (8.81% ± 1.24) and 2R-isosakuranetin (6.75% ± 0.19) demonstrate that isosakuranetin in the 2S-configuration is more readily

excreted in urine than 2R-isosakuranetin. Conversely, isosakuranetin glucuro-conjugates are more readily eliminated in the 2R-configuration. The CL_R of 2R-isosakuranetin is higher than 2S-isosakuranetin (2.04E-03 ± 3.00E-04 L/h/kg and 1.74E-03 ± 2.16E-04 L/h/kg, respectively). Nevertheless, the CL_H of both 2S- and 2R-isosakuranetin are higher than the CL_R, suggesting that the two enantiomers are excreted mainly via non-renal routes.

Table 5.2. Stereospecific pharmacokinetics of isosakuranetin after IV administration in rats. The $t\frac{1}{2}$ and k_E from serum are presented for comparison (10 mg/kg) (n = 4, mean ± S.E.M.)

Pharmaceutical Parameter	Units	2S-Isosakuranetin	2R-Isosakuranetin
k_E urine	h^{-1}	1.60E-02 ± 2.40E-03	2.38E-02 ± 3.42E-03[a]
(k_E serum)	(h^{-1})	(3.74 ± 0.45)	(4.08 ± 0.34)
$AUC_{0\text{-INF}}$	µg×h/ml	253.06 ± 37.15	165.71 ± 23.12
$f_{e\text{-}u}$	%	8.81 ± 1.24	6.75 ± 0.99
$f_{e\text{-}g}$	%	0.36 ± 0.04	0.38 ± 0.05
CL_T	L/h/kg	1.98E-02 ± 1.43E-03	3.02E-02 ± 1.65E-03[a]
CL_R	L/h/kg	1.74E-03 ± 2.61E-04	2.04E-03 ± 3.00E-04
CL_H	L/h/kg	1.80E-02 ± 2.12E-03	2.81E-02 ± 2.45E-03[a]
V_{SS}	L/kg	1.23 ± 0.17	1.27 ± 0.18
$t\frac{1}{2}$ urine	h	43.29 ± 6.01[a]	29.07 ± 4.02
($t\frac{1}{2}$ serum)	(h)	(0.19 ± 0.01)	(0.17 ± 0.02)
ER	-	1.01E-02 ± 1.23E-03	1.57E-02 ± 2.12E-03[a]

2S-isosakuranetin and 2R-isosakuranetin are reported to have CL_H values (1.80E-02 ± 2.12E-03 L/h/kg and 2.81 ± 2.45E-03 L/h/kg, respectively) that are lower than the hepatic plasma flow in rats (1.79 L/h/kg). Similarly, the ER obtained from urine is low (<0.3). These results suggest that 2S- and 2R-isosakuranetin are low hepatic extraction compounds.

In summary, though isosakuranetin enantiomers have long half-lives, 2S-isosakuranetin remains in the body 1.5-fold longer than 2R-isosakuranetin. 2S-isosakuranetin and 2R-isosakuranetin exit the central compartment and penetrate deep into tissues. The

enantiomers of isosakuranetin are metabolized in the liver, where glucuro-conjugates are formed, and are excreted mainly via non-renal routes. 2S-isosakuranetin is more readily excreted in urine than the 2R-enantiomer.

Previous pharmacokinetic studies of isosakuranetin are limited and have not taken into consideration the chiral nature of isosakuranetin. The effect of cancer on flavonoid metabolism was studied in rats after the administration of naringin [65]. Naringenin conjugates mainly as glucuronides, as well as non-conjugates of hesperetin and isosakuranetin were detected in plasma, urine, liver and kidney. The concentration of naringenin in cancer-bearing rats was demonstrated to be lower than in healthy rats; however, no effect was seen for isosakuranetin or hesperetin in plasma concentrations. Isosakuranetin was described to derive from the hydroxylation of the C-3' in naringenin. Previous studies have described other flavonoids with chemical structures similar to isosakuranetin to be metabolized primarily in the liver [136].

5.4.7 Taxifolin Serum Disposition

The assay methodology described in Chapter IV was applied to the study of taxifolin disposition in Sprague-Dawley rats (n = 4). Taxifolin has been previously detected in human serum after the administration of pine bark extract in the racemic form, but the disposition of the stereoisomers of taxifolin has not been previously reported [134].

Following IV administration of racemic taxifolin (40 mg/kg), the serum disposition of taxifolin stereoisomers was examined (**Fig. 5.8**). Taxifolin stereoisomers were detected in serum mostly as glucuronidated metabolites. The serum concentration vs. time profiles of

(2S3R)-(+)-, (2S3S)-(-)-, (2R3R)-(+)-, and (2R3S)-(-)-taxifolin demonstrate stereoselective disposition and were characterized by a rapid decline in concentrations up to half an hour.

The glucuro-conjugated forms of (2S3R)-(+)-, (2S3S)-(-)-, (2R3R)-(+)-taxifolin showed a serum concentration-time profile with a biexponential pattern; a rapid decline in the first half an hour after I.V. administration (distribution phase), followed by a rapid elimination (elimination phase). On the other hand, a slight increase in concentration at 30 minutes was observed for the (2R3S)-(-)-taxifolin glucuronidated metabolite which suggests the possibility of enterohepatic recycling as observed previously for homoeriodicytol.
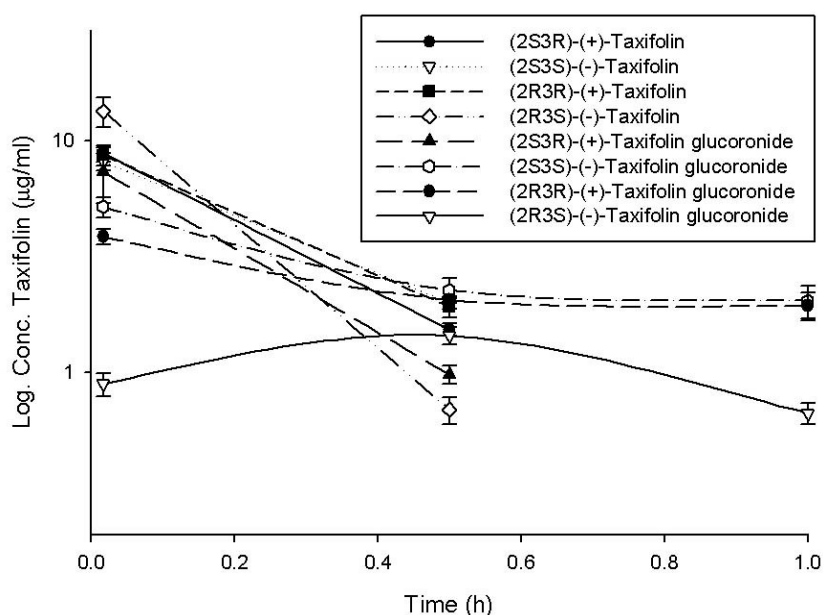
Figure 5.8. Disposition in serum of (2S3R)-(+)-, (2S3S)-(-)-, (2R3R)-(+)-, and (2R3S)-(-)-taxifolin and the corresponding glucuro-conjugates following administration of (+/-)-taxifolin (40 mg/kg) to rats (n = 4, mean ± S.E.M.)

Similar to what was observed for the isosakuranetin glucuronides, the taxifolin glucuronides showed a serum drug concentration curve characteristic of a multicompartamental model. This was not observed for the non-conjugated forms perhaps due to low assay sensitivity in serum. Although serum samples were collected and analyzed up to

120 hours, the stereoisomers of taxifolin were detectable only until 30 minutes post-dose in the non-conjugated forms, and at 1 hour post-dose for the glucuro-conjugated metabolites.

5.4.8 Taxifolin Urinary Excretion

The HPLC method described in Chapter IV was also applied to the stereospecific determination of taxifolin in the urinary excretion analysis in rats (n = 4). Taxifolin has been previously detected in human urine after the administration of pycnogenol [133]; however, no stereospecific analysis has been reported.

Following IV administration of racemic taxifolin (40 mg/kg), (2S3R)-(+)-, (2S3S)-(-)-, (2R3R)-(+)-, and (2R3S)-(-)-stereoisomers were detected in urine. The cumulative total amount excreted in urine versus time plots were characterized by a rapid increase in concentrations (**Fig. 5.9**) and suggested stereospecific differences for the four stereoisomers of taxifolin. (2S3R)-(+)-taxifolin was predominant over the other three stereoisomers in the conjugated and non-conjugated forms. However, unlike what was observed for homoeriodicytol and isosakuranetin, the non-conjugated form was predominant instead of the glucuro-conjugate. The stability of glucuronidated conjugates of taxifolin remains to be determined; some drugs have previously shown spontaneous hydrolysis of glucuro-conjugates, i.e. naproxen [160].

The cumulative total amount excreted in urine-time plot demonstrated that the glucuronides of the stereoisomers of taxifolin produced by phase II metabolism also exhibit stereoselective excretion (**Fig. 5.9**). The (2S3R)-(+)-taxifolin glucuronide was predominant, followed by the glucuro-conjugate metabolite of (2R3S)-(-)-taxifolin.
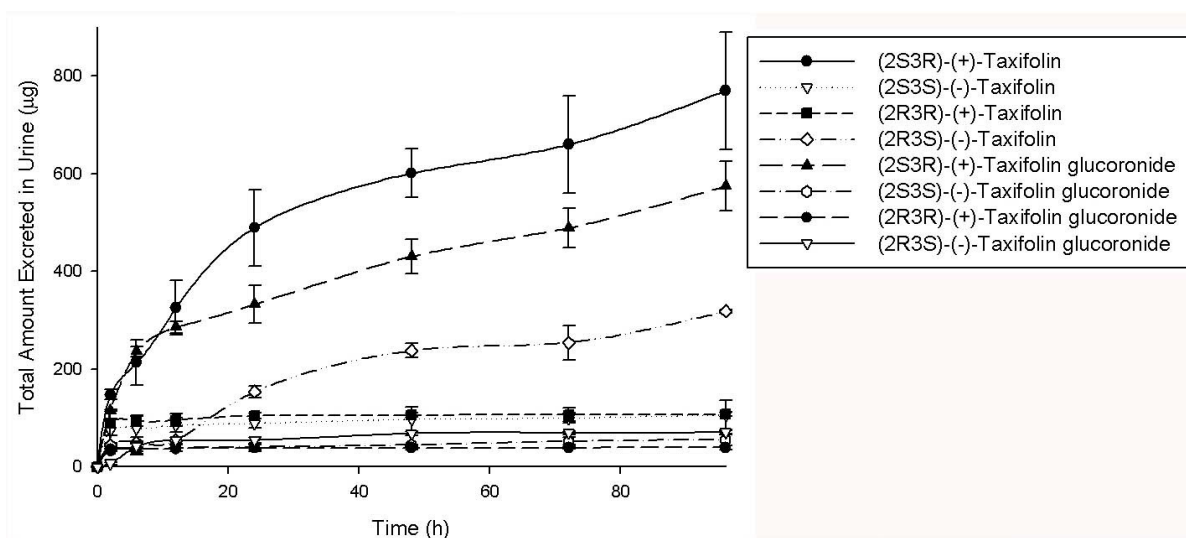
Figure 5.9. Total amount excreted in urine of (2S3R)-(+)-, (2S3S)-(-)-, (2R3R)-(+)-, and (2R3S)-(-)-taxifolin and its glucuro-conjugates following administration of (+/-)-taxifolin (40 mg/kg) to rats (n = 4, mean ± S.E.M.).

The rate of urinary excretion-time plot was also obtained from urine (**Fig 5.10**) and (2S3R)-(+)-taxifolin was predominant in the conjugated and non-conjugated forms. The rate of urinary excretion-time profile also demonstrated stereospecific differences between (2S3R)-(+)-, (2S3S)-(-)-, (2R3R)-(+)-, and (2R3S)-(-)-taxifolin since (2S3R)-(+)-taxifolin was more readily excreted than (2R3S)-(-)-, (2R3R)-(+)-, and (2R3S)-(-)-taxifolin. However, no significant differences were seen in the rate of excretion of (2S3S)-(-)-taxifolin and (2R3R)-(+)-taxifolin.

The rate of urinary excretion-time profiles of the glucuro-conjugates also showed stereospecific excretion. The (2S3R)-(+)-taxifolin glucuronide was more readily excreted than (2S3S)-(-)-, (2R3R)-(+)-, and (2R3S)-(-)-taxifolin glucuronides. Significant differences, however, were not seen among (2S3S)-(-)-taxifolin glucuronide, (2R3R)-(+)-taxifolin glucuronide, and (2R3S)-(-)-taxifolin glucuronide.
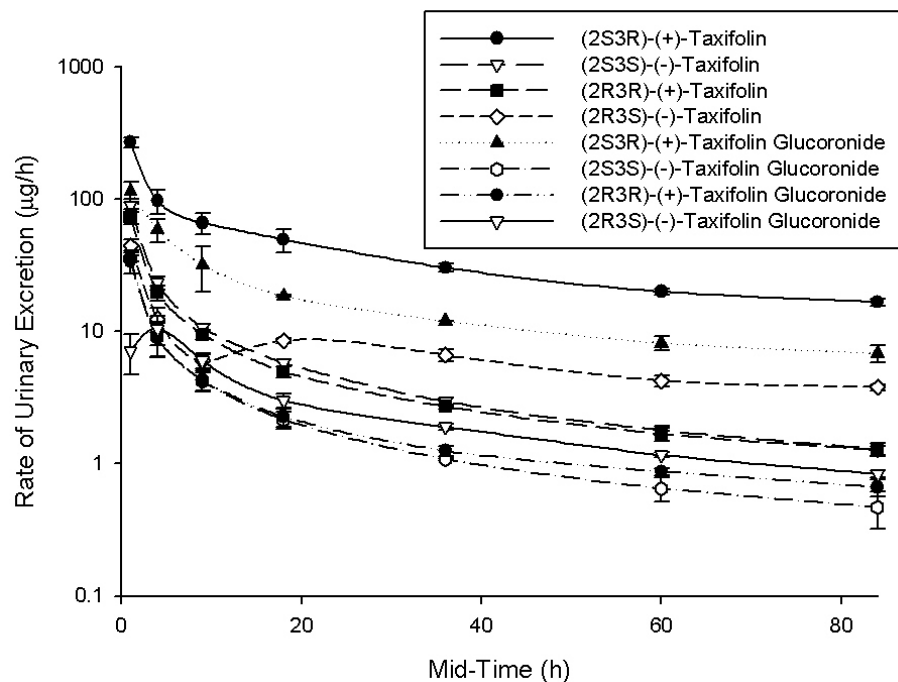
Figure 5.10. Rate of urinary excretion plot of (2S3R)-(+)-taxifolin, (2S3S)-(-)-taxifolin, (2R3R)-(+)-taxifolin, (2R3S)-(-)-taxifolin and their respective glucuronides after I.V. administration of (+/-)-homoeriodicytol (40 mg/kg) to rats (n = 4, mean ± S.E.M.)

5.4.9 Taxifolin Pharmacokinetics

After analyzing serum and urine using the validated HPLC method described in Chapter IV, the pharmacokinetic parameters were obtained. The AUC_{0-INF}, V_{SS}, CL_T, $t\frac{1}{2}$ and k_E were obtained from serum; $t\frac{1}{2}$, k_E and f_e were obtained from urine. Similar to what was reported for homoeriodicytol and isosakuranetin, when compared to the half-lives obtained from serum, the half-lives for all four stereoisomers of taxifolin obtained from urine were significantly higher.

The discrepancy in half-life values for serum and urine in taxifolin may suggest issues with the lack of assay sensitivity in serum; therefore, urine may be a better biological fluid for taxifolin pharmacokinetic studies. Therefore, the pharmacokinetic parameters of taxifolin

stereoisomers were calculated using the k_E from urine in the noncompartmental analysis (**Table 5.3**). When comparing values for the pharmacokinetic parameters calculated using k_E from serum and the k_E obtained from urine, the $AUC_{0\text{-}INF}$, and t½ are underestimated; whilst V_{SS}, clearance, and ER were overestimated. This indicates that similar to what was reported for homoeriodicytol, isosakuranetin, and other flavonoids the pharmacokinetic parameters obtained from urine may be a better estimate for taxifolin that the serum values.

Thus, (2S3R)-(+)-taxifolin (30.91 ± 4.29 h), (2S3R)-(-)-taxifolin (32.61 ± 2.89 h), (2R3R)-(+)-taxifolin (14.63 ± 4.79 h), and (2R3S)-(-)-taxifolin (31.73 ± 4.23 h) are reported to have long half-lives. The V_{SS} of (2S3R)-(+)-taxifolin (0.11 ± 0.01 L/kg), (2S3R)-(-)-taxifolin (1.76 ± 0.25 L/kg), (2R3R)-(+)-taxifolin (1.68 ± 0.24 L/kg), and (2R3S)-(-)-taxifolin (0.09 ± 0.01 L/kg) are higher than the blood volume (0.054 L/kg). However, (2S3R)-(-)- and (2R3S)-(+)-taxifolin have V_{SS} that are lower than the total water volume (0.668 L/kg), while (2S3S)-(-)- and (2R3R)-(+)-taxifolin are higher. The V_{SS} of (2S3R)-(+)-, (2S3S)-(-)-, (2R3R)-(+)-, and (2R3S)-(-)-taxifolin represent 16%, 263%, 251% and 13% of the total water volume, respectively. This indicates that the stereoisomers of taxifolin are differentially distributed in the body. (2S3R)-(+)-taxifolin is distributed intracellularly, (2R3S)-(-)-taxifolin distributes extracellularly, while (2S3S)-(-)- and (2R3R)-(+)-taxifolin are deeply distributed into tissues. These findings suggest that the stereoisomers of taxifolin exit the vascular system and are either distributed intra- or extracellularly, or even penetrate deep into tissues depending on their stereochemical configuration.

The $AUC_{0\text{-}INF}$ were comparable for (2S3R)-(+)-taxifolin and (2S3S)-(-)-taxifolin (462.34 ± 65.35 µg × h/ml and 498.37 ± 73.45 µg × h/ml, respectively); the $AUC_{0\text{-}INF}$ for (2R3R)-(+)-taxifolin was approximately 47% lower (235.53 ± 32.49 µg × h/ml), and the

$AUC_{0\text{-INF}}$ for (2R3S)-(-)-taxifolin was 1.5-fold higher (725.94 ± 100.45 µg × h/ml). In comparison, the CL_T for (2S3R)-(+)-taxifolin and (2R3S)-(-)-taxifolin were similar (2.38E-03 ± 3.31E-04 L/h/kg, and 2.01E-03 ± 1.99E-04 L/h/kg, respectively), whereas the CL_T for (2S3S)-(-)-taxifolin (3.75E-02 ± 1.11E-03 L/h/kg) and (2R3R)-(+)-taxifolin (7.97E-02 ± 5.90E-03 L/h/kg) were 15.8-fold and 33.5-fold higher.

The $f_{e\text{-}u}$ for (2S3R)-(+)- and (2R3S)-(-)-taxifolin indicate that approximately 55% and 22% of these stereoisomers are excreted unchanged in urine, respectively. On the other hand, less than 1% of (2S3S)-(-)- and (2R3R)-(+)-taxifolin is excreted unchanged in urine. Similarly, (2S3R)-(+)- and (2R3S)-(-)-taxifolin in the glucuronidated forms are more readily excreted in urine than the glucuro-conjugates of (2S3S)-(-)- and (2R3R)-(+)-taxifolin. The CL_R of (2S3R)-(+)-taxifolin (1.25E-03 ± 1.60E-04 L/h/kg) is 5.9-fold, 2.7-fold, and 2.9-fold higher than the CL_R of (2S3S)-(-)-, (2R3R)-(+)-, and (2R3S)-(-)-taxifolin.

The reported CL_H of (2S3R)-(+)-taxifolin (1.13E-03 ± 1.00E-04 L/h/kg), (2S3S)-(-)-taxifolin (3.73E-02 ± 5.78E-03 L/h/kg), (2R3R)-(+)-taxifolin (7.92E-02 ± 1.11E-03 L/h/kg), and (2R3S)-(-)-taxifolin (1.57E-03 ± 2.01E-04 L/h/kg) are lower than the hepatic plasma flow in rats (1.79 L/h/kg) and represent 0.6%, 2.8%, 4.4%, and 0.09% of 1.79 L/h/kg, respectively. The ER for these stereoisomers are low (<0.3). These results suggest that (2S3S)-(-)-taxifolin and (2R3R)-(+)-taxifolin are low hepatic extraction compounds. Nevertheless, (2S3S)-(-)-, (2R3R)-(+)- and (2R3S)-(-)-taxifolin are mainly excreted via non-renal routes.

In summary, the stereoisomers of taxifolin have long half-lives (> 14 h), with (2R3R)-(+)- having shorter half-life than the other three stereoisomers (14.63 ± 2.18 h). The stereoisomers of taxifolin exit the central compartment and are either distributed intracellularly, extracellularly, or even reach deep into tissues depending on their

stereochemistry. (2S3R)-(+)-, (2S3S)-(-)-, (2R3R)-(+)-, and (2R3S)-(-)-taxifolin are metabolized in the liver to a lesser degree than homoeriodicytol and isosakuranetin. (2S3S)-(-)-, (2R3R)-(+)-, and (2R3S)-(-)-taxifolin are mainly excreted via non-renal routes; whereas (2S3R)-(+)-taxifolin is mainly excreted by the kidneys.

Table 5.3. Stereospecific pharmacokinetics of taxifolin after IV administration in rats (40mg/kg). The $t\frac{1}{2}$ and k_E from serum are presented for comparison (n = 4, mean ± S.E.M.). a, $P < 0.05$.

Pharmaceutical Parameter	Units	(2S3R)(+)-Taxifolin	(2S3S)-(-)-Taxifolin	(2R3R)-(+)-Taxifolin	(2R3S)-(-)-Taxifolin
k_E urine	h^{-1}	2.24E-02 ± 3.35E-03	2.13E-02 ± 3.20E-03	4.72E-02 ± 2.30E-03[a]	2.18E-02 ± 3.27E-03
(k_E serum)	(h^{-1})	(3.62 ± 0.54)	(2.92 ± 0.34)	(3.14 ± 0.24)	(6.18 ± 0.92)
AUC_{0-INF}	μg×h/ml	462.34 ± 65.35	498.37 ± 73.45	235.53 ± 32.49[a]	725.94 ± 100.45[a]
f_{e-u}	%	52.24 ± 7.95[a]	0.57 ± 0.03	0.58 ± 0.07	21.86 ± 3.23
f_{e-g}	%	22.52 ± 3.09[a]	0.09 ± 0.01	0.01 ± 1.23E-03	0.29 ± 0.01
CL_T	L/h/kg	2.38E-03 ± 3.31E-04	3.75E-02 ± 1.11E-03	7.97E-02 ± 5.90E-03[a]	2.01E-03 ± 1.99E-04
CL_R	L/h/kg	1.25E-03 ± 1.60E-04[a]	2.13E-04 ± 4.58E-05	4.65E-04 ± 1.19E-05	4.38E-04 ± 3.01E-05
CL_H	L/h/kg	1.13E-03 ± 1.00E-04	3.73E-02 ± 5.38E-03	7.92E-02 ± 1.11E-03[a]	1.57E-03 ± 2.01E-04
V_{SS}	L/kg	0.11 ± 0.01	1.76 ± 0.25	1.68 ± 0.24	0.09 ± 0.01
$t\frac{1}{2}$ urine	h	30.91 ± 4.02	32.61 ± 4.58	14.63 ± 2.18[a]	31.73 ± 3.75
($t\frac{1}{2}$ serum)	(h)	(0.19 ± 0.02)	(0.24 ± 0.02)	(0.22 ± 0.03)	(0.11 ± 0.01)
ER	-	6.13E-04 ± 9.01E-05	2.08E-02 ± 3.11E-03	4.43E-02 ± 3.64E-03	8.74E-04 ± 1.32E-04

Previous studies have reported taxifolin as a metabolite of maritime pine bark extract [134]. After oral administration of single (300 mg) and multiple doses (200 mg × 5 days) of maritime pine bark extract to humans, taxifolin, catechin, caffeic acid, ferulic acid, and δ-(3.4-dihydroxy-phenyl)-γ-valerolactone were detected in plasma samples up to 14 hours. The AUC_{0-INF} reported for taxifolin was 231.11 ± 85.98 ng×h/ml, whereas elimination half-life was 8.89 ± 2.81 hours.

It has been previously reported that taxifolin is not metabolized by rat liver microsomes *in vitro* [136]. This findings support that fact that the glucuronidated forms of (2S3R)-(+)-taxifolin, (2S3S)-(-)-taxifolin, (2R3R)-(+)-taxifolin and (2R3S)-(-)-taxifolin were found in low concentrations in serum and urine.

5.5 CONCLUSIONS

In summary, the developed stereospecific HPLC methods for homoeriodicytol, isosakuranetin, and taxifolin have been applied for the first time to pharmacokinetic studies of the stereoisomers of these chiral flavonoids in rats. It has been demonstrated that small differences in the stereochemical structure of the stereoisomers of these flavonoids have a great impact on their pharmacokinetic profile and disposition.

Previous pharmacokinetic studies of homoeriodicytol, isosakuranetin, and taxifolin are limited, and have not taken into consideration the chiral nature of these compounds. To our knowledge, this is the first study that has assessed the stereospecific pharmacokinetics of homoeriodicytol, isosakuranetin, and taxifolin after intravenous administration of the pure racemates to rats. Previous studies of the three flavonoids have focused only on the racemic mixtures and have utilized achiral analysis in serum, urine, and tissues. Most of the previous studies only collect samples up to 24 hours post-dose, which could result in the underestimation of the overall elimination phase and therefore affect the calculation of pharmacokinetic parameters.

It was also observed that some discrepancy existed between half-lives in serum and urine for homoeriodicytol, isosakuranetin, and taxifolin. Assay sensitivity in serum may explain this inconsistency; therefore, it is likely that serum half-lives significantly underestimate overall half-lives of homoeriodicytol, isosakuranetin, and taxifolin. In addition,

it was observed that homoeriodicytol, isosakuranetin, and taxifolin were detected in urine up to 96 hours, whereas these compounds were detected in serum for up to two hours. Thus, a more accurate estimation of pharmacokinetic parameters can be obtained from urine.

The limited sensitivity in serum may be overcome using other methods of analysis such as high performance liquid chromatography – mass spectrometry (HPLC-MS), liquid chromatograph – mass spectrometry – mass spectrometry (LC-MS-MS), or gas chromatography – mass spectrometry (GC-MS) that allow for detection of much lower concentrations compared to HPLC – UV/Vis. These findings demonstrate the challenges of experimentally understanding disposition of these homoeriodicytol, isosakuranetin, and taxifolin as others have found with flavonoids and stilbenes [152-154]. Urinary data is of tremendous utility in describing the pharmacokinetics of these compounds since serum concentrations are low and clearance from serum is extremely rapid.

Based on the pharmacokinetic data obtained, homoeriodicytol, isosakuranetin, and taxifolin appear to exit the systemic circulation in order to distribute into tissues. High V_{SS} values were reported for the stereoisomers of homoeriodicytol, isosakuranetin, and taxifolin, except for (2S3R)-(+)-taxifolin and (2R3S)-(-)-taxifolin. Clearance occurs mainly via non-renal routes, assuming that the hepatic clearance is equivalent to non-renal clearance. Low fraction excreted in urine (f_e) values were seen in all stereoisomers of homoeriodicytol, isosakuranetin, and taxifolin, except for (2S3R)-(+)-taxifolin and (2R3S)-(-)-taxifolin.

The pharmacokinetics of homoeriodicytol reveals disposition, metabolism, and elimination that are dependent on the stereochemistry of the enantiomers. Both R(+)-homoeriodicytol and S(-)-homoeriodicytol have long half-lives, they exit the central compartment and penetrate into tissues. R(+)-homoeriodicytol and S(-)-homoeriodicytol are

metabolized in the liver into glucuro-conjugates and are mainly cleared by non-renal routes. S(-)-homoeriodicytol excretion in urine is higher than R(+)-homoeriodicytol.

The disposition, metabolism, and excretion of isosakuranetin enantiomers are stereoselective processes. Though isosakuranetin enantiomers have long half-lives, 2S-isosakuranetin remains in the body 1.5-fold longer than 2R-isosakuranetin. 2S-isosakuranetin and 2R-isosakuranetin exit the central compartment and penetrate deep into tissues. They are metabolized in the liver, where glucuro-conjugates are formed, and are excreted mainly via non-renal routes. 2S-isosakuranetin is more readily excreted in urine than the 2R-enantiomer.

The stereoisomers of taxifolin have comparably long half-lives, with (2R3R)-(+)- having a shorter half-life than the other three stereoisomers. The stereoisomers of taxifolin exit the central compartment and are either distributed intracellularly, extracellularly, or even distribute deep into tissues depending on their stereochemistry. (2S3R)-(+)-, (2S3S)-(-)-, (2R3R)-(+)-, and (2R3S)-(-)-taxifolin are metabolized in the liver to a lesser degree than homoeriodicytol and isosakuranetin. (2S3S)-(-)-, (2R3R)-(+)-, and (2R3S)-(-)-taxifolin are mainly excreted via non-renal routes; whereas (2S3R)-(+)-taxifolin is mainly excreted by the kidneys.

The differences in disposition, metabolism, and excretion of the stereoisomers of homoeriodicytol, isosakuranetin, and taxifolin would have not been apparent if achiral methods of analysis were used as previously reported in pharmacokinetic studies of these compounds which provide less scientifically insightful results. These findings further demonstrate the utility of developing chiral methods of analysis for xenobiotics with a chiral nature to provide a more comprehensive understanding of their disposition.

6 *In vitro* Pharmacological activity of Homoeriodictyol, Isosakuranetin, and Taxifolin

6.1 INTRODUCTION

This chapter describes the *in vitro* pharmacological activities of homoeriodicytol, isosakuranetin, and taxifolin in selected assays. An exploratory approach demonstrates the anti-cancer, anti-inflammatory, and anti-oxidant activities, as well as cyclooxygenases (COX) and histone deacetylases (HDAC) inhibitory activities of the racemic and enantiomeric forms of each compound. Similarly, the effect of the aglycone forms of these compounds are compared to the pharmacological activities of some glycosylated forms.

6.2 BACKGROUND

Previous studies have suggested some pharmacological activity for homoeriodicytol, isosakuranetin, and taxifolin including anti-cancer, anti-inflammatory, anti-adipogenic, and anti-oxidant activities (Chapter I). However, the importance of the study of the enantiomers of these three compounds in terms of eliciting activity has not been evaluated. Similarly, the importance of the potential activity of the glycosylated forms of these compounds has not been ascertained previously.

When compounds with similar actions are present together, the combined effect may be predicted by additivity if the individual drugs are equally active. However, the effect of a combination of some drugs such as enantiomers can be exaggerated or attenuated. The exaggerated effect is termed synergistic, whereas the blunted effect is termed sub-additive or antagonistic [161]. In each of these cases, the individual compounds may contribute differentially to the effect. Assessment of activity that departs from additivity suggests that some kind of interaction is occurring when both compounds are present together.

Therefore, understanding the role of each flavonoid enantiomer in the pharmacological activity described for the racemic mixtures as well as the differences between the activity of aglycones and glycosides is important. One of the inherit difficulties of assessing the individual activity of enantiomers can be their lack of commercial availability. Furthermore, some enantiomers can racemize or isomerize (Chapter I, [124,162]). The degree of purity of the enantiomer is also critically important. The methods of stereoseparation usually require high resolution of the assay to obtain stereochemically pure enantiomers.

This chapter describes and compares the anti-cancer, anti-inflammatory, anti-adipogenic, and anti-oxidant activities as well as the COX and HDAC inhibitory activities of

the stereoisomers of homoeriodicytol (R(+) and (S(-)), isosakuranetin (2S and 2R) and taxifolin ((2S3R)-(+), (2S3S)-(-), (2R3R)-(+), and (2R3S)-(+)).

6.3   METHODS

6.3.1 Attempts at Isolation of the Pure Stereoisomers

The validated HPLC methods described in Chapters II – IV were used in attempts to isolate pure stereoisomers.   Racemic mixtures of homoeriodicytol, isosakuranetin, and taxifolin were obtained from commercial sources. The HPLC conditions described for each compound were used and a series of injections were performed followed by the collection of the chromatographic peaks of each stereoisomer in separate 50.0 ml conical tubes. Pure stereoisomers were collected and dried down to completion under nitrogen gas using a rotary evaporator (Organomation Associates, Inc., Berlin, MA, USA). Issues with the isomerization of taxifolin [123] and the need of high quantities of stereoisomers for the resolution of their absolute configuration in circular dichroism experiments limited the amount available for the pharmacological studies. Similarly, in the case of homoeriodicytol, the racemization of the compound (Chapter II) also limited the ability to obtain pure R(+)-homoeriodicytol. Isomerization and racemization of chiral flavonoids has been documented in the literature for some chiral flavonoids (Chapter I). However, isolation of isosakuranetin enantiomers was successfully conducted and racemization was not apparent for this flavonoid.

6.3.2 In vitro Anti-cancer activity

6.3.2.1 Chemicals and Reagents

Racemic homoeriodicytol, isosakuranetin, taxifolin, and S(-)-homoeriodicytol were purchased from Indofine Chemical Company (Hillsborough, NJ, USA). (2R3R)-(+)-Taxifolin was purchased from Extrasynthèse (Genay, France). 2S-isosakuranetin and 2R-isosakuranetin were individually isolated using stereospecific HPLC (Chapter III). Pure 2S-isosakuranetin and 2R-isosakuranetin were collected and the mobile phase was evaporated using a nitrogen evaporator. Trypsin-Ethylenediamenetetraacetic acid (EDTA), trypan blue, phosphate-buffered saline (PBS), 4-methylumbelliferone, resazurin, cell culture tested sodium carbonate, HEPES, β-glucosidase, sodium pyruvate, McCoy's 5A medium, penicillin-streptomycin, and insulin were purchased from Sigma (St. Louis, MO, USA). Dulbecco's Modified Eagle Medium/Nutrient Mixture F-12 Ham (DMEM/F-12) without phenol red and RMPI 1640 medium were purchased from Gibco Industries Inc. (Langley, OK, USA). Fetal bovine serum (FBS) was purchased from Equitech-Bio Inc. (Kerrville, TX, USA). Dimethyl sulfoxide (DMSO) was purchased from Sigma Chemicals (St Louis, MO, USA).

6.3.2.2 Cell Culture

The cell lines used in these series of experiments were A-375 (human malignant melanoma), HCT-116 (human colorectal carcinoma), MDA-MB-231 (Her-2/Neu positive, estrogen negative breast adenocarcinoma), Hep-G2 (human hepatocellular carcinoma), SK-BR-3 (breast adenocarcinoma), and PC3 (prostate carcinoma). All cell lines were obtained from the American Type Culture Association (ATCC, Manassas, VA, USA). All media preparation and other cell culture work were performed in a laminar flow hood. The blower

and UV light in the cell culture hood were turned on 15 - 20 minutes before each use. The working surface was sterilized with 75% ethanol before and after each use. A-375 and Hep-G2 cells were maintained in 12.0 – 15.0 ml DMEM medium; MDA-MB-231 and PC-3 cells were maintained in 12.0 – 15.0 ml RPMI medium; and HCT-116 and SK-BR-3 cells were maintained in 12.0 – 15.0 ml McCoy's 5A medium. All cell lines were supplemented with 10% heat-inactivated FBS. The Hep-G2 cell line was also supplemented with insulin (4.0 mg/ml). In addition, all cell lines were treated with penicillin-streptomycin (10.0 mg/l). All cell lines were placed in 75 cm^2 tissue cell culture flasks (15 cm × 8.5 cm × 3.5 cm, TPP, Switzerland), and incubated at 37°C in a 5% CO_2 atmosphere using a Forma Scientific CO_2 water jacketed incubator from Thermo Scientific (Waltham, MA, USA).

6.3.2.3 Cell Subculture and Cell Number

Thirty minutes prior to subculturing cell lines, media, PBS, and a trypsin-EDTA solution were placed in a 37°C Precision Scientific Inc. reciprocal shaking water bath (Artisan Scientific Corporation, Champaign, IL, USA). The trypsin-EDTA solution was comprised of 0.5% trypsin and 0.2% EDTA/0.9% NaCl diluted in PBS to prepare a 10% working solution. Next, the cell flask was removed from the 5% CO_2 incubator and cells were observed under the light microscope to determine the percent confluency and their general health. A percentage of confluency of 50-75% was desired; after confluency was determined, media were aspirated and the cells were washed with 5.0 ml PBS. After a gentle wash, PBS was aspirated and 1.0 ml of the trypsin-EDTA working solution was added; then the flask was placed in the 5% CO_2 incubator for 2 – 4 minutes depending on the cell line. The flask was then removed from the incubator and when cell detachment was confirmed with the light

microscope, trypsin-EDTA containing detached cells was transferred to a 15 ml conical tube containing 9.0 ml PBS. The conical tube was centrifuged at 700 r.p.m. for 5 minutes. Following centrifugation, the conical tube was removed and the supernatant was aspirated, leaving the cell pellet undisturbed. Resuspension of cells was attained by adding 5.0 ml of fresh media followed by careful pipetting for 3 minutes; 10.0 µl of resuspended cells was removed and diluted 4 times in trypan blue. The trypan blue solution was added to a Hausser BRIGHT-LINE counting chamber (1.0 mm deep) from Optic Planet, Inc. (Northbrook, IL, USA) where the number of live cells was verified, and the number of dead cells was recorded. If it was determined that the number of dead cells surpassed 10% of the total population of healthy cells, the cells were excluded from future experiments and a new generation of the cell line was thawed.

The total number of cells in the flask was determined using the following equation:

$$Cells/ml = (\# \ cells/4) \times (dilution) \times (1 \times 10^4)$$

Media containing cells and fresh media were added in determined volumes to a fresh 75 cm^2 flask depending on the observed cell number attained with the previous equation, and the desired cell seeding number. The flask was then placed into the 5% CO_2 incubator at 37°C. Cell subculture was performed 2-3 times per week depending on the growth rate of each particular cell line and the observed confluency.

The optimal cell seeding numbers for each cell line was determined by preliminary cell seeding number experiments. Cells were seeded in number 1×10^4, 2×10^4, 3×10^4 and so on until a final seeding number of 5×10^4 per well in a 96-well plate (Costar 3595, Costar Corp., Cambridge, MA, USA) was attained. The 96-well plates were incubated in a 5% CO_2 atmosphere for 72 h. After incubation, medium was aspirated; 20.0 µl of 10% Alamar blue

(resazurin) fluorescent dye solution was added to the cells. The 96-well plates were incubated at 37°C in 5% CO_2 atmosphere for 3 hours, then removed from the incubator and placed at room temperature in a drawer to protect them from light for 30 minutes. Next, the 96-well plates were placed into a Synergynt multi-well plate reader (Biotek® Instruments Inc., Winnoski, VT, USA) using Gen 5 software from Biotek®. Fluorescence was read at an excitation of 530 nm and an emission of 590 nm. Standard curves of cell seeding number and fluorescence were generated. The optimal cell seeding number for each cell line to be used in this series of experiments was chosen form the linear portion of the generated curve. All cell lines were seeded at a density of 5,000 cells per well.

6.3.2.4   Anti-cancer Models

Counted and seeded A-375, MDA-MB-231, HCT-116, HepG2, PC3, and SK-BR-3 cells were placed on 96-well plates, then incubated at 37°C in a 5% CO_2 atmosphere for 24 hours. On the day of the experiment, homoeriodicytol, isosakuranetin, taxifolin, S(-)-homoeriodicytol, and (2R3R)-(+)-taxifolin were dissolved in DMSO and diluted with the corresponding media to yield concentrations of 250.0, 100.0, 50.0, 10.0, 5.0, and 1.0 µg/ml per enantiomer. Media were aspirated from the wells, and cells were treated with media containing homoeriodicytol, isosakuranetin, taxifolin, S(-)-homoeriodicytol, and (+)-taxifolin at different concentrations (1.0 – 250.0 µg/ml); DMSO in media and media alone were used as controls. Treated and control cells were incubated at 37°C in a 5% CO_2 atmosphere for 72 hours.

6.3.2.5   Description of the Alamar Blue Assay

After 72 hours incubation, the 96-well plates were removed from the incubator; 20.0 μl of 10% Alamar blue (resazurin) fluorescent dye was added to the control and treatment groups in the 96-well plates; they were incubated at 37°C in a 5% CO_2 atmosphere for an additional 3 hours. Following 3 hours incubation, the 96-well plates were placed in a darkened environment for 30 minutes at room temperature; then placed into a Synergynt multi-well plate reader using Gen 5 software from Biotek[®]. Fluorescence was read at an excitation of 530 nm and an emission of 590 nm. The viable cell number (as a percent of control) in each cell line was measured and for each cell line exposed to varying concentrations of homoeriodicytol, isosakuranetin, taxifolin, S(-)-homoeriodicytol, and (2R3R)-(+)-taxifolin the IC_{50} was calculated.

6.3.2.6   Data Analysis

Data were analyzed as mean percent of viable cells ± standard deviation in Microsoft Excel[®] (Microsoft Office Professional Edition, Copyright ©1985-2003 Microsoft Corporation) and then graphed using Sigma Plot[®] software (Version 10.0, Build 0.0.54, Copyright ©2006 Systat Software, Inc.). Next, the individual mean percent of viable cells was modeled using the inhibitory effect model WinNonlin[®] (Version 5.2, Build 200701231637, Pharsight WinNonlin copyright ©1998-2007) pharmacodynamic software. This model allowed the calculation of the concentration that inhibits 50% cell viability (IC_{50}) for each cell line investigated. The IC_{50} values were obtained using the following equation:

$$E^* = E_{max}{}^{\S} \left((1 - C^{\dagger})/(C + IC_{50})\right)$$

[*] Viability
[§] Maximum viability

[†] Concentration

Data were expressed as the mean ± standard error of the mean (S.E.M.) of IC_{50} values across replicates.

6.3.3 In vitro Anti-inflammatory activity

6.3.3.1   Chemicals and Reagents

Racemic homoeriodicytol, and taxifolin were purchased from Indofine Chemical Company (Hillsborough, NJ, USA). Trypsin-ethylenediamenetetraacetic acid (EDTA), trypan blue, phosphate-buffered saline (PBS), resazurin, cell culture tested sodium carbonate, 4-(2-hydroxyethyl-1-piperazineethanesulphonic acid (HEPES), McCoy's 5A medium, penicillin-streptomycin, and dimethyl sulfoxide (DMSO) were purchased from Sigma (St. Louis, MO, USA). Fetal bovine serum (FBS) was purchased from Equitech-Bio Inc. (Kerrville, TX, USA). The prostaglandin E_2 (PGE_2) Direct Biotrak[TM] Assay Kit was purchased from GE Healthcare (previously Amersham Biosciences Corp., Piscataway, NJ, USA, catalog No. RPN222).

6.3.3.2   Cell Culture

The cell line employed in this series of experiments was HT-29 (colon adenocarcinoma) purchased from American Type Culture Collection (ATCC, Manassas, VA, USA). The cell line was maintained in McCoy 5A medium with 10% heat-inactivated FBS, penicillin-streptomycin (10.0 mg/l), and HEPES (6.0 g/l); and incubated at 37°C in a 5% CO_2 atmosphere.

6.3.3.3   Cell Subculture and Cell Number

Thirty minutes prior to subculturing cell lines, medium, PBS, and a trypsin-EDTA solution were placed in a 37°C water bath. The trypsin-EDTA solution was comprised of 0.5% trypsin and 0.2% EDTA/0.9% NaCl diluted in PBS to prepare a 10% working solution. Next, the cell flask was removed from the 5% CO_2 incubator and cells were observed under the light microscope to determine the percent confluency and their general health. A percentage of confluency of 60-80% was desired; after confluency was determined, medium was aspirated and the cells were washed with 5.0 ml PBS. After a gentle wash, PBS was aspirated and 2.0 ml of the trypsin-EDTA working solution was added; then the flask was placed in the 5% CO_2 incubator for 2 – 4 minutes. The flask was then removed from the incubator and when cell detachment was confirmed with the light microscope, trypsin-EDTA containing detached cells was transferred to a 15 ml conical tube containing 8.0 ml PBS. The conical tube was centrifuged at 700 r.p.m. for 5 minutes. Following centrifugation, the conical tube was removed and the supernatant was aspirated, leaving the cell pellet undisturbed. Resuspension of cells was attained by adding 5.0 ml of fresh medium followed by careful pipetting for 3 minutes; 10.0 µl of resuspended cells was removed and diluted 4 times in trypan blue. The trypan blue solution was added to a Hausser BRIGHT-LINE counting chamber (1.0 mm deep) from Optic Planet, Inc. (Northbrook, IL, USA) where the number of live cells was verified, and the number of dead cells was recorded. If it was determined that the number of dead cells surpassed the 10% of the total population of healthy cells, the cells were excluded from future experiments and a new generation of the cell line was thawed.

The total number of cells in the flask was determined using the following equation:

$$Cells/ml = (\# \ cells/4) \times (dilution) \times (1 \times 10^4)$$

Media containing cells and fresh media were added in determined volumes to a fresh 75 cm^2 flask depending on the observed cell number attained with the previous equation, and the desired cell seeding number. The flask was then placed into the 5% CO_2 incubator at 37°C. Cell subculture was performed 2-3 times per week depending on the growth rate and the observed confluency.

The optimal cell seeding numbers was determined by preliminary cell seeding number experiments. Cells were seeded in number 1×10^4, 2×10^4, 3×10^4 and so on until a final seeding number of 5×10^4 per well in a 96-well plate (Costar 3595, Costar Corp., Cambridge, MA, USA) was achieved. The 96-well plates were incubated in a 5% CO_2 atmosphere for 72 hours. After incubation, medium was aspirated and 20.0 µl of 10% Alamar blue (resazurin) fluorescent dye solution was added to the cells. The 96-well plates were incubated at 37°C in 5% CO_2 atmosphere for 3 hours, then removed from the incubator and placed at room temperature in a drawer to protect them from light for 30 minutes. Next, the 96-well plates were placed into a Synergynt multi-well plate reader (Biotek® Instruments Inc., Winnoski, VT, USA) using Gen 5 software from Biotek®. Fluorescence was read at an excitation of 530 nm and an emission of 590 nm. Standard curves of cell seeding number and fluorescence were generated. The optimal cell seeding number for HT-29 cells was chosen form the linear portion of the generated curve. This cell line was seeded at a density of 20,000 cells per well.

6.3.3.4   In vitro Colitis Model

The employed *in vitro* colitis model was adapted from previously described methodology [153]. HT-29 (colorectal adenocarcinoma) cells were counted and seeded on 96-well plates. The seeded cells were then incubated at 37°C in a 5% CO_2 atmosphere until they

reached monolayer confluency of 60 – 80% at 72 hours. Cells were then serum starved for 24 hours. On the day of the experiment, homoeriodicytol, isosakuranetin, and taxifolin were dissolved in 1.0 µl DMSO and diluted in 1.0 ml medium to yield concentrations of 1.0, 10.0, 50.0, and 100.0 µg/ml per flavonoid.

The cells were divided into one of four groups: (1) cells treated with vehicle (1.0 µl DMSO in 1.0 ml medium) in the presence of 250.0 µl TNF-α, (2) cells treated with vehicle (1.0 µl DMSO in 1.0 ml medium) without TNF-α, (3) cells treated with the compounds (1.0 – 100.0 µg/ml) with 250.0 µl TNF-α, and (4) cells treated with the compounds (1.0 – 100.0 µg/ml) without TNF-α. Medium was aspirated from each well and then cells were treated with the compounds or vehicle in triplicate. Depending on the group, either 250.0 µl TNF-α (20.0 ng/ml) in medium or 250.0 µl of blank media was added. Medium from each group of triplicates was collected at 24 hours and stored at -80ºC for further analysis; the desired biomarkers were measured within 72 hours.

Prostaglandin E_2 (PGE$_2$) levels were measured using the prostaglandin E_2 (PGE$_2$) Direct Biotrak^{TM} assay kit. Assay buffer, lyophilized PGE$_2$ antibody, lyophilized horseradish peroxidase (HRP)-PGE$_2$ conjugate, wash buffer, 3,3'5,5'-tetramethylbenzidine (TMB) substrate, lysis reagent 1, lysis reagent 2, and PGE$_2$ standard were prepared on the day of the experiment following the manufacturer's instructions. A serial dilution of the PGE$_2$ standard was used to construct a standard curve. Assay blanks, standards and the collected media from each treatment and control group were placed in the 96-well plate supplied in the kit and incubated for 30 minutes at room temperature after the addition of lyophilized PGE$_2$ antibody. PGE$_2$ from samples was measured using a Synergynt multi-well plate reader (Biotek$^{®}$ Instruments Inc., Winnoski, VT, USA) using Gen 5 software from Biotek$^{®}$. Absorbance was

read at 450 nm. The average optical density was calculated for each set of replicates. The PGE$_2$ content of the samples was compared to the percent bound for standards (%B/B$_0$).

6.3.3.5   Relevance of the Selected Inflammatory Mediator in the *In Vitro* Model of Colitis

Prostaglandin E$_2$ (PGE$_2$) is normally involved in gastrointestinal (GI) motility, bicarbonate secretion, mucus secretion, and cytoprotection of the GI tract [163]. During inflammation, radiation-induced injury, and GI tumorgenesis differential expression of EP receptors has been reported. EP receptors consist of four different subtypes – EP$_1$, EP$_2$, EP$_3$, and EP$_4$ – and are cellular membrane receptors for PGE$_2$. Previously, upregulation of EP$_4$ in T lymphocytes as well as EP$_2$ and EP$_3$ in epithelial cells have been reported in ulcerative colitis [163]. The function of prostaglandins, in particular PGE$_2$ in the gastrointestinal tract is determined by the PGE$_2$-EP coupling, and can be either pro- or anti-inflammatory. For example, EP$_4$ signaling outcomes vary between early onset – pro-inflammatory on mucosal epithelial cells – and the late progressive stage of colitis – anti-inflammatory on immune cells in the lamina propia [163]. The PGE$_2$ concentration was measured and the IC$_{50}$ values were calculated for HT-29 colon adenocarcinoma cells exposed to varying concentrations of (+/-)-homoeriodicytol and (+/-)-taxifolin.

6.3.3.6   Description of the Prostaglandin E$_2$ (PGE$_2$) Assay

The prostaglandin E$_2$ (PGE$_2$) Direct Biotrak^{TM} assay kit was purchased from GE Healthcare (previously Amersham Biosciences Corp., Piscataway, NJ, USA, catalog No. RPN222). This competitive enzymeimmunoassay (EIA) system uses novel lysis reagents to

facilitate the extraction of PGE_2 from cell cultures without the need to remove the extracting agents prior to measurement, ensuring PGE_2 is directly available for later analysis. Intracellular PGE_2 is released after hydrolysis, and is later sequestered to ensure PGE_2 is free for subsequent analysis. More details are available in the manufacturer's instruction manual.

6.3.3.7   Statistical Analysis

All experiments were repeated at least in duplicate; data are expressed as the mean ± standard error of the mean (S.E.M.). Comparisons among control and treatment groups were made using General Linear Model (GLM) ANOVA with Newman-Keuls multiple comparison test using NCSS Statistical and Power Analysis software (NCSS, Kaysville, UT, USA). With all analyses a $P < 0.05$ was considered significant.

6.3.4 In vitro Cyclooxygenase-1 and -2 (COX) Inhibitory Activity

6.3.4.1   Chemicals and Reagents

Racemic taxifolin and isosakuranetin were purchased from Indofine Chemical Company (Hillsborough, NJ, USA). S-isosakuranetin and 2R-isosakuranetin were individually isolated using stereospecific HPLC (Chapter III). Pure 2S-isosakuranetin and 2R-isosakuranetin were collected and the mobile phase was evaporated using a nitrogen evaporator. Dimethyl sulfoxide (DMSO) was purchased from Sigma (St. Louis, MO, USA). The COX Inhibitor Screening Assay Kit was purchased from Cayman Chemical Company (Ann Arbor, MI, USA, catalog No. 560131).

6.3.4.2 Pre-Assay Preparations

On the day of the experiment, homoeriodicytol, S(-)-homoeriodicytol, isosakuranetin, poncirin, didymin, taxifolin, astilbin, and (2R3R)-(+)-taxifolin were dissolved in DMSO to yield concentrations of 1.0, 10.0, 50.0, and 100.0 µg/ml. Standards and samples used in the assay were prepared two days in advance. On day 1, the reaction buffer, COX-1 (bovine), COX-2 (human recombinant), heme, arachidonic acid, hydrocholic adic, and stannous chloride ($SnCl_2$) were prepared according to the manufacturer's instructions. Inactivated enzymes (COX-1 and COX-2) were used to generate background values; active enzymes were used to asses 100% initial activity for COX-1 and COX-2. All samples prepared this day were stored at 4ºC. On day 2, the reagents for the assay were prepared and COX inhibitory activity was assessed. The inhibitory activity of the compounds was tested individually for COX-1 and COX-2. The wash buffer, prostaglandin (PG) standard, PG screening AChE tracer, and PG screening antiserum were prepared following the manufacturer's instructions. COX reactions were performed in serial dilutions for the background samples, the 100% initial activity samples, and the COX inhibitor samples. Controls, standards, and samples were placed in 96-well plates and incubated overnight at room temperature. On day 3, the plate was developed using Ellman's reagent for 60 – 90 minutes. The COX inhibitor activity of the compounds was measured using a Synergynt multi-well plate reader (Biotek[®] Instruments Inc., Winnoski, VT, USA) using Gen 5 software from Biotek[®]. Absorbance was read at 405 – 420 nm. The COX inhibitor activity of the samples was compared to the percentage of standard bound/ maximum bound (%B/B_0).

6.3.4.3   Description of the COX Inhibitor Screening Assay

The COX Inhibitor Screening Assay Kit was purchased from Cayman Chemical Company (Ann Arbor, MI, USA, catalog No. 560131) and it directly measures the level of $PGF_{2\alpha}$ produced from PGH_2 after $SnCl_2$ reduction. $PGF_{2\alpha}$ is quantified via enzyme immunoassay (EIA) using a broadly specific antibody that binds PG compounds. This assay includes both ovine COX-1 and human recombinant COX-2 enzymes in order to screen isozyme-specific inhibitors. For more details see the manufacturer's instruction manual. The inhibition of COX – expressed as percentage of COX activity – for (+/-)-homoeriodicytol, S(-)-homoeridictyol, (+/-)-isosakuranetin, poncirin, didymin, (+/-)-taxifolin, astilbin, and (2R3R)-(+)-taxifolin was measured and the IC_{50} values were calculated.

6.3.4.4   Statistical Analysis

Compiled data were present as mean and standard error of the mean (mean ± S.E.M.). General Linear Model (GLM) Analysis of Variance (ANOVA) with Newman-Keuls multiple comparison test was utilized with a p-value < 0.05 been statistically significant (NCSS Statistical and Power Analysis, Kaysville, UT).

6.3.5 In vitro Anti-oxidant activity

6.3.5.1   Chemicals and Reagents

Racemic homoeriodicytol, isosakuranetin, taxifolin, and S(-)-homoeriodicytol were purchased from Indofine Chemical Company (Hillsborough, NJ, USA). (2R3R)-(+)-Taxifolin, didymin (2S-isosakuranetin-7-rutinoside), and poncirin (2S-isosakuranetin-7-neohesperidoside) were purchased from Extrasynthèse (Genay, France). Dimethyl sulfoxide

(DMSO) was purchased from Sigma (St. Louis, MO, USA). The Anti-oxidant Assay Kit was purchased from Cayman Chemical Company (Ann Arbor, MI, USA, catalog No. 709001).

6.3.5.2   Pre-Assay Preparations

On the day of the experiment, homoeriodicytol, S(-)-homoeriodicytol, isosakuranetin, poncirin, didymin, taxifolin, astilbin, and (2R3R)-(+)-taxifolin were dissolved in DMSO to yield concentrations of 1.0, 10.0, 50.0, and 100.0 µg/ml per enantiomer. The assay buffer, chromogen, trolox and hydrogen peroxide were prepared on the day of the experiment following the manufacturer's instructions. A trolox standard curve was constructed using a serial of dilutions. Controls, standards, and treatments at different concentrations (1.0 – 100.0 µg/ml) were placed in 96-well plates and hydrogen peroxide was used to start the oxidative reaction. The anti-oxidant activity of the compounds was measured using a Synergynt multi-well plate reader (Biotek® Instruments Inc., Winnoski, VT, USA) using Gen 5 software from Biotek® after five minutes of exposure to hydrogen peroxide. Absorbance was read at 750 nm to decrease interference. The anti-oxidant capacity of the samples was compared to that of trolox.

6.3.5.3   Description of the Anti-oxidant Assay

The Cayman Anti-oxidant Assay Kit measures the total anti-oxidant capacity based on the ability of the anti-oxidants in the sample to inhibit the oxidation of $ABTS^+$ to $ABTS^{•+}$. For more details see the manufacturer's instruction manual. The anti-oxidant capacity expressed as trolox equivalent anti-oxidant capacity (TEAC) of (+/-)-homoeriodicytol, S(-)-

homoeriodicytol, (+/-)-isosakuranetin, and (+/-)-taxifolin was measured and the IC$_{50}$ values were calculated.

6.3.5.4   Statitistical Analysis

Compiled data were present as mean and standard error of the mean (mean ± S.E.M.). General Linear Model (GLM) Analysis of Variance (ANOVA) with Newman-Keuls multiple comparison test was utilized with a p-value < 0.05 being statistically significant (NCSS Statistical and Power Analysis, Kaysville, UT).

6.3.6 In vitro Histone deacetylases (HDAC) Activity

6.3.6.1   Chemicals and Reagents

Taxifolin and homoeriodicytol were purchased from Indofine Chemical Company (Hillsborough, NJ, USA). Dimethyl sulfoxide (DMSO) was purchased from Sigma (St. Louis, MO, USA). The HDAC Activity Assay Kit was purchased from Cayman Chemical Company (Ann Arbor, MI, USA, catalog No. 10011563).

6.3.6.2   Pre-Assay Preparations

On the day of the experiment, homoeriodicytol, S(-)-homoeriodicytol, isosakuranetin, poncirin, didymin, taxifolin, astilbin, and (2R3R)-(+)-taxifolin were dissolved in DMSO to yield concentrations of 1.0, 10.0, 50.0, and 100.0 µg/ml. The assay buffer, HDAC1-positive control (human recombinant), Trichostatin A, HDAC substrate, deacetylated standard and developer were prepared on the day of the experiment following the manufacturer's

instructions. The flavonoids at different concentrations were treated with and without Trichostatin A. Serial dilutions of the deacetylated standard were used to construct a standard curve. Controls, standards, and treatments at different concentrations (1.0 – 100.0 µg/ml) were placed in 96-well plates. HDAC substrate was used to initiate the reaction (30 minutes), followed by the developer (15 minutes). The HDAC activity of the compounds was measured using a Synergynt multi-well plate reader (Biotek® Instruments Inc., Winnoski, VT, USA) using Gen 5 software from Biotek®. Fluorescence was read using an excitation wavelength of 340 – 360 nm and an emission wavelength of 440 – 465 nm. A comparison of the Trichostatin A-treated samples with their corresponding counterparts to yield the corrected sample fluorescence was performed. The deacetylated concentration of samples was compared to the standard curve; the HDAC activity of the samples was then calculated.

6.3.6.3   Description of the HDAC Activity Assay

The HDAC Activity Assay kit consists of two steps: 1) An acetylated lysine substrate is incubated with samples containing HDAC activity; then 2) a fluorescent product is released as the substrate is sensitized when deacetylation occurs after treatment with HDAC developer. The samples treated with the compounds are compared with a HDAC deacetylated standard. The assay measures Class I and II HDAC activity using a fluorescent reaction product analyzed with excitation wavelengths of 340-360 nm and emission wavelengths of 440-465 nm using a Synergynt multi-well plate reader (Biotek® Instruments Inc., Winnoski, VT, USA) using Gen 5 software from Biotek®. For more details see the instruction manual. The HDAC activity of (+/-)-homoeriodicytol, S(-)-homoeriodicytol, (+/-)-isosakuranetin, poncirin,

didymin, (+/-)-taxifolin, astilbin and (2R3R)-(+)-taxifolin was measured and the IC$_{50}$ were calculated.

6.3.6.4   Statistical Analysis

Compiled data were present as mean and standard error of the mean (mean ± S.E.M.). General Linear Model (GLM) Analysis of Variance (ANOVA) with Newman-Keuls multiple comparison test was utilized with a p-value < 0.05 been statistically significant (NCSS Statistical and Power Analysis, Kaysville, UT).

6.3.7 In vitro Anti-adipogenic Activity

6.3.7.1   Chemicals and Reagents

Racemic homoeriodicytol, isosakuranetin, taxifolin, and S(-)-homoeriodicytol were purchased from Indofine Chemical Company (Hillsborough, NJ, USA). (2R3R)-(+)-Taxifolin was purchased from Extrasynthèse (Genay, France). Trypsin-Ethylenediamenetetraacetic acid (EDTA), trypan blue, phosphate-buffered saline (PBS), 4-methylumbelliferone, resazurin, cell culture tested sodium carbonate, HEPES, sodium pyruvate, penicillin-streptomycin, and insulin were purchased from Sigma (St. Louis, MO, USA). Dulbecco's Modified Eagle Medium/Nutrient Mixture F-12 Ham (DMEM/F-12) without phenol red medium was purchased from Gibco Industries Inc. (Langley, OK, USA). Fetal bovine serum (FBS) was purchased from Equitech-Bio Inc. (Kerrville, TX, USA). The Adipogenesis Assay kit was purchased from Cayman Chemical Company (Ann Arbor, MI, USA, catalog No. 10006908).

6.3.7.2   Cell Culture

The cell line used in these series of experiments was 3T3-L1 cells (pre-adipocyte fibroblasts) purchased from American Type Culture Collection (ATCC, Manassas, VA, USA). Medium preparation and other cell culture work were performed in a laminar flow hood. The blower and UV light in the hood were turned on 15 - 20 minutes before each use. The working surface was sterilized with 75% ethanol before and after each use. 3T3-L1 cells were maintained in 12.0 – 15.0 ml DMEM medium and supplemented with 10% heat-inactivated FBS, and penicillin-streptomycin (10.0 mg/l). 3T3-L1 cells were placed in 75 cm^2 tissue cell culture flasks (15 cm × 8.5 cm × 3.5 cm, TPP, Switzerland), and incubated at 37°C in a 5% CO_2 atmosphere using a Forma Scientific CO_2 water jacketed incubator from Thermo Scientific (Waltham, MA, USA).

6.3.7.3   Cell Subculture and Cell Number

Thirty minutes prior to subculturing cell lines, medium, PBS, and a trypsin-EDTA solution were placed in a 37°C water bath. The trypsin-EDTA solution was comprised of 0.5% trypsin and 0.2% EDTA/0.9% NaCl diluted in PBS to prepare a 10% working solution. Next, the cell flask was removed from the 5% CO_2 incubator and cells were observed under the light microscope to determine the percent confluency and their general health. A percentage of confluency < 50% was desired to prevent differentiation; after confluency was determined, medium was aspirated and the cells were washed with 5.0 ml PBS. After a gentle wash, PBS was aspirated and 2.0 ml of the trypsin-EDTA working solution was added; then the flask was placed in the 5% CO_2 incubator for 2 – 4 minutes. The flask was then removed from the incubator and when cell detachment was confirmed with the light microscope,

trypsin-EDTA detached cells were transferred to a 15 ml conical tube containing 8.0 ml PBS. The conical tube was centrifuged at 700 r.p.m. for 5 minutes. Following centrifugation, the conical tube was removed and the supernatant was aspirated, leaving the cell pellet undisturbed. Resuspension of cells was attained by adding 5.0 ml of fresh medium followed by careful pipetting for 3 minutes; 10.0 µl of resuspended cells was removed and diluted 4 times in trypan blue. The trypan blue solution was added to a Hausser BRIGHT-LINE counting chamber (1.0 mm deep) from Optic Planet, Inc. (Northbrook, IL, USA) where the number of live cells was verified, and the number of dead cells was recorded. If it was determined that the number of dead cells surpassed the 10% of the total population of healthy cells, the cells were excluded from future experiments and a new generation of the cell line was thawed.

The total number of cells in the flask was determined using the following equation:

$$Cells/ml = (\text{\# cells}/4) \times (dilution) \times (1 \times 10^4)$$

Media containing cells and fresh media were added in determined volumes to a fresh 75 cm^2 flask depending on the observed cell number attained with the previous equation, and the desired cell seeding number. The flask was then placed into the 5% CO_2 incubator at 37°C. Cell subculture was performed 2-3 times per week depending on the growth rate and the observed confluency.

The optimal cell seeding numbers was determined by preliminary cell seeding number experiments. Cells were seeded in number 1×10^4, 2×10^4, 3×10^4 and so on until a final seeding number of 5×10^4 per well in a 96-well plate (Costar 3595, Costar Corp., Cambridge, MA, USA) was attained. The 96-well plates were incubated in a 5% CO_2 atmosphere for 72 hours. After incubation, medium was aspirated and 20 µl of 10% Alamar blue (resazurin)

fluorescent dye solution was added to the cells. The 96-well plates were incubated at 37°C in 5% CO_2 atmosphere for 3 hours, then removed from the incubator and placed at room temperature in a drawer to protect them from light for 30 minutes. Next, the 96-well plates were placed into a Synergynt multi-well plate reader (Biotek® Instruments Inc., Winnoski, VT, USA) using Gen 5 software from Biotek®. Fluorescence was read at 492 nm. Standard curves of cell seeding number and fluorescence were generated. The optimal cell seeding number for 3T3-L1 cells was chosen form the linear portion of the generated curve. This cell line was seeded at a density of 3.0×10^4 cells per well.

6.3.7.4   Adipogenesis Model

The employed adipogenesis model uses 3T3-L1 cells (pre-adipocyte fibroblasts) to study the induction and inhibition of adipogenesis. On the day of the experiment, homoeriodicytol, S(-)-homoeriodicytol, isosakuranetin, poncirin, didymin, taxifolin, astilbin, and (2R3R)-(+)-taxifolin were dissolved in DMSO to yield concentrations of 1.0, 10.0, 50.0, and 100.0 µg/ml per enantiomer. Three kinds of media were prepared: (1) regular DMEM medium with 10% FBS for controls; (2) induction medium containing insulin, 3-isobutyl-1-methylxanthine (IBMX) and dexamethasone; and (3) insulin medium containing insulin. Compounds at different concentrations were diluted in induction and insulin media (treatment groups). 3T3-L1 cells were seeded on 96-well plates (3×10^4 cells/well) and allowed to reach confluency. Two days post-confluency, induction medium was used to replace regular DMEM medium in the treatment groups to promote differentiation, whereas control groups received fresh regular DMEM medium (induction day). Three days after the induction, insulin medium was used to replace the induction medium in the treatment group in order to promote

further differentiation; control groups received fresh regular DMEM medium. Insulin medium was replaced once at day 5 after the induction. When 80% of the cells achieved differentiation, the lipid accumulation within cells was assessed using the Adipogenesis Assay kit purchased from Cayman Chemical Company (Ann Arbor, MI, USA, catalog No. 10006908). The fixative, wash buffer and Oil Red O were prepared on the day of the experiment following the manufacturer's instructions. The assay uses Oil Red O as an indicator of the degree of adipogenesis. The Oil Red O extracted from cells was measured spectrophotmetrically at 492 nm using a Synergynt multi-well plate reader (Biotek[®] Instruments Inc., Winnoski, VT, USA) using Gen 5 software from Biotek[®]. The anti-adipogenic activity of the compounds was compared to the percentage of Oil Red O Stain Material (OROSM).

6.3.7.5   Description of the Anti-adipogenic Assay

The Adipogenesis Assay kit uses a well characterized cell line often used to study the differentiation of adipocytes. 3T3-L1 cells have been used to investigate insulin-induced glucose uptake and mechanisms of obesity development. The fibroblast-like pre-adipocytes undergo a series of morphological and biochemical changes, accumulating lipid droplets during terminal differentiation. For more details see the manufacturer's instruction manual. The anti-adipogenic activity expressed as oil red O stained material (OROSM) for (+/-)-homoeriodicytol, S(-)-homoeriodicytol, (+/-)-isosakuranetin, poncirin, didymin, (+/-)-taxifolin, astilbin, and (2R3R)-(+)-taxifolin was measured and the IC_{50} values were calculated.

6.3.7.6 Statistical Analysis

Compiled data were present as mean and standard error of the mean (mean ± S.E.M.). General Linear Model (GLM) Analysis of Variance (ANOVA) with Newman-Keuls multiple comparison test was utilized with a p-value < 0.05 being statistically significant (NCSS Statistical and Power Analysis, Kaysville, UT).

6.4 RESULTS AND DISCUSSION

In vitro studies of the pharmacological activity of the stereoisomers of homoeriodictyol (R(+) and S(-)), isosakuranetin (2S and 2R), and taxifolin ((2S3R)-(+), (2S3S)-(-), (2R3R)-(+), and (2R3S)-(+)) are necessary because as demonstrated by the results obtained in the pharmacokinetic studies, the differences in the stereochemistry of these compounds can impact their disposition, metabolism, and elimination by the body, and it is also likely that enantiomers produce different pharmacological effects in biological systems depending on their stereochemical configuration.

Due to the prohibitive costs of commercially available flavonoids, *in vitro* studies can be of significant utility in exploratory pharmacology for the screening of the pharmacological activity of these compounds; if the desired pharmacological effect is obtained with either stereoisomer, more in-depth studies can be performed with the active stereoisomers in the future. It has been previously reported that for some racemic xenobiotics, a detrimental effect is apparent when given as a mixture while the pure stereoisomer may produce a desired effect, i.e. the theratogenic effect of thalidomide results from DNA intercalation of the S-enantiomer in the racemate, but R-thalidomide does not produce such an effect [164].

However, some chiral drugs like ibuprofen that have a carbon chiral center, are marketed as the racemic mixture because of the expense and futility of making the pure active

S-enantiomeric compound. Furthermore, some studies have demonstrated that an isomerase converts R-ibuprofen into the active S-enantiomer, making the production of pure S-ibuprofen, which is costly, unnecessary [165].

Therefore, *in vitro* studies of each stereoisomer of homoeriodictyol, isosakuranetin, and taxifolin are needed. Although the isolation of stereoisomers is possible with the validated HPLC methods described in Chapters II – IV, the cost of the starting racemic compounds is often a limiting factor to extensive studies in an academic laboratory. Prices range from $7 to $30 per milligram, and so the number of assays that can be performed is limited due to financial constraints. In addition, it is a time consuming process, taking between two to six weeks to collect the amount of individual enantiomers necessary for one single assay. Consequently, as many assays were performed with pure compounds as possible within the inherent time and cost constraints. In addition, for the stereoisomers that are commercially available, issues with stereochemical purity must be taken into consideration. The importance of characterizing the purity of commercially available isomers has been previously reported for other compounds such as dihydroouabain [166]. Therefore, it is important to consider the commercial sources of the pure stereoisomers to ensure the purity of these compounds. Finally, the stability of the compounds needs to be taken into consideration. Taxifolin and homoeriodictyol have been reported to undergo isomerisation [123] or racemization (Chapter II), respectively; which makes the production of pure stereoisomers testable in biological systems exceedingly difficult.

6.4.1 In vitro Anti-Cancer Activity

The Alamar blue (resazurin) fluorescent cell viability measurement is an easy and accurate assay to determine the cytotoxicity of many cell lines. Viable cells are capable of metabolizing the non-fluorescent dye resazurin into its fluorescent counterpart, resorufin; on the other hand, metabolism of resazurin in non-viable cells is not achieved. The fluorescence emission can be quantified using a plate reader and the number of viable cells after treatment can be determined.

6.4.1.1   Homoeriodictyol

The cytotoxic effects of homoeriodictyol on different cancer cell lines are presented in **Fig. 6.1.** It can be observed that (+/-)-homoeriodicytol and S(-)-homoeriodicytol showed concentration-dependent anti-cancer activity, and racemic homoeriodicytol was most effective in A-375 melanoma cells, whereas, S(-)-homoeriodicytol was most effective in HCT-116 colon cancer cells.

Figure 6.1. Effects of racemic homoeriodicytol (**1**) and S-(+)-homoeridictyol (**2**) on the viability of different cancer cell lines (means ± S.E.M.).

The IC_{50} values of (+/-)-homoeriodictyol and S(-)-homoeriodicytol are summarized in **Table 6.1**. (+/-)-Homoeriodictyol was most effective in reducing the number of viable cancer cells in the A-375 melanoma cell line (IC_{50} = 56.62 ± 3.95 µg/ml) and least effective in Sk-Br-3 breast cancer cells (IC_{50} = 305.20 ± 45.78 µg/ml). On the other hand, S(-)-homoeriodicytol was most effective in HCT-116 colon cancer cells (IC_{50} = 39.50 ± 5.92 µg/ml), and least effective in the Sk-Br-3 breast cell line (IC_{50} = 282.38 ± 42.36 µg/ml).

If the S(-) and R(+) enantiomers of homoeriodicytol were equally active in cancer cell growth inhibition, the IC_{50} values of S(-)-homoeriodicytol would be expected to be half of the IC_{50} values obtained for (+/-)-homoeriodicytol, the racemic (50:50) mixture of the S(-) and R(+) forms. Some chiral compounds that show similarity in their chemical structures have been reported to have an additive effect when administered together [167]. An additive effect means that the resulting effect is the sum of the individual effects, i.e. the effect of toluene (C_7H_8) and p-xylene (C_8H_{10}) in the central nervous system (CNS) [167].

Table 6.1. IC_{50} values in µg/ml (mM) of (+/-)-homoeriodicytol and S(-)-homoeriodicytol across different cancer cell lines (n = 3, mean, S.E.M.). a, $P < 0.05$, racemate vs. enantiomer.

Cancer cell line	Compound (IC_{50})	
	(+/-)-Homoeriodictyol	S(-)-Homoeriodictyol
A-375 (melanoma)	56.62 ± 3.95	59.67 ± 6.81
	(187.32 ± 13.06)	(197.39 ± 22.52)
HCT-116 (colon)	117.20 ± 17.58[a]	39.50 ± 5.92
	(387.71 ± 58.16)	(130.67 ± 19.60)
Hep-G2 (liver)	90.96 ± 13.64	77.39 ± 11.61
	(300.91 ± 45.14)	(256.04 ± 38.41)
MDA-MB-231 (breast)	81.48 ± 12.22	108.67 ± 16.30
	(269.54 ± 40.43)	(359.52 ± 53.93)
PC-3 (prostate)	107.90 ± 16.18[a]	77.25 ± 11.59
	(356.95 ± 53.54)	(255.57 ± 38.33)
Sk-Br-3 (breast)	305.20 ± 45.78	282.38 ± 42.36
	(1009.68 ± 151.45)	(934.17 ± 140.13)

However, the results obtained in A-375 melanoma, Hep-G2 liver cancer, MDA-MB-231 breast cancer, PC-3 prostate cancer, and SK-Br-3 breast cancer indicate that S(-)-homoeriodicytol and R(+)-homoeriodicytol do not have the same activity in cell growth inhibition since the IC_{50} values for S(-)-homoeriodicytol are comparable to the IC_{50} values for the racemic mixture, (+/-)-homoeriodicytol and not half of the values as proposed for an additive effect model. Only in one cell line (HCT-116 colon carcinoma) the effect of S(-)-homoeriodicytol in inhibiting cell growth is three-fold lower than the effect of (+/-)-homoeriodicytol and less than the expected for an additive effect model.

Therefore, these results may suggest that S(-)-homoeriodicytol and R(+)-homoeriodicytol may cause their effect on cell growth inhibition independently and differentially interacting with cell receptors [167]. The effect of S(-)-homoeriodicytol in cell growth inhibition could also suggest that R(+)-homoeriodicytol has a potentiating effect in the activity of S(-)-homoeriodicytol in A-375 melanoma, and MDA-MB-231 breast cancer cell lines [167]. This would mean that R(+)-homoeriodicytol by itself does not have a toxic effect in cancer cells, but when combined with S(-)-homoeriodicytol, the R(+)-isomer enhances the effect of S(-)-homoeriodicytol in cell growth inhibition. This type of effect has been described for other xenobiotics, i.e. 2-propanol and carbon tetrachloride. 2-propanol by itself does not present liver toxicity; however, when administered with carbon tetrachloride, 2-propanol induces enzymes that enhance the formation of toxic carbon tetrachloride metabolites [167].

A synergistic effect may also explain the results seen in the MDA-MB-231 breast cancer cell line. In this case, the effect seen for the two enantiomers in the racemic mixture (81.48 ± 12.22 µg/ml) is much higher than the effect seen for S(-)-homoeriodicytol alone

(108.67 ± 16.50 µg/ml). It is also higher than the predicted in an additive effect model (half of (+/-)-homoeriodicytol, ~40.74 µg/ml). An antagonistic effect model may explain the effects seen in HCT-116 colon cancer, Hep-G2 liver cancer, PC-3 prostate cancer, and SK-Br-3 breast cancer. The effect of S(-)-homoeriodicytol in inhibiting cancer cell growth is greater (lower IC_{50}) than the effect seen for the racemic mixture.

Therefore, testing the effect of R(+)-homoeriodicytol would be necessary to clearly understand the role of each enantiomer in cancer cell growth inhibition. However, issues with possible instability of (+/-)-homoeriodicytol racemization need to be resolved before these type of investigations are experimentally possible.

The HPLC method developed in Chapter II would allow for the isolation of R(+)-homoeriodicytol from (+/-)-homoeriodicytol; however, the cost of this compound, which can run as high as $15 per milligram, may be a limiting factor. Nevertheless, it was demonstrated that for most cancer cell lines, S(-)-homoeriodicytol shows similar effects in cancer cell growth inhibition to the effects seen for (+/-)-homoeriodicytol. In order to elucidate the mechanism of action of S(-)-homoeriodicytol and R(+)-homoeriodicytol in cancer cell growth inhibition, the direct anti-cancer activity of R(+)-homoeriodicytol needs to be assessed.

Previous studies have demonstrated the anti-cancer activity of homoeriodicytol. Nevertheless, these studies only considered the activity of the racemic mixture; no stereospecific studies of R(+)-homoeriodicytol and S(-)-homoeriodicytol are available in the literature. These findings suggest that R(+)- and S(-)-homoeriodicytol have different activity in cancer cell growth in all cell lines studied, and therefore, further studies are necessary to elucidate the activity of R(+)-homoeriodicytol in cancer.

6.4.1.2 Isosakuranetin

The cytotoxic effects of isosakuranetin on different cancer cell lines are presented in **Fig. 6.2.** It can be observed that isosakuranetin presents a concentration-dependent anticancer activity, and that racemic isosakuranetin was very effective in Hep-G2 liver cancer cells. Therefore, the effect of the individual stereoisomers of isosakuranetin was tested in Hep-G2 (**Fig. 6.2.2**). 2S-isosakuranetin and 2R-isosakuranetin have similar effect on the inhibition of Hep-G2 liver cancer cells. Nevertheless, when both 2R- and 2S-isosakuranetin are present in the racemic mixture, a synergistic effect is evident. The effect seen in Hep-G2 liver cancer cells did not correspond to an additive effect model. (+/-)-Isosakuranetin was far more effective in reducing cancer cell growth than the 2S or 2R enantiomers administered alone. Due to the limited amount of pure stereoisomers isolated, only one cell line has been tested. These results suggest that 2S-isosakuranetin and 2R-isosakuranetin are likely to have different effects in cancer cell growth in other cell lines; however, this hypothesis remains to be explored.

(1)   **(2)**
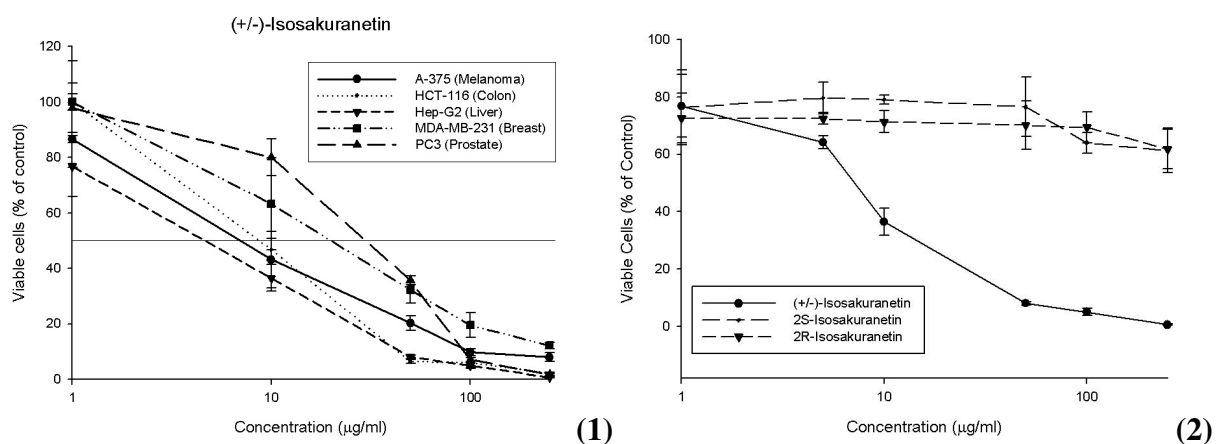
Figure 6.2. Effects of (+/-)-isosakuranetin in the viability of different cancer cell lines **(1)** and comparison of the effect of (+/-)-isosakuranetin, 2S-isosakuranetin, and 2R-isosakuranetin in Hep-G2 liver cancer cells (means ± S.E.M.).

Table 6.2 summarizes the IC_{50} values of (+/-)-isosakuranetin in the five cancer cell lines studied. (+/-)-Isosakuranetin was most effective in the inhibition of cancer cell growth in HCT-116 colon cancer cells (IC_{50} = 5.98 ± 0.90 µg/ml), and least effective in reducing the number of cancer cells in the PC-3 prostate cancer cell line (IC_{50} = 21.68 ± 3.25 µg/ml). Overall, (+/-)-isosakuranetin was the most effective of all the flavonoids studied since lower IC_{50} values compared to (+/-)-homoeriodicytol, S(-)-homoeriodicytol, (+/-)-taxifolin, astilbin, and (2R3R)-(+)-taxifolin were obtained for (+/-)-isosakuranetin in all cancer cell lines tested.

Table 6.2. IC_{50} values in µg/ml (mM) of (+/-)-isosakuranetin, 2S-isosakuranetin, and 2R-isosakuranetin across different cancer cell lines (n = 3, mean, S.E.M.); n.d.; not determined. a, $P < 0.05$, racemate vs. enantiomer; b, $P < 0.05$, 2S vs. 2R.

Cancer cell line	Compound (IC_{50})		
	(+/-)-Isosakuranetin	2S-Isosakuranetin	2R-Isosakuranetin
A-375 (melanoma)	9.79 ± 1.47 (34.19 ± 4.86)	n.d	n.d.
HCT-116 (colon)	5.98 ± 0.90 (20.89 ± 2.97)	n.d	n.d.
Hep-G2 (liver)	6.68 ± 0.72[a] (23.32 ± 3.31)	5.09E+08 ± 4.65E+06[b] (1.78E+09 ± 1.62E+07)	2.47E+08 ± 1.23E+06 (8.63E+08 ± 4.30E+06)
MDA-MB-231 (breast)	20.07 ± 3.01 (70.11 ± 9.96)	n.d	n.d
PC-3 (prostate)	21.68 ± 3.25 (75.73 ± 10.76)	n.d	n.d

6.4.1.3 Taxifolin

The cytotoxic effects of taxifolin on different cancer cell lines are presented in **Fig. 6.3.** It can be observed that (2R3R)-(+)-taxifolin and astilbin, the rhamnoside of (2R3R)-(+)-taxifolin, were most effective in MDA-MB-231 breast cancer cells, whereas (+/-)-taxifolin was most effective in HCT-116 colon cancer cells.
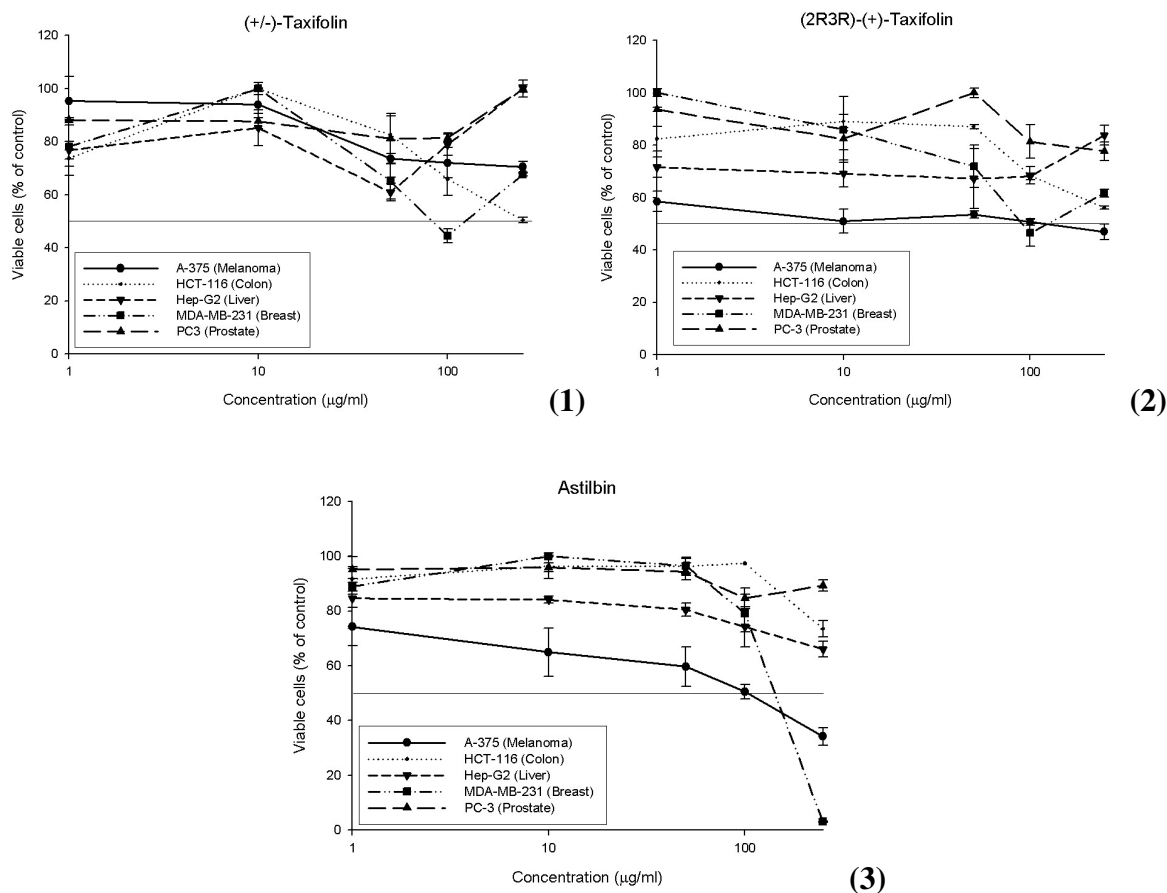
Figure 6.3. Effects of racemic taxifolin **(1)**, (2R3R)-(+)-taxifolin **(2)** and **(3)** astilbin – a rhamnoside of taxifolin – on the viability of different cancer cell lines (means ± S.E.M.).

It is apparent from the experimental results that at higher concentrations (100 – 250.0 µg/ml) the inhibitory effect of (2R3R)-(+)-taxifolin (XLogP = 1.5), (+/-)-taxifolin (XLogP = 1.5), and astilbin (XLogP = 0.4) on cell growth is not as effective in some of the cancer cell lines studied. This might be explained by further understanding the solubility of these compounds. It is plausible that at high concentrations these compounds come out of solution due to their lipophilic nature and poor water solubility. In this case, the actual concentration of the compound remaining in solution and interacting with the cancer cells may vary considerably. Interestingly, in the case of astilbin (a more polar glycoside flavonoid), high concentrations may actually have a protective effect in PC-3 cells.

The IC_{50} values of (+/-)-taxifolin, (2R3R)-(+)-taxifolin, and astilbin are summarized in Table 6.3. (+/-)-Taxifolin was most effective in reducing the number of cancer cells in HCT-116 colon cancer cells ($IC_{50} = 346.18 \pm 51.93$ µg/ml), and least effective in A-375 melanoma cells ($IC_{50} = 594.56 \pm 89.18$ µg/ml). Both (2R3R)-(+)-taxifolin ($IC_{50} = 237.52 \pm 35.63$ µg/ml) and astilbin ($IC_{50} = 143.18 \pm 21.48$ µg/ml) were most effective in the inhibition of cancer cells in the MDA-MB-231 breast cancer cell line; however, (2R3R)-(+)-taxifolin was least effective in PC-3 prostate cancer cells ($IC_{50} = 1254.93 \pm 188.24$ µg/ml), whereas its rhamnoside, astilbin, was least effective in reducing the number of cancer cells in the HCT-116 colon cell line ($IC_{50} = 346.18 \pm 51.93$ µg/ml). Overall, (+/-)-taxifolin, (2R3R)-(+)-taxifolin, and astilbin performed poorly in inhibiting cell growth in cancer cell lines. The aglycone form of (2R3R)-(+)-taxifolin was more effective that the rhamnoside in HCT-116 colon cancer and Hep-G2 liver cancer cells which suggests that the sugar moiety partially hinders the pharmacological activity of the enantiomer in these cell lines. On the other hand, astilbin was more effective than the aglycone form in A-375 melanoma, MDA-MB-231 breast cancer, and PC-3 prostate cancer. This might be due to the more hydrophilic nature of the rhamnoside form of (2R3R)-(+)-taxifolin; and greater availability and cellular penetration.

Table 6.3. IC_{50} values in µg/ml (mM) of (+/-)-taxifolin, (2R3R)-(+)-taxifolin, and astilbin – a rhamnoside of taxifolin – across different cancer cell lines (n = 3, mean, S.E.M.). a, P < 0.05, racemate vs. enantiomer; b, P < 0.05 aglycone vs. glycoside.

Cancer cell line	Compound (IC_{50})		
	(+/-)-Taxifolin	(2R3R)-(+)-Taxifolin	Astilbin
A-375 (melanoma)	594.56 ± 89.18	1069.25 ± 160.39[a,b]	233.42 ± 33.13
	(1954.17 ± 293.13)	(3514.37 ± 527.16)	(518.26 ± 73.55)
HCT-116 (colon)	346.18 ± 51.93	446.61 ± 66.99	984.47 ± 147.67[b]
	(1137.80 ± 170.67)	(1467.89 ± 220.18)	(2185.80 ± 327.87)
Hep-G2 (liver)	505.00 ± 75.75	504.90 ± 74.73	834.35 ± 69.18
	(1659.81 ± 248.97)	(1659.48 ± 248.92)	(1852.50 ± 153.59)
MDA-MB-231 (breast)	431.50 ± 64.73[a]	237.52 ± 35.63[b]	143.18 ± 21.48
	(1418.24 ± 212.74)	(780.69 ± 117.10)	(317.91 ± 47.69)
PC-3 (prostate)	504.99 ± 75.73	1254.93 ± 188.24[a,b]	504.99 ± 75.75
	(1659.77 ± 248.97)	(4124.65 ± 618.70)	(1121.23 ± 168.18)

(+/-)-Taxifolin is composed of four stereoisomers, therefore, predictions of their individual effects in cancer cell growth are much more complex than in the case of (+/-)-homoeriodicytol and (+/-)-isosakuranetin, as these two flavonoids only have two stereoisomers. The results suggest that enantiomeric synergism may be observed in A-375 melanoma, HCT-116 colon cancer, and PC-3 prostate cancer treated with (+/-)-taxifolin. The effects seen in these cell lines are higher (lower IC_{50}) than the effect of (2R3R)-(+)-taxifolin alone. On the other hand, in Hep-G2 liver cancer the effects of (2R3R)-(+)-taxifolin and (+/-)-taxifolin are comparable, in which case a plausible hypothesis is that other three stereoisomers, (2S3R)-(+), (2S3S)-(-), and (2R3R)-(+), may be inactive in this cancer cell line. In MDA-MB-231 breast cancer it appears that (2S3R)-(+)-, (2S3S)-(-)-, and (2R3R)-(+)-taxifolin may have an antagonistic effect on the cell growth inhibitory activity of (2R3R)-(+)-taxifolin.

Unlike (+/-)-homoeriodicytol, in which the racemic mixture of the R(+) and S(-) enantiomers is close to 50:50, the commercially available racemic mixture of taxifolin consists of four stereoisomers in the following percentages: (2S3R)-(+)-taxifolin and (2R3S)-(-)-taxifolin each represents approximately 3% of the racemic mixture, whereas (2S3S)-(-)-taxifolin and (2R3R)-(+)-taxifolin each corresponds to approximately 47% of the racemic mixture.

Even though the separation of each stereoisomer is accomplished with the stereospecific HPLC method described in Chapter IV, the isolation of all four stereoisomers is extremely time consuming and the low percentage of two of the four stereoisomers in the racemic mixture is a limiting factor for preparative isolation. Likewise, the high cost of this compound, as much as $7 per milligram, also limited the number of assays performed with the taxifolin pure stereoisomers.

Previous studies have demonstrated the anti-cancer activity of taxifolin. However, these studies took in consideration the racemic form but not the stereoisomers. These findings suggest that stereoisomers of (+/-)-taxifolin may have different effects in cancer cell growth inhibition. Further studies are necessary to elucidate the effect of taxifolin stereochemistry in *in vitro* cancer model.

In summary, homoeriodicytol, isosakuranetin, and taxifolin demonstrated concentration-dependent anti-cancer activity. The evaluated stereoisomers (S(-)-homoeriodicytol, 2S-isosakuranetin, 2R-isosakuranetin, and (2R3R)-(+)-taxifolin) suggest that each stereoisomer contributed differently to the anti-cancer effect seen in the racemic mixtures.

6.4.2 In vitro Anti-inflammatory Activity

Prostaglandin E_2 (PGE_2) results from the metabolism of arachidonic acid in several cell types, and does not exist preformed in any cell reservoir. In the assay used, intracellular PGE_2 is released after cell membrane hydrolysis or dissociation from receptors and proteins. Then, unlabelled PGE_2 from the samples and the HRP-PGE_2 conjugate compete for the binding sites on the lyophilized PGE_2 antibody attached to the goat anti-mouse IgG coating the wells in the plate. Finally, the reaction is stopped and spectrometric measurement of PGE_2 content is performed.

Prostaglandins (PG) are 20 carbon fatty acid derivatives, found in all tissues and organs. PGs can be synthesized from several essential fatty acid precursors including arachidonic acid. Phospholipids in the cellular membrane are converted into arachidonic acid

released to the cytoplasm by phospholipase A_2 (PLA_2); PGs derived from arachidonic acid are named series-2 PGs including PGE_2, PGD_2, PGI_2, $PGF_{2\alpha}$ and TXA_2 [163].

TNF-α has been reported to induce inflammation in HT-29 colon adenocarcinoma cells *in vitro* and *in vivo* [168]; it was therefore used to stimulate PGE_2 cell production. TNF-α is a potent immuno-modulator and its excessive production has been associated with inflammatory bowel disease and colitis.

6.4.2.1   Homoeriodictyol

HT-29 cells treated with and without TNF-α and with the respective homoeriodictyol treatment showed concentration-dependent anti-inflammatory activity (**Fig. 6.4** and **Table 6.4**) by reducing the PGE_2 content. Homoeriodictyol appears to have a protective effect in HT-29 colon adenocarcinoma cells since the detected level of PGE_2 decreased in relation to homoeriodictyol concentration whether TNF- α was present or not.
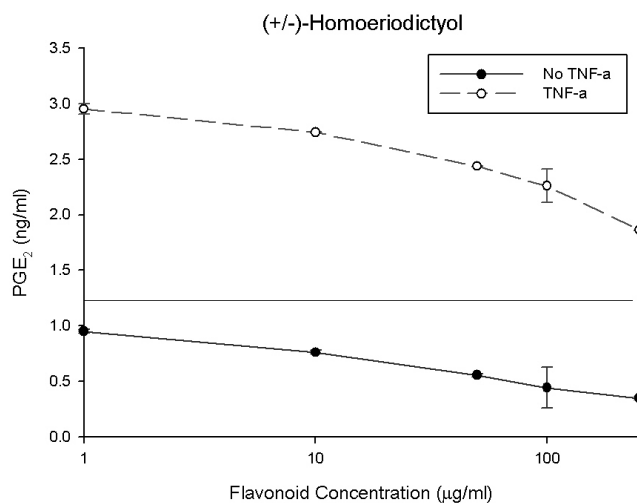
Figure 6.4. Prostaglandin E_2 (PGE_2) production (n = 3, mean ± S.E.M.) in the HT-29 cell culture medium at 72 hours after treatment with homoeriodictyol (1.0 – 250.0 µg/ml). Values are expressed as ng/ml. The line represents the baseline level in which HT-29 cells have not been exposed to an inflammatory insult.

Previous studies have demonstrated the anti-inflammatory activity of homoeriodicytol; however, no stereospecific studies have been reported in the literature. This is the first time the effect of homoeriodicytol in PGE_2 levels in HT-29 colon adenocarcinoma cells *in vitro* is evaluated. It would be important, nevertheless, to study the anti-inflammatory activity of the enantiomers of homoeriodicytol to understand their individual role in PGE_2 reduction. The expense of commercially available pure stereoisomers is a limiting factor, and even though the pure stereoisomers could be isolated form (+/-)-homoeriodicytol using the validated HPLC method described in Chapter II, this is a time consuming process that requires high quantities of the racemic compound.

These findings suggest that homoeriodicytol may have a protective effect in the GI tract since the enantiomers are mostly excreted via non-renal routes (Chapter V), which translates into high concentrations of homoeriodicytol in the GI tract. Therefore, homoeriodicytol may be used in pathologies of the GI tract such as colitis and inflammatory bowel disease, and consumption of products with high homoeriodicytol content may have a protective effect in gastrointestinal pathologies.

6.4.2.2   Taxifolin

HT-29 cells treated with and without TNF-α and with the respective taxifolin treatment show concentration-dependent anti-inflammatory activity (**Fig. 6.5)** due to the reduction of PGE_2 levels. Taxifolin, like homoeriodicytol, appears to have a protective effect due to its effect in the concentration of PGE_2 in the presence or absence of TNF- α.
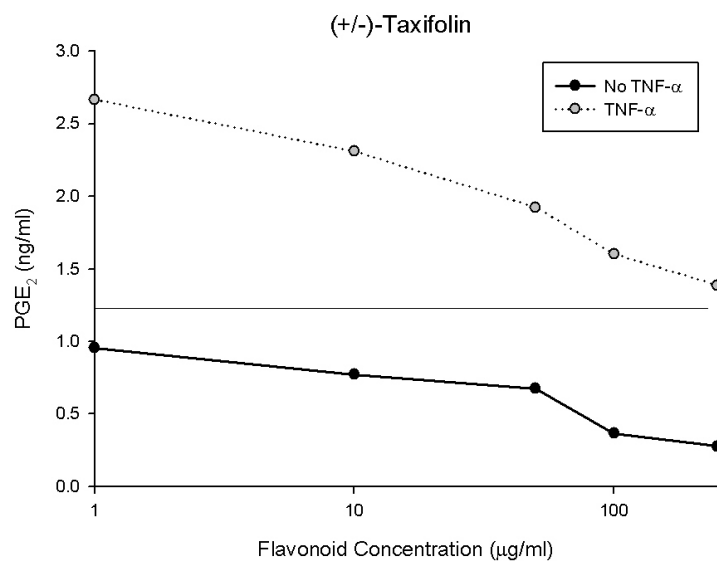
Figure 6.5. Prostaglandin E_2 (PGE_2) production (n = 3, mean ± S.E.M.) in the HT-29 cell culture medium at 72 hours after treatment with taxifolin (1.0 – 100.0 µg/ml). Values are expressed as ng/ml. The line represents the baseline level in which HT-29 cells have not been exposed to an inflammatory insult.

Previous studies have reported the anti-inflammatory activity of (+/-)-taxifolin; however, the stereochemistry of taxifolin has not been considered. This is the first time the effect of taxifolin in PGE_2 levels in a colitis *in vitro* model is studied. Even though the validated HPLC method for taxifolin (Chapter IV) allows for the isolation of the pure stereoisomers, considerable expense and time consuming preparative methods and isomerization are limiting factors.

Table 6.4 summarizes the IC_{50} values for (+/-)-homoeriodicytol and (+/-)-taxifolin for PGE_2 reduction. (+/-)-Homoeriodictyol exhibited a lower IC_{50} value than (+/-)-taxifolin; however, the difference was not significant.

Table 6.4. IC$_{50}$ values in µg/ml (mM) for (+/-)-homoeriodicytol and (+/-)-taxifolin for PGE$_2$ reduction (n = 3, mean ± S.E.M).

Compound	IC$_{50}$
(+/-)-Homoeriodictyol	143.32 ± 21.50 (474.14 ± 71.12)
(+/-)-Taxifolin	160.05 ± 24.01 (526.03 ± 78.90)

This is the first time that (+/-)-homoeriodicytol and (+/-)-taxifolin are evaluated for their effect in a colitis *in vitro* model in HT-29 colon adenocarcinoma cells. (+/-)-Homoeriodictyol and (+/-)-taxifolin demonstrated concentration-dependent reduction of PGE$_2$ levels in HT-29 cells. Further follow-up studies are necessary with the pure stereoisomers of homoeriodicytol and taxifolin to elucidate their potential differences in anti-inflammatory activity in colitis.

These findings suggest that like homoeriodicytol, taxifolin may also have a protective effect in the GI tract since it is mostly excreted via non-renal routes (Chapter V). Therefore, taxifolin may also be potentially used in pathologies of the GI tract such as colitis and inflammatory bowel disease. Consumption of products with high taxifolin content may have a protective effect in diseases of the gastrointestinal tract.

6.4.3 In vitro Cyclooxygenases Activity

Cyclooxygenases (COXs) contain cyclooxygenase and peroxidase activities. PGs can be synthesized from several essential fatty acid precursors including arachidonic acid. COXs activity will result in the production of PGG$_2$ and PGH$_2$ which are unstable endoperoxide intermediates [163]. COX catalyzes the conversion of arachidonic acid to PGH$_2$, the first step in the biosynthesis of prostaglandins (PGs), thromboxanes, and prostacyclins. Two distinct

isoforms of COX are known: COX-1, which is constitutively expressed in a variety of cell types and is involved in normal cellular homeostasis; and COX-2, which production is induced by mitogenic stimuli and is responsible for the biosynthesis of PGs under acute inflammatory conditions. Cyclooxygenases have been involved in gastric and colorectal carcinogenesis; and in particular, COX-2 polymorphisms were demonstrated to be present in patients with gastric or colorectal lesions [169].

The inhibitory effect of (+/-)-isosakuranetin, 2S-isosakuranetin, 2R-isosakuranetin, and (+/-)-taxifolin in COX-1 and COX-2 activity was assessed. Ibuprofen was used as a positive control for the COX-1 assay due to its inhibitory activity towards both COX-1 and COX-2. For the COX-2 assay, ibuprofen and etodolac were employed as positive controls since etodolac is suggested to be a more selective COX-2 inhibitor.

6.4.3.1   Isosakuranetin

Racemic isosakuranetin and its enantiomers, 2R-isosakuranetin, and 2S-isosakuranetin, were assessed for their COX-1 and COX-2 inhibitory activity using a commercially available ELISA assay. The inhibitory effect of (+/-)-isosakuranetin, 2R-isosakuranetin and 2S-isosakuranetin in COX-1 activity is presented in **Fig. 6.6**; the IC_{50} values were also calculated (**Table 6.5**). 2R-Isosakuranetin and 2S-isosakuranetin had similar COX-1 inhibitory activity, but were not as active as (+/-)-ibuprofen (higher IC_{50}). On the other hand, the racemic mixture, (+/-)-isosakuranetin, is far less effective than 2R- and 2S-isosakuranetin alone. These results suggest an antagonistic effect in COX-1 inhibition when 2R-isosakuranetin and 2S-isosakuranetin are administered together, opposite to the findings of racemic, 2R and 2S isosakuranetin in HepG-2 liver cancer.
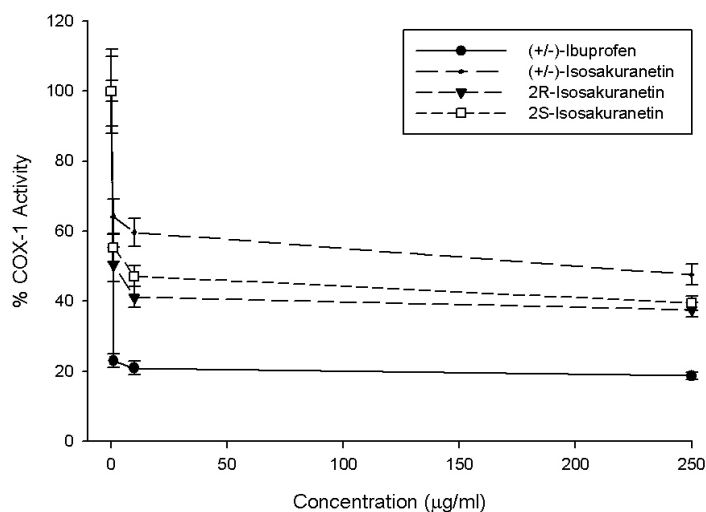
Figure 6.6. Cyclooxygenase-1 (COX-1) activity after addition of racemic isosakuranetin, 2R-isosakuranetin, 2S-isosakuranetin and ibuprofen (positive control) at concentrations 1.0 – 250.0 µg/ml (n = 3, mean ± S.E.M). Values are expressed as percentage (%).

The COX-2 inhibitory activity of (+/-)-isosakuranetin, 2S-isosakuranetin, and 2R-isosakuranetin was also evaluated (**Fig. 6.7** and **Table 6.6**) and was demonstrated to be concentration-dependent for the three compounds. 2R-Isosakuranetin was more effective in inhibiting the activity of COX-2 than 2S-enantiomer. When both 2R and 2S enantiomers are present in the racemic mixture, an antagonistic effect was evident. Nevertheless, neither one of the enantiomers nor the racemic mixture of isosakuranetin were as effective as (+/-)-ibuprofen or (+/-)-etodolac in inhibiting COX-2 activity.

Poncirin (2S-isosakuranetin neohesperidoside) has been previously reported to have anti-inflammatory activity by inhibiting COX-2 expression [53]. However, the COX-2 inhibitory effect of the aglycone forms has not been previously evaluated. This is the first time the COX-2 inhibitory effects of the racemic mixture and the enantiomeric forms of isosakuranetin are evaluated.
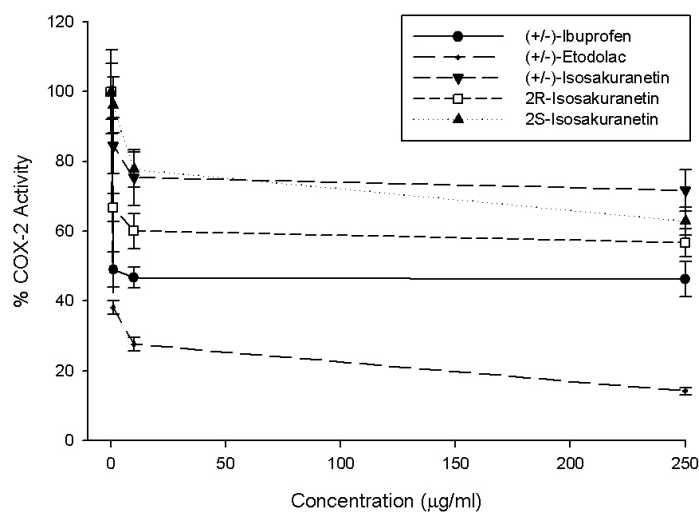
Figure 6.7. Cyclooxygenase-2 (COX-2) activity after addition of racemic isosakuranetin, 2R-isosakuranetin, 2S-isosakuranetin, ibuprofen, and etodolac (positive controls) at concentrations 1.0 – 250.0 µg/ml (n = 3, mean ± S.E.M.). Values are expressed as percentage (%).

Furthermore, the COX-2 to COX-1 ratio was calculated to assess the preferential inhibitory activity for either one of the COX isoforms (**Fig. 6.8**). The lower the ratio, the lower the COX-1 inhibitory effect; and therefore, potentially lower the gastric side effect profile. (+/-)-Etodolac exhibited more selective COX-2 inhibition whereas (+/-)-ibuprofen exhibited essentially equal inhibition of both COX-1 and COX-2. (+/-)-Isosakuranetin, 2S-isosakuranetin, and 2R-isosakuranetin showed selective COX-2 inhibition comparable to (+/-)-etodolac.
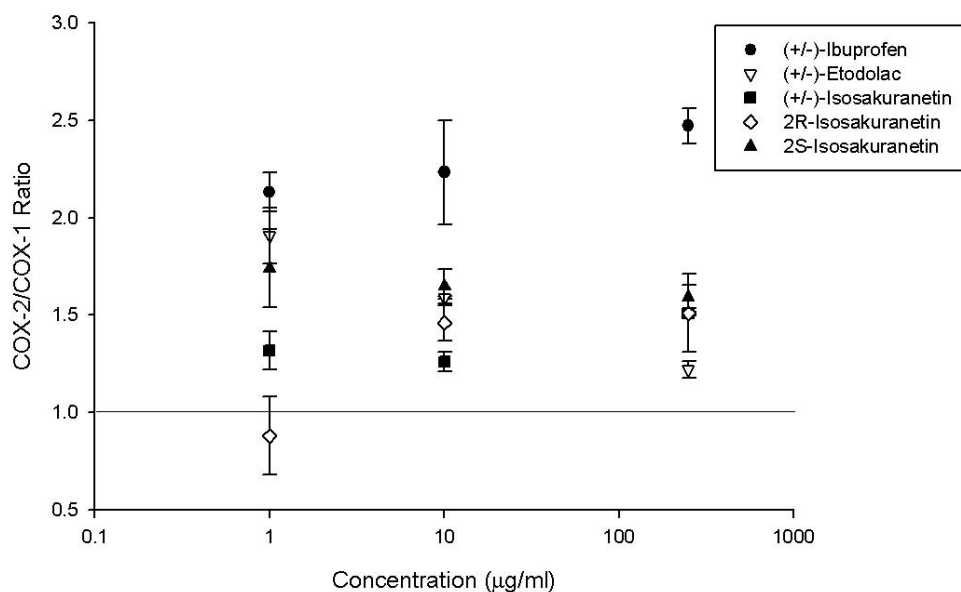
Figure 6.8. Cyclooxygenase-2 (COX-2) to cyclooxygenase-1 (COX-1) ratio of racemic isosakuranetin, ibuprofen, and etodolac as positive controls at concentrations 1.0 – 250.0 µg/ml (n = 3, mean ± S.E.M.). Values are expressed as percentage (%). The line represents a ratio of 1 that would indicate equal inhibitory activity for both COX isomers.

6.4.3.2   Taxifolin

Racemic taxifolin was assessed for its COX-1 and COX-2 inhibitory activity using a commercially available ELISA assay. The inhibitory effect of (+/-)-taxifolin in COX-1 activity is presented in **Fig. 6.9**. (+/-)-Taxifolin demonstrated less COX-1 inhibitory activity than (+/-)-ibuprofen (**Table 6.5**). This is the first time the COX-1 inhibitory activity of (+/-)-taxifolin is reported.
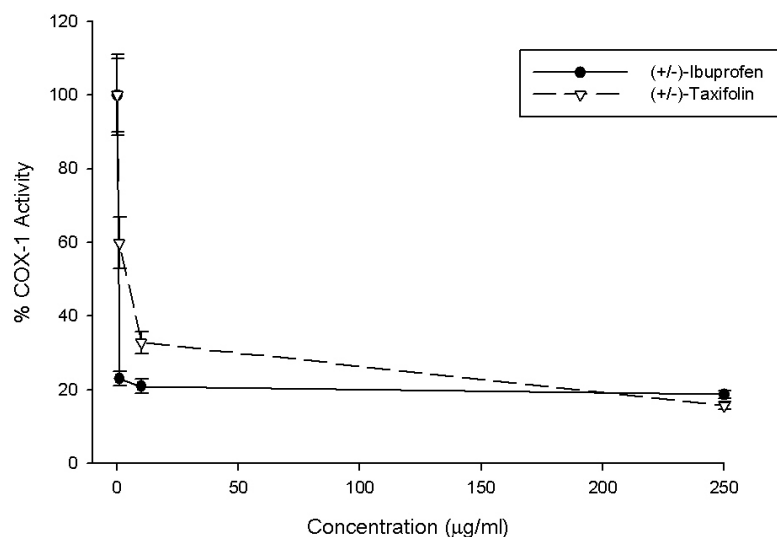
Figure 6.9. Cyclooxygenase-1 (COX-1) activity after addition of racemic taxifolin and ibuprofen (positive control) at concentrations 1.0 – 250.0 µg/ml (n = 3, mean ± S.E.M.). Values are expressed as percentage (%).

The COX-2 inhibitory activity of (+/-)-taxifolin was also evaluated (**Fig. 6.10**), and the IC_{50} was calculated (**Table 6.6**). (+/-)-Taxifolin exhibited higher inhibitory activity (lower IC_{50}) than (+/-)-ibuprofen and (+/-)-etodolac in the COX-2 inhibition assay. The lower IC_{50} value of (+/-)-taxifolin may suggest that this flavonoid is a more specific COX-2 inhibitor than (+/-)-ibuprofen and even (+/-)-etodolac. These results are in agreement with the observations that (+/-)-taxifolin inhibits inflammation in a HT-29 colitis model by decreasing the PGE_2 levels in a concentration dependent manner.
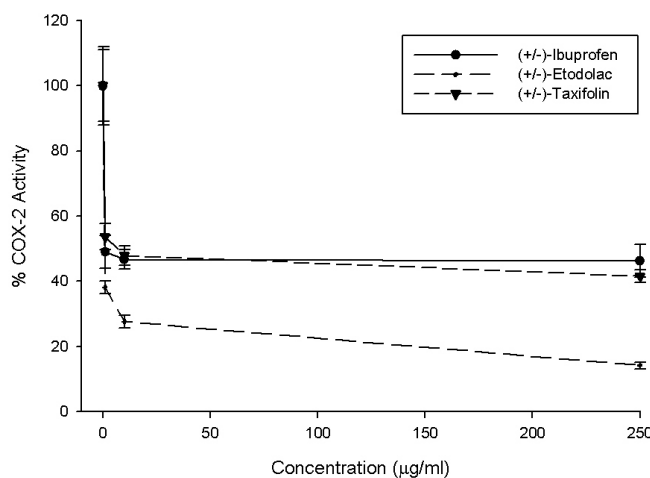
Figure 6.10. Cyclooxygenase-2 (COX-2) activity after addition of racemic taxifolin and ibuprofen and etodolac (positive controls) at concentrations 1.0 – 250.0 µg/ml (n = 3, mean ± S.E.M.). Values are expressed as percentage (%).

Furthermore, the COX-2 to COX-1 ratio was calculated to assess the preferential inhibitory activity for one of the COX isozymes involved primarily in inflammation. As shown in **Figure 6.11, (+/-)-**etodolac exhibited more selective COX-2 inhibition, while (+/-)-ibuprofen inhibited COX-1 and COX-2 to the same extent. Racemic taxifolin exhibited higher inhibition for COX-2, comparable to the selective COX-2 inhibition by (+/-)-etodolac, and at low concentrations it showed greater COX-2 inhibition than (+/-)-etodolac.
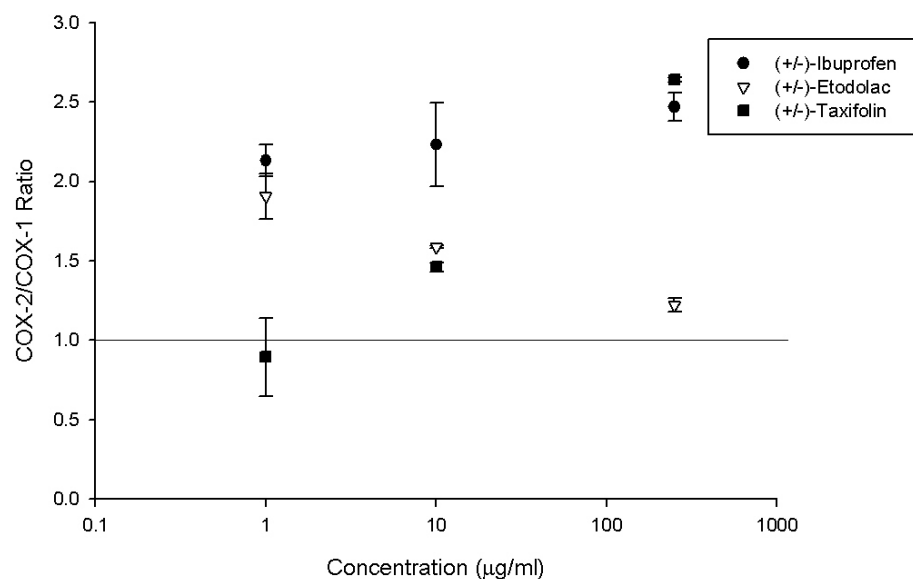
Figure 6.11. Cyclooxygenase-2 (COX-2) to cyclooxygenase-1 (COX-1) ratio of racemic taxifolin, ibuprofen, and etodolac as positive controls at concentrations $1.0 - 250.0$ µg/ml (n = 3, mean ± S.E.M.). Values are expressed as percentage (%). The line represents a ratio of 1 that would indicate equal inhibitory activity for both COX isomers.

Table 6.5. IC_{50} values in µg/ml (mM) of (+/-)-ibuprofen, (+/-)-etodolac (+/-)-isosakuranetin, 2R-isosakuranetin, 2S-isosakuranetin, and (+/-)-taxifolin for COX-1 inhibition (n = 3, mean ± S.E.M). a, $P < 0.05$, compared to ibuprofen; b, $P < 0.05$, racemate vs. enantiomers.

Compound	IC_{50}
(+/-)-Ibuprofen	$4.11E\text{-}08 \pm 6.17E\text{-}09$
	$(1.99E\text{-}07 \pm 2.99E\text{-}08)$
(+/-)-Isosakuranetin	$1.87E\text{+}08 \pm 14.70^{a}$
	$(6.51E\text{+}08 \pm 9.77E\text{+}07)$
2R-Isosakuranetin	$0.11 \pm 1.43E\text{-}02^{a,b}$
	(0.37 ± 0.06)
2S-Isosakuranetin	$0.08 \pm 1.23E\text{-}02^{a,b}$
	(0.29 ± 0.04)
(+/-)-Taxifolin	1.37 ± 0.02^{a}
	(4.50 ± 0.68)

Table 6.6. IC_{50} values in µg/ml (mM) of ibuprofen, etodolac (+/-)-isosakuranetin, 2R-isosakuranetin, 2S-isosakuranetin, and (+/-)-taxifolin for COX-2 inhibition (n = 3, mean ± S.E.M). a, $P < 0.05$, compared to ibuprofen; b, $P < 0.05$, compared to etodolac; c, $P < 0.05$, racemate vs. enantiomers.

Compound	IC_{50}
(+/-)-Ibuprofen	0.76 ± 0.01 (2.64 ± 0.20)
(+/-)-Etodolac	2.87E-02 ± 3.23E-03 (0.14 ± 0.02)
(+/-)-Isosakuranetin	0.81 ± 1.22E-02[b] (2.84 ± 0.43)
2R-Isosakuranetin	0.10 ± 1.23E-02[a,b,c] (0.35 ± 0.05)
2S-Isosakuranetin	7.22 ± 0.99[a,b,c] (25.22 ± 3.78)
(+/-)-Taxifolin	1.99E-02 ± 2.45E-03[a,b] (6.54E-02 ± 9.81E-03)

In summary, (+/-)-isosakuranetin, 2S-isosakuranetin, 2R-isosakuranetin, and (+/-)-taxifolin demonstrated COX-1 and COX-2 inhibitory activity. (+/-)-Taxifolin showed selective COX-2 inhibition greater than (+/-)-etodolac at low concentrations. These findings suggest that the anti-inflammatory activity reported for (+/-)-taxifolin may be related to its selective COX-2 inhibitory activity. The stereoseparation of all four taxifolin stereoisomers has been proven to be technically difficult (Chapter I). Similar to what has been reported with other chiral xenobiotics, configurational stability of taxifolin has been a limiting factor in the development of methods of stereoseparation [7]. Isomerization of taxifolin has been reported by Kielhmann and Edmond [123], which has limited the commercial development of pure stereoisomers; thus, only the (2R3R)-(+)-is commercially available. Though the isolation of the stereoisomers of taxifolin is possible, concerns with the configurational stability of these compounds limited the number of investigations performed.

6.4.4 In vitro Anti-oxidant activity

The principle behind this assay is the formation of the ferryl myoglobin radical from metmyoglobin and hydrogen peroxide which then oxidizes ABTS to produce a radical cation, $ABTS^{\bullet+}$. This technique measures the total anti-oxidant capacity of a compound relying on the ability of the anti-oxidants in the sample to inhibit the oxidation of ABTS to $ABTS^{\bullet+}$ by metmyoglobin – the oxidized form of the oxygen-carrier protein myoglobin – rather than the direct reduction of ferryl myoglobin [170]. The capacity of the anti-oxidants in the sample to prevent ABTS oxidation is compared with that of Trolox$^{®}$, a water-soluble tocopherol analogue used as positive control.

The anti-oxidant activity of (+/-)-homoeriodicytol, S(-)-homoeriodicytol, (+/-)-isosakuranetin, didymin, poncirin, (+/-)-taxifolin, (2R3R)-(+)-taxifolin and astilbin was assessed.

6.4.4.1   Homoeriodictyol

The anti-oxidant activity of racemic and S(-)-homoeriodicytol was assessed using the ABTS method. S(-)-homoeriodicytol showed greater anti-oxidant activity (lower IC_{50}) than (+/-)-homoeriodicytol (**Fig. 6.12** and **Table 6.7**); this may suggest an antagonistic effect when the S(-)- and R(+)-enantiomers are given together in the racemic mixture. In addition, both racemic and enantiomeric homoeriodicytol showed concentration-dependent anti-oxidant activity.
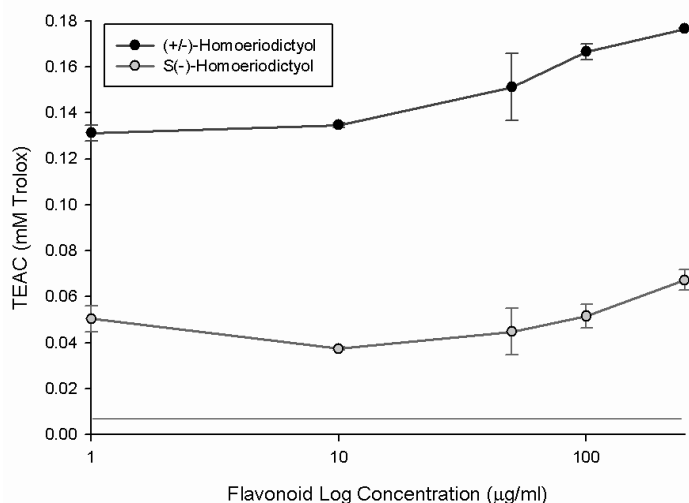
Figure 6.12. Trolox® equivalent anti-oxidant capacity (TEAC) of homoeriodicytol and S(-)-homoeriodicytol (n = 4, mean ± S.E.M.). The line represents the baseline level indicating the effect of DMSO alone.

Furthermore, (+/-)-homoeriodicytol (1.65 ± 0.24 µg/ml) showed anti-oxidant activity comparable to α-tocopherol (1.87 ± 0.28 µg/ml), whereas S(-)-homoeriodicytol (3.57E-02 ± 5.35E-03 µg/ml) demonstrated much greater anti-oxidant activity than α-tocopherol (**Table 6.7**). These results are quite unexpected, considering that the functional source of the anti-oxidant activity of racemic and enantiomeric homoeriodicytol is the free hydroxyl moieties present in the flavonoid backbone. These findings suggest that possible issues with the purity of the compound have to be assessed since they may be a source of interference for the anti-oxidant activity seen in S(-)-homoeriodicytol or enhanced activity of the racemate [171].

The anti-oxidant activity of homoeriodicytol has been previously studied; however, these studies have only taken into consideration the racemic mixture. The enantiomeric form of homoeriodicytol has been evaluated for its anti-oxidant activity for the first time. The findings suggest that the R(+) and S(-)-homoeriodicytol have different anti-oxidant activity. Further studies are necessary to elucidate the anti-oxidant activity of R(+)-homoeriodicytol.

Even though the HPLC method described in Chapter II allows the isolation of R(+)-homoeriodicytol, the cost of the racemic compound and the time need to collect enough pure enantiomer for the assay are limiting factors. Similar to what was seen for taxifolin and other chiral xenobiotics, the stability of homoeriodicytol may also be prohibitive for biological characterization.

6.4.4.2   Isosakuranetin

The anti-oxidant activity of isosakuranetin and two of its glycosides was assessed using the ABTS method. Poncirin, a neohesperidose of 2S-isosakuranetin, showed greater anti-oxidant activity (lower IC_{50}) than isosakuranetin and didymin, a rutinose of 2S-isosakuranetin (**Fig. 6.13** and **Table 6.7**) suggesting greater anti-oxidant activity for the 2S-configuration when attached to a neohesperidose sugar. (+/-)-Isosakuranetin, poncirin, and didymin demonstrated greater anti-oxidant activity than α-tocopherol.
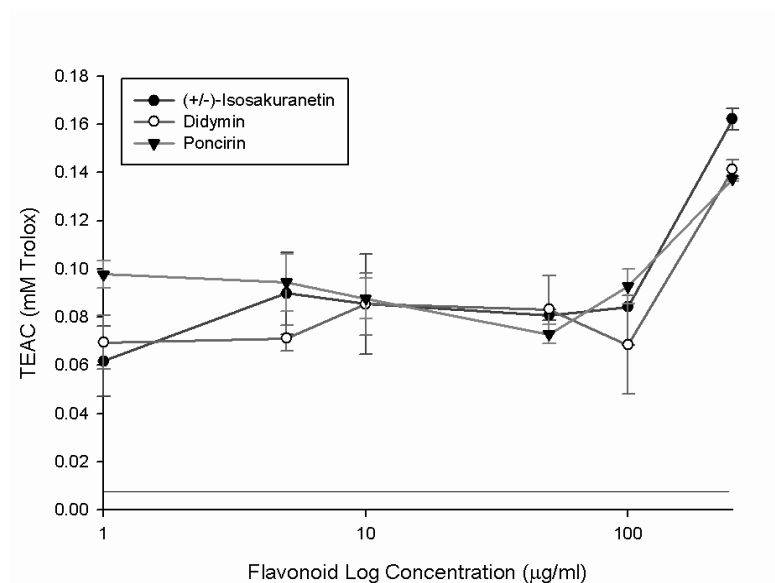
Figure 6.13. Trolox® equivalent anti-oxidant capacity (TEAC) of isosakuranetin, poncirin, and didymin (n = 4, mean ± S.E.M.). The line represents the baseline level indicating the effect of DMSO alone.

Previous studies have demonstrated the anti-oxidant activity of racemic isosakuranetin; however, the enantiomers of isosakuranetin have not been previously evaluated. Further studies are necessary to evaluate the anti-oxidant capacity of 2R- and 2S-isosakuranetin, and although the method of separation described in Chapter III can be used to isolate these enantiomers, the cost of the compound and the time needed to collect the individual enantiomers are limiting factors. Alternative ways of preparately isolating or synthesizing isosakuranetin enantiomers are necessary.

6.4.4.3   Taxifolin

The anti-oxidant activity of racemic and enantiomeric taxifolin, as well as its rhamnoside was assessed using the ABTS method. (2R3R)-(+)-taxifolin and astilbin, a rhamnoside of (2R3R)-(+)-taxifolin, showed comparable concentration-dependent anti-oxidant activity (**Fig. 6.14**). The anti-oxidant activity of (+/-)-taxifolin was comparable to (2R3R)-(+)-taxifolin at concentrations 1.0 to 50.0 µg/ml; however, at higher concentrations (100.0 and 250.0 µg/ml) the anti-oxidant activity of (2R3R)-(+)-taxifolin was much greater than that of the racemic form.

The IC_{50} values for (+/-)-taxifolin, (2R3R)-(+)-taxifolin, and astilbin to inhibit the formation of ABTS radical were calculated (**Table 6.7**). (+/-)-Taxifolin showed greater anti-oxidant capacity than the (2R3R)-(+)-taxifolin. The IC_{50} value of (2R3R)-(+)-taxifolin is lower than the expected for an additive effect model (a fourth of (+/-)-taxifolin = 5.07E-05 µg/ml) which suggests that a synergistic interaction is responsible for the (+/-)-taxifolin anti-

oxidant activity or impurities in the racemate or (2R3R)-(+)-taxifolin influence anti-oxidant activity.
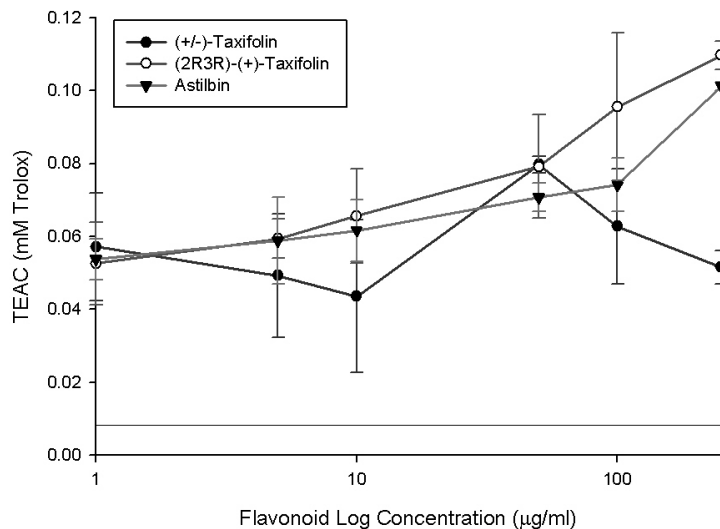
Figure 6.14. Trolox® equivalent anti-oxidant capacity (TEAC) of racemic taxifolin, (2R3R)-(+)-taxifolin and astilbin, a glycoside of (2R3R)-(+)-taxifolin (n = 4, mean ± S.E.M.). The line represents the baseline level indicating the effect of DMSO alone.

The IC_{50} values of the racemic flavonoids, the enantiomeric forms and glycosides to inhibit ABTS radical formation were calculated (**Table 6.7**). The IC_{50} values were compared to α-tocopherol, a recognized anti-oxidant. S(-)-Homoeriodictyol showed greater anti-oxidant capacity than (+/-)-homoeriodicytol. In comparison, (+/-)-taxifolin showed greater anti-oxidant activity compared to the (2R3R)-(+)-stereoisomer; and the rhamnoside of (2R3R)-(+)-taxifolin, astilbin, showed lower anti-oxidant activity than the aglycone. (+/-)-Isosakuranetin also demonstrated anti-oxidant activity comparable to α-tocopherol, and the neohesperidose of 2S-isosakuranetin (poncirin) showed greater anti-oxidant activity than the rutinose (didymin).

Table 6.7. IC_{50} values in µg/ml (mM) for (+/-)-homoeriodicytol, S(-)-homoeriodicytol, (+/-)-isosakuranetin, didymin, poncirin, (+/-)-taxifolin, (2R3R)-(+)-taxifolin, astilbin, and tocopherol as positive control to inhibit ABTS radical formation (n = 4, mean ± S.E.M.). a, P < 0.05, compared to α-tocopherol; b, P < 0,05, racemate vs. stereoisomers.

Compound	IC_{50}
α-Tocopherol	$1.87 \pm 2.80E\text{-}01$
	(4.34 ± 0.65)
(+/-)-Homoeriodictyol	$1.65 \pm 2.47E\text{-}01^{b}$
	(5.44 ± 0.82)
S(-)-Homoeriodictyol	$3.57E\text{-}02 \pm 5.35E\text{-}03^{a}$
	(0.12 ± 0.02)
(+/-)-Isosakuranetin	$1.47 \pm 2.21E\text{-}01$
	(5.14 ± 0.77)
Didymin	$2.22E\text{-}01 \pm 3.34E\text{-}02^{a}$
	(0.78 ± 0.12)
Poncirin	$1.26E\text{-}03 \pm 1.88E\text{-}04^{a}$
	$(4.38E\text{-}03 \pm 6.58E\text{-}04)$
(+/-)-Taxifolin	$2.03E\text{-}04 \pm 3.05E\text{-}05^{a}$
	$(6.67E\text{-}04 \pm 1.00E\text{-}05)$
(2R3R)-(+)-Taxifolin	$3.15E\text{-}01 \pm 4.72E\text{-}02^{a,b}$
	(1.03 ± 0.01)
Astilbin	$7.45E\text{-}01 \pm 1.12E\text{-}01^{a}$
	(1.65 ± 0.25)

In summary, the anti-oxidant capacity of homoeriodicytol, isosakuranetin, and taxifolin was evaluated to assess the effect of each stereoisomer. The findings suggest that the stereoisomers of each compound may be differentially responsible for the anti-oxidant capacity of (+/-)-homoeriodicytol, (+/-)-isosakuranetin, and (+/-)-taxifolin.

6.4.5 In vitro Histone Deacetylases (HDAC) Activity

Nucleosomes contain two molecules each of the histones H2A, H2B, H3, and H4; forming the fundamental repeating units of eukaryotic chromatin which fold chromosomal DNA. Acetylation, phosphorylation, ubiquination, and methylation can modify the histone amino termini extending from the core of the nucleosome during post-translation events. Acetylation in particular, modifies ε-amino groups of specific histone lysines due to histone

acetyltransferases (HATs) activity. This translates into open chromatin structure and gene activation. On the other hand, deacetylation removes the acetyl groups from histone lysine residues by hydrolysis through histone deacetylases (HDACs). This translates into chromatin condensation and transcriptional repression. Therefore, HDAC inhibition accomplishes transcriptional activation of DNA due to chromatin relaxation. If transcriptional changes in key genes are accomplished by HDAC inhibitors, angiogenesis and cell cycling are blocked; whereas, apoptosis and differentiation are promoted [172]. Due to their effect in these key events of tumor proliferation, HDAC inhibitors are currently being studied as potential anti-cancer agents [173].

The HDAC inhibitory activity of homoeriodicytol, isosakuranetin, and taxifolin was assessed using an ELISA assay. Trichostatin A (TSA) was used for its known HDAC inhibitory activity. TSA has been reported to enhance G(2)/M cell cycle arrest, promote apoptosis through multiple pathways, and interfere with DNA damage repair processes [174].

6.4.5.1 Homoeriodictyol

Racemic homoeriodicytol was assessed for its HDAC inhibitory activity using a commercially available ELISA assay. The HDAC activity decreased in a concentration-dependent manner with (+/-)-homoeriodicytol (1.0 – 100.0 µg/ml) in the presence or absence of trichostatin A, an HDAC inhibitor. In fact, all concentrations of (+/-)-homoeriodicytol decreased the activity of HDAC below baseline levels (**Fig. 6.15**).

The inhibitory effect of homoeriodicytol in HDAC activity has not been previously studied. These findings suggest that (+/-)-homoeriodicytol may act as an anti-cancer agent by inhibiting HDAC activity. Future studies with the stereoisomers of homoeriodicytol are

necessary to understand their role in HDAC inhibition. The anti-cancer studies in different cell lines suggest that R(+)-homoeriodicytol and S(-)-homoeridictyol may produce their anti-cancer effect by different mechanisms. Therefore, it is important to understand the inhibitory effect of R(+)-homoeridictyol and S(-)-homoeriodicytol independently.
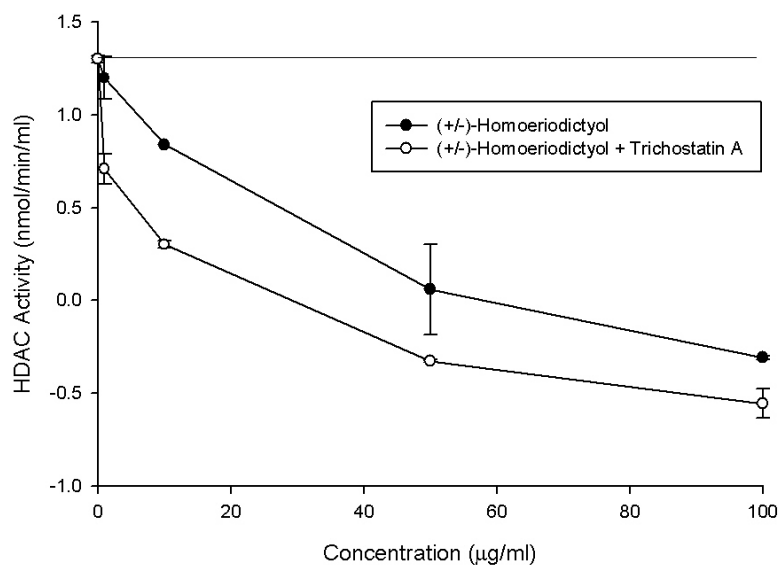
Figure 6.15. HDAC activity of (+/-)-homoeriodicytol (n = 3, mean ± S.E.M.). The line represents the baseline level indicating the effect of DMSO alone.

6.4.5.2   Taxifolin

Racemic taxifolin was assessed for its HDAC inhibitory activity using a commercially available ELISA kit (**Fig. 6.16**). (+/-)-Taxifolin did not show a clear concentration-dependent inhibition of HDAC activity (1.0 – 100.0 µg/ml) in the presence or absence of trichostatin A, an HDAC inhibitor. Only the lowest and highest concentrations of (+/-)-taxifolin tested (1.0 and 100.0 µg/ml) reduced HDAC activity below baseline level. In comparison, 10.0 and 50.0

µg/ml of (+/-)-taxifolin seemed to promote HDAC activity instead. (+/-)-Taxifolin was not as effective as (+/-)-homoeriodicytol in inhibiting the activity of histone deacetyltransferases.
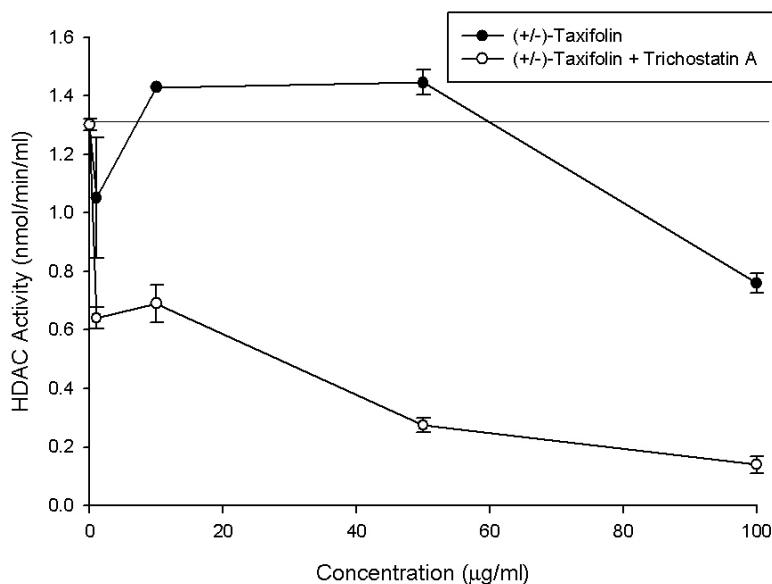
Figure 6.16. HDAC activity of (+/-)-taxifolin (n = 3, mean ± S.E.M.). The line represents the baseline level indicating the effect of DMSO alone.

The effect of taxifolin in HDAC activity has not been previously studied. The results obtained in different cancer cell lines may suggest issues with taxifolin solubility. Future studies are necessary to understand the role of taxifolin stereoisomers in the inhibition of HDAC activity. The anti-cancer studies in different cancer cell lines suggest that the stereoisomers of taxifolin may have different mechanisms of action in cancer. Therefore, studies of the inhibitory HDAC activity of each stereoisomer of taxifolin would be interesting to examine.

The IC_{50} values for (+/-)-homoeriodicytol and (+/-)-taxifolin to inhibit HDAC activity are reported in **Table 6.8**. (+/-)-Homoeriodictyol (42.61 ± 6.39 mM) showed greater inhibition of HDAC activity (lower IC_{50}) compared to (+/-)-taxifolin (345.06 ± 51.76 mM).

Table 6.8. IC_{50} values in µg/ml (mM) for (+/-)-homoeriodicytol and (+/-)-taxifolin to inhibit HDAC activity (n = 3, mean ± S.E.M.). a, P < 0.05.

Compound	IC_{50}
(+/-)-Homoeriodictyol	12.88 ± 1.93 (42.61 ± 6.39)
(+/-)-Taxifolin	104.98 ± 15.47[a] (345.06 ± 51.76)

In summary, the effect of homoeriodicytol and taxifolin in HDAC activity was reported for the first time. These findings support the results obtained in cancer cell line models. (+/-)-Homoeriodictyol inhibits HDAC activity more effectively than (+/-)-taxifolin. Further studies are necessary to elucidate the role of each stereoisomer in HDAC activity inhibition.

6.4.6 In vitro Anti-Adipogenic Activity

Adipose tissue in mammals is present as white adipose tissue (WAT), and brown adipose tissue (BAT). WAT stores excess energy as triglyceride in lipid droplets, whereas BAT uses lipids to generate heat during thermogenesis. Multipotent mesenchymal precursor cells originate adipocytes when committed to pre-adipocytes, either remaining dormant or becoming differentiated adipocytes. 3T3-L1 cells are a well characterized cell line used in the study of adipocyte differentiation [175]. This model system has helped elucidate the molecular basis and signaling pathways of adipogenesis. During terminal differentiation, the fibroblast-like pre-adipocytes undergo morphological and biochemical changes that result in the accumulation of lipid droplets *in vitro* and *in vivo* [175]. Oil Red O staining is used in

lipid droplets as an indicator of the degree of adipogenesis. The inhibitory effect of homoeriodicytol and taxifolin on the accumulation of lipid droplets in adipocytes *in vitro* was assessed using an ELISA assay.

6.4.6.1   Homoeriodictyol

The effect of racemic homoeriodicytol and S(-)-homoeridictyol on oil red O stained material (OROSM) in 3T3-L1 pre-adipocytes indicated a reduction in intracellular triglyceride formation and accumulation after differentiation into adipocytes (**Fig. 6.17** and **Table 6.8**). (+/-)-Homoeriodictyol and S(-)-homoeriodicytol were effective in a concentration dependent manner in the reduction of intracellular triglycerides; in fact, S(-)-homoeriodicytol was more effective (lower IC_{50}) than the racemic mixture. This suggests that there is an antagonistic effect when R(+)-homoeriodicytol and S(-)-homoeriodicytol are present together.
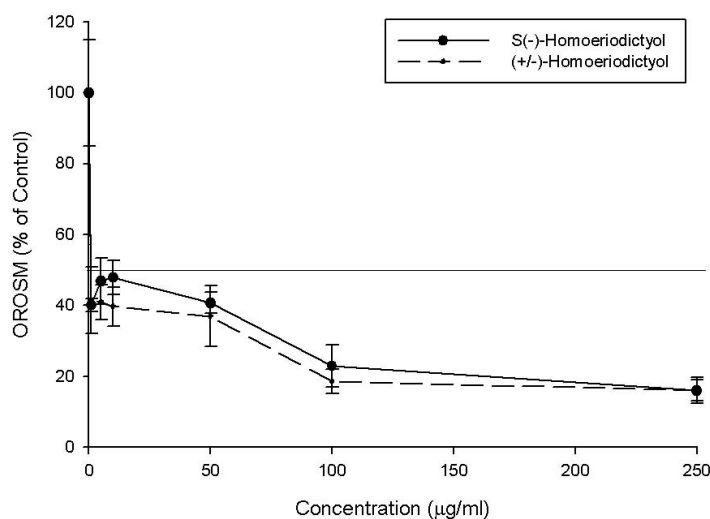
Figure 6.17. Effect of (+/-)-homoeriodicytol and S(-)-homoeriodicytol on oil red O stained material (OROSM) in 3T3-L1 adipocytes. 3T3-L1 pre-adipocytes were harvested 8 days after the initiation of differentiation and were stained with oil red O. Cells were treated with 0.0 – 250.0 µg/ml of (+/-)-homoeriodicytol and S(-)-homoeriodicytol for 72 hours at 37°C (n = 3, mean ± S.E.M.)

The effect of (+/-)-homoeriodicytol in adipogenesis has not been previously evaluated. These findings suggest that R(+)-homoeridictyol and S(-)-homoeriodicytol may have different effects in the accumulation of triglycerides in adipocytes. Future studies need to evaluate the effect of R(+)-homoeriodicytol in lipid droplet formation *in vitro*.

6.4.6.2   Isosakuranetin

The effect of (+/-)-isosakuranetin, didymin (2S-isosakuranetin rutinoside), and poncirin (2S-isosakuranetin neohesperidose) on oil red O stained material (OROSM) in 3T3-L1 pre-adipocytes is demonstrated in **Fig. 6.18** and **Table 6.8**. (+/-)-Isosakuranetin demonstrated to be effective in reducing the OROSM in a concentration dependent manner for concentrations between 1.0 and 50.0 µg/ml; whereas at higher concentrations (100.0 and 250.0 µg/ml) (+/-)-isosakuranetin seemed to induce the accumulation of intracellular triglyceride lipids measured with the OROSM. Poncirin was shown to be ineffective in reducing the OROSM in 3T3-L1 adipocytes and in fact promoted the accumulation of lipid droplets. On the other hand, didymin was demonstrated to both inhibit and induce triglycerides formation in adipocytes depending on the concentration. These data suggest that 2S-isosakuranetin has a greater effect in inhibiting the accumulation and formation of triglycerides in adipocytes when attached to a rutinose sugar.
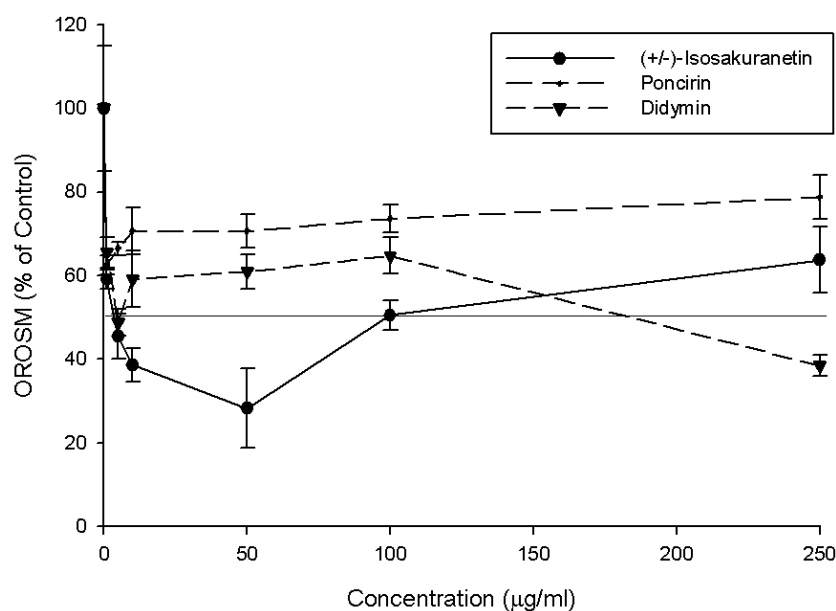
Figure 6.18. Effect of (+/-)-isosakuranetin, poncirin, and didymin on oil red O stained material (OROSM) in 3T3-L1 adipocytes. 3T3-L1 pre-adipocytes were harvested 8 days after the initiation of differentiation and were stained with oil red O. Cells were treated with 0.0 – 250.0 µg/ml of homoeriodicytol for 72 hours at 37°C (n = 3, mean ± S.E.M.)

The effect of isosakuranetin in adipogenesis has not been previously studied. Further studies are necessary to elucidate the effects of 2S-isosakuranetin and 2R-isosakuranetin in formation and accumulation of triglycerides in adipocytes *in vitro*.

6.4.6.3　Taxifolin

The effect of racemic taxifolin, (2R3R)-(+)-taxifolin, and astilbin ((2R3R)-(+)-taxifolin rhamnoside) on oil red O stained material (OROSM) in 3T3-L1 pre-adipocytes is shown in **Fig. 6.19** and **Table 6.8.** (2R3R)-(+)-Taxifolin was demonstrated to reduce intracellular triglyceride lipids accumulation and formation in adipocytes. (+/-)-Taxifolin reduced the formation of lipid droplets in adipocytes at low concentrations; however, at 10.0 and 50.0 µg/ml it seemed to promote the formation of triglycerides *in vitro*. Similarly, astilbin

reduced lipid droplets formation at low concentrations, but at high concentrations it promoted the formation of triglycerides.

These results suggest that possible issues with solubility of these compounds need to be carefully assessed. It might be possible that these compounds precipitate out of solution and therefore, the effect seen in inhibiting triglyceride formation might therefore be less than expected.
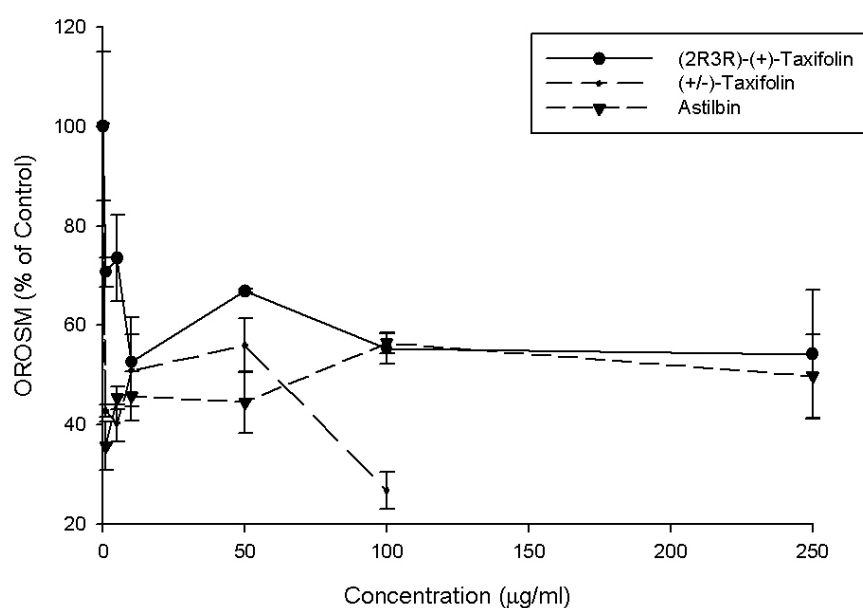
Figure 6.19. Effect of (+/-)-taxifolin, (2R3R)-(+)-taxifolin, and astilbin on oil red O stained material (OROSM) in 3T3-L1 adipocytes. 3T3-L1 pre-adipocytes were harvested 8 days after the initiation of differentiation and were stained with oil red O. Cells were treated with 0.0 – 250.0 µg/ml of homoeriodicytol for 72 hours at 37°C (n = 3, mean ± S.E.M.)

The effect of taxifolin in adipogenesis has not been previously evaluated. Further studies with (2S3R)-(+)-taxifolin, (2S3S)-(-)-taxifolin, and (2R3S)-(-)-taxifolin will contribute to our understanding of differences in stereochemistry of taxifolin in triglyceride formation and accumulation *in vitro*.

The IC_{50} values for (+/-)-homoeriodicytol, S(-)-homoeriodicytol, (+/-)-isosakuranetin, didymin, poncirin, (+/-)-taxifolin, (2R3R)-(+)-taxifolin, and astilbin for reduction on OROSM are shown in **Table 6.9.** Overall, the aglycones were more effective when compared to the glycosides. (+/-)-Taxifolin was demonstrated to be more effective (lower IC_{50}) than (+/-)-homoeridictyol, S(-)-homoeriodicytol, (+/-)-isosakuranetin, and (2R3R)-(+)-taxifolin in reducing the accumulation and formation of triglycerides in adipocytes cells *in vitro*.

Table 6.9. IC_{50} values in µg/ml (mM) for (+/-)-homoeriodicytol, S(-)-homoeriodicytol, (+/-)-isosakuranetin, didymin, poncirin, (+/-)-taxifolin, (2R3R)-(+)-taxifolin, and astilbin for reduction on oil red O stained material (OROSM) in 3T3-L1 adipocytes (n = 3, mean ± S.E.M.). a, $P < 0.05$, racemate vs. stereoisomer.

Compound	IC_{50}
(+/-)-Homoeriodictyol	0.80 ± 1.50
	(2.65 ± 0.40)
S(-)-Homoeriodictyol	0.82 ± 0.10
	(2.71 ± 0.41)
(+/-)-Isosakuranetin	50.84 ± 7.53
	(177.59 ± 26.64)
Didymin	51.08 ± 7.56
	(85.91 ± 12.89)
Poncirin	1233.26 ± 184.25
	(2074.24 ± 311.14)
(+/-)-Taxifolin	0.66 ± 0.09
	(2.17 ± 0.33)
(2R3R)-(+)-Taxifolin	7.81 ± 1.17[a]
	(25.67 ± 3.85)
Astilbin	0.62 ± 0.08
	(1.38 ± 0.21)

In summary, the effect of homoeriodicytol, isosakuranetin, and taxifolin in adipogenesis were studied for the first time. A concentration-dependent decrease in lipid droplets formation was evident in (+/-)-homoeriodicytol and S(-)-homoeriodicytol, but not in the other compounds studied. Nevertheless, a decrease in triglycerides in adipocytes was seen after treatment with (+/-)-isosakuranetin, didymin, and (+/-)-taxifolin, whereas poncirin and astilbin promoted triglyceride accumulation. Further studies are necessary to elucidate the role

of each stereoisomer of homoeriodicytol, isosakuranetin, and taxifolin in triglyceride formation and accumulation in adipocytes *in vitro*.

6.5 CONCLUSIONS

Overall, these studies have demonstrated that homoeriodicytol, isosakuranetin, and taxifolin have pharmacological activity in a variety of exploratory and well established *in vitro* assays. Interestingly, these investigations have revealed that small structural differences in the chemical structure of these compounds result in significant pharmacodynamic differences. These structural differences include glycosides, aglycones, enantiomers, and hydroxyl and methoxy substitution patterns.

Homoeriodictyol, isosakuranetin, and taxifolin demonstrated concentration-dependent anti-cancer activity. The results obtained with the pure stereoisomers, S(-)-homoeriodicytol, 2S-isosakuranetin, 2R-isosakuranetin, and (2R3R)-(+)-taxifolin, suggest that each stereoisomer contributed differently to the anti-cancer effect seen in the racemic mixtures.

(+/-)-Homoeriodictyol and (+/-)-taxifolin were evaluated for their effect in a colitis *in vitro* model in HT-29 colon adenocarcinoma cells for the first time. (+/-)-Homoeriodictyol and (+/-)-taxifolin demonstrated concentration-dependent reduction of PGE_2 levels in HT-29 cells. Further studies are necessary with the pure stereoisomers of homoeriodicytol and taxifolin to elucidate their potential differences in anti-inflammatory activity in colitis. Given the pharmacokinetics of these compounds and the extensive non-renal clearance, homoeriodicytol and taxifolin may be of potential therapeutic use in the treatment of pathologies of the GI tract such as inflammatory bowel disease.

(+/-)-Isosakuranetin, 2S-isosakuranetin, 2R-isosakuranetin, and (+/-)-taxifolin showed COX-1 and COX-2 inhibitory activity. Furthermore, (+/-)-taxifolin showed selective COX-2

inhibition greater than (+/-)-etodolac at low concentrations. These findings suggest that the anti-inflammatory activity reported for (+/-)-taxifolin may be related to its selective COX-2 inhibitory activity.

The anti-oxidant capacity of homoeriodicytol, isosakuranetin, and taxifolin was evaluated to assess the effect of each stereoisomer. The findings suggest that the stereoisomers of each compound may be differentially responsible for the anti-oxidant capacity of (+/-)-homoeriodicytol, (+/-)-isosakuranetin, and (+/-)-taxifolin.

The effect of homoeriodicytol and taxifolin in HDAC activity was evaluated for the first time. These findings support the results obtained in cancer cell line models and suggest that their anti-cancer activity may be associated with their HDAC inhibitory activity. The results suggested that (+/-)-homoeriodicytol inhibits HDAC activity more effectively than (+/-)-taxifolin. Further studies are necessary to elucidate the role of each stereoisomer in HDAC activity inhibition, and the possible synergistic activity of these compounds in cancer chemotherapy.

The effect of homoeriodicytol, isosakuranetin, and taxifolin in adipogenesis were studied for the first time. A concentration-dependent decrease in lipid droplets formation was evident in (+/-)-homoeriodicytol and S(-)-homoeriodicytol, but not in the other compounds studied. Nevertheless, a decrease in triglycerides in adipocytes was seen after treatment with (+/-)-isosakuranetin, didymin, and (+/-)-taxifolin, whereas poncirin and astilbin promoted triglyceride accumulation. Further studies are necessary to elucidate the role of each stereoisomer of homoeriodicytol, isosakuranetin, and taxifolin in triglyceride formation and accumulation in adipocytes *in vitro*.

These studies demonstrated the utility and necessity of developing stereoselective HPLC methods for chiral flavonoids. The validated HPLC methods described in Chapter III were successfully used to isolate the stereoisomers of isosakuranetin that are not commercially available. Nonetheless, the expense and time needed to collect enough quantity of the compounds limited the number of investigations able to be conducted. A number of technical issues require further experimental scrutiny including: purity of the compounds obtained from commercial suppliers, isomerization, racemization, stability, stereoselective release, and solubility.

7 <u>Analysis of Selected Polyphenol Content in Tomatoes (*Solanum lycopersicum* L.)</u>

7.1 INTRODUCTION

This chapter describes the quantification of the content of selected polyphenols – ellagic acid, fisetin, hesperetin, kaempferol, quercetin, phloretin, myricetin, R(+)-naringenin, S(-)-naringenin, and taxifolin – in tomatoes grown in two distinct soil fertility management systems – organic and conventional – in a glasshouse at the Pullman campus of Washington State University. Polyphenol quantification was accomplished using reverse phase high performance liquid chromatography, RP-HPLC.

7.2 BACKGROUND

The tomato (*Solanum lycopersicum* L.), a Solanaceae member, is native to Central, South and southern North America. Tomatoes are grown worldwide for their edible fruits, and the United States is the second largest tomato producer in the world after China [176]. California and Florida are the states with the largest production of processed and fresh tomatoes, respectively in the United States [177]. Tomato consumption has been linked to health benefits due to the presence of lycopene (MW = 536.87 g/mol; XLogP = 10.2); however, the United States' Food and Drug Administration (FDA) has found no credible evidence to support the association between lycopene consumption and reduced risk of certain cancers [178]. Nevertheless, this has not prevented the processed-tomato industry from using qualified health claims on their product labels since the standards for health claims are less stringent than for drugs [179]. Lycopene as a food component and tomatoes as food were evaluated separately by the FDA for lung, colorectal, gastric, breast, cervical, ovarian, endometrial, and pancreatic cancers [178]. The FDA reported that there is limited credible evidence that tomato consumption is associated with a reduced risk of prostate, gastric, ovarian, and pancreatic cancers, whereas in lung, colorectal, breast, cervical, and endometrial cancers the evidence does not support the health benefit claims associated with tomato consumption. In the case of lycopene, dietary lycopene intake was demonstrated to be poorly correlated to serum lycopene levels. Moreover, the FDA concluded that there is no credible evidence supporting the relationship between lycopene consumption and any of the cancers evaluated in the studies that exist to date [178].

Tomato consumption has been correlated with the low mortality rate from coronary heart disease (CHD) in the Mediterranean region of Southern Europe [180]. The Mediterranean-style diet consists of a non-strict vegetarian diet rich in oleic acid, omega-3

fatty acids, fiber, B vitamins, and anti-oxidants, and low in saturated and polyunsaturated fats [180]. Various studies have produced contradictory results regarding the role of the health systems and welfare on the effect of the Mediterranean-style diet and CHD. A randomized single-blinded secondary prevention trial concluded that a 50 to 70% reduction in the risk of cardiovascular complications was achieved in patients following a Mediterranean dietary pattern for 46 months [181]. Following this report, the American Heart Association stated that the Mediterranean diet had a high content of alpha-linolenic acid, but that high dietary diversity is a more important factor rather than a single food or beverage in the diet [180]. However, the National Cancer Institute has included tomatoes in the list of cancer preventive plant-food sources along with garlic, ginger, onion, and legumes [3].

Analysis of the polyphenolic content in tomatoes has been limited. Transgenic tomatoes obtained by overexpression of the gene encoding stilbene synthase were used to analyze the content of stilbenes using HPLC and photodiodearray (PDA) detection [182]. Rutin – a quercetin glycoside – and naringenin demonstrated the highest concentrations in peel (80.32 and 31.68 mg/kg, respectively) and whole fruit (4.32 and 23.92 mg/kg, respectively) of wild-type tomatoes. However, transgenic tomatoes showed lower concentrations of these flavonoids in both peel (39.13 and 13.2 mg/kg, respectively) and whole fruit (3.27 and 8.42 mg/kg, respectively). The highest amount of stilbenes was found in their glycosylated form in peel of tomato at mature stages of ripening. To our knowledge, there have not been extensive studies that describe the content of selected polyphenols in different hybrid tomato cultivars using two distinct fertility management systems. Moreover, the stereospecific content of R(-)-naringenin and S(+)-naringenin has not been determined in tomato except in studies in our laboratories at Washington State University [152,183,184].

7.3   METHODS

7.3.1 HPLC Apparatus and Conditions

The HPLC system used was a Shimadzu HPLC (Kyoto, Japan), consisting of an LC-10ATVP pump, a SIL-10AF auto injector, a SPD-M10A VP spectrophotometric diodearray detector, and a SCL-10A VP system controller. Data collection and integration were accomplished using Shimadzu EZ Start 7.1.1 SP1 software. The analytical column used was Chiralcel® OD-RH column (150mm × 4.6mm i.d., 5-µm particle size, Chiral Technologies Inc., PA, USA) protected by a Chiralcel OD-RH guard column (0.4cm x 1cm, 5-µm particle size). The mobile phase consisted of acetonitrile, water and phosphoric acid (30:70:0.04, v/v/v), filtered and degassed. Separation was carried out isocratically at $25 \pm 1°C$, a flow rate of 0.4 ml/min, with ultraviolet (UV) detection at 292 nm.

7.3.2 Chemicals and Reagents

Racemic taxifolin was purchased from Indofine Chemical Company (Hillsborough, NJ, USA). Diadzein, ellagic acid, fisetin, hesperetin, kaempferol, quercetin, phloretin, myricetin, naringenin, formic acid, and β-glucuronidase from *Helix pomatia* Type-HP-2 were purchased from Sigma Chemicals (St Louis, MO, USA). HPLC grade acetonitrile, methanol, and water were purchased from J. T. Baker (Phillipsburg, NJ, USA). Phosphoric acid was purchased from Aldrich Chemical Co. Inc. (Milwaukee, WI, USA).

7.3.3 Stock and Working Standard Solutions

Diadzein, ellagic acid, fisetin, hesperetin, kaempferol, quercetin, phloretin, myricetin, naringenin, and taxifolin solutions of 100.0 μg/ml were dissolved in methanol. Diadzein was used as internal standard (IS). These solutions were protected from light and stored at -20°C between uses, for no longer than three months. Calibration standard curves in water were prepared from the stock solutions by sequential dilution, yielding concentrations of 0.5, 1.0, 5.0, 10.0, 50.0 and 100.0 μg/ml. Diadzein was used as internal standard (IS).

7.3.4 Plant Material

Three hybrid tomato (*Solanum lycopersicum* L.) cultivars varying in fruit size from small ('Octavio'), to medium ('First Lady'), to large ('Big Beef') were grown in Spring/Summer 2007 in the Agricultural Research Center's Plant Growth Facilities at the Pullman campus of Washington State University. Either cultivar was grown in each organic (75% v/v Sunshine Organic Planting Mix, Sun-Gro Horticulture, 25% v/v Whitney Farms Planting Compost, 5% v/v Palouse silt-loam top soil) or conventional (100% Sunshine LC1 Professional Growing Media, Sun-Gro Horticulture) growth media and fertilized with either organic (BioLink 5-5-5 Organic All-Purpose and Organic Micronutrient Fertilizers, Westbridge) or conventional (Peters Professional 20-20-20 General Purpose and Soluble Trace Element Mix Fertilizers, Scotts Co.) liquid fertilizers, with approximately equal amounts of total nitrogen for each fertilizer treatment. A 4-block Randomized Complete Block (RCB) design in a glasshouse (14 hours, 21.1°C/ 10 hours, 18.3°C day/night temperatures) was used, and 1000 W metal-halide lamps were used to supplement natural daylight.

7.3.5 Sample Preparation

Extraction of ellagic acid, fisetin, hesperetin, kaempferol, quercetin, phloretin, myricetin, naringenin, and taxifolin for analysis of polyphenolic content from *Solanum lycopersicum* L. samples was accomplished as follows: 0.1 g of sample (pericarp) was measured and frozen under liquid nitrogen. Each sample was prepared in duplicate; the frozen samples were placed into an extraction glass tube and 1.0 ml of methanol was added. Extraction was performed for 1 minute using a Thomas tissue grinder (Thomas Scientific, Swedesboro, NJ, USA). The extraction mix and fruit tissue were placed into a 2.0 ml Eppendorf tube, 0.5 ml of methanol was added to the extraction glass for rinsing and combined with the extraction mix. A total volume of 1.5 ml was obtained per extraction; the samples were vortexed for 30 seconds and centrifuged at 5,000 r.p.m. for 5 minutes. One of the duplicates was treated to extract only aglycones (free) and the second of the duplicates was treated with β-glucuronidase from *Helix pomatia* Type HP-2 to cleave any glycosides to aglycones (total) [147]. The supernatant of the free samples was transferred into 2.0 ml Eppendorf tubes, and 25.0 µl of IS was added, samples were vortexed for 10 seconds, dried to completion under nitrogen gas using an analytical evaporator, and stored at 4°C before analysis. The supernatant of the total samples was transferred into 15 ml conical tubes. The total samples were dried to completion under nitrogen gas, then 1.0 ml of HPLC-grade water, 110.0 µl 0.78 M sodium acetate-acetic acid buffer (pH 4.8), and 100.0 µl 0.1 M ascorbic acid were added. The samples were vortexed for 30 seconds, and incubated for 17 - 24 hours at 37°C in a shaking incubator following the addition of 200.0 µl of crude preparation of β-glucuronidase from *Helix pomatia* Type HP-2. After incubation, 1.0 ml of ice-cold

acetonitrile was added to stop the enzymatic activity of β-glucuronidase, the samples were vortexed for 10 seconds, and centrifuged at 5,000 r.p.m. for 5 minutes. The supernatant was collected into 15 ml conical tubes and dried to completion under nitrogen gas using an analytical evaporator after 25.0 µl of IS was added; then were subsequently stored at 4°C before analysis. When all samples were ready for analysis, free and total samples were reconstituted in 200.0 µl of mobile phase, vortexed for 30 seconds, and centrifuged at 5,000 r.p.m. for 5 minutes; 150.0 µl were injected into the HPLC system for analysis. Glycoside content was calculated by subtracting the concentration of the free samples from the incubated total samples.

7.3.6 Data Analysis

Data analysis was performed using Excel 4.0. Quantification was based on calibration curves constructed using PAR of ellagic acid, fisetin, hesperetin, kaempferol, quercetin, phloretin, myricetin, naringenin, and taxifolin to IS, against ellagic acid, fisetin, hesperetin, kaempferol, quercetin, phloretin, myricetin, naringenin, and taxifolin concentrations using unweighted least squares linear regression.

7.4   RESULTS AND DISCUSSION

7.4.1 Chromatography

Separation of ellagic acid, fisetin, hesperetin, kaempferol, quercetin, phloretin, myricetin, R(+)- and S(-)- naringenin, taxifolin and the internal standard (IS) diadzein in tomatoes was successfully achieved **(Fig. 7.1.2).** No interfering peaks co-eluting with the compounds of interest were detected **(Fig. 7.1.1)**. The retention times of ellagic acid, taxifolin,

myricetin, fisetin, quercetin, phloretin, R(+)-naringenin, S(-)-naringenin, hesperetin, and kaempferol were approximately 14, 15, 17, 18, 30, 38, 55, 60, 70, and 80 minutes, respectively. The IS diadzein eluted at approximately 24 minutes (**Fig. 7.1**). Optimal separation was achieved when the combination of acetonitrile, water and phosphoric acid was 30:70:0.04 (v/v/v) and the flow rate 0.37 ml/min. The total run time of the method was 90 minutes.
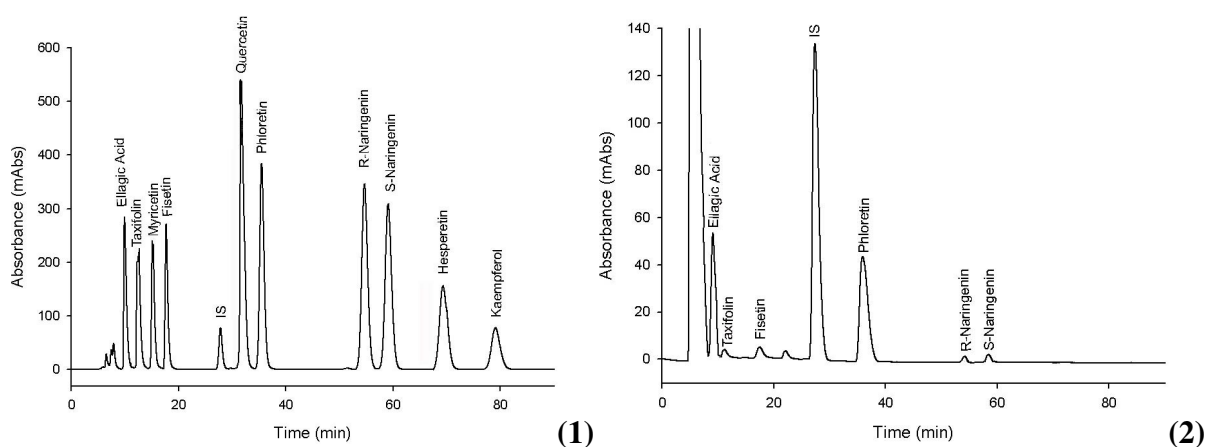
Figure 7.1. Representative chromatographs of standards and a tomato (*Solanum lycopersicum*) sample. (**1**) Ellagic acid, taxifolin, myricetin, fisetin, quercetin, phloretin, R(+)-naringenin, S(-)-naringenin, hesperetin, and kaempferol standards(10.0 µg/ml) in water (**2**) Compounds detected in an actual tomato sample. Diadzein was used as internal standard (IS) and it eluted at approximately 24 minutes.

To our knowledge, this is the first report identifying the presence of taxifolin in tomatoes. Subsequent to this study, the chiral method of analysis presented in Chapter IV was ultimately developed. In addition, homoeriodicytol and isosakuranetin were not present in tomatoes. The stereospecific content of (+/-)-taxifolin was subsequently analyzed in selected tomato samples (**Fig. 7.2**). There were no interfering peaks eluting with the compounds of interest. The validated HPLC method described in Chapter IV was used to analyzed the

content of (2S3R)-(+)-taxifolin (56.20% ± 5.06), (2S3S)-(-)-taxifolin (2.88% ± 0.35), (2R3R)-(+)-taxifolin (26.76% ± 3.75), and (2R3S)-(-)-taxifolin (14.16% ± 1.70) in tomato samples with high (+/-)-taxifolin content. (2S3R)-(+)-taxifolin and (2R3R)-(+)-taxifolin were predominant in the tomato samples studied. To our knowledge, this is the first report of the stereospecific content of taxifolin in tomatoes.
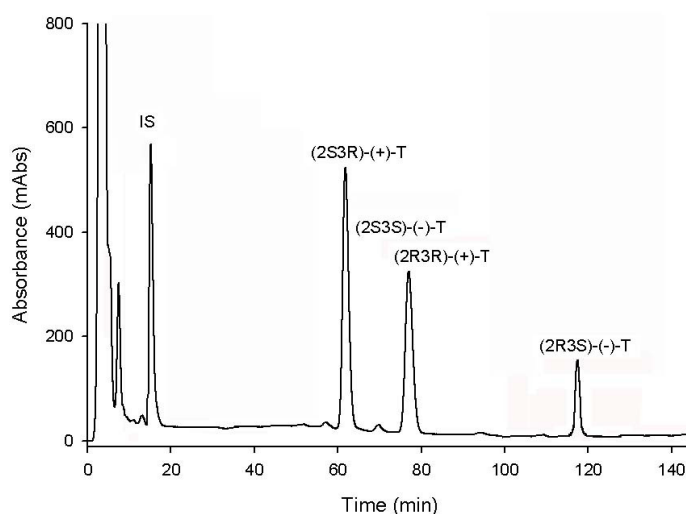
Figure 7.2. Representative chromatograph of tomato (*Solanum lycopersicum*) samples. The stereoisomers of (+/-)-taxifolin were detected in tomato samples using the validated HPLC method described in Chapter IV.

7.4.2 Polyphenol Content of Tomatoes

7.4.2.1 Aglycone Content of Selected Polyphenols

The content of ellagic acid, taxifolin, myricetin, fisetin, quercetin, phloretin, R(+)-naringenin, S(-)-naringenin, hesperidin, and kaempferol was quantified in both conventionally- and organically-grown tomatoes harvested in WSU facilities as described in section 7.3.4. The content of these selected flavonoids in the 'First Lady' tomato cultivar is presented in **Fig. 7.3.**

Myricetin (12.22 ± 3.41 mg/100 g FW) was predominant in conventionally-grown tomatoes, whereas kaempferol (0.85 ± 0.09 mg/100 g FW) was the aglycone with the lowest concentration. In comparison, organically grown 'First Lady' tomatoes showed hesperetin (8.85 ± 8.66 mg/100 g FW) to be the aglycone with the highest concentration and kaempferol (0.07 ± 0.07 mg/100 g FW) the polyphenol with the lowest concentration.

These results do not support previous findings that reported racemic naringenin as the polyphenol with the highest concentration in tomatoes [182]. This discrepancy (seen for both the aglycone and glycoside content of tomatoes) may be due to the fact that a different cultivar was analyzed; Nicoletti *et. al.* studied the polyphenolic content of red fruit of the 'Money Maker' tomato in Italy. In the red fruit of 'Money Maker', racemic naringenin and rutin were reported to be the predominant polyphenols for the aglycone and glycoside forms, respectively [182]. Even though a myricetin analysis method was developed by Nicoletti *et. al.*, no quantification data were reported for this polyphenol in 'Money Maker'.

In conventionally grown 'First Lady' tomatoes, myricetin was the polyphenol in the aglycone form with the highest concentration followed by fisetin, ellagic acid, taxifolin, R(+)-naringenin, quercetin, S(-)-naringenin, hesperetin, phloretin, and kaempferol (**Fig. 7.3**). On the other hand, 'First Lady' tomatoes grown using organic soil fertility conditions showed hesperetin to be the polyphenol with the highest concentration followed by fisetin, myricetin, quercetin, ellagic acid, R(+)-naringenin, S(-)-naringenin, phloretin, and kaempferol (**Fig. 7.3**).

These findings suggest that the use of varied soil fertility conditions may result in disproportionate polyphenolic content of these aglycones in tomatoes. However, these preliminary data do not include separate analysis of the polyphenolic content in the epidermis of tomatoes. Polyphenols are usually accumulated in this layer of cells in fruit were they can

exert their protective properties against environmental stresses [4]. Therefore, the analysis of epidermal peel samples is important to assess the total polyphenolic content in fruit of 'First Lady'. The evaluation of the polyphenolic composition in epidermal tissue in 'First Lady' tomato cultivar remains to be determined.
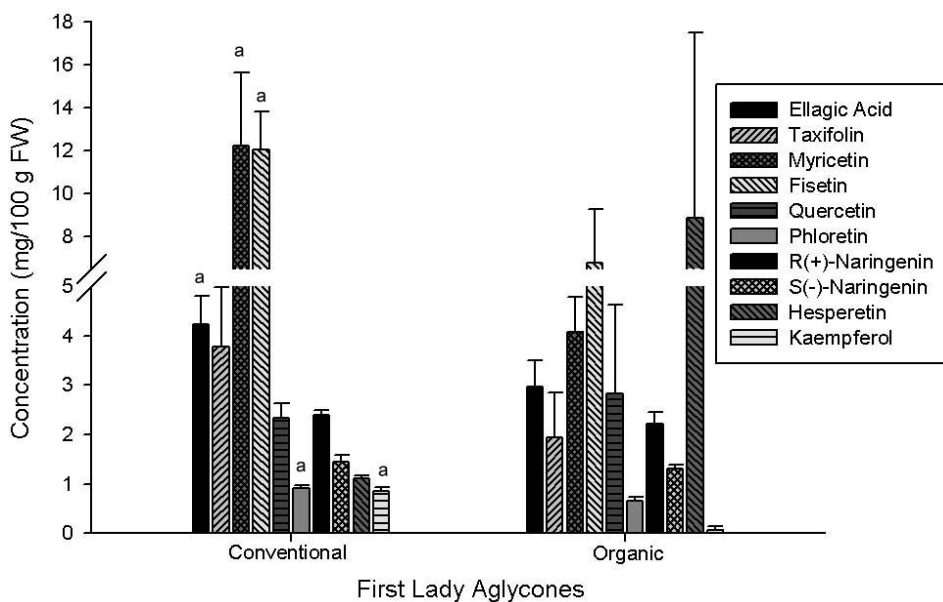
Figure 7.3. Content of ellagic acid, taxifolin, myricetin, fisetin, quercetin, phloretin, R(+)-naringenin, S(-)-naringenin, hesperetin, and kaempferol in conventionally grown and organically grown 'First Lady' tomatoes (n = 32, mean ± S.E.M.). a, P < 0.05, conventional vs. organic.

7.4.2.2 Glycoside Content of Selected Polyphenols

The content of ellagic acid glycoside, taxifolin glycoside, myricetin glycoside, fisetin glycoside, quercetin glycoside, phloridzin, R(+)-naringin, S(-)-naringin, hesperidin, and kaempferol glycoside was also quantified in both organically and conventionally grown tomatoes (**Fig. 7.4**). 'First Lady' tomatoes grown with a conventional soil fertility management showed greater concentration of myricetin glycoside (104.00 ± 42.13 mg/100 g FW) while R(+)-naringin (0.39 ± 0.11 mg/100 g FW) was demonstrated to have the lowest

concentration. Likewise, organically grown 'First Lady' tomatoes also exhibited myricetin glycoside (321.40 ± 175.64 mg/100 g FW) as the glycoside with the highest concentration, but in tomatoes grown organically, phloridzin (0.22 ± 0.12 mg/100 g FW) was demonstrated to have the lowest concentration.

These results do not support previous findings that report rutin, or quercetin-3-rutinoside, as the polyphenol with the highest concentration in the glycosylated form in the 'Money Maker' cultivar [182]. Similarly, a study of the glycosides in tomatoes reported quercetin glycosides, phloretin glycosides, and kaempferol glycosides to be predominant in 'Romana', 'Elanto', and 'Favorita' cultivars [185]. As mentioned before, this discrepancy may be due to the difference in cultivars analyzed.

In 'First Lady' tomatoes, quercetin glycoside was the second highest polyphenol detected in this group, followed by taxifolin glycoside, fisetin glycoside, hesperidin, ellagic acid glycoside, phloridzin, S(-)-naringin, kaempferol glycoside, and R(+)-naringin in conventional tomatoes (**Fig. 7.4**). Further studies are necessary to determine if the quercetin glycoside detected with the HPLC method developed corresponds to quercetin-3-rutinoside. In comparison, glycoside concentrations from the highest to the lowest in organic tomatoes were myricetin glycoside, taxifolin glycoside, ellagic acid glycoside, hesperedin, fisetin glycoside, quercetin glycoside, S(-)-naringin, kaempferol glycoside, R(+)-naringin, and phloridzin (**Fig. 7.4**).
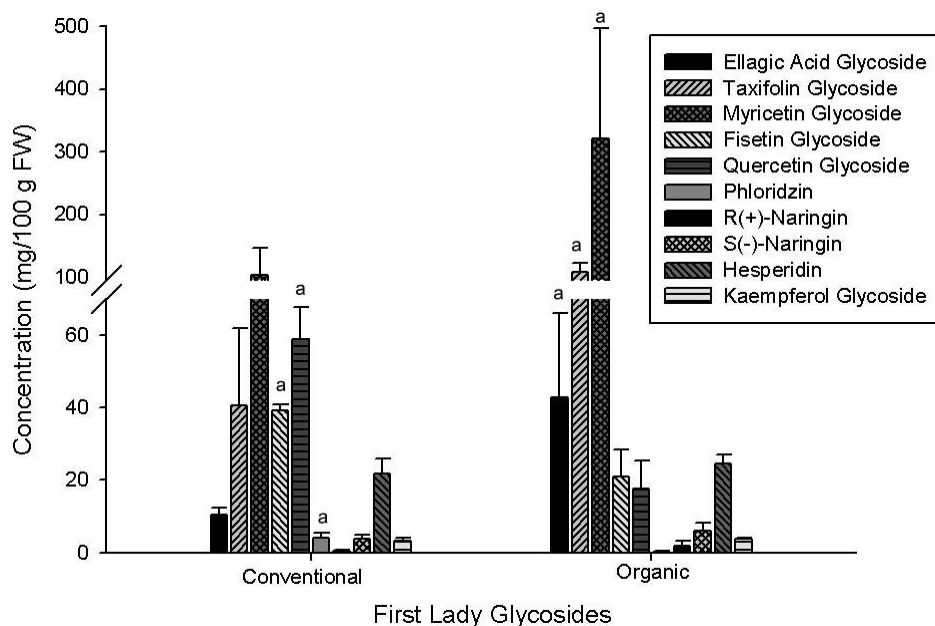
Figure 7.4. Content of ellagic acid glycoside, taxifolin glycoside, myricetin glycoside, fisetin glycoside, quercetin glycoside, phloridzin, R(+)-naringin, S(-)-naringin, hesperidin, and kaempferol glycoside in conventionally grown and organically grown 'First Lady' tomatoes (n = 32, mean ± S.E.M.). a, $P < 0.05$, conventional vs. organic.

Similar to the findings of aglycone content, these data suggest that the use of varied soil fertility management may result in differences in the polyphenolic content of the glycoside forms of polyphenols. Moreover, polyphenols are mostly found as glycosides and other conjugates in nature [6]. Therefore, the analysis of the content of these polyphenols and their glycosidic forms in epidermal peel is important to complete the analysis of the total polyphenolic content in fruit of 'First Lady' tomato.

7.4.2.3   Comparisons

Occurrence of polyphenols in tomato fruits has been reported to be exclusively restricted to the peel [185]; and previous studies have reported only negligible quantities in

the remaining parts of the fruit [185]. However, the present findings report high polyphenolic content in flesh tissue of tomatoes.

The aglycone content in 'First Lady' tomatoes ranged from 0.85 to 12.22 mg/100 g fresh weight (FW) for conventionally grown tomatoes and from 0.07 to 8.85 mg/100 g FW for organically-grown tomatoes. Glycoside content in 'First Lady' tomatoes ranged from 0.39 to 104.00 mg/100 g FW in tomatoes grown under conventional soil fertility conditions and from 0.22 to 321.40 mg/100 g FW for tomatoes grown organically (**Table 7.1**).

The R(+)-naringenin and S(-)-naringenin content in tomatoes is reported for the first time. Previous studies outside of Washington State University have not considered the stereochemical analysis of naringenin in tomatoes. Nevertheless, S(-)-naringenin has been reported to be predominant over R(+)-naringenin in fruit juices [152], and differences in the pharmacokinetics of R(+)-naringenin and S(-)-naringenin have also been reported [152]. Similar differences in the disposition of naringenin are seen in tomatoes. In both conventional and organic tomatoes, S(-)-naringenin has higher concentrations than R(+)-naringenin.

Table 7.1. Content (mg/100 g FW) of selected polyphenols in organically grown and conventionally grown 'First Lady' tomatoes (n = 32, mean ± S.E.M.). a, P < 0.05, conventional vs. organic.

Compound (mg/100 g FW)		Conventional	Organic
Ellagic Acid	Glycoside	10.52 ± 1.80	42.74 ± 23.10
	Aglycone	4.24 ± 0.57[a]	2.98 ± 0.53
	Total	**14.75 ± 2.37**	**45.72 ± 23.63[a]**
Taxifolin	Glycoside	40.42 ± 21.34	108.01 ± 14.60[a]
	Aglycone	3.78 ± 1.20	1.94 ± 0.91
	Total	**44.21 ± 22.54**	**109.96 ± 15.51[a]**
Myricetin	Glycoside	104.00 ± 42.13	321.40 ± 175.64
	Aglycone	12.22 ± 3.41[a]	4.08 ± 0.70
	Total	**116.22 ± 45.54**	**325.48 ± 176.34**
Fisetin	Glycoside	39.05 ± 1.68[a]	20.87 ± 7.45
	Aglycone	12.06 ± 1.77[a]	6.76 ± 2.53
	Total	**51.12 ± 3.45[a]**	**27.63 ± 9.98**
Quercetin	Glycoside	58.91 ± 8.84[a]	17.69 ± 7.53
	Aglycone	2.34 ± 0.30	2.83 ± 1.80
	Total	**61.25 ± 9.14[a]**	**20.51 ± 9.32**
Phloretin	Glycoside	4.05 ± 1.30[a]	0.22 ± .012
	Aglycone	0.92 ± 0.05[a]	0.66 ± 0.07
	Total	**4.97 ± 1.34[a]**	**0.88 ± 0.19**
R(+)-Naringenin	Glycoside	0.39 ± 0.11	1.98 ± 0.95[a]
	Aglycone	2.39 ± 0.10	2.21 ± 0.24
	Total	**2.78 ± 0.22**	**4.19 ± 1.19**
S(-)-Naringenin	Glycoside	3.68 ± 1.31	5.94 ± 2.21
	Aglycone	1.44 ± 0.14	1.32 ± 0.08
	Total	**5.12 ± 1.45**	**7.27 ± 2.29**
Hesperetin	Glycoside	21.71 ± 4.13	24.37 ± 8.47
	Aglycone	1.11 ± 0.07	8.85 ± 8.66
	Total	**22.82 ± 4.20**	**33.21 ± 17.13**
Kaempferol	Glycoside	3.30 ± 0.77	3.85 ± 0.29
	Aglycone	0.85 ±0.09[a]	0.07 ± 0.07
	Total	**4.15 ± 0.85**	**3.92 ± 0.36**
Total Glycosides		**286.03 ± 83.41**	**547.08 ± 240.36**
Total Aglycones		**41.35 ± 7.70**	**31.69 ± 15.59**
TOTAL POLYPHENOLS		327.38 ± 91.10	578.76 ± 255.94

Overall, organically grown tomatoes demonstrated a concentration of total selected polyphenols 1.8-fold higher than conventionally-grown tomatoes (578.76 ± 255.94 mg/100 g FW and 327.38 ± 91.10 mg/100 g FW, respectively). Moreover, myricetin was the predominant polyphenol in tomatoes produced in both organic and conventional farming systems (325.48 ± 176.34 mg/100 g FW and 116.22 ± 45.54 mg/100 g FW). Previous studies of the composition of polyphenols in another tomato cultivar ('Money Maker') indicated that the content of polyphenolic compounds was dependent on the cultivar of tomato analyzed [182]. However, no studies have analyzed the effect of the soil fertility management system on polyphenolic composition in tomatoes. The present findings suggest that differences in content and concentration of polyphenols in the flesh samples of 'First Lady' tomato analyzed may be related to the soil fertility conditions (**Fig. 7.5**).
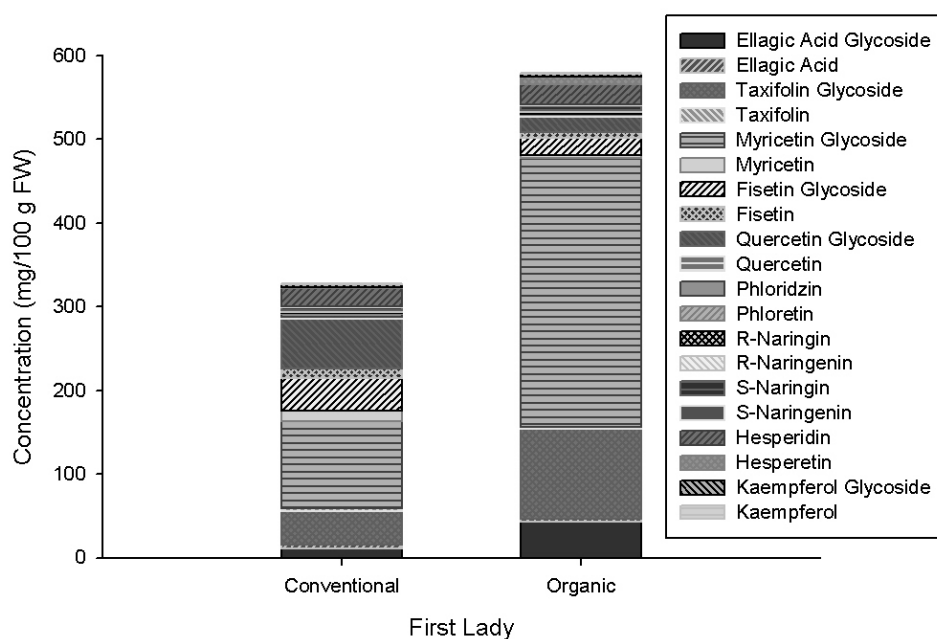
Figure 7.5. Content of ellagic acid, taxifolin, myricetin, fisetin, quercetin, phloretin, R(+)-naringenin, S(-)-naringenin, hesperetin, kaempferol and their respective glycosides in conventionally grown and organically grown 'First Lady' tomatoes (n = 32, mean values).

Nevertheless, the analysis of the epidermal peel of 'First Lady' tomatoes is necessary and will provide more conclusive evidence on the effect of the farming method in polyphenolic content in tomatoes.

7.5 CONCLUSIONS

A novel HPLC method for ellagic acid, taxifolin, myricetin, fisetin, quercetin, phloretin, R(+)-naringenin, S(-)-naringenin, hesperetin, and kaempferol, and their glycosides is sensitive, reproducible and accurate. The method was applied for the first time in the analysis and quantification of these selected polyphenols in tomatoes grown using conventional and organic soil fertility management. The organically grown 'First Lady' tomatoes showed a 1.8-fold higher concentration of total selected polyphenols compared to 'First Lady' tomatoes grown conventionally.

The content and concentration of ellagic acid, taxifolin, myricetin, fisetin, quercetin, phloretin, R(+)-naringenin, S(-)-naringenin, hesperetin, and kaempferol varied depending on the soil fertility system used. Moreover, ellagic acid, taxifolin, fisetin, and hesperidin were reported in tomato extracts for the first time. Previous reports of naringenin content in tomatoes did not analyze the enantiomeric content of this polyphenol [182]. S(-)-naringenin, R(+)-naringenin and their glycosides were reported in tomatoes for the first time and similarly to what has been reported in fruit juices, the S(-)-enantiomer is predominant in both organic and conventional tomatoes.

After serendipitous discovery of taxifolin in tomatoes, the stereospecific analysis of (+/-)-taxifolin was achieved in selected samples of tomatoes and demonstrated differential disposition in favor of (2S3R)-(+)-taxifolin and (2R3R)-(+)-taxifolin. This is the first report of the presence of taxifolin in tomatoes which subsequently resulted in the development of the

chiral method of analysis presented in Chapter IV and further demonstrates the importance of chiral analysis techniques.

These findings contribute to our understanding of the complex relationship between the polyphenolic content of fruit and farming systems. However, further studies of the polyphenolic content in epidermal peel of the fruits of the 'First Lady' cultivar of tomatoes are necessary to have more conclusive evidence of the effect of the soil fertility management on polyphenolic composition. Future studies will also include the analysis of other cultivars of tomatoes to examine their effects on the polyphenolic content. The importance of analysis of both aglycone and glycoside forms in addition to enantiomeric forms in horticultural studies of tomato polyphenols is highlighted.

8 <u>Analysis of Selected Polyphenol Content in Apples (*Malus* x *domestica*) and Assessment of Pharmacological Activity</u>

8.1 INTRODUCTION

The first section of this chapter describes the quantification of the content of selected polyphenols in apples – ellagic acid, hesperetin, kaempferol, quercetin, phloretin, R(+)-naringenin and S(-)-naringenin – using reverse phase high performance liquid chromatography, RP-HPLC. The second section of this chapter describes the pharmacological activity of selected apple extracts in *in vitro* anti-cancer and anti-inflammatory models, as well as anti-oxidant, and anti-adipogenic assays.

8.2 BACKGROUND

The apple (*Malus* x *domestica*), a Rosaceae member, originated in Kazakhstan and constitutes the largest agricultural product in the state of Washington [186]. Apples are consumed worldwide for their fruits and their consumption has been suggested to be linked to numerous health benefits due to their polyphenol content [187]. The relationship between the anti-oxidant content in apple peel and the whole fruit in two growing seasons of 19 cultivars was studied [187]. The total polyphenolic content was measured using HPLC or the Folin-Ciocalteu method; and polyphenol concentrations were reported to be 3-fold higher in peel than in flesh. Likewise, specific anti-oxidative enzymes were measured: glutathione reductase, ascorbate peroxidase, and catalase. These enzymes were demonstrated to have different activity in the nineteen different cultivars analyzed.

Content and composition of phenolic compounds in apples vary depending on several factors including: cultivar, area of cultivation, and time and year of harvest [188]. The influence of cultivar, rural practice (or farming system), and growing region on polyphenolic composition was studied in four apple cultivars in Italy [189]. The total polyphenolic content and the majority of single polyphenols were higher in peel than in flesh. Procyanidins, flavanols, and flavonols were predominant in peel (77 – 95%), whereas hydroxycinnamics, anthocyanins, and dihydrochalcones were detected at lower concentrations. The cultivar effect was the most important factor in determining the anti-radical activity [190]; 'Golden Delicious' and 'Annurca' were reported to have the lowest and highest radical scavenging activity respectively of all four cultivars analyzed. In another study, the polyphenolic content of apple was measured using HPLC in eight cultivars in Canada [190]. Five groups were described to be the main polyphenols in apples: hydroxycinnamic acids, flavan-3-ols/procyanidins, anthocyanins, flavonols, and dihydrochalcones; mainly associated with

sugar moieties including galactose, glucose, rhamnose, xylose, arabinose, and rutinose. The highest concentration of polyphenols was detected in the peel of 'Red Delicious'; whereas the 'McIntosh' cultivar had the highest concentration for flesh. To our knowledge, there are no studies in the United States and specifically in the state of Washington that analyze the content of selected polyphenol of several apple cultivars at various harvest maturities and harvest years, and with different fertility management alternatives and storage conditions.

Apple consumption has been linked to diverse health benefits. Apples have been reported to reduce cardiovascular disease, asthma, pulmonary dysfunction, diabetes, obesity and cancer [188]. *In vitro* studies demonstrated that apple components have anti-mutagenic potential, modulate phase 1 and phase 2 carcinogen metabolism, inhibit cell proliferation, induce apoptosis, inhibit signaling pathways involved in carcinogenesis, and have anti-oxidant and anti-inflammatory properties [188]. However, an evaluation of these properties has not been attributed to any specific component of the apple extracts. On the other hand, *in vivo* studies showed reduction of tumors in mice with chemically-induced skin papillomas and colon carcinogenesis, as well as in transgenic multiple intestinal neoplastia mice [188]. Finally, epidemiological studies demonstrated the cancer preventive potential of apples for lung and colorectal cancer in the United States, Netherlands, Uruguay, and South Korea [188]. Evidence supporting the pharmacological activity *in vitro* of apple components in cancer, inflammation, oxidation, and adipogenesis is available; however, the evaluation of apple cultivars produced specifically in Washington is nonexistent. The importance of identifying the disease prevention potential of apples produced in Washington relies on the possibility of enhancing health and reducing healthcare cost due to consumption of beneficial polyphenols

in apples and apple juices which can enhance the economic competitiveness of Washington produce.

8.3   METHODS

8.3.1 HPLC Apparatus and Conditions

The HPLC system used was a Shimadzu HPLC (Kyoto, Japan), consisting of an LC-10ATVP pump, a SIL-10AF auto injector, a SPD-M10A VP spectrophotometric diodearray detector, and a SCL-10A VP system controller. Data collection and integration were accomplished using Shimadzu EZ Start 7.1.1 SP1 software. The analytical column used was Chiralcel® OD-RH column (150mm × 4.6mm i.d., 5-µm particle size, Chiral Technologies Inc., PA, USA) protected by a Chiralcel OD-RH guard column (0.4cm x 1cm, 5-µm particle size). The mobile phase consisted of acetonitrile, water and phosphoric acid (30:70:0.04, v/v/v), filtered and degassed. Separation was carried out isocratically at 25 ± 1°C, a flow rate of 0.4 ml/min, with ultraviolet (UV) detection at 292 nm.

8.3.2 Chemicals and Reagents

Diadzein, ellagic acid, hesperetin, kaempferol, quercetin, phloretin, naringenin, formic acid, and β-glucuronidase from *Helix pomatia* Type-HP-2 were purchased from Sigma Chemicals (St Louis, MO, USA). HPLC grade acetonitrile, methanol, and water were purchased from J. T. Baker (Phillipsburg, NJ, USA). Phosphoric acid was purchased from Aldrich Chemical Co. Inc. (Milwaukee, WI, USA).

8.3.3 Stock and Working Standard Solutions

Diadzein, ellagic acid, fisetin, hesperetin, kaempferol, quercetin, phloretin, myricetin, naringenin, and taxifolin solutions of 100.0 µg/ml were dissolved in methanol. Diadzein was used as internal standard (IS). These solutions were protected from light and stored at -20°C between uses, for no longer than three months. Calibration standard curves in water were prepared daily from the stock solutions by sequential dilution yielding concentrations of 0.5, 1.0, 5.0, 10.0, 50.0 and 100.0 µg/ml of each compounds.

8.3.4 Plant and Juice Material

Five distinct apple cultivars found in the state of Washington were analyzed: 'Gala', 'Golden Delicious', 'Red Delicious', 'Granny Smith', and 'Fuji'. The examined cultivars of apple were obtained from local growers. Apples were collected from healthy, mature orchards, representing cultivars that are important in Washington's apple industry. Fruit of each cultivar were harvested from exposed and shaded canopy locations over several dates, representing different harvest maturities, during two years, 2005 and 2006. Depending upon the commercial storage requirements of each cultivar, harvest samples were treated or not with diphenylamine (DPA) or 1-methylcyclopropene (MCP), and stored in regular- and controlled-atmosphere (RA and CA) storage under appropriate conditions of O_2, CO_2, and temperature.

Fruit from these harvest/storage treatments, along with matched at-harvest samples, were separated into peel and flesh tissues and immediately frozen in liquid nitrogen either at termination of the storage period or at harvest in the orchard. A second group of fruit removed from storage was left on a laboratory bench at room temperature (20-25°C) for a week to simulate shelf-life conditions, and then sampled and frozen as described. All samples were

stored in an ultra-low temperature freezer (-80°C) until analyzed. Organic (Knudson and Nantu brands) and conventional (Martinelli and Safeway brands) apple juices were purchased from local grocery stores.

8.3.5 Sample Preparation

Extraction of ellagic acid, hesperetin, kaempferol, quercetin, phloretin, and naringenin from *Malus* x *domestica* for analysis of selected polyphenolic content in the fruit peel and flesh of all harvest/storage treatments and farming systems was accomplished as follows: 0.1 g of sample (peel or flesh) was measured and frozen under liquid nitrogen. Each sample was prepared in duplicate; the frozen samples were placed into the extraction glass tube and 1.0 ml of methanol was added. Extraction was performed for 1 minute using a Thomas tissue grinder (Thomas Scientific, Swedesboro, NJ, USA). The extraction mix and the fruit tissue were placed into a 2.0 ml Eppendorf tube, 0.5 ml of methanol was added to the extraction glass for rinsing and combined with the extraction mix. A total volume of 1.5 ml was obtained per extraction; the samples were vortexed for 30 seconds and centrifuged at 5,000 r.p.m. for 5 minutes. One of the duplicates was treated to extract only aglycones (free) and the second of the duplicates was treated with β-glucuronidase from *Helix pomatia* Type HP-2 to cleave any glycosides to aglycones (total) [147]. The supernatant of the free samples was transferred into 2.0 ml Eppendorf tubes, and 25.0 µl of IS was added, samples were vortexed for 10 seconds, dried to completion under nitrogen gas using an analytical evaporator, and stored at 4°C before analysis. The supernatant of the total samples was transferred into 15 ml conical tubes. The total samples were dried to completion under nitrogen gas, then 1.0 ml of HPLC-grade water, 110.0 µl 0.78 M sodium acetate-acetic acid buffer (pH 4.8), and 100.0 µl 0.1 M

ascorbic acid were added. The samples were vortexed for 30 seconds, and incubated for 17 - 24 hours at 37°C in a shaking incubator following the addition of 200.0 µl of crude preparation of β-glucuronidase from *Helix pomatia* Type HP-2. After incubation, 1.0 ml of ice-cold acetonitrile was added to stop the enzymatic activity of β-glucuronidase, the samples were vortexed for 10 seconds, and centrifuged at 5,000 r.p.m. for 5 minutes. The supernatant was collected into 15 ml conical tubes and dried to completion under nitrogen gas using an analytical evaporator after 25.0 µl of IS was added; and were subsequently stored at 4°C before analysis. When all samples were ready for analysis, free and total samples were reconstituted in 200.0 µl of mobile phase, vortexed for 30 seconds, and centrifuged at 5,000 r.p.m. for 5 minutes; 150.0 µl were injected into the HPLC system for analysis. Glycoside content was calculated by subtracting the concentration of the free samples from the incubated total samples. All compounds were quantitatively expressed on the basis of concentration per fresh weight, as well as an estimate of total content in the edible portion of a 200 g apple.

Samples of conventional and organic apple juices were purchased from grocery stores in the Moscow – Pullman area. One milliliter of apple juice was added into 15 ml conical tubes corresponding to free and total duplicates. Three milliliters of HPLC-grade water were added to all samples, followed by 25.0 µl of diadzein (IS) to the free samples only. Free samples were dried to completion using a nitrogen evaporator, and stored at 4°C until process. To the total samples, 330.0 µl 0.78 M sodium acetate-acetic acid buffer (pH 4.8), and 300.0 µl 0.1 M ascorbic acid were added, samples were vortexed for 30 seconds, and 600.0 µl crude preparation of *Helix pomatia* glucuronidase type H-2 was added and gently mixed. Total samples were incubated in a water bath at 37°C for 17-24 hours; 25.0 µl of IS were added, followed by 3.0 ml of cold acetonitrile. Samples were vortexed for 30 seconds, centrifuged for

5 minutes at 5,000 r.p.m. and the supernatant was collected into new eppendorf tubes, and dried until completion under compressed nitrogen gas. The stored free samples were removed from the refrigerator (4°C), and left at room temperature for 5 minutes. Free and total samples were reconstituted at the same time, 400.0 µl of mobile phase was added to each sample, samples were vortexed for 30 seconds, centrifuged for 5 minutes at 5,000 r.p.m. and the supernatant was carefully transferred to HPLC vials; 150.0 µl of sample was injected into the HPLC system for analysis.

8.3.6 Data Analysis

Quantification was based on calibration curves constructed using PAR of ellagic acid, fisetin, hesperetin, kaempferol, quercetin, phloretin, myricetin, naringenin, and taxifolin to IS, against ellagic acid, fisetin, hesperetin, kaempferol, quercetin, phloretin, myricetin, naringenin, and taxifolin concentrations using unweighted least squares linear regression.

8.3.7 Pharmacological Activity of Apple Extracts

8.3.7.1 *In vitro* Anti-cancer activity

8.3.7.1.1 *Chemicals and Reagents*

Trypsin-Ethylenediamenetetraacetic acid (EDTA), trypan blue, phosphate-buffered saline (PBS), 4-methylumbelliferone, resazurin, cell culture tested sodium carbonate, HEPES, β-glucosidase, sodium pyruvate, McCoy's 5A medium, penicillin-streptomycin, and insulin were purchased from Sigma (St. Louis, MO, USA). Dulbecco's Modified Eagle Medium/Nutrient Mixture F-12 Ham (DMEM/F-12) without phenol red and RMPI 1640

medium were purchased from Gibco Industries Inc. (Langley, OK, USA). Fetal bovine serum (FBS) was purchased from Equitech-Bio Inc. (Kerrville, TX, USA). Dimethyl sulfoxide (DMSO) was purchased from Sigma Chemicals (St Louis, MO, USA). Apple samples were obtained from Washington State Tree Fruit Research Commission.

8.3.7.1.2   *Cell Culture*

The experimental conditions were similar to those utilized in Chapter VI with minor modifications. The cell lines used in these series of experiments were A-375 (human malignant melanoma), HCT-116 (human colorectal carcinoma), MDA-MB-231 (Her-2/Neu positive, estrogen negative breast adenocarcinoma), Hep-G2 (human hepatocellular carcinoma), and PC-3 (prostate carcinoma). A-375 and Hep-G2 cells were maintained in 12.0 – 15.0 ml DMEM medium; MDA-MB-231 and PC-3 cells were maintained in 12.0 – 15.0 ml RPMI medium; and HCT-116 cells were maintained in 12.0 – 15.0 ml McCoy's 5A medium. All cell lines were supplemented with 10% heat-inactivated FBS. The Hep-G2 cell line was also supplemented with insulin (4.0 mg/ml). In addition, all cell lines were treated with penicillin-streptomycin (10.0 mg/l). All cell lines were placed in 75 cm^2 tissue cell culture flasks (15 cm × 8.5 cm × 3.5 cm, TPP, Switzerland), and incubated at 37°C in a 5% CO_2 atmosphere using a Forma Scientific CO_2 water jacketed incubator from Thermo Scientific (Waltham, MA, USA).

8.3.7.1.3   *Cell Subculture and Cell Number*

The experimental conditions for the cancer cell lines tested were similar to those described in Chapter VI (Section 6.3.2.3).

8.3.7.1.4   *Anti-Cancer Models*

Counted and seeded A-375, MDA-MB-231, HCT-116, HepG2, PC3, and SK-BR-3 cells were placed on 96-well plates, then incubated at 37°C in a 5% CO_2 atmosphere for 24 hours. On the day of the experiment, 'Red Delicious' apple extracts were dissolved in DMSO and diluted with the corresponding media to yield concentrations of 1.0, 10.0, 50.0, 100.0, 250.0, 500.0, and 1,000.0 µg/ml. Media were aspirated from the wells, and cells were treated with media containing 'Red Delicious' apple extracts (1.0 – 1,000.0 µg/ml); DMSO in media and media alone were used as controls. Treated and control cells were incubated at 37°C in a 5% CO_2 atmosphere for 72 hours.

8.3.7.1.5   *Description of the Alamar Blue Assay*

After 72 hours incubation, the 96-well plates were removed from the incubator; 20.0 µl of 10% Alamar blue (resazurin) fluorescent dye was added to the control and treatment groups in the 96-well plates; they were incubated at 37°C in a 5% CO_2 atmosphere for an additional 3 hours. Following 3 hours incubation, the 96-well plates were placed in a darkened environment for 30 minutes at room temperature; then placed into a Synergynt multi-well plate reader using Gen 5 software from Biotek[®]. Fluorescence was read at an excitation of 530 nm and an emission of 590 nm. The viable cell number (as a percent of control) in each cell line was measured and for each cell line exposed to varying concentrations of 'Red Delicious' apple extracts the IC_{50} was calculated.

8.3.7.1.6   *Data Analysis*

Data were analyzed as mean percent of viable cells ± standard deviation in Microsoft Excel[®] (Microsoft Office Professional Edition, Copyright ©1985-2003 Microsoft Corporation) and then graphed using Sigma Plot[®] software (Version 10.0, Build 0.0.54, Copyright ©2006 Systat Software, Inc.). Next, the individual mean percent of viable cells was modeled using the inhibitory effect model WinNonlin[®] (Version 5.2, Build 200701231637, Pharsight WinNonlin copyright ©1998-2007) pharmacodynamic software. This model allowed the calculation of the concentration that inhibits 50% cell viability (IC_{50}) for each cell line investigated. The IC_{50} values were obtained using the following equation:

$$E^* = E_{max}^{\S} \left((1 - C^{\dagger})/(C + IC_{50}) \right)$$

[*] Viability
[§] Maximum viability
[†] Concentration

Data were expressed as the mean ± standard error of the mean (S.E.M.) of IC_{50} values across replicates.

8.3.7.2   *In vitro* Anti-inflammatory Activity

8.3.7.2.1   *Chemicals and Reagents*

Trypsin-ethylenediamenetetraacetic acid (EDTA), trypan blue, phosphate-buffered saline (PBS), resazurin, cell culture tested sodium carbonate, 4-(2-hydroxyethyl-1-piperazineethanesulphonic acid (HEPES), McCoy's 5A medium, Debulcco's modified Eagle's medium/nutrient mixture F-12 Ham (DMEM/F-12) without phenol red, penicillin-streptomycin, and dimethyl sulfoxide (DMSO), and human recombinant interleukin-1β expressed in *Escherichia coli* were purchased from Sigma (St. Louis, MO, USA). Fetal

bovine serum (FBS) was purchased from Equitech-Bio Inc. (Kerrville, TX, USA). The prostaglandin E_2 (PGE_2) Direct Biotrak^{TM} Assay Kit was purchased from GE Healthcare (previously Amersham Biosciences Corp., Piscataway, NJ, USA, catalog No. RPN222). The Nitric Oxide Quantitation Kit was purchased from Active Motif (Carlsbad, CA, USA, catalog No. 40020). The TNF-α (human) EIA Assay Kit was purchased from Cayman Chemical (Ann Arbor, MI, USA, catalog No. 589201). The RayBio$^®$ Human MMP-3 ELISA Kit was purchased from RayBiotech, Inc. (Norcross, GA, USA, catalog No. ELH-MMP3-001). The sGAG Assay Kit was purchased from Kamiya Biomedical Company (Seattle, WA, USA, catalog No. BP-004).

8.3.7.2.2   *Cell Culture*

The cell lines employed in this series of experiments were HT-29 (colon adenocarcinoma) purchased from American Type Culture Collection (ATCC, Manassas, VA, USA) and canine chondrocytes (CnC) purchased from Cell Applications, Inc. (San Diego, CA, USA). HT-29 cells were maintained in McCoy 5A medium, and CnC cells were maintained in DMEM/F-12 medium without phenol red. HT-29 cells were supplemented with 10% heat-inactivated FBS and HEPES (6.0 g/l), and CnC were supplemented with 20% heat-inactivated FBS. Both cell lines were additionally supplemented with penicillin-streptomycin (10.0 mg/l); and incubated at 37°C in a 5% CO_2 atmosphere.

8.3.7.2.3   *Cell Subculture and Cell Number*

The subculture of HT-29 cells is discussed in Chapter VI, Section 6.3.3.3. A percentage of confluency of 85 - 95% was desired for CnC cells. The optimal cell seeding

number for CnC cells was chosen form the linear portion of the generated curve. CnC cells were seeded at a density of 5,000 cells per well.

8.3.7.2.4   *Anti-Inflammatory Models*

8.3.7.2.4.1 In Vitro Arthritis Model

The employed method was adapted from previously described methodology [191] with some modifications. For our *in vitro* arthritis model, canine chondrocytes (CnC) were counted and seeded on 96-well plates. The seeded cells were incubated at 37ºC in a 5% CO_2 atmosphere for 24 hours.

Following incubation, medium from each well was aspirated, and cells were treated with 100.0 µl of interleukin- 1β (IL-1β, 10.0 ng/ml); the 96-well plates were then incubated at 37ºC in a 5% CO_2 atmosphere for 2 hours. On the day of the experiment, apple extracts were dissolved in DMSO to yield concentrations of 1.0, 10.0, 100.0 and 250.0 µg/ml and serial dilutions in medium were performed for free and total samples of apple peel and flesh tissues. Following incubation, cells exposed to IL-1β were treated with 200.0 µl of medium containing different concentrations of free and total preparations of peel and flesh from apples (1.0 – 250.0 µg/ml) in triplicate. Control groups were treated with either DMSO diluted in medium or medium alone. Treated and control groups were incubated at 37ºC in a 5% CO_2 atmosphere for 72 hours. After the 96-well plates were removed from the incubator, medium from each group of triplicates was collected and stored at - 80ºC until further analysis; the desired biomarkers were measured within 72 hours.

Prostaglandin E_2 (PGE_2) levels were measured using the prostaglandin E_2 (PGE_2) Direct Biotrak^{TM} assay kit. Assay buffer, lyophilized PGE_2 antibody, lyophilized horseradish

peroxidase (HRP)-PGE_2 conjugate, wash buffer, 3,3'5,5'-tetramethylbenzidine (TMB) substrate, lysis reagent 1, lysis reagent 2, and PGE_2 standard were prepared on the day of the experiment following the manufacturer's instructions. A serial dilution of the PGE_2 standard was used to construct a standard curve. Assay blanks, standards and the collected media from each treatment and control group were placed in the 96-well plate supplied in the kit and incubated for 30 minutes at room temperature after the addition of lyophilized PGE_2 antibody. PGE_2 from samples was measured using a Synergynt multi-well plate reader (Biotek® Instruments Inc., Winnoski, VT, USA) using Gen 5 software from Biotek®. Absorbance was read at 450 nm. The average optical density was calculated for each set of replicates. The PGE_2 content of the samples was compared to the percent bound for standards (%B/B_0).

Tumor necrosis factor-α (TNF-α) levels were measured within 72 hours using the TNF-α (human) EIA Assay Kit. Assay buffer, wash buffer, TNF-α standard, sample matrix blank, Ellman's reagent, tween 20, non-specific mouse serum, human plasma, and TNF-α acetyl cholinesterase: Fab' conjugate (AChE:Fab') were prepared on the day of the experiment following the manufacturer's instructions. A serial dilution of the TNF-α standard was used to construct a standard curve. Assay blanks, controls, standards and the collected media from each treatment and control group were placed in the 96-well plate supplied in the kit, and incubated overnight at 4ºC after AChE:Fab' was added. The next day the plate was developed using Ellman's reagent. Standard wells needed to be visibly yellow for the plate to be ready for TNF-α measurement. TNF-α content was measured using a Synergynt multi-well plate reader (Biotek® Instruments Inc., Winnoski, VT, USA) using Gen 5 software from Biotek®. Absorbance was read at 412 nm. The TNF-α content of CnC media samples was compared to the standard curve.

Nitric oxide (NO) levels were measured within 72 hours using the Nitric Oxide Quantitation Kit. Assay buffer, nitrate reductase, cofactors, nitrate standard, nitrite standard, and Griess reagent were prepared on the day of the experiment following the manufacturer's instructions. Serial dilutions were used to construct standard curves for nitrate and nitrite. Assay blanks, controls, standards and the collected media from each treatment and control group were placed in 96-well plates and incubated for 30 minutes at room temperature following the addition of Griess reagent. NO content was measured using a Synergynt multi-well plate reader (Biotek® Instruments Inc., Winnoski, VT, USA) using Gen 5 software from Biotek®. Absorbance was read at 550 nm. The NO content of CnC media samples was compared to the nitrate and nitrite standard curves.

Matrix metallopeptidase-3 (MMP-3) levels were measured within 72 hours using the RayBio® Human MMP-3 ELISA Kit. Assay diluent buffer, wash solution, biotinylated anti-human MMP-3 antibody, recombinant human MMP-3 standard, HRP-streptavidin solution, 3,3',5,5'-tetramethylbenzidine (TMB)-One-Step substrate reagent, and stop solution were prepared on the day of the experiment following the manufacturer's instructions. A serial dilution of the recombinant human MMP-3 standard was used to construct a standard curve. Assay blanks, controls, standards and the collected media from each treatment and control group were placed in the 96-well plate provided with the kit, and incubated overnight at 4ºC after the addition of biotilylated anti-human MMP-3 antibody. The next day the plate was developed using HRP-streptavidin solution and TMB-One-Step substrate reagent. MMP-3 content was measured using a Synergynt multi-well plate reader (Biotek® Instruments Inc., Winnoski, VT, USA) using Gen 5 software from Biotek®. Absorbance was read at 450 nm. The MMP-3 content of CnC media samples was compared to the standard curve.

Sulphated glucosaminoglycans (sGAG) levels were measured within 72 hours using the sGAG Assay Kit. Alcian Blue working solution, guanidine (Gu)-HCl, DMSO solution, SAT solution, Gu-Prop solution, calibrators, and control (1.1 ml cartilage extract diluted in water) were prepared on the day of the experiment following the manufacturer's instructions. The six different calibrators were used to construct a standard curve. Controls, standards and the collected media from each treatment and control group were placed in eppendorf tubes and incubated overnight at 4ºC following the addition of Alcian Blue working solution. After incubation, samples were centrifuged for 15 minutes at 12,000 r.p.m., and the pellet resuspended in DMSO. The DMSO-resuspended samples were again centrifuged for 15 minutes at 12,000 r.p.m., and the new pellet resuspended in Gu-Prop solution. The content of the samples in the eppendorf tubes was transferred to a 96-well plate in duplicate. sGAG content was measured using a Synergynt multi-well plate reader (Biotek® Instruments Inc., Winnoski, VT, USA) using Gen 5 software from Biotek®. Absorbance was read at 595 nm. The sGAG content of CnC media samples was compared to the standard curve.

8.3.7.2.4.2 *In Vitro* Colitis Model

The employed *in vitro* colitis model was adapted from previously described methodology [153]. HT-29 (colorectal adenocarcinoma) cells were counted and seeded on 96-well plates. The seeded cells were then incubated at 37°C in a 5% CO_2 atmosphere until they reached monolayer confluency of 60 – 80% at 72 hours. Cells were then serum starved for 24 hours. On the day of the experiment, apple extracts were dissolved in 1.0 µl DMSO and serial dilutions in 1.0 ml medium were performed; 0.2, 2.0, and 20.0 µg/ml samples of free and total preparations of peel and flesh were prepared.

The cells were divided into one of four groups: (1) cells treated with vehicle (1.0 µl DMSO in 1.0 ml medium) in the presence of 250.0 µl TNF-α, (2) cells treated with vehicle (1.0 µl DMSO in 1.0 ml medium) without TNF-α, (3) cells treated with the compounds (1.0 – 100.0 µg/ml) with 250.0 µl TNF-α, and (4) cells treated with the compounds (0.2 – 20.0 µg/ml) without TNF-α. Medium was aspirated from each well and then cells were treated with the compounds or vehicle in triplicate. Depending on the group, either 250.0 µl TNF-α (20.0 ng/ml) in medium or 250.0 µl of blank media was added. Medium from each group of triplicates was collected at 24 hours and stored at -80ºC for further analysis; the desired biomarkers were measured within 72 hours.

Prostaglandin E_2 (PGE_2) levels were measured using the prostaglandin E_2 (PGE_2) Direct Biotrak^{TM} assay kit. Assay buffer, lyophilized PGE_2 antibody, lyophilized horseradish peroxidase (HRP)-PGE_2 conjugate, wash buffer, 3,3'5,5'-tetramethylbenzidine (TMB) substrate, lysis reagent 1, lysis reagent 2, and PGE_2 standard were prepared on the day of the experiment following the manufacturer's instructions. A serial dilution of the PGE_2 standard was used to construct a standard curve. Assay blanks, standards and the collected media from each treatment and control group were placed in the 96-well plate supplied in the kit and incubated for 30 minutes at room temperature after the addition of lyophilized PGE_2 antibody. PGE_2 from samples was measured using a Synergynt multi-well plate reader (Biotek® Instruments Inc., Winnoski, VT, USA) using Gen 5 software from Biotek®. Absorbance was read at 450 nm. The average optical density was calculated for each set of replicates. The PGE_2 content of the samples was compared to the percent bound for standards (%B/B_0).

8.3.7.2.5   *Description of the Prostaglandin E₂ (PGE₂) Assay*

The prostaglandin E$_2$ (PGE$_2$) Direct Biotrak^{TM} assay kit was purchased from GE Healthcare (previously Amersham Biosciences Corp., Piscataway, NJ, USA, catalog No. RPN222). This competitive enzymeimmunoassay (EIA) system uses novel lysis reagents to facilitate the extraction of PGE$_2$ from cell cultures without the need to remove the extracting agents prior to measurement, ensuring PGE$_2$ is directly available for later analysis. Intracellular PGE$_2$ is released after hydrolysis, and is later sequestered to ensure PGE$_2$ is free for subsequent analysis. More details are available in the manufacturer's instruction manual. The concentration of PGE$_2$ was measured and the IC$_{50}$ values were calculated for HT-29 colorectal adenocarcinoma and CnC canine chondrocyte cells exposed to varying concentrations of 'Red Delicious' and 'Golden Delicious' apple extracts.

8.3.7.2.6   *Description of the Tumor Necrosis Factor-α (TNF-α) Assay*

The TNF-α (human) EIA Assay Kit was purchased from Cayman Chemical (Ann Arbor, MI, USA, catalog No. 589201). This immunometric assay is based on a double-antibody 'sandwich' technique. Each well of the plate supplied with the kit has been coated with a monoclonal antibody specific for TNF-α, which will bind any TNF-α introduced into the well. After being added to the well, AChE:Fab' binds selectively to a different epitope on the TNF-α molecule. The two antibodies form a 'sandwich' by binding on opposite sides of the TNF-α molecule. The concentration of the analyte is determined by measuring the enzymatic activity of AChE. Addition of Ellman's reagent produces a yellow-colored product which can be measured spectrometrically. More details are available in the manufacturer's instruction manual. The concentration of TNF-α was measured and the IC$_{50}$ values were

calculated for HT-29 colorectal adenocarcinoma cells exposed to varying concentrations of 'Red Delicious' and 'Golden Delicious' apple extracts.

8.3.7.2.7 *Description of the Nitric Oxide (NO) Assay*

The Nitric Oxide Quantitation Kit was purchased from Active Motif (Carlsbad, CA, USA, catalog No. 40020). This assay allows for the monitoring of nitric oxide production based on nitrate and nitrite determination. In the cell, NO is eventually metabolized to nitrite (NO_2^-) and nitrate (NO_3^-); therefore, to quantify total NO production the sum of both nitrite and nitrate is commonly used. The addition of two cofactors to the nitrate reductase reaction accelerates the conversion of nitrate to nitrite while simultaneously degrading excess NADPH to NADP. Colorimetric determination can be directly measured by using the Griess reagent without the need for lactate dehydrogenase treatment. More details are available in the manufacturer's instruction manual. The concentration of NO was measured and the IC_{50} values were calculated for HT-29 colorectal adenocarcinoma cells exposed to varying concentrations of 'Red Delicious' and 'Golden Delicious' apple extracts.

8.3.7.2.8 *Description of the Matrix Metallopeptidase-3 (MMP-3) Assay*

The RayBio® Human MMP-3 ELISA Kit was purchased from RayBiotech, Inc. (Norcross, GA, USA, catalog No. ELH-MMP3-001). This assay uses a double-antibody 'sandwich' technique. The supplied 96-well plate is coated with an antibody specific for human MMP-3. MMP-3 present in samples is bound to the wells by the immobilized antibody. Then the biotilylated anti-human MMP-3 antibody is added; the two antibodies form a 'sandwich' by binding on opposite sides of the MMP-3 molecule. After the addition of TMB-

substrate solution color develops in proportion to the amount of MMP-3 bound. The stop solution changes the color from blue to yellow and the intensity of the color is measured spectrometrically. More details are available in the manufacturer's instruction manual. The concentration of MMP-3 was measured and the IC_{50} values were calculated for HT-29 colorectal adenocarcinoma cells exposed to varying concentrations of 'Red Delicious' and 'Golden Delicious' apple extracts.

8.3.7.2.9   *Description of the Sulphated Glycosaminoglycans (sGAG) Assay*

The sGAG Assay Kit was purchased from Kamiya Biomedical Company (Seattle, WA, USA, catalog No. BP-004). This assay uses the dye Alcian Blue, a tetravalent cation with a hydrophobic core commonly used as a histological tissue staining reagent. The ionic bonding between cationic dyes such as Alcian Blue and the negatively charged GAGs are generally proportional to the number of negative charges present as sulfated groups on the GAG chain when performed at low pH and high ionic strength. More details are available in the manufacturer's instruction manual. The concentration of sGAG was measured and the IC_{50} values were calculated for HT-29 colorectal adenocarcinoma cells exposed to varying concentrations of 'Red Delicious' and 'Golden Delicious' apple extracts.

8.3.7.2.10   *Statistical Analysis*

All experiments were minimally repeated in duplicate; data are expressed as the mean ± standard error of the mean (S.E.M.). Comparisons among control and treatment groups were made using General Linear Model (GLM) ANOVA with Newman-Keuls multiple comparison

test using NCSS Statistical and Power Analysis software (NCSS, Kaysville, UT, USA). With all analyses a $P < 0.05$ was considered significant.

8.3.7.3   *In vitro* Anti-oxidant activity

8.3.7.3.1   *Chemicals and Reagents*

Dimethyl sulfoxide (DMSO) was purchased from Sigma (St. Louis, MO, USA). The Anti-oxidant Assay Kit was purchased from Cayman Chemical Company (Ann Arbor, MI, USA, catalog No. 709001).

8.3.7.3.2   *Pre-Assay Preparations*

On the day of the experiment, peel and flesh of 'Red Delicious' were dissolved in DMSO to yield concentrations of 1.0, 10.0, 50.0, 100.0, 250.0, 500.0, and 1,000.0 µg/ml. The assay buffer, chromogen, trolox and hydrogen peroxide were prepared on the day of the experiment following the manufacturer's instructions. A trolox standard curve was constructed using a serial of dilutions. Controls, standards, and treatments at different concentrations (1.0 – 1,000.0 µg/ml) were placed in 96-well plates and hydrogen peroxide was used to start the oxidative reaction. The anti-oxidant activity of the compounds was measured using a Synergynt multi-well plate reader (Biotek[®] Instruments Inc., Winnoski, VT, USA) using Gen 5 software from Biotek[®] after five minutes of exposure to hydrogen peroxide. Absorbance was read at 750 nm to decrease interference. The anti-oxidant capacity of 'Red Delicious', apple extracts was compared to that of trolox.

8.3.7.3.3   *Description of the Anti-Oxidant Assay*

The Cayman Anti-oxidant Assay Kit measures the total anti-oxidant capacity based on the ability of the anti-oxidants in the sample to inhibit the oxidation of $ABTS^+$ to $ABTS^{\bullet+}$. For more details see the manufacturer's instruction manual. The anti-oxidant capacity expressed as trolox equivalent anti-oxidant capacity (TEAC) of extracts of 'Red Delicious' was measured and the IC_{50} values were calculated.

8.3.7.3.4   *Statitistical Analysis*

All experiments were repeated at least in duplicate; data are expressed as the mean ± standard error of the mean (S.E.M.). Comparisons among control and treatment groups were made using General Linear Model (GLM) ANOVA with Newman-Keuls multiple comparison test using NCSS Statistical and Power Analysis software (NCSS, Kaysville, UT, USA). With all analyses a $P < 0.05$ was considered significant.

8.3.7.4   *In vitro* Anti-adipogenic Activity

8.3.7.4.1   *Chemicals and Reagents*

Trypsin-Ethylenediamenetetraacetic acid (EDTA), trypan blue, phosphate-buffered saline (PBS), 4-methylumbelliferone, resazurin, cell culture tested sodium carbonate, HEPES, sodium pyruvate, penicillin-streptomycin, and insulin were purchased from Sigma (St. Louis, MO, USA). Dulbecco's Modified Eagle Medium/Nutrient Mixture F-12 Ham (DMEM/F-12) without phenol red medium was purchased from Gibco Industries Inc. (Langley, OK, USA). Fetal bovine serum (FBS) was purchased from Equitech-Bio Inc. (Kerrville, TX, USA). The

Adipogenesis Assay kit was purchased from Cayman Chemical Company (Ann Arbor, MI, USA, catalog No. 10006908).

8.3.7.4.2 *Cell Culture*

The experimental conditions for the 3T3-L1 cells (pre-adipocyte fibroblasts) were similar to those described in Chapter VI (Section 6.3.7.2).

8.3.7.4.3 *Cell Subculture and Cell Number*

The experimental conditions were similar to those described in Chapter VI, Section 6.3.7.3.

8.3.7.4.4 *Adipogenesis Model*

The *in vitro* adipogenesis model using 3T3-L1 cells (pre-adipocyte fibroblasts) was described in detail in Chapter VI, Section 6.3.7.4. Apple extracts were dissolved in DMSO to yield concentrations of 0.2, 2.0 and 20.0 µg/ml.

8.3.7.4.5 *Description of the Anti-adipogenic Assay*

The Adipogenesis Assay kit uses a well characterized cell line often used to study the differentiation of adipocytes. 3T3-L1 cells have been used to investigate insulin-induced glucose uptake and mechanisms of obesity development. The fibroblast-like pre-adipocytes undergo a series of morphological and biochemical changes, accumulating lipid droplets during terminal differentiation. For more details see the manufacturer's instruction manual.

The anti-adipogenic activity expressed as the percentage of Oil Red O Stained Material (OROSM) was measured and the IC_{50} values were calculated for 3T3-L1 cells exposed to varying concentrations of 'Gala' and 'Red Delicious' apple extracts.

8.3.7.4.6   *Statistical Analysis*

All experiments were repeated at least in duplicate; data are expressed as the mean ± standard error of the mean (S.E.M.). Comparisons among control and treatment groups were made using General Linear Model (GLM) ANOVA with Newman-Keuls multiple comparison test using NCSS Statistical and Power Analysis software (NCSS, Kaysville, UT, USA). With all analyses a $P < 0.05$ was considered significant.

8.4   RESULTS AND DISCUSSION

8.4.1 Chromatography

Separation of ellagic acid, hesperetin, kaempferol, quercetin, phloretin, and R(+)- and S(-)- naringenin, and the internal standard (IS) diadzein in apples was achieved successfully **(Figure 8.1).** No interfering peaks co-eluting with the compounds of interest were detected **(Figs. 8.1.1)**. The retention times of ellagic acid, quercetin, phloretin, R(+)-naringenin, S(-)-naringenin, hesperetin, and kaempferol were approximately 8, 31, 35, 43, 49, 60 and 70 minutes, respectively. The IS diadzein eluted at approximately 26 minutes **(Fig. 8.1.2)**. Optimal separation was achieved when the combination of acetonitrile, water and phosphoric acid was 30:70:0.04 (v/v/v) and the flow rate 0.4 ml/min. The total run time of the method was 80 minutes.
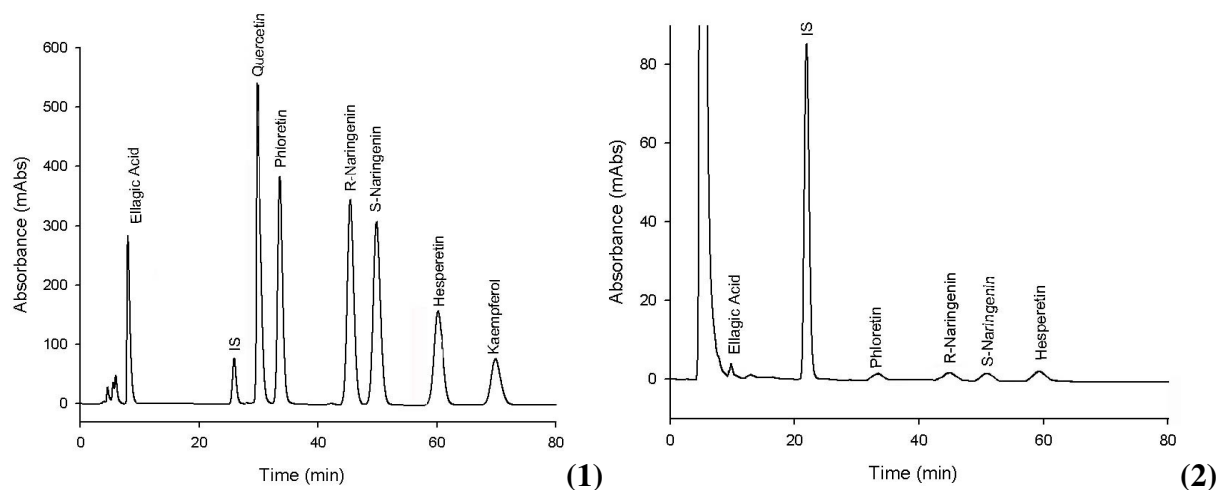
Figure 8.1. Representative chromatographs of apple (*Malus* x *domestica*) samples. **(1)** Ellagic acid, quercetin, phloretin, R(+)-naringenin, S(-)-naringenin, hesperetin, and kaempferol (10.0 µg/ml) in water **(2)** Compounds detected in an actual apple sample. Diadzein was used as internal standard (IS) and it eluted at approximately at 26 minutes.

A peak adjacent to ellagic acid was serendipitously later identified to be (+/-)-taxifolin after completion of this study, leading to studies in Chapter IV and V. (+/-)-Homoeriodictyol and (+/-)-isosakuranetin were not identified in apples.

8.4.2 Polyphenol Content of Apples

8.4.2.1   Apple Cultivars

The content of ellagic acid, quercetin, phloretin, R(+)-naringenin, S(-)-naringenin, and kaempferol was analyzed in five different apple cultivars: 'Gala', 'Golden Delicious', 'Red Delicious', 'Granny Smith', and 'Fuji' from commercial apple orchards in North-Central Washington in 2005 at harvest and after 3 – 6 months of controlled-atmosphere (CA) storage (Low O_2, high CO_2). For each set, half of the apples were sampled immediately after harvest or after two weeks shelf-life at room temperature (RT). Both, the peel and flesh of apples

were compared for their polyphenolic content in the five cultivars analyzed. The results of four groups are presented: immediately after harvest (harvest, 0 weeks), and after two weeks shelf-life RT (harvest, 2 weeks); and immediately after 3 – 6 months of CA storage (storage, 0 weeks) and after two weeks shelf-life RT (storage, 2 weeks).

Immediately after harvest (harvest, 0 weeks), 'Gala' and 'Fuji' were the cultivars with the highest concentrations of total polyphenols followed by 'Red Delicious', 'Golden Delicious', and 'Granny Smith' (**Fig. 8.2** and **Table 8.1**). The content of polyphenols in all apple cultivars was mostly as glycosides, similar to the results reported for tomatoes (Chapter VII). In all the apple cultivars analyzed, the glycoside content in flesh and peel was between 3-fold and 7-fold higher than the aglycone content. Moreover, polyphenols have been reported to be found in nature mostly as glycosides and other conjugates [6]. Furthermore, these findings are in accordance with previous studies of apples in Italy [189].
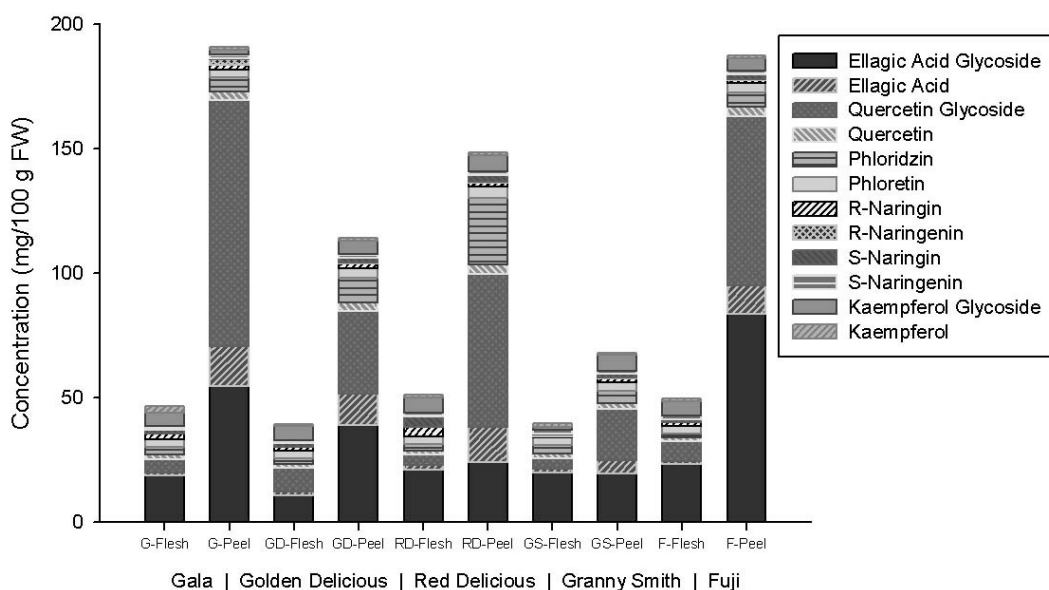
Figure 8.2. Content of selected polyphenols in five apple cultivars immediately after harvest (harvest, 0 weeks): 'Gala' (G), 'Golden Delicious' (GD), 'Red Delicious' (RD), 'Granny Smith' (GS), and 'Fuji' (F). Flavonoids were measured in both flesh and peel as aglycones and glycosides and included: ellagic acid, quercetin, phloretin, R(+)-naringenin, S(-)-naringenin, and kaempferol.

Overall, peel tissue was found to have higher concentrations of total polyphenols when compared to flesh in 'Gala' (4.1-fold), 'Golden Delicious' (2.9-fold), 'Red Delicious' (2.9-fold), 'Granny Smith' (1.7-fold), and 'Fuji' (3.8-fold). These findings are in accordance with previous reports that demonstrated polyphenols to be in higher concentrations in peel of apple cultivars in Italy [189].

In 'Gala', 'Golden Delicious', 'Red Delicious', 'Granny Smith' and 'Fuji' ellagic acid was predominant in flesh tissue. Likewise, in 'Golden Delicious', 'Granny Smith', and 'Fuji' ellagic acid was also predominant in peel tissue; only in 'Gala' and 'Red Delicious' quercetin was predominant in peel tissue. On the other hand, R(+)-naringenin was reported to have the lowest concentration in both peel and flesh of all apple cultivars except for peel of 'Gala' in which S(-)-naringenin was found in the lowest concentration.

Table 8.1. Concentration (mg/100 g FW) of ellagic acid, quercetin, phloretin, R(+)-naringenin, S(-)-naringenin, kaempferol and the respective glycosides in flesh and peel tissue samples of five apple cultivars immediately after harvest (harvest, 0 weeks): 'Gala', 'Golden Delicious', 'Red Delicious', 'Granny Smith', and 'Fuji'.

Compound (mg/ 100 g FW)		Gala		Golden Delicious		Red Delicious		Granny Smith		Fuji	
		Flesh	Peel	Flesh	Peel	Flesh	Peel	Flesh	Peel	Flesh	Peel
Ellagic Acid	Glycoside	18.80	54.62	10.68	39.05	21.24	23.97	19.92	19.57	23.52	83.76
	Aglycone	1.20	16.18	1.48	12.41	1.62	14.20	1.36	5.28	1.00	11.17
	Total	20.00	70.80	12.16	51.46	22.87	36.16	21.28	24.85	24.52	94.93
Quercetin	Glycoside	5.27	98.68	9.53	33.42	4.25	61.29	4.34	20.75	7.93	68.17
	Aglycone	1.87	3.21	1.78	3.22	1.73	3.87	1.78	2.30	1.72	3.69
	Total	7.14	101.89	11.31	36.64	5.98	65.16	6.11	23.05	9.65	71.85
Phloretin	Glycoside	3.23	5.84	2.07	9.91	2.55	27.00	3.46	4.72	1.36	5.60
	Aglycone	3.06	3.30	3.18	3.93	3.11	4.51	3.18	3.66	3.19	3.81
	Total	6.29	9.14	5.25	13.85	5.67	31.51	6.65	8.38	4.55	9.41
R-Naringenin	Glycoside	1.96	1.74	1.48	1.78	3.51	1.61	0.46	1.43	1.30	1.37
	Aglycone	0.16	2.40	0.10	0.30	0.08	0.20	0.64	0.12	0.08	0.22
	Total	2.12	4.13	1.58	2.07	3.59	1.82	1.11	1.55	1.38	1.59
S-Naringenin	Glycoside	1.65	0.22	1.33	2.23	4.35	2.79	0.25	1.66	1.29	1.88
	Aglycone	1.48	1.46	1.34	1.55	1.28	1.49	1.51	1.41	1.30	1.59
	Total	3.13	1.68	2.67	3.78	5.63	4.28	1.76	3.07	2.59	3.47
Kaempferol	Glycoside	5.11	2.13	5.53	5.14	6.45	6.18	1.24	6.23	5.96	4.85
	Aglycone	3.02	0.94	0.97	1.22	0.89	1.30	1.46	0.98	1.03	1.11
	Total	8.12	3.07	6.49	6.36	7.33	7.48	2.70	7.22	7.00	5.96
Total Glycosides		36.01	163.22	30.62	91.54	42.35	122.84	29.67	54.37	41.36	165.62
Total Aglycones		10.78	27.49	8.85	22.63	8.70	25.57	9.92	13.75	8.32	21.59
TOTAL POLYPHENOLS		46.79	190.71	39.47	114.17	51.06	148.41	39.60	68.12	49.68	187.22

After two weeks shelf-life RT the polyphenol content of apples at harvest (harvest, 2 weeks) was measured (**Fig. 8.3** and **Table 8.2**). 'Red Delicious' was the cultivar with the highest total polyphenol concentration followed by 'Gala', 'Golden Delicious', 'Fuji', and 'Granny Smith'. Samples were taken from different apple fruits immediately after harvest and after two weeks; differences in the polyphenol content of individual apple fruits are expected. However, the data were representative of the apples analyzed at harvest and after two weeks. These results suggest that shelf-life may have an effect in the content of polyphenols in apples.

The content of polyphenols in all apple cultivars was determined to be found mostly as glycosides. In the apple cultivars analyzed the glycoside content in flesh and peel was

between 2-fold and 6-fold higher than the aglycone content. These findings are similar to the polyphenol concentration reported immediately after harvest.
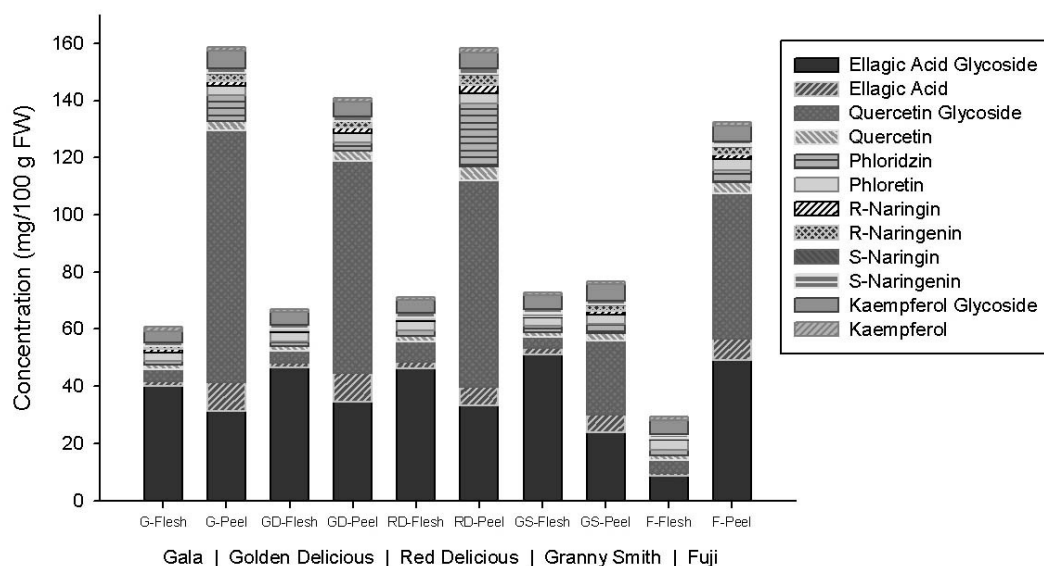
Figure 8.3. Content of selected flavonoids in five apple cultivars after two weeks shelf life RT (harvest, 2 weeks): 'Gala' (G), 'Golden Delicious' (GD), 'Red Delicious' (RD), 'Granny Smith' (GS), and 'Fuji' (F). Flavonoids were measured in both flesh and peel as aglycones and glycosides and included: ellagic acid, quercetin, phloretin, R(+)-naringenin, S(-)-naringenin, and kaempferol.

Higher concentrations of total polyphenols were reported in peel compared to flesh in 'Gala' (3-fold), 'Golden Delicious' (2-fold), 'Red Delicious' (2.2-fold), and 'Fuji' (4.4-fold). However, similar concentrations of total polyphenols were found in the peel and flesh of 'Granny Smith'. The findings in 'Granny Smith' differ from the results reported immediately after harvest in which peel had higher total polyphenol concentration than flesh.

Ellagic acid was predominant in peel and flesh of all apple cultivars except in peel of 'Gala', 'Golden Delicious' and 'Red Delicious' in which quercetin was predominant. The S(-)-naringenin was reported to have the lowest concentration in peel of all the apple cultivars studied. In comparison, R(+)-naringenin had the lowest concentration in flesh of all the apple cultivars except 'Gala' in which S(-)-naringenin has the lowest concentration. These findings

suggest possible isomerization of naringenin in some of the apple cultivars because immediately after harvest R(+)-naringenin had the lowest concentrations in peel and flesh.

Nevertheless, all flavonoids have been reported to derive from the intermediate S(-)-naringenin which can be oxidized into flavone or hydroxylated into 2R3R-dihydroflavonol [192]. Substitution reactions may then proceed at any stage and lead to different polyphenol products. These findings may suggest that when oxidation and hydroxylation reactions take place; they reduce the concentration of S(-)-naringenin and subsequently form other polyphenols [182,193]. These findings are the first of their kind in apples since naringenin has not been previously reported in apples in the literature.

Table 8.2. Concentration (mg/100 g FW) of ellagic acid, quercetin, phloretin, R(+)-naringenin, S(-)-naringenin, kaempferol and the respective glycosides in flesh and peel tissue samples of five apple cultivars after two weeks shelf-life RT (harvest, 2 weeks): 'Gala', 'Golden Delicious', 'Red Delicious', 'Granny Smith', and 'Fuji'.

Compound (mg/ 100 g FW)		Gala		Golden Delicious		Red Delicious		Granny Smith		Fuji	
		Flesh	Peel	Flesh	Peel	Flesh	Peel	Flesh	Peel	Flesh	Peel
Ellagic Acid	Glycoside	40.02	31.26	46.52	34.59	46.27	33.35	51.19	23.78	8.56	49.01
	Aglycone	1.60	10.07	1.68	10.12	2.07	6.55	2.27	6.22	0.96	7.70
	Total	**41.62**	**41.34**	**48.21**	**44.71**	**48.35**	**39.90**	**53.46**	**30.00**	**9.53**	**56.71**
Quercetin	Glycoside	4.23	88.26	4.15	74.10	7.24	72.15	3.67	25.85	4.55	50.66
	Aglycone	1.79	3.07	1.79	3.68	1.91	4.78	1.77	2.60	1.83	4.07
	Total	**6.03**	**91.33**	**5.94**	**77.78**	**9.15**	**76.94**	**5.43**	**28.45**	**6.38**	**54.73**
Phloretin	Glycoside	1.11	9.04	1.56	2.66	2.09	21.99	2.15	3.13	1.86	4.17
	Aglycone	3.12	3.36	3.18	3.48	3.21	3.67	3.09	3.59	3.49	3.79
	Total	**4.23**	**12.40**	**4.73**	**6.15**	**5.30**	**25.66**	**5.24**	**6.72**	**5.35**	**7.96**
R-Naringenin	Glycoside	1.08	1.65	0.52	1.80	0.51	2.75	0.25	1.29	0.30	1.69
	Aglycone	0.98	2.53	0.61	2.17	0.78	3.66	0.60	1.96	0.42	2.52
	Total	**2.06**	**4.18**	**1.12**	**3.97**	**1.29**	**6.41**	**0.85**	**3.25**	**0.72**	**4.21**
S-Naringenin	Glycoside	0.10	0.35	0.09	0.21	0.10	0.49	0.37	0.17	0.08	0.35
	Aglycone	1.35	1.61	1.35	1.50	1.38	1.94	1.53	1.40	1.31	1.67
	Total	**1.44**	**1.96**	**1.45**	**1.70**	**1.48**	**2.44**	**1.90**	**1.57**	**1.38**	**2.02**
Kaempferol	Glycoside	3.75	6.01	4.50	5.11	4.81	5.24	4.98	5.65	4.80	5.55
	Aglycone	1.80	1.53	0.92	1.43	0.95	1.77	1.04	1.14	1.26	1.16
	Total	**5.55**	**7.55**	**5.43**	**6.54**	**5.76**	**7.01**	**6.02**	**6.78**	**6.06**	**6.71**
Total Glycosides		50.29	136.58	57.34	118.46	61.02	135.98	62.61	59.87	20.15	111.44
Total Aglycones		10.63	22.17	9.54	22.38	10.30	22.37	10.29	16.91	9.27	20.90
TOTAL POLYPHENOLS		60.92	158.75	66.88	140.84	71.32	158.35	72.90	76.78	29.42	132.34

The content of polyphenols was analyzed after 3 – 6 months of CA storage (storage, 0 weeks). 'Gala' and 'Golden Delicious' were the cultivars with the highest concentrations of total polyphenols followed by 'Fuji', 'Red Delicious', and 'Granny Smith' (**Fig. 8.4** and **Table 8.3**). All the apple cultivars studied demonstrated higher concentration of glycosides compared to aglycone forms. The glycoside forms in peel and flesh were between 3.3-fold and 12-fold higher than the aglycone forms. These findings are similar to the content of glycosides immediately after harvest and after two weeks shelf-life.

Similarly, all polyphenols were found to be concentrated in peel which was also the case in the analysis immediately after harvest and after two weeks shelf-life. The polyphenol content in peel was higher in 'Gala' (1.7-fold), 'Golden Delicious' (3-fold), 'Red Delicious' (1.3-fold), 'Granny Smith' (2.6-fold), and 'Fuji' (3-fold) cultivars.
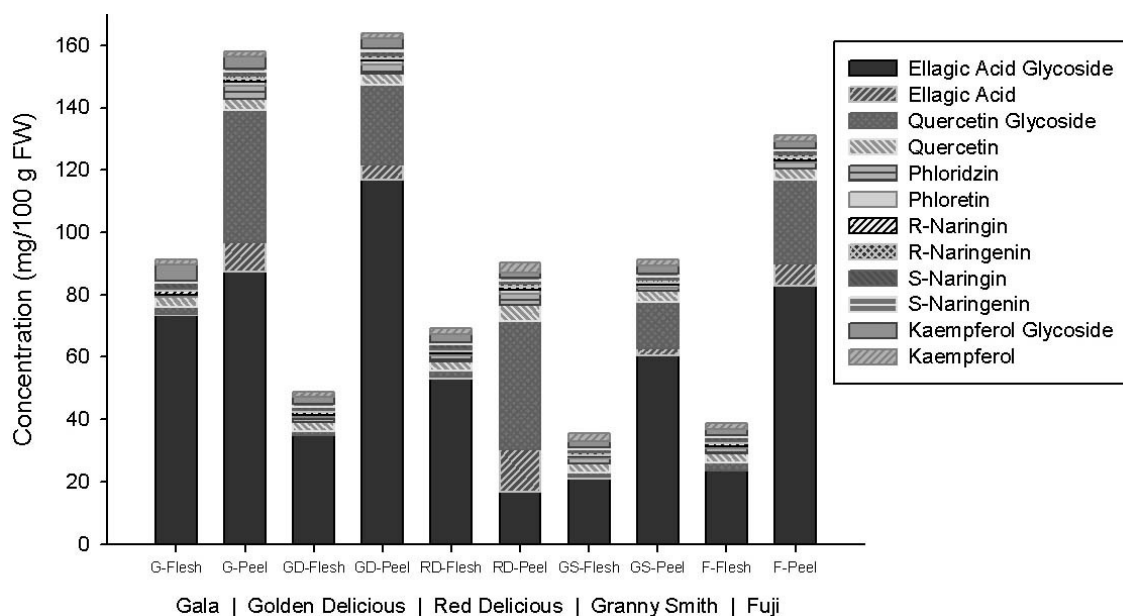
Figure 8.4. Content of selected flavonoids in five apple cultivars after 3 – 6 months of CA storage (storage, 0 weeks): 'Gala' (G), 'Golden Delicious' (GD), 'Red Delicious' (RD), 'Granny Smith' (GS), and 'Fuji' (F). Flavonoids were measured in both flesh and peel as aglycones and glycosides and included: ellagic acid, quercetin, phloretin, R(+)-naringenin, S(-)-naringenin, and kaempferol.

Ellagic acid was predominant in both peel and flesh of all five cultivars, except for the peel of 'Red Delicious' in which quercetin was predominant. In comparison, the lowest polyphenol in both peel and flesh of all the apple cultivars studied was R(+)-naringenin. These findings are in accordance with the results in the analysis of polyphenol content after harvest and after two weeks shelf-life.

Table 8.3. Concentration (mg/100 g FW) of ellagic acid, quercetin, phloretin, R(+)-naringenin, S(-)-naringenin, kaempferol and the respective glycosides in flesh and peel tissue samples of five apple cultivars after 3 – 6 months of storage (storage, 0 weeks): 'Gala', 'Golden Delicious', 'Red Delicious', 'Granny Smith', and 'Fuji'.

Compound (mg/ 100 g FW)		Gala		Golden Delicious		Red Delicious		Granny Smith		Fuji	
		Flesh	Peel	Flesh	Peel	Flesh	Peel	Flesh	Peel	Flesh	Peel
Ellagic Acid	Glycoside	73.49	87.38	34.93	117.00	53.16	16.79	20.94	60.34	23.55	82.78
	Aglycone	0.42	9.30	0.07	4.78	0.52	13.46	0.52	2.48	0.02	7.12
	Total	73.91	96.68	35.00	121.79	53.68	30.25	21.46	62.81	23.58	89.89
Quercetin	Glycoside	2.25	42.64	1.23	25.42	1.86	41.16	1.46	14.75	2.46	26.83
	Aglycone	2.99	3.41	3.00	3.62	2.90	5.13	2.96	3.68	2.93	3.67
	Total	5.24	46.05	4.23	29.03	4.76	46.29	4.42	18.44	5.40	30.50
Phloretin	Glycoside	0.19	4.38	1.62	3.05	1.96	3.63	1.52	1.01	1.80	1.85
	Aglycone	0.63	0.99	0.61	1.11	0.58	1.24	0.59	1.01	0.58	0.75
	Total	0.82	5.37	2.22	4.16	2.54	4.87	2.11	2.02	2.38	2.61
R-Naringenin	Glycoside	1.22	1.13	0.71	0.87	0.81	0.97	0.57	0.61	0.80	0.93
	Aglycone	0.79	0.88	0.82	0.90	0.79	0.98	0.84	1.02	0.81	0.85
	Total	2.01	2.01	1.53	1.77	1.59	1.95	1.41	1.63	1.61	1.79
S-Naringenin	Glycoside	1.89	1.57	1.10	1.21	1.35	1.06	0.98	0.98	1.16	1.41
	Aglycone	0.70	0.78	0.72	0.92	0.69	1.11	0.73	0.89	0.71	0.73
	Total	2.59	2.36	1.82	2.13	2.05	2.17	1.71	1.87	1.87	2.13
Kaempferol	Glycoside	5.21	3.78	2.41	3.23	2.63	1.56	1.96	2.39	1.95	2.32
	Aglycone	1.50	1.70	1.72	1.67	1.85	3.19	2.53	1.94	2.00	1.87
	Total	6.71	5.48	4.13	4.90	4.48	4.75	4.49	4.33	3.94	4.19
Total Glycosides		84.25	140.88	42.00	150.79	61.78	65.17	27.43	80.08	31.72	116.13
Total Aglycones		7.03	17.07	6.94	12.99	7.33	25.11	8.17	11.02	7.06	14.99
TOTAL POLYPHENOLS		91.28	157.95	48.94	163.77	69.11	90.28	35.60	91.10	38.78	131.11

Lastly, the polyphenol concentration was measured in samples of apples stored under CA conditions after two weeks shelf life RT (storage, 2 weeks). 'Gala' was the cultivar with the highest concentration followed by 'Red Delicious', 'Golden Delicious', 'Fuji' and

'Granny Smith' (**Fig. 8.5** and **Table 8.4**). The content of polyphenols in 'Gala', 'Golden Delicious', 'Red Delicious', and 'Granny Smith' apple cultivars was mostly evident as glycosides. The glycoside content in flesh and peel of these apple cultivars was between 3-fold and 12-fold higher than the aglycones. However, the aglycone content was higher than the glycoside content in peel of the 'Fuji' cultivar. These findings are unexpected since greater concentrations of glycosides were measured in 'Fuji' after CA storage. This kind of conversion has only been reported in transgenic apples [194]. Therefore, further studies are necessary to fully comprehend this variation and instability of the glycoside forms in this cultivar.
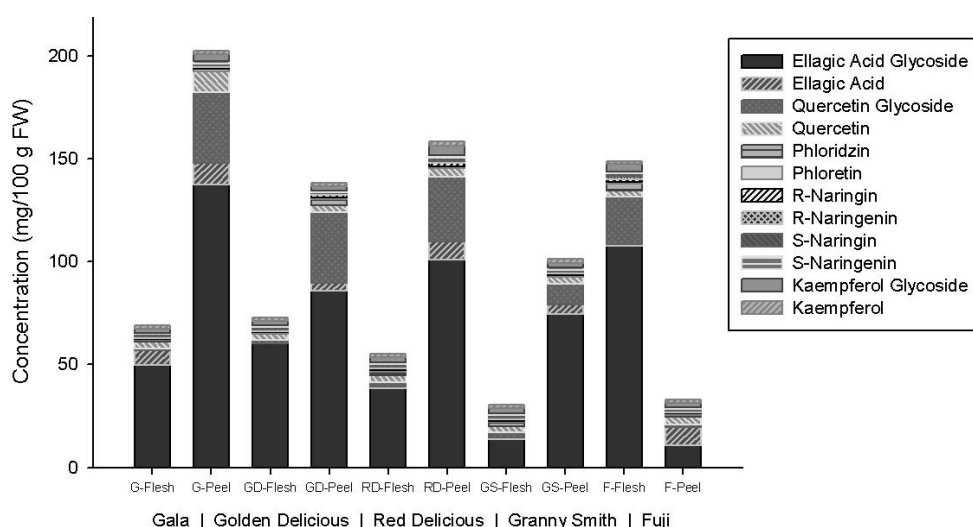
Figure 8.5. Content of selected flavonoids in five stored apple cultivars of after 2 weeks shelf life (storage, 2 weeks): 'Gala' (G), 'Golden Delicious' (GD), 'Red Delicious' (RD), 'Granny Smith' (GS), and 'Fuji' (F) conditions. Flavonoids were measured in both flesh and peel as aglycones and glycosides and included: ellagic acid, quercetin, phloretin, R(+)-naringenin, S(-)-naringenin, and kaempferol.

Higher concentrations of ellagic acid were demonstrated in both peel and flesh of all apple cultivars which is in accordance with the findings in the other three treatments studied. Unlike what was reported for the polyphenolic content in apples at harvest and after storage,

most of the apple cultivars exhibited phloretin as the polyphenol with the lowest concentrations. R(+)-naringenin was the polyphenol with the lowest concentration in peel of 'Gala', 'Granny Smith', and 'Fuji'. In addition, S(-)-naringenin had the lowest concentration in peel of 'Golden Delicious' and flesh of 'Red Delicious'.

Phloretin had the lowest concentrations in peel of the majority of apple cultivars. Phloretin is formed in apples by chalcone synthase activity [195] from naringenin precursors. These findings suggest that in some apple cultivars the formation of naringenin was favored over the formation of phloretin. Nevertheless, the knowledge of the biosynthetic pathways of dihydrochalcones (the class to which phloretin and naringenin belong) remains limited [195]. Further studies are necessary to understand the biosynthetic pathway possibly responsible for the differences after two weeks shelf-life of stored apples.

Table 8.4. Concentration (mg/100 g FW) of ellagic acid, quercetin, phloretin, R(+)-naringenin, S(-)-naringenin, kaempferol and the respective glycosides in flesh and peel tissue samples of five stored apple cultivars after two weeks shelf-life (storage, 2 weeks): 'Gala', 'Golden Delicious', 'Red Delicious', 'Granny Smith', and 'Fuji' (mean values).

Compound (mg/ 100 g FW)		Gala		Golden Delicious		Red Delicious		Granny Smith		Fuji	
		Flesh	Peel	Flesh	Peel	Flesh	Peel	Flesh	Peel	Flesh	Peel
Ellagic Acid	Glycoside	49.70	137.54	60.04	85.80	38.43	100.87	13.52	74.44	107.65	10.65
	Aglycone	7.01	10.54	0.28	3.99	0.71	8.75	0.85	4.87	0.64	8.91
	Total	56.71	148.08	60.32	89.79	39.14	109.62	14.37	79.30	108.29	19.55
Quercetin	Glycoside	1.17	34.33	1.61	34.11	2.36	31.62	2.68	9.83	23.15	1.19
	Aglycone	3.13	9.93	2.99	3.55	3.01	4.04	2.93	3.45	3.16	4.03
	Total	4.30	44.27	4.60	37.65	5.37	35.65	5.61	13.29	26.31	5.23
Phloretin	Glycoside	0.76	0.08	0.003	2.85	2.04	0.06	2.00	0.04	3.15	0.65
	Aglycone	0.62	1.18	0.60	0.92	0.60	0.94	0.59	0.86	0.73	0.75
	Total	1.38	1.26	0.61	3.76	2.64	1.00	2.59	0.90	3.87	1.40
R-Naringenin	Glycoside	0.56	0.73	0.69	0.98	0.90	1.65	0.82	0.80	1.61	0.55
	Aglycone	0.84	1.01	0.83	0.85	0.84	0.79	0.81	0.86	0.84	0.91
	Total	1.39	1.74	1.52	1.83	1.74	2.44	1.62	1.66	2.46	1.45
S-Naringenin	Glycoside	0.93	0.92	1.07	0.78	1.43	1.79	1.24	0.93	2.09	0.75
	Aglycone	0.74	1.23	0.73	0.77	0.73	1.16	0.72	0.90	0.75	0.72
	Total	1.67	2.15	1.81	1.55	2.16	2.95	1.96	1.83	2.84	1.47
Kaempferol	Glycoside	2.09	3.27	2.19	2.01	2.65	4.63	2.56	2.29	3.50	2.19
	Aglycone	1.62	1.78	1.79	1.64	1.61	2.04	1.74	2.04	1.54	1.88
	Total	3.70	5.05	3.98	3.66	4.26	6.67	4.30	4.33	5.04	4.07
Total Glycosides		55.21	176.87	65.60	126.52	47.81	140.62	22.82	88.33	141.15	15.97
Total Aglycones		13.95	25.69	7.24	11.72	7.50	17.71	7.63	12.99	7.66	17.20
TOTAL POLYPHENOLS		69.15	202.56	72.84	138.24	55.31	158.33	30.45	101.32	148.81	33.17

In summary, the polyphenol content of 'Gala', 'Golden Delicious', 'Red Delicious', 'Granny Smith', and 'Fuji' is higher in peel than in flesh as previously reported in apple cultivars in Italy [189]. Moreover, the polyphenols analyzed were mostly found as glycosides, similar to previous studies of apples, and to the reported findings in tomatoes (Chapter VII). Of all the polyphenols studied, ellagic acid and R(+)-naringenin had the highest and lowest concentrations, respectively in most of the apple cultivars at harvest and after CA storage. To our knowledge, this is the first report of naringenin enantiomeric content in apples.

8.4.2.2   Storage Conditions and Farming System

The content of selected flavonoids was measured in 'Gala' apples obtained from a research site on a commercial orchard in Washington state. The content of ellagic acid, quercetin, phloretin, R(+)-naringenin, S(-)-naringenin, and kaempferol was assessed in apples in the aglycone and glycosylated forms and the content of these flavonoids was compared between apples sampled at harvest and after being stored under controlled-atmosphere (CA) conditions and between apples grown using conventional and organic farming systems (**Fig. 8.6**). Conventionally grown apples showed no difference in the total content of selected polyphenols at harvest and after CA storage. On the other hand, organically grown apples showed higher content of these selected polyphenols after CA storage when compared to the content of polyphenols at harvest. Previous studies have demonstrated the effect of storage in the polyphenol content of apples to be similar to what is reported for the organic apples [196,197]. Postharvest storage was reported to increase the anti-oxidant activity in correlation with an increase of the concentration of polyphenols, in particular in the cultivar 'Annurca'. The genetic characteristics of the 'Annurca' cultivar as well as the harvest time were suggested to be involved in the increase of polyphenol content. Therefore, further studies are necessary to characterize the genetic and metabolomic profile of organic apples.
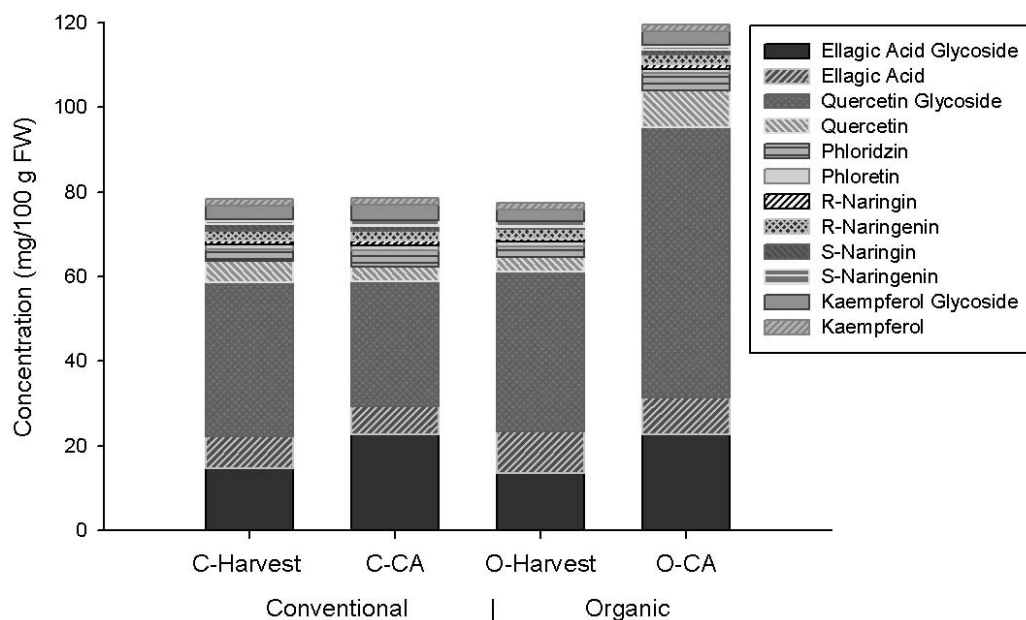
Figure 8.6. Content of selected flavonoids in conventionally and organically grown apples at harvest and under control-atmosphere (CA) storage conditions. Flavonoids were measured as aglycones and glycosides and included: ellagic acid, quercetin, phloretin, R(+)-naringenin, S(-)-naringenin, and kaempferol.

The concentrations of ellagic acid, quercetin, phloretin, R(+)-naringenin, S(-)-naringenin, kaempferol and their glycosides at harvest and after CA storage are summarized in **Table 8.5**. Quercetin glycoside and ellagic acid glycoside were the polyphenols in the glycosylated form with the highest concentrations in both conventionally and organically grown apples at harvest and after storage followed by kaempferol glycoside, phloridzin, R(+)-naringin, and S(-)-naringin. The aglycone with the highest concentration was ellagic acid at harvest and after storage followed by quercetin R(+)-naringenin, kaempferol, S(-)-naringenin, and phloretin regardless of the method of storage or farming system. Of all the polyphenols analyzed, only quercetin and phloridzin have been previously described in apple extracts [189,190]. Overall, the glycoside form of all six flavonoids was 3-fold to 4-fold higher than the aglycone form. These findings are in accordance with previously reported results of

analysis of apple polyphenol content that described polyphenols to be mainly associated with glycosylated sugar moieties [190].

Table 8.5. Concentration (mg/100 g FW) of ellagic acid, quercetin, phloretin, R-naringenin, S-naringenin, kaempferol and the respective glycosides in conventionally and organically grown apples (mean ± S.E.M.).

Compound (mg/100 g FW)		Conventional		Organic	
		Harvest	CA	Harvest	CA
Ellagic Acid	Glycoside	14.70	22.61	13.51	22.69
	Aglycone	7.45	6.67	9.79	8.71
	Total	**22.15**	**29.28**	**23.30**	**31.40**
Quercetin	Glycoside	36.53	29.57	37.93	63.87
	Aglycone	4.91	3.40	3.37	8.70
	Total	**41.44**	**32.97**	**41.30**	**72.57**
Phloretin	Glycoside	2.92	3.98	2.55	4.06
	Aglycone	1.00	1.01	1.02	1.04
	Total	**3.92**	**4.99**	**3.57**	**5.10**
R-Naringenin	Glycoside	0.97	1.31	0.76	1.14
	Aglycone	2.35	2.29	2.31	2.26
	Total	**3.32**	**3.60**	**3.07**	**3.40**
S-Naringenin	Glycoside	1.57	1.04	0.55	1.07
	Aglycone	1.22	1.32	1.28	1.19
	Total	**2.79**	**2.36**	**1.83**	**2.26**
Kaempferol	Glycoside	2.97	3.72	2.81	3.12
	Aglycone	1.68	1.59	1.60	1.66
	Total	**4.65**	**5.31**	**4.41**	**4.78**
Total Glycosides		59.66	62.23	58.11	95.35
Total Aglycones		18.61	16.28	19.37	23.56
TOTAL POLYPHENOLS		**78.27**	**78.51**	**77.48**	**118.91**

8.4.2.3   Apple Juices

The content of selected polyphenols was also studied in conventional and organic apple juices. Juices were purchased from local grocery stores and analyzed as described in section 8.3.5. Conventional juices showed similar content of total polyphenols; whereas, the organic brand Knudsen showed total polyphenols concentration 1.6-fold higher than the other brand of organic juice, Nantu (**Fig. 8.7** and **Table 8.6**). Similar to what was seen in fresh

apples, the predominant polyphenol was ellagic acid in three of the four juices studied. Only in Knudsen juice (organic) the content of kaempferol was predominant. The polyphenol with the lowest concentration was S(-)-naringenin. Previous reports of isomerization after food processing have been reported in vegetables [198]. This process may explain some of the differences seen at the lowest concentrations of fresh apples and apple juices.
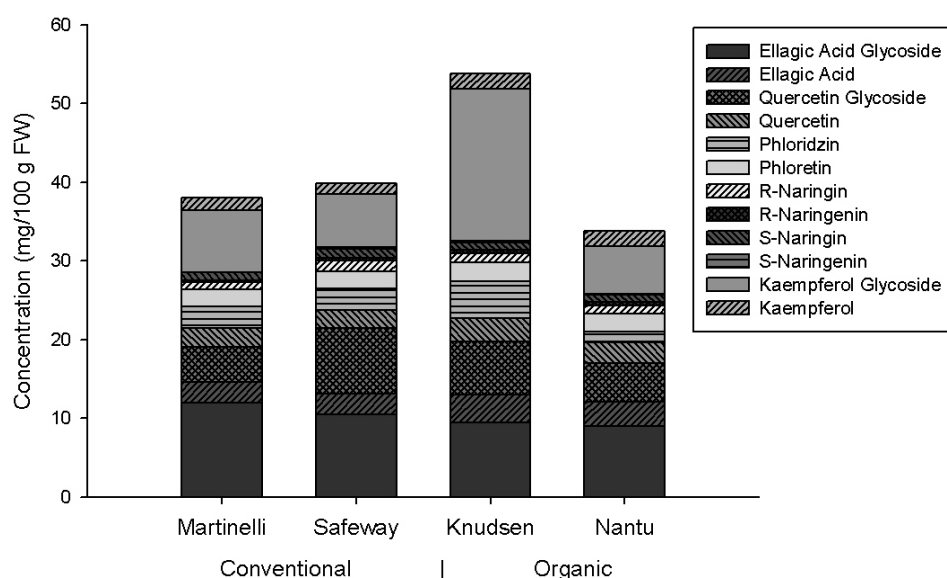
Figure 8.7. Content of ellagic acid, quercetin, phloretin, R(+)-naringenin, S(-)-naringenin, kaempferol and the respective glycosides in conventional and organic apple juices.

Higher concentrations of glycosides were seen both in organic and conventional juices. The glycoside content of apple juices was between 2.2-fold and 3.5-fold higher than the aglycones. Lower concentrations of total polyphenols in juices compared to fresh fruit were observed. These findings are in accordance with previous studies in which oxygenation during processing was demonstrated to significantly reduce all classes of polyphenols [199].

Table 8.6. Concentration (mg/100 g FW) of ellagic acid, quercetin, phloretin, R-naringenin, S-naringenin, kaempferol and the respective glycosides in conventional and organic apple juices (mean values).

Compound (mg/100 g FW)		Conventional		Organic	
		Martinelli	Safeway	Knudsen	Nantu
Ellagic Acid	Glycoside	12.02	10.49	9.44	9.06
	Aglycone	2.57	2.61	3.58	3.08
	Total	14.59	13.10	13.02	12.14
Quercetin	Glycoside	4.46	8.40	6.75	4.90
	Aglycone	2.45	2.24	2.99	2.61
	Total	6.91	10.64	9.74	7.51
Phloretin	Glycoside	2.71	2.74	4.69	1.41
	Aglycone	2.20	2.18	2.33	2.24
	Total	4.91	4.92	7.02	3.65
R-Naringenin	Glycoside	0.89	1.42	1.14	1.03
	Aglycone	0.27	0.29	0.45	0.42
	Total	1.16	1.71	1.60	1.45
S-Naringenin	Glycoside	0.93	1.19	0.98	0.92
	Aglycone	0.09	0.16	0.19	0.16
	Total	1.02	1.35	1.17	1.08
Kaempferol	Glycoside	7.81	6.79	19.29	2.04
	Aglycone	1.60	1.38	2.04	1.96
	Total	9.41	8.16	21.33	8.00
Total Glycosides		28.82	31.02	42.29	23.36
Total Aglycones		9.18	8.86	11.58	10.48
TOTAL POLYPHENOLS		38.00	39.88	53.87	33.82

The content of polyphenols in apple juices has been previously reported [200-204]. However, to our knowledge this is the first time the stereospecific content of naringenin is reported in apple juices.

8.4.3 Pharmacological Activity of Apple Extracts

8.4.3.1   In vitro Anti-cancer Activity

The Alamar blue (resazurin) fluorescent cell viability measurement is an easy and accurate assay to determine the cytotoxicity of many cell lines. Viable cells are capable of

metabolizing the non-fluorescent dye resazurin into its fluorescent counterpart, resorufin; on the other hand, metabolism of resazurin in non-viable cells is not achieved. The fluorescence emission can be quantified using a plate reader and the number of viable cells after treatment can be determined.

Flesh and peel samples of 'Red Delicious' apple were treated with and without β-glucuronidase from *H. pomatia* type HP-2 to release the sugar groups from the glycoside forms which increased the available aglycones. The apple extracts of flesh and peel tissue of 'Red Delicious' demonstrated concentration-dependent anti-cancer activity (**Fig. 8.8 and 8.9**). Extracts of the flesh of 'Red Delicious' apple that did not receive β-glucuronidase treatment (free samples) showed greater reduction in the number of Hep-G2 liver cancer cells (IC_{50} = 245.09 ± 30.50 µg/ml); whereas, they showed least effect in PC-3 prostate cancer (2.67E05 ± 537.41 µg/ml) and HCT-116 colon cancer (2.05E05 ± 512.09 µg/ml) cell lines (**Fig. 8.8.1** and **Table 8.7**). On the other hand, extracts of the flesh of 'Red Delicious' apple that underwent treatment with β-glucuronidase from *H. pomatia* type HP-2 (total samples) to cleave any glycosides into aglycones showed greater reduction in the number of MDA-MB-231 breast cancer cells (250.05 ± 81.02 µg/ml), and demonstrated least effect in PC-3 prostate cancer cells (1.59E05 ± 421.75 µg/ml) (**Fig. 8.8.2**).
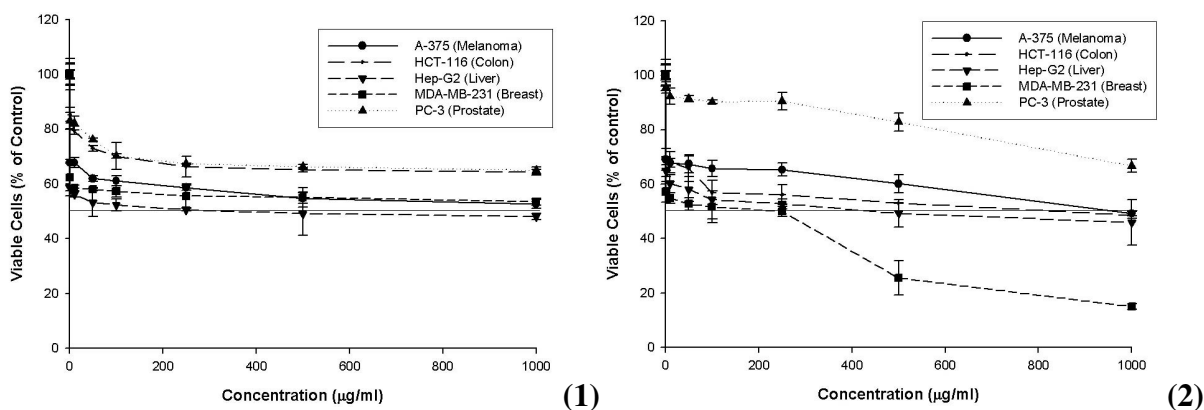
Figure 8.8. Effects of flesh 'Red Delicious' apple extracts treated without (free) **(1)** and with (total) **(2)** β-glucuronidase from *H. pomatia* type HP-2 in the viability of five different cancer cell lines (n = 4, mean ± S.E.M.).

The apple extracts of peel tissue of 'Red Delicious' demonstrated concentration-dependent anti-cancer activity (**Fig. 8.3**). Extracts of the peel of 'Red Delicious' apple that did not receive β-glucuronidase treatment showed greater reduction in the number of MDA-MB-231 breast cancer cells (96.15 ± 12.24 µg/ml); whereas, they were demonstrated least effect in PC-3 prostate cancer cell lines (4.95E04 ± 740.73 µg/ml) (**Fig. 8.3.1**).

Similar results were obtained with extracts of the peel of 'Red Delicious' apple that underwent treatment with β-glucuronidase from *Helix pomatia* type HP-2; the anti-cancer effect was more effective in A-375 melanoma (9.80 ± 1.30 µg/ml) and least effective in PC-3 prostate cancer (5.69E04 ± 513.14 µg/ml; **Fig. 8.3.2** and **Table 8.7**).
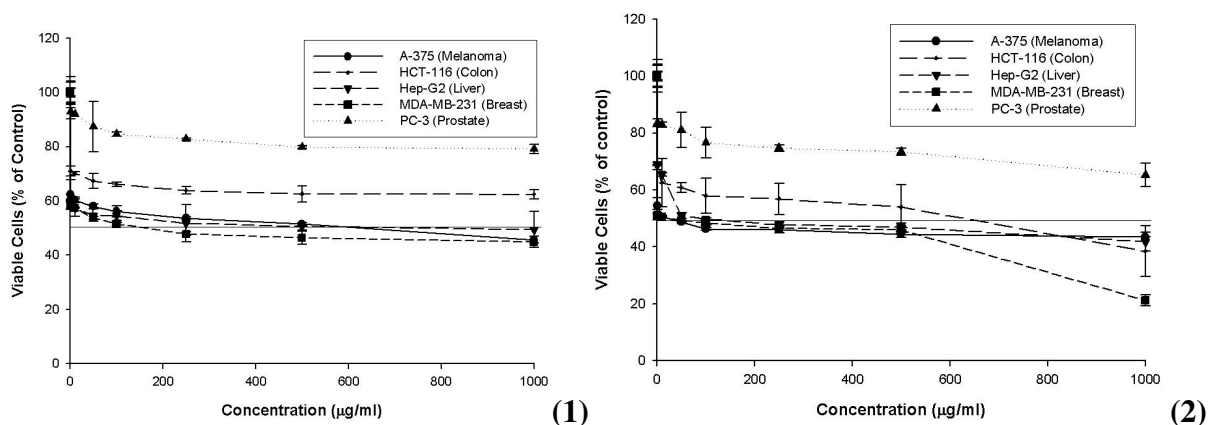
Figure 8.9. Effects of peel 'Red Delicious' apple extracts treated without (free) **(1)** and with (total) **(2)** β-glucuronidase from *H. pomatia* type HP-2 in the viability of five different cancer cell lines (n = 4, mean ± S.E.M.).

Table 8.7. IC_{50} values (µg/ml) of 'Red Delicious' apple extracts treated with (total) and without (free) β-glucuronidase across different cancer cell lines (n = 4, mean ± S.E.M.). a, P < 0.05, free vs. total; b, P < 0.05, flesh vs. peel.

Apple Cultivar	Tissue	β-glucuronidase Treatment (Y/N)	Cell line	IC_{50} (µg/ml)
Red Delicious	Flesh	N	A-375	$1.85E+03 \pm 276.67^{a,b}$
			HCT-116	$2.05E+05 \pm 512.09^{a,b}$
			Hep-G2	245.09 ± 30.50
			MB-MDA-231	$2.23E+03 \pm 250.51^{a,b}$
			PC-3	$2.67E+05 \pm 537.41^{a,b}$
Red Delicious	Flesh	Y	A-375	980.60 ± 82.14^{b}
			HCT-116	970.70 ± 40.50^{b}
			Hep-G2	$510.10 \pm 76.01^{a,b}$
			MB-MDA-231	250.05 ± 81.02^{b}
			PC-3	$1.59E+05 \pm 421.75^{b}$
Red Delicious	Peel	N	A-375	480.76 ± 44.06^{a}
			HCT-116	$3.50E+04 \pm 750.68^{a}$
			Hep-G2	$490.19 \pm 50.71^{a,b}$
			MB-MDA-231	96.15 ± 12.24^{a}
			PC-3	$4.95E+04 \pm 750.73$
Red Delicious	Peel	Y	A-375	9.80 ± 1.30
			HCT-116	462.93 ± 23.42
			Hep-G2	100.23 ± 8.53
			MB-MDA-231	10.01 ± 1.48
			PC-3	$5.69E+04 \pm 513.14^{a}$

The cancer preventive activity of apples or apple components *in vitro* and *in vivo* has been previously reported [188]. Apple components have been described to have anti-mutagenic potential by modulation of phase 1 and 2 carcinogen metabolism, inhibition of cell proliferation and cancer signaling pathways, as well as apoptosis induction [205-208]. Apple extracts demonstrated to reduce the activity of Cyp1A1 (cytochrome P450, family 1, subfamily A, polypeptide 1) in Caco-2 colon cancer cells. Likewise, quercetin was reported to be a Cyp1A1 inhibitor. Cyp1A1 plays a role in drug metabolism of intestinal cells by activating certain chemical carcinogens, i.e. polycyclic aromatic hydrocarbons, and inhibition of Cyp1A1 may contribute to the chemopreventive properties described for apple extracts [208]. Apple extracts were shown to inhibit cell growth; polyphenols and triterpenoids in apple peel demonstrated inhibition of Hep-G2 liver cancer and Caco-2 colon cancer cell proliferation [207]. It was suggested that the effect of polyphenols on cell growth was due to the production of hydrogen peroxide (H_2O_2) [209]; however, it was later demonstrated that H_2O_2 formation occurred only in bicarbonate-buffered solutions [210]. Addition of HEPES to the media was sufficient to avoid H_2O_2 production [188]. Fridrich *et. al.* demonstrated that apple polyphenols diminished the phosphorylation of the epidermal growth factor (EGF) receptor in HT-29 colon carcinoma cells; therefore, inhibiting cancer signaling pathways [206]. The effect of apple extracts in the induction of apoptosis was investigated by Chen *et. al* [205]. Apple extracts inhibited 20S proteasome activity associated with cancer cell apoptosis. *In vivo* studies have shown that polyphenol-rich apple extracts are effective and safe in reducing tumors in chemically-induced peel papillomas and colon carcinogenesis in mice. Likewise, polyphenols in apples have shown anti-cancer activity against multiple intestinal neoplasia in transgenic mice [188]. These findings are limited to studies of apples

in Germany. In the United States, studies have been performed with apples grown in New York and Michigan, but since the content and composition of polyphenolic compounds in apples may be dependent on factors including the area of cultivation, studies of Washington State apples are relevant to our understanding of the relationship between polyphenolic content and anti-cancer activity. To our knowledge, the biological activity and content analysis of apple extracts has not been investigated in apple cultivars in the state of Washington. Similarly, no studies have compared the effects of different apple cultivars in different *in vitro* cancer cell models.

In summary, the apple extracts of flesh and peel tissues of the 'Red Delicious' cultivar demonstrated concentration-dependent anti-cancer activity. Peel was more effective in inhibiting cell growth than flesh regardless of the cell line analyzed. Extracts in which the glycosides were cleaved using β-glucuronidase demonstrated higher inhibition of cancer cell growth than extracts without the treatment.

8.4.3.2   In vitro Anti-inflammatory Activity

Apples have been reported to inhibit COX-1 and COX-2 activity [211,212]. Apple juice extracts have also been tested for their anti-inflammatory activity; phloretin and (-)-epicatechin were the most potent COX-1 inhibitors [212]. In another study, apple extracts of fresh apples were tested for their role in the inhibition of nuclear factor (NF)-κB activation which is involved in chronic inflammatory diseases [211]. Exposure of human umbilical vascular endothelial cells (HUVECs) to 20, 200, and 2,000 nM of apple extracts resulted in reduced P-IκBα expression [211]. The inhibition of COX in turn reduces prostaglandin (PG) levels. Excess PGs can cause cellular injury and uncontrolled inflammation. *In vitro* studies

have demonstrated the anti-inflammatory activity of some apple components [188]. Nevertheless, studies that compare the effect of different apple cultivars grown in the state of Washington in arthritis or colitis models are nonexistent.

8.4.3.2.1 *In vitro Arthritis Model*

No study to date has reportedly used a chondrocyte (CnC) model to measure the anti-inflammatory activity of apples or apple components in arthritis. However, pterostilbene, a natural compound found in grapes and blueberries has been reported to decrease the level of some inflammatory mediators – i.e. MMP-3, sGAG, and TNF-α – in chondrocyte cells [153].

In order to begin exploration of pathogenic mechanisms involved in rheumatoid arthritis, certain mediators were measured including PGE_2, TNF-α, NO, sGAG, and MMP-3. The effect of 'Red Delicious' and 'Golden Delicious' apple extracts in PGE_2 levels produced by chondrocyte cells was evaluated (**Fig. 8.10** and **Table 8.8**). The chondrocyte controls produced low PGE_2 levels (0.44 ± 0.02 ng/ml) compared to chondrocytes treated with IL-1β (0.69 ± 0.01 ng/ml). The extracts of flesh and peel of 'Red Delicious' and 'Golden Delicious' reduced PGE_2 levels in a concentration-dependent manner.

Figure 8.10. Prostaglandin E_2 (PGE_2) production in the chondrocyte cell culture medium at 72 hours after treatment with **(1)** flesh and **(2)** peel extracts from 'Red Delicious' and 'Golden Delicious' apple extracts treated with (total) and without (free) β-glucuronidase (n = 3, mean ± S.E.M.). Values are expressed as ng/ml. The line represents the baseline level in which chondrocyte cells have not been exposed to inflammatory insult.

Extracts of peel of 'Golden Delicious' that received the β-glucuronidase from *H. pomatia* type HP-2 treatment demonstrated to be the most effective in reducing PGE_2 levels in chondrocytes (442.85 ± 57.72 µg/ml; **Table 8.8**).

Table 8.8. IC_{50} values (µg/ml) of 'Red Delicious' and 'Golden Delicious' apple extracts treated with (total) and without (free) β-glucuronidase for PGE_2 reduction in chondrocyte cells (n = 3, mean ± S.E.M.). a, $P < 0.05$, free vs. total; b, $P < 0.05$, flesh vs. peel.

Apple Cultivar	Tissue	β-glucoronidase Treatment (Y/N)	IC_{50} (µg/ml)
Red Delicious	Flesh	N	592.85 ± 88.21
		Y	535.71 ± 42.36
	Peel	N	521.43 ± 36.52
		Y	578.57 ± 67.34
Golden Delicious	Flesh	N	470.58 ± 42.36
		Y	635.71 ± 92.89[a,b]
	Peel	N	522.05 ± 32.29
		Y	442.85 ± 57.72

The effect of 'Red Delicious' and 'Golden Delicious' apple extracts in TNF-α levels produced by chondrocyte cells was evaluated (**Fig. 8.11**). The untreated controls exhibited

low concentrations of TNF-α (7.45 ± 0.28 pg/ml) compared to chondrocytes treated with IL-1β (8.88 ± 0.07 ng/ml).
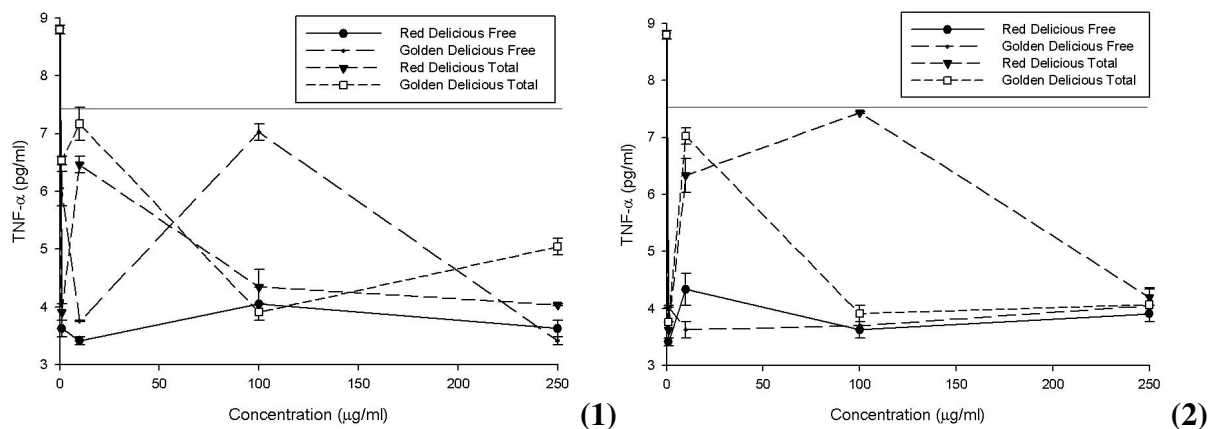
Figure 8.11. Tumor necrosis factor-α (TNF-α) production in the chondrocyte cell culture medium at 72 hours after treatment with **(1)** flesh and **(2)** peel extracts from 'Red Delicious' and 'Golden Delicious' apple extracts treated with (total) and without (total) β-glucuronidase (n = 3, mean ± S.E.M.). Values are expressed as pg/ml. The line represents the baseline level in which chondrocyte cells have not been exposed to inflammatory insult.

'Red Delicious' and 'Golden Delicious' extracts of peel and flesh did not have a clear effect in TNF-α levels. At some concentrations the treatment with apple extracts increased TNF-α levels; whereas, an increase in TNF-α levels was observed at 10.0 and 100 μg/ml of apple extract treatment. These findings suggest an anti-inflammatory effect with the reduction of PGE$_2$ levels but not TNF-α levels by the 'Red Delicious' and 'Golden Delicious' apple extracts.

Furthermore, the effect of 'Red Delicious' and 'Golden Delicious' apple extracts in reducing experimental chondro-degeneration *in vitro* was evaluated. The effect of 'Red Delicious' and 'Golden Delicious' apple extracts on NO (as nitrite) levels produced by chondrocyte cells was evaluated (**Fig. 8.12**). The chondrocyte controls produced low nitrite

levels (5.48 ± 0.03 μM) due to the constitutive nitric oxide synthase compared to chondrocytes treated with IL-1β (8.68 ± 0.13 μM). Neither 'Red Delicious' nor 'Golden Delicious' apple extracts showed an effect on NO synthesis in this *in vitro* arthritis model. Moreover, the extracts exhibited a slight increase in nitrite production at all concentrations of apple extracts studied.
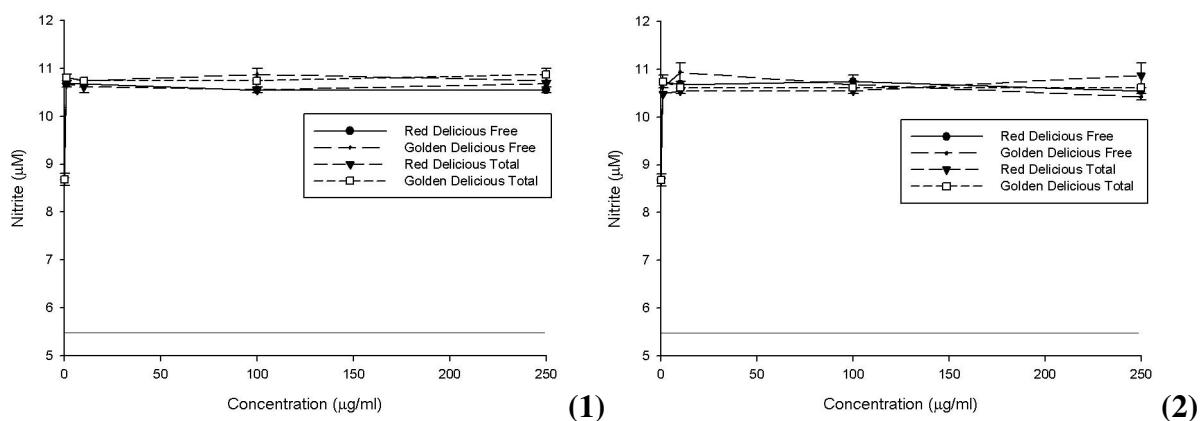
Figure 8.12. Nitric oxide (NO) production in the chondrocyte cell culture medium at 72 hours after treatment with **(1)** flesh and **(2)** peel extracts from 'Red Delicious' and 'Golden Delicious' apples (n = 3, mean ± S.E.M.). Values are expressed as μM. The line represents the baseline level in which chondrocyte cells have not been exposed to inflammatory insult.

The effect of 'Red Delicious' and 'Golden Delicious' apple extracts on MMP-3 levels produced by chondrocyte cells was evaluated (**Fig. 8.13**). The untreated controls exhibited low concentrations of MMP-3 levels (0.033 ± 0.001 ng/ml) compared to chondrocytes with IL-1β (0.084 ± 0.0003 ng/ml). The flesh extracts of 'Golden Delicious' and 'Red Delicious' increased the MMP-3 levels in chondrocytes at high concentrations (100.0 and 250.0 μg/ml). However, at low concentrations (1.0 and 10.0 μg/ml), the apple extracts decreased the MMP-3 concentrations in chondrocytes below baseline levels.

The peel extracts of 'Red Delicious' and 'Golden Delicious' also showed a decrease in the MMP-3 levels at low (1.0 and 10.0 µg/ml) and high (250.0 µg/ml) concentrations. However, the MMP-3 levels increased at 100.0 µg/ml.
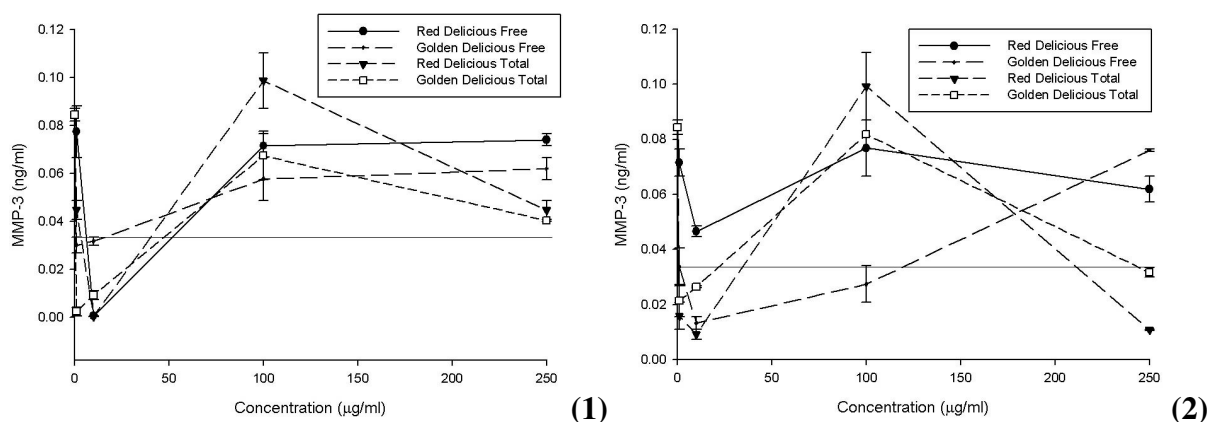
Figure 8.13. Matrix metallopeptidase-3 (MMP-3) production in the chondrocyte cell culture medium at 72 hours after treatment with **(1)** flesh and **(2)** peel extracts from 'Red Delicious' and 'Golden Delicious' apples (n = 3, mean ± S.E.M.). Values are expressed as ng/ml. The line represents the baseline level in which chondrocyte cells have not been exposed to inflammatory insult.

The effect of 'Red Delicious' and 'Golden Delicious' apple extracts on sGAG levels produced by chondrocyte cells was evaluated (**Fig. 8.14**). The untreated controls produced low levels of sGAG (46.25 ± 0.02 µg/ml) compared to chondrocytes treated with IL-1β (53.89 ± 0.59 µg/ml). There was a decrease in sGAG levels in chondrocytes treated with apple flesh extracts. However, flesh of 'Red Delicious' actually increased the sGAG levels (**Fig. 8.14.1**).

The peel extracts of 'Red Delicious' and 'Golden Delicious' showed an increase at low concentrations (1.0 and 10.0 µg/ml) and a decrease in sGAG levels at high concentrations (100.0 and 250.0 µg/ml; **Fig. 8.14.2**).

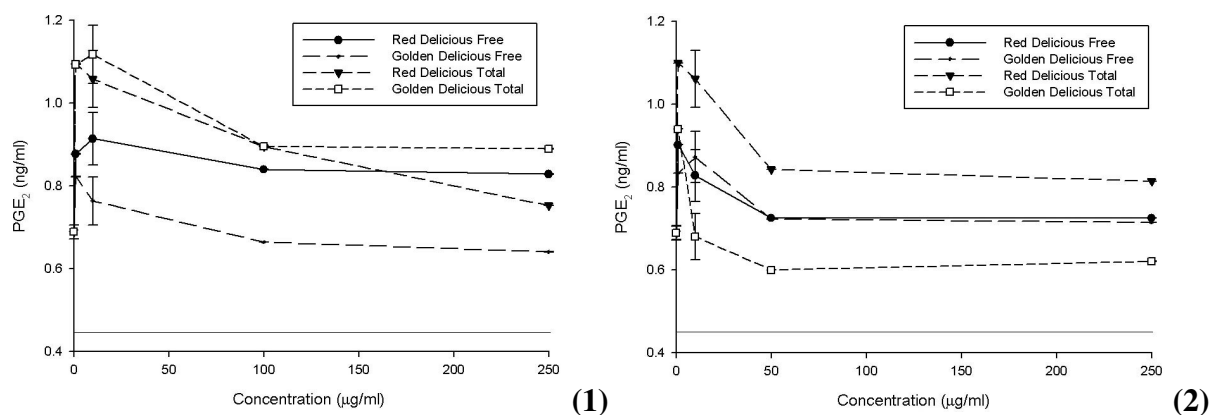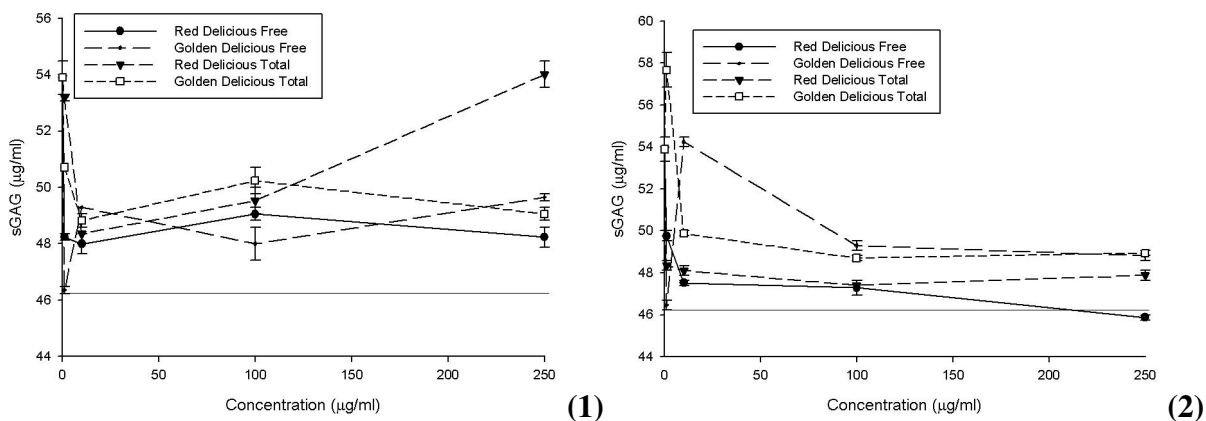**Figure 8.14.** Sulphated glycosaminoglycans (sGAG) production in the chondrocyte cell culture medium at 72 hours after treatment with **(1)** flesh and **(2)** peel extracts from 'Red Delicious' and 'Golden Delicious' apples (n = 3, mean ± S.E.M.). Values are expressed as µg/ml. The line represents the baseline level in which chondrocyte cells have not been exposed to inflammatory insult.

These results suggest that at low concentrations, apple extracts may have a protective effect on chondrocytes *in vitro*. No changes were observed in NO levels. MMP-3 levels decreased with low concentrations of apple extracts; whereas, sGAG levels decreased with high concentrations of apple extracts. Low concentrations are probably more physiologically relevant to the *in vivo* situation.

The anti-inflammatory activity of 'Red Delicious' and 'Golden Delicious' apple extracts in an *in vitro* arthritis model was studied. Several inflammatory markers in arthritis were measured including PGE_2, NO, TNF-α, MMP-3, and sGAG. Controls for each mediator measured showed a low level of mediator production which markedly increased after treatment with IL-1β. Degenerative arthropathies such as arthritis are characterized by a progressive destruction of the articular joint tissue which results in metabolic modifications in cartilaginous tissue. Degenerative, oxidative, and inflammatory mechanisms cause an imbalance between the reparative and destructive processes of articular cartilage.

Inflammation is characterized by the extravasation and infiltration of leukocytes into the affected tissue regardless of the cause of inflammation [213]. Interactions of white cell adhesion molecules with those on endothelial cells mediate the inflammatory events. Macrophages and other antigen presenting cells phagocytize and kill microorganisms and produce TNF-α, interleukin (IL)-1, matrix metalloproteases including MMP-3, which can cleave collagen and proteoglycans in cartilage. In addition, activation of phospholipase A_2 results in the synthesis of prostaglandins, leukotrienes and platelet-activating factor which are also involved in the inflammatory response. The expression of the inducible form of COX, COX-2, also contributes to the formation of prostaglandins [213]. Cytokines like TNF-α and IL-1 induce the transcription of inducible nitric oxide synthase (iNOS) in leukocytes, fibroblasts and other cell types accounting for higher NO levels [214]. NO is involved in vasodilation present in acute inflammation; experimental models of acute inflammation demonstrated a dose-dependent protective effect of iNOS inhibitors suggesting that NO promotes edema and vascular permeability [214].

In rheumatoid arthritis an inflammatory response occurs in affected joints where immune complexes are deposited and eicosanoids amplify inflammation [22]. Lymphocytes and macrophages accumulate in the synovium and polymorphonuclear leukocytes (PMNs) localize in the synovial fluid. Eicosanoids are produced by PMNs mainly as leukotrienes in order to facilitate T-cell proliferation and act as chemoattractants. Other eicosanoid produced include PGE_2 and TXA_2 [22]. Synovial fluid from patients with arthritis was demonstrated to contain peroxynitrite and other products that result from NO oxidation. NO has been reported to stimulate the synthesis of inflammatory prostaglandins by activating COX-2 [214]. Therefore, inhibition of NO may have a beneficial effect on joint diseases that present

inflammation [214]. sGAG has been used as a biomarker of proteoglycan turnover [215] and was reported to increase following joint injury consistent with altered cartilage metabolism following injury and inflammation [215].

Elevated levels of IL-1β have been reported in synovial fluid of arthritic patients and are considered one of the most potent catabolic factors in arthropathies like arthritis [216]. The *in vitro* canine model utilized to assess the effect of apple extracts in arthritis may produce valuable information for the possible effects of apple consumption in humans and may also provide information of the differences in intra-species comparisons. Moreover, flavonoids are a constituent in many nutraceutical supplements for dogs, i.e. PhyCox-JS$^{®}$ [217] of which there are ongoing studies at Washington State University including our laboratory.

In order to effectively study a wide concentration-response window, concentrations between 1.0 and 250.0 µg/ml apple extracts were studied. Nevertheless, low concentrations give more valuable information to predict the possible effects *in vivo*. The *in vitro* activity of apple extracts suggests that they may act on the pathogenic mechanisms of arthritis in inflammation (PGE$_2$) and chondro-degeneration (MMP-3).

8.4.3.2.2   *In vitro Colitis Model*

Prostaglandins (PG) are produced throughout the gut; in particular PGE$_2$ is very important to maintain the normal physiological function of the GI tract. PGE$_2$ is involved in gastric mucosal protection and motility during normal GI function [163]; however, PGE$_2$ is also implicated in the pathology of diseases like inflammatory bowel disease (IBD), entero-invasive bacterial diseases, and colorectal cancers [163].

The effect of 'Gala' and 'Red Delicious' apple extracts harvested in 2005 and 2006 in the PGE_2 levels produced by HT-29 colon adenocarcinoma cells was evaluated (**Fig. 8.15** and **Fig. 8.16**). This study demonstrated the anti-inflammatory activity of apple extracts in a colitis model *in vitro* to be concentration-dependent (**Fig. 8.15**). Peel and flesh apple extracts of Red Delicious and 'Gala' cultivars harvested in 2005 and 2006 demonstrated a rapid decrease in PGE_2 levels at low concentrations (0.2 µg/ml) and a slight decrease at 2.0 and 20.0 µg/ml apple extracts. 'Red Delicious' exhibited more effective reduction of PGE_2 levels in HT-29 cells compared to 'Gala'. Peel tissue demonstrated higher reduction of PGE_2 levels when compared to flesh. No significant differences were observed between apple extracts of the same cultivar harvested in two different years, except for flesh of 'Red Delicious' that was reported to be less effective (higher IC_{50}) in the apples harvested in 2006 (**Table 8.9**).
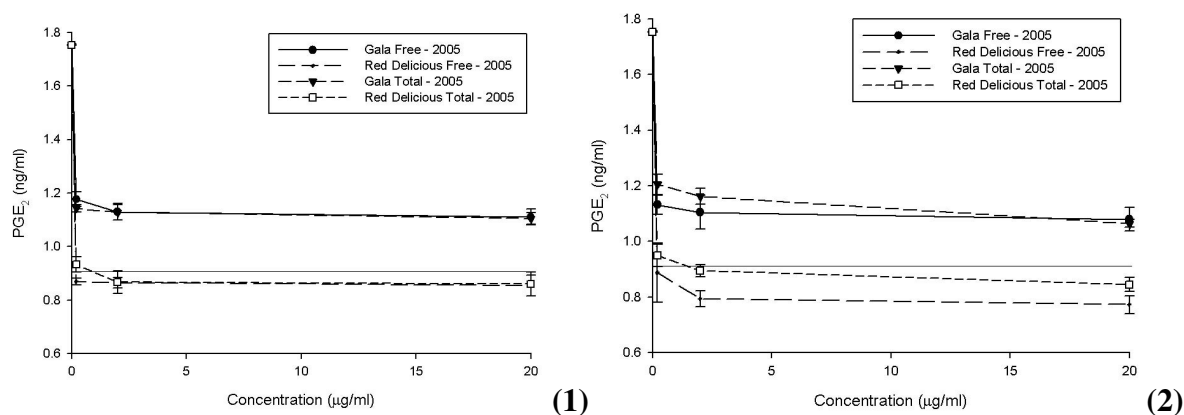
Figure 8.15. Prostaglandin E_2 (PGE_2) production in the HT-29 cell culture medium at 72 hours after treatment with (**1**) flesh and (**2**) peel extracts from 'Gala' and 'Red Delicious' apples harvested in 2005 (n = 3, mean ± S.E.M.). Values are expressed as ng/ml. The line represents the baseline level in which HT-29 cells have not been exposed to inflammatory insult.
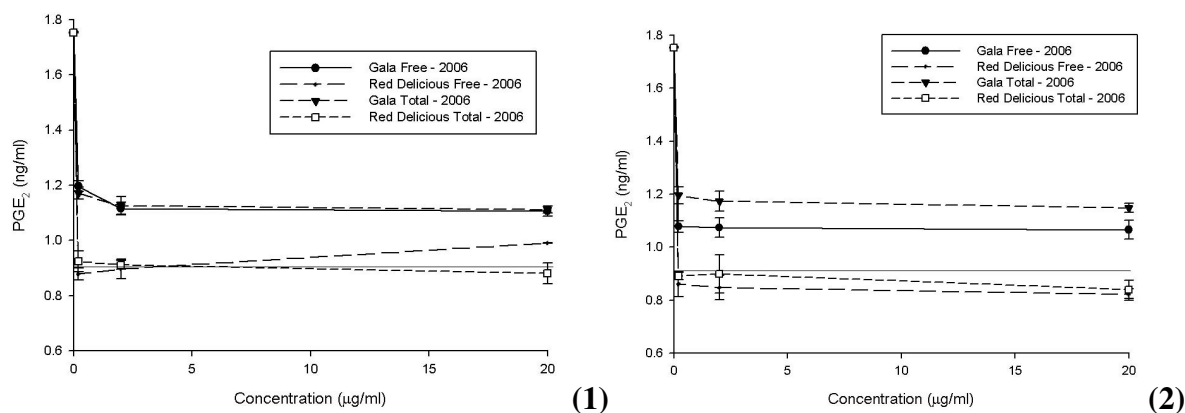
Figure 8.16. Prostaglandin E_2 (PGE_2) production in the HT-29 cell culture medium at 72 hours after treatment with **(1)** flesh and **(2)** peel extracts from 'Gala' and 'Red Delicious' apples harvested in 2006 (n = 3, mean ± S.E.M.). Values are expressed as ng/ml. The line represents the baseline level in which HT-29 cells have not been exposed to inflammatory insult.

Table 8.9. IC_{50} values (µg/ml) of 'Gala' and 'Red Delicious' apple extracts treated with (total) and without (free) β-glucuronidase for PGE_2 reduction in canine chondrocyte cells (n = 3, mean ± S.E.M.). a, $P < 0.05$, free vs. total; b, $P < 0.05$, flesh vs. peel.

Apple Cultivar	Year	Tissue	β-glucoronidase Treatment (Y/N)	IC_{50} (µg/ml)
Gala	2005	Flesh	N	25.22 ± 3.78
			Y	25.00 ± 3.75
		Peel	N	24.54 ± 0.22
			Y	24.09 ± 0.35
	2006	Flesh	N	25.12 ± 3.74
			Y	25.22 ± 3.06
		Peel	N	24.32 ± 3.04
			Y	26.13 ± 3.09
Red Delicious	2005	Flesh	N	0.20 ± 0.01
			Y	2.01 ± 0.05[a]
		Peel	N	0.21 ± 0.04
			Y	2.02 ± 0.10[a]
	2006	Flesh	N	0.21 ± 0.03
			Y	20.00 ± 3.05[a,b]
		Peel	N	0.21 ± 0.03
			Y	0.20 ± 0.04

Previous studies in HT-29 adenocarcinoma cells treated with apple juice polyphenols for 24 hours resulted in a 1.6- to 2.1-fold induction of mRNA levels of several phase II metabolism enzymes that have been associated with cancer chemoprevention [188]. However, this study failed to assess the effect of apple polyphenols in the production levels of inflammatory markers like PGE_2. In addition, to our knowledge no studies have compared the effects of different apple cultivars in a colitis *in vitro* model.

These findings suggest that apple extracts effectively reduce the levels of PGE_2 in colitis *in vitro*. 'Red Delicious' was demonstrated to be more effective than 'Gala' if these results are extended to the *in vivo* situation, and may have a protective effect in the GI tract in pathologies like colitis and IBD.

8.4.3.3   In vitro Anti-Oxidant Activity

The principle behind this assay is the formation of the ferryl myoglobin radical from metmyoglobin and hydrogen peroxide which then oxidizes ABTS to produce a radical cation, $ABTS^{\bullet+}$. The assay measures the total anti-oxidant capacity relying on the ability of the anti-oxidants in the sample to inhibit the oxidation of ABTS to $ABTS^{\bullet+}$ by metmyoglobin, the oxidized form of the oxygen-carrier protein myoglobin [170]. The capacity of the anti-oxidants in the sample to prevent ABTS oxidation was compared with that of Trolox®, a water-soluble tocopherol analogue used as positive control.

The anti-oxidant activity of flesh and peel of 'Red Delicious' was measured using the ABTS method (**Fig. 8.17** and **Table 8.10**). The apple extracts of flesh and peel demonstrated concentration-dependent anti-oxidant activity.
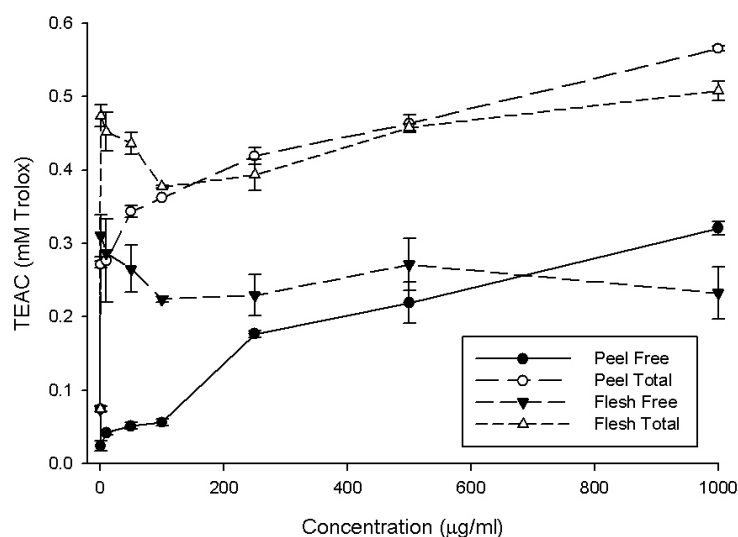
Figure 8.17. Trolox® equivalent anti-oxidant capacity (TEAC) of extracts of flesh tissue of 'Red Delicious', with (total) and without (free) enzymatic hydrolysis with β-glucuronidase (n = 3, mean ± S.E.M.).

Table 8.10. IC$_{50}$ values (µg/ml) of 'Red Delicious' apple extracts treated with (total) and without (free) β-glucuronidase to inhibit ABTS radical formation (n = 3, mean ± S.E.M.). a, P < 0.05, free vs. total.

Apple Variety	Tissue	β-glucoronidase Treatment (Y/N)	IC$_{50}$ (µg/ml)
Red Delicious	Flesh	N	380.41 ± 45.64[a]
		Y	292.90 ± 29.29
	Peel	N	383.55 ± 34.19[a]
		Y	253.92 ± 22.85

The anti-oxidant content of apples has been previously studied [187-189]. The relationship between the anti-oxidant content in apple peel and the whole fruit in two growing seasons of 19 cultivars in Poland was tested [187]. Some of the cultivars studied in Poland were 'Fuji', 'Gala', 'Golden Delicious', and 'Granny Smith'. Total polyphenols were measured using HPLC or the Fiolin-Ciolcalteu method and were described to be approximately three times higher in the peel as compared to flesh [187]. This study included

the assessment of the activity of anti-oxidative enzymes such as glutathione reductase (GR), ascorbate peroxidase (APX), and catalase (CAT). 'Fuji' showed the highest GR activity, 'Fuji' and 'Gala' showed the highest difference of APX activity between tissues (peel and whole fruit).

Apple phytochemicals have also been reported to possess anti-oxidant activity against peroxyl radicals [188]. Lipophilic fractions of apple extracts with quercetin glycosides and oligomeric procyanidins demonstrated radical scavenger activity against 1,1-diphenyl-2-picrylhydrazyl (DPPH) and superoxide anion radicals [188]. Apple juice extracts and polyphenols from apple pomace were shown to reduce the oxidative DNA damage induced by hydrogen peroxide in colon cancer cell lines *in vitro* [188]. The anti-radical activity of apples was strongly related to the polyphenolic content in apples studied in Italian cultivars collected from different regions and with different farming systems [189].

Epidemiological studies in Germany demonstrated that consumption of organic or conventional 'Golden Delicious' apples resulted in the protection of lymphocyte DNA from hydroxyl radicals [188]. The type of apple production; however, had no effect on polyphenol levels or on any biological effect measured.

To our knowledge, the studies of the anti-oxidant activity of apple extracts have been performed in apple cultivars found in Italy, Poland, and Germany and a strong association with the polyphenolic content was only demonstrated in the Italian study [189]. Davis *et. al.* described the effect of apple extracts on the NF-κB activation system in HUVEC cells which is known to respond to oxidative stress using apples from Washington State purchased from a local grocery [211]. The study included 'Fuji', 'Golden Delicious', 'Red Delicious', and 'Granny Smith' apples; but no results were presented for the analysis of the anti-oxidant

activity of the apple cultivars. Apple extracts were shown to decrease NF-κB signaling and IκBα protein phosphorylation which are indicative of an anti-oxidant effect [211]. Therefore, some apple cultivars grown in Washington State were analyzed for their anti-oxidant activity.

Overall, peel tissue was demonstrated to have higher anti-oxidant activity than flesh in accordance with previous studies of the anti-oxidant activity of apple cultivars [187] and reports that relate the polyphenol content with anti-oxidant activity [189]. However, the peel and flesh extracts of 'Red Delicious' treated with β-glucuronidase showed greater anti-oxidant activity than apple extracts without the treatment. This demonstrates that almost half of the compounds in apples associated with the anti-oxidant activity reported in this fruit are attached to a sugar moiety. When the sugar moiety is release by the action of β-glucuronidase an increase in the anti-oxidant activity is observed in both flesh and peel.

8.4.3.4   In vitro Anti-Adipogenic Activity

Adipose tissue in mammals is present as white adipose tissue (WAT), and brown adipose tissue (BAT). WAT stores excess energy as triglyceride in lipid droplets, whereas BAT uses lipids to generate heat during thermogenesis. Multipotent mesenchymal precursor cells originate adipocytes when committed to pre-adipocytes, either remaining dormant or becoming differentiated adipocytes. 3T3-L1 cells are a well characterized cell line used in the study of adipocyte differentiation [175]. This model system has helped elucidate the molecular basis and signaling pathways of adipogenesis. During terminal differentiation, the fibroblast-like pre-adipocytes undergo morphological and biochemical changes that result in the accumulation of lipid droplets *in vitro* and *in vivo* [175]. Oil Red O staining is used in lipid droplets as an indicator of the degree of adipogenesis.

The effect of 'Gala' and 'Red Delicious' apple extracts on oil red O stained material (OROSM) in 3T3-L1 pre-adipocytes is demonstrated in **Figs. 8.18 - 8.19** and **Table 8.11**. Flesh and peel samples of 'Gala' and 'Red Delicious' were treated with (total samples) and without (free samples) β-glucuronidase. Apples harvested in two different years (2005 and 2006) were evaluated for their effect in the formation and accumulation of triglycerides in the form of lipid droplets after differentiation of pre-adipocytes into adipocytes *in vitro*.

The effect of 'Gala' and 'Red Delicious' apple extracts from 2005 on oil red O stained material (OROSM) in 3T3-L1 pre-adipocytes is demonstrated in **Figs. 8.18** and **Table 8.11**. 'Red Delicious' demonstrated to be more effective in the inhibition of lipid droplets formation and accumulation in adipocytes than 'Gala'. In 'Red Delicious' and 'Gala' extracts the inhibitory effect in the formation of triglycerides in adipocytes was greater for flesh than peel; and the apple extracts with the β-glucuronidase treatment had a higher inhibitory effect than the apple extracts that did not receive the treatment.
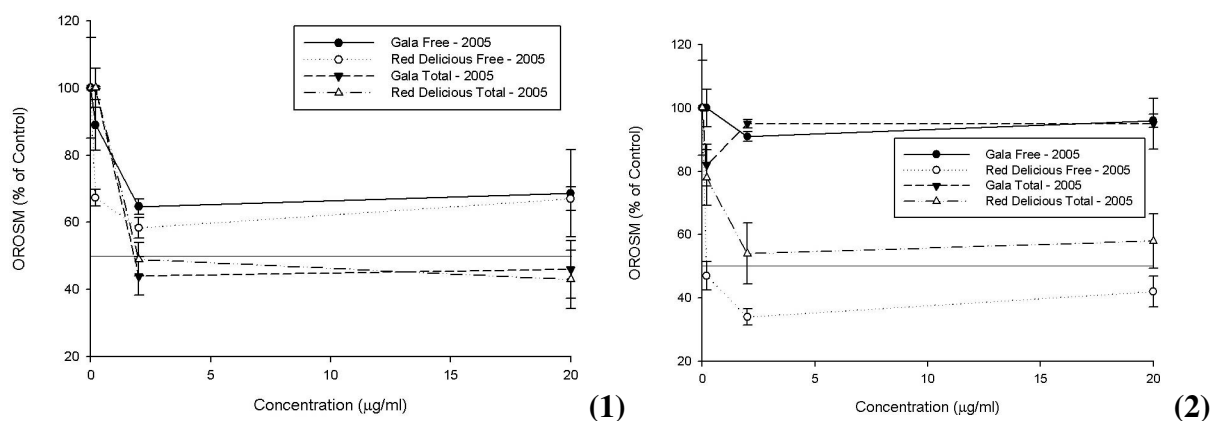
Figure 8.18. Effect of selected apple extracts on oil red O stained material (OROSM) in 3T3-L1 adipocytes. 3T3-L1 pre-adipocytes were harvested 8 days after the initiation of differentiation and were stained with oil red O (n = 3, mean ± S.E.M.). Cells were treated with 0.0 – 20.0 µg/ml of flesh (**1**) and peel (**2**) from 'Gala' and 'Red Delicious' apple extracts harvested in 2005 at 37°C.

The effect of 'Gala' and 'Red Delicious' apple extracts from the 2006 harvest on oil red O stained material (OROSM) in 3T3-L1 pre-adipocytes is demonstrated in **Figs. 8.19** and **Table 8.11**. Similar to what was seen in the apple extracts of 'Gala' and 'Red Delicious' harvest in 2005, most of the 'Red Delicious' extracts were demonstrated to be more effective than 'Gala'. Likewise, flesh of 'Gala' and 'Red Delicious' demonstrated greater inhibitory activity in the accumulation and formation of triglycerides in adipocytes compared to peel.
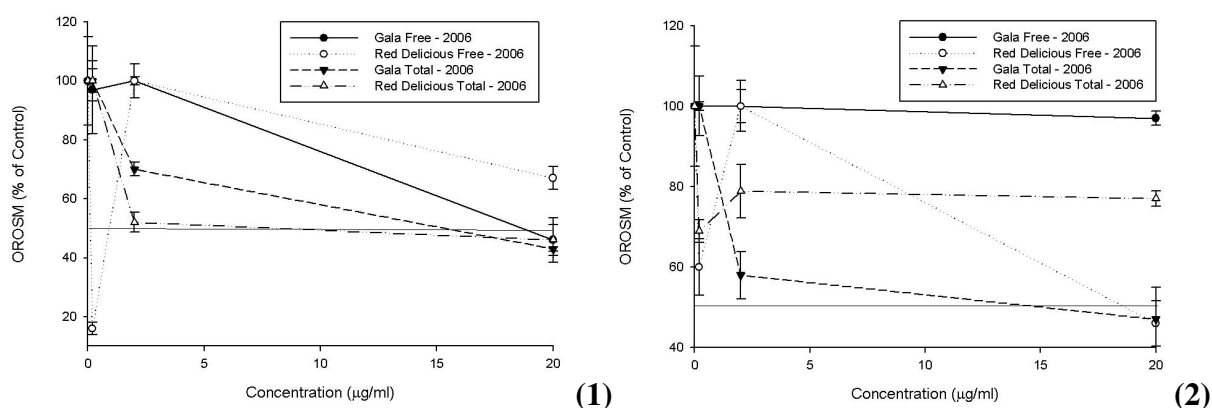
Figure 8.19. Effect of selected apple extracts on oil red O stained material (OROSM) in 3T3-L1 adipocytes. 3T3-L1 pre-adipocytes were harvested 8 days after the initiation of differentiation and were stained with oil red O (mean ± S.E.M.). Cells were treated with 0.0 – 20.0 µg/ml of flesh **(1)** and peel **(2)** from 'Gala' and 'Red Delicious' apple extracts harvested in 2006 at 37°C.

Table 8.11. IC$_{50}$ values (µg/ml) of 'Red Delicious' and 'Gala' apple extracts treated with (total) and without (free) β-glucuronidase for reduction of oil O red stained material (OROSM) in 3T3-L1 adipocyte cells (n = 3, mean ± S.E.M.). a, P < 0.05, free vs. total; b, P < 0.05, flesh vs. peel.

Apple Cultivar	Tissue	Year	β-glucoronidase Treatment (Y/N)	IC$_{50}$ (µg/ml)
Gala	Flesh	2005	N	27.60 ± 4.15[a]
			Y	1.76 ± 0.23
	Peel		N	38.40 ± 4.28[b]
			Y	38.00 ± 2.49[b]
	Flesh	2006	N	18.40 ± 2.58
			Y	17.20 ± 2.07
	Peel		N	38.80 ± 4.66[a,b]
			Y	18.80 ± 2.59
Red Delicious	Flesh	2005	N	26.80 ± 3.15[a,b]
			Y	2.10 ± 0.05
	Peel		N	0.18 ± 0.03
			Y	2.16 ± 0.29[a]
	Flesh	2006	N	6.40E-03 ± 0.01
			Y	2.08 ± 0.30[a]
	Peel		N	18.40 ± 1.92[b]
			Y	30.80 ± 4.15[a,b]

Previous studies have looked at the effect of apple consumption in obesity *in vivo*. Obese Zucker rats fed apples demonstrated a decrease in cholesterol and low-density lipoproteins (LDL) levels compared to lean rats, in which no change in cholesterol occurred. [193]. Combination of apple pectin and apple phenolic fractions were demonstrated to lower plasma and liver cholesterol, triglycerides, and apparent cholesterol absorption to a much greater extent than apple pectin or apple polyphenols alone [218]. However, to our knowledge no *in vitro* adipogenesis model has been use to evaluate the differential effect of peel and flesh tissues of apple extracts.

In summary, the effect of 'Gala' and 'Red Delicious' apple extracts in the formation and accumulation of triglycerides in adipocytes demonstrated differences between the apple

cultivars and tissues studied. Flesh of 'Red Delicious' demonstrated the highest inhibitory effect on triglyceride formation in adipocytes. The treatment with β-glucuronidase demonstrated an increase in the inhibitory effect of most apple extracts and is representative of the action of intestinal bacteria in the GI tract. These results support previous findings that apple consumption decreases cholesterol and low-density lipoproteins *in vivo* [193].

8.5 CONCLUSIONS

A novel HPLC method for ellagic acid, quercetin, phloretin, R(+)-naringenin, S(-)-naringenin and kaempferol is sensitive, reproducible, and accurate. The method was applied for the first time in the analysis and quantification of these selected polyphenols in apples grown in Washington State. These phytochemicals varied in their stability in fresh fruit and in products processed from them like juices. Five different apple cultivars were studied, and ellagic acid was demonstrated to be the predominant polyphenol in 'Gala', 'Golden Delicious', 'Red Delicious', 'Granny Smith' and 'Fuji'. In addition, this is the first report of the enantiomeric content of naringenin in apples; similar to findings in other fruits studied, the S(-)-enantiomer of naringenin is predominant in different apple cultivars. In general, the peel of fresh fruit had higher concentrations of polyphenols when compared to flesh. Moreover, the effect of the farming system utilized to grow apples demonstrated that organically grown apples had greater polyphenol content than apples grown using a conventional farming system.

In addition, the pharmacological activity of apples that are grown and sold in Washington was evaluated. In order to identify the disease prevention benefits of apple consumption associated with polyphenol content, cancer, inflammation, and adipogenesis models were used. Similarly, the anti-oxidant capacity of apple cultivars produced in Washington was evaluated. Fruit extracts exhibited dose-dependent anti-cancer, anti-

inflammatory and anti-oxidant activities that may suggest a potential phytoprotective effect of apple consumption in GI tract pathologies. The anti-adipogenic activity of apple extracts contribute to our understanding of the beneficial effects of apple consumption in the prevention of obesity. These findings may help to elucidate the health benefits of fruit consumption and its relationship with polyphenolic content. Such cross disciplinary studies are essential to further advance our knowledge in this field.

9 <u>Conclusions and Future Directions</u>

9.1 SUMMARY

The specific aims of the studies presented in this thesis were:

1. To develop and validate novel, sensitive, specific, and stereospecific RP-HPLC assays in biological fluids for homoeriodicytol, isosakuranetin, and taxifolin (Chapters II-IV).

2. To characterize the stereospecific pharmacokinetic parameters of homoeriodicytol, isosakuranetin, and taxifolin in a rat model as well as the stereospecific quantification of homoeriodicytol, isosakuranetin, and taxifolin in fruits and herbs (Chapter V).

3. To evaluate the pharmacological activity of homoeriodicytol, isosakuranetin, and taxifolin in *in vitro* cancer, inflammation, oxidation, and adipogenesis models (Chapter VI).

4. To delineate the selected polyphenol content of hybrid tomato cultivars using two distinct fertility management alternatives (Chapter VII).

5. To analyze the selected polyphenol content of several apple cultivars at various harvest maturities, harvest years, and fertility management alternatives; and under commercial storage and shelf-life conditions; and to characterize the pharmacological activity of apple extracts in *in vitro* cancer, inflammation, oxidation, and adipogenesis models (Chapter VIII).

These studies have demonstrated that homoeriodicytol, isosakuranetin, and taxifolin have unique pharmacokinetic disposition and content in fruit and juice as well as unique activity in different *in vitro* assays. In this thesis the current methods of analysis, pharmacological and pharmacokinetic studies, and commercial uses of homoeriodicytol, isosakuranetin, and taxifolin were reviewed (Chapter I). This bibliographic review

demonstrated the lack of studies that take into account the chirality of these compounds. Therefore, the validated HPLC methods to separate and quantify the selected chiral flavonoids: homoeriodicytol, isosakuranetin, and taxifolin in biological matrices were developed and described for the first time (Chapters II – IV). These methods were utilized in the assessment of homoeriodicytol, isosakuranetin, and taxifolin in serum and urine samples in the study of the pharmacokinetics of these compounds in the rat animal model (Chapter V). In addition, the pharmacological effect of the chiral nature of these compounds was evaluated in cancer, inflammation, and adipogenesis models *in vitro.* Likewise, the anti-oxidant capacity, COX, and HDAC inhibitory activities of the racemic and enantiomeric forms of homoeriodicytol, isosakuranetin, and taxifolin were assessed (Chapter VI). These studies demonstrated the utility and necessity of developing stereoselective HPLC methods for racemic flavonoids. The validated HPLC method for the stereoselective separation of isosakuranetin was successfully utilized to isolate the stereoisomers that were not commercially available. Nonetheless, the expense, stability, and time needed to collect enough quantity of the compounds limited the capacity of investigations. Studies of the polyphenolic content of tomatoes and apples were performed using novel HPLC methods of analysis (Chapters VII and VIII). The content of the S(-) and R(+) enantiomers of naringenin were reported for the first time in tomatoes and apples. These studies demonstrated the utility and necessity of developing chiral methods of analysis for polyphenols that show stereoselectivity. These findings contributed to our understanding of the relationship between the polyphenol content of tomatoes and apples with the farming systems utilized to grow the fruit as well as the cultivar of fruit selected. In addition, the pharmacological activity of selected apple extracts was evaluated (Chapter VIII) in cancer, inflammation and

adipogenesis models. Similarly, the anti-oxidant capacities of various apple cultivars were compared. Fruit extracts exhibited dose-dependent anti-cancer, anti-inflammatory, and anti-oxidant activities that suggest a protective effect of apple consumption against gastrointestinal pathologies.

The developed stereospecific HPLC methods for homoeriodicytol, isosakuranetin, and taxifolin have been applied for the first time to pharmacokinetic studies of the stereoisomers of these chiral flavonoids in rats. It has been demonstrated that small differences in the stereochemical structure of the stereoisomers of these flavonoids have a great impact in their pharmacokinetic profile.

Previous pharmacokinetic studies of homoeriodicytol, isosakuranetin, and taxifolin are limited, and have not taken into consideration the chiral nature of these compounds. To our knowledge, these are the first studies that have assessed the stereospecific pharmacokinetics of homoeriodicytol, isosakuranetin, and taxifolin after intravenous administration of the pure racemates to rats. Previous studies of the three flavonoids have focused only on the racemic mixtures and have utilized achiral analysis in serum, urine, and tissues. Most of the previous studies only collect samples up to 24 hours post-dose, which could result in the underestimation of the elimination phase and therefore of the pharmacokinetic parameters.

It was also observed that some discrepancy existed between half-lives in serum and urine for homoeriodicytol, isosakuranetin, and taxifolin. Assay sensitivity in serum may explain this inconsistency; therefore, it is likely that serum half-lives significantly underestimate overall half-lives of homoeriodicytol, isosakuranetin, and taxifolin. In addition, it was observed that homoeriodicytol, isosakuranetin, and taxifolin were detected in urine up to 96 hours, whereas these compounds were detected in serum for up to two hours. Thus, a

more accurate determination of pharmacokinetic parameters can be obtained from an analysis of urinary excretion.

The limited assay sensitivity in serum may be overcome using other methods of analysis such as high performance liquid chromatography – mass spectrometry (HPLC-MS), liquid chromatograph – mass spectrometry – mass spectrometry (LC-MS-MS), or gas chromatography – mass spectrometry (GC-MS) that allow for detection of much lower concentrations. These findings demonstrate the challenges of experimentally understanding the disposition of homoeriodicytol, isosakuranetin, and taxifolin, consistent with other flavonoids studies [152-154]. Urinary data is of tremendous utility in describing the pharmacokinetics of these compounds since plasma concentrations are low and clearance from plasma is quite rapid.

Based on the pharmacokinetic data obtained, homoeriodicytol, isosakuranetin, and taxifolin appear to exit the systemic circulation in order to distribute into tissues. High V_{SS} values were reported for the stereoisomers of homoeriodicytol, isosakuranetin, and taxifolin, except for (2S3R)-(+)-taxifolin and (2R3S)-(-)-taxifolin. Clearance occurs mainly via non-renal routes, assuming that the hepatic clearance is equivalent to non-renal clearance. Low fraction excreted in urine (f_e) values were seen in all stereoisomers of homoeriodicytol, isosakuranetin, and taxifolin, except for (2S3R)-(+)-taxifolin and (2R3S)-(-)-taxifolin.

The pharmacokinetics of homoeriodicytol reveals distribution, metabolism, and elimination that are dependent on the stereochemistry of the enantiomers. Both R(+)-homoeriodicytol and S(-)-homoeriodicytol have long half-lives, they exit the central compartment and penetrate into tissues. R(+)-homoeriodicytol and S(-)-homoeriodicytol are

metabolized in the liver into glucuro-conjugates and are mainly cleared by non-renal routes. S(-)-homoeriodicytol excretion in urine is higher than R(+)-homoeriodicytol.

The disposition, metabolism, and excretion of Isosakuranetin are stereoselective processes. Though isosakuranetin enantiomers have long half-lives, 2S-isosakuranetin remains in the body 1.5-fold longer than 2R-isosakuranetin. 2S-isosakuranetin and 2R-isosakuranetin exit the central compartment and penetrate deep into tissues. They are metabolized in the liver, where glucuro-conjugates are formed, and are excreted mainly via non-renal routes. 2S-isosakuranetin is more readily excreted in urine than the 2R-enantiomer.

The stereoisomers of taxifolin have comparably long half-lives, with (2R3R)-(+)-having shorter half-life than the other three stereoisomers. The stereoisomers of taxifolin exit the central compartment and are either distributed intracellularly, extracellularly, or even reach deep into tissues depending on their stereochemistry. (2S3R)-(+)-, (2S3S)-(-)-, (2R3R)-(+)-, and (2R3S)-(-)-taxifolin are metabolized in the liver to a lesser degree than homoeriodicytol and isosakuranetin. (2S3S)-(-)-, (2R3R)-(+)-, and (2R3S)-(-)-taxifolin are mainly excreted via non-renal routes; whereas (2S3R)-(+)-taxifolin is mainly excreted by the kidneys.

The differences in disposition, metabolism, and excretion of the stereoisomers of homoeriodicytol, isosakuranetin, and taxifolin would have not been apparent if achiral methods of analysis were used as those previously reported in pharmacokinetic studies of these compounds which provide less comprehensive results. These findings demonstrate the utility of developing chiral methods of analysis for chemical compounds of a chiral nature.

The exploratory pharmacological studies of racemates and stereoisomers of homoeriodicytol, isosakuranetin, and taxifolin *in vitro* revealed that small structural

differences in the chemical structure of these compounds result in significant pharmacodynamic differences similar to what was observed in the pharmacokinetic studies. These structural differences include the presence or absence of sugar moieties, enantiomeric forms, and hydroxyl and methoxy substitution patterns. The stereoisomers of homoeriodicytol, isosakuranetin, and taxifolin demonstrated concentration-dependent anti-cancer activity that appeared to contribute differently to the anti-cancer effect observed with racemates. Furthermore, racemic homoeriodicytol and taxifolin exhibited HDAC inhibitory activity, suggesting that the anti-cancer activity observed *in vitro* may be associated with the HDAC pathway. Racemic homoeriodicytol and taxifolin demonstrated concentration-dependent reduction of PGE_2 levels in an *in vitro* HT-29 colitis model. Further studies are necessary with the pure stereoisomers of these compounds to elucidate their potential differences in anti-inflammatory activity in colitis *in vitro*. The pharmacokinetics of these compounds and the extensive non-renal clearance indicate that homoeriodicytol and taxifolin may be of potential therapeutic use in the treatment of pathologies of the GI tract such as inflammatory bowel disease. Racemic taxifolin demonstrated selective COX-2 inhibition greater than etodolac which suggests that the anti-inflammatory activity observed in the *in vitro* colitis model may be related to the inhibition of COX-2 by taxifolin. Finally, a concentration-dependent decrease in the formation of triglycerides in adipocytes *in vitro* was evident with the racemate and S(-)-enantiomer of homoeriodicytol suggesting a potential therapeutical use of these compounds in hyperlipidemia. The pharmacological studies of the racemates and stereoisomers of homoeriodicytol, isosakuranetin, and taxifolin demonstrated the utility and necessity of developing stereoselective HPLC methods for chiral flavonoids and are in accordance with reports on the pharmacological activity of other polyphenols [152,153].

Nonetheless, the expense, stability, and time needed to collect enough quantities of the pure compounds limited the investigations.

A novel HPLC method for the simultaneous analysis of ellagic acid, taxifolin, myricetin, fisetin, quercetin, phloretin, R(+)-naringenin, S(-)-naringenin, hesperetin, and kaempferol was applied in the analysis and quantification of these selected polyphenols in tomatoes for the first time. The analysis of the enantiomeric content of naringenin was reported for the first time in tomatoes and demonstrated that the S(-)-enantiomer is predominant in both organic and conventional tomatoes. Further studies are necessary to elucidate the polyphenolic content of peel in tomatoes, as well as the content of these selected polyphenols in other tomato cultivars.

A novel HPLC method for the simultaneous analysis of ellagic acid, phloretin, R(+)-naringenin, S(-)-naringenin, and kaempferol was applied in the analysis and quantification of these selected polyphenols in different apple cultivars grown in Washington State. The enantiomeric content of naringenin was also reported in apples for the first time. Similar to the findings in tomatoes, the S(-)-enantiomer of naringenin was demonstrated to be predominant in different apple cultivars. In general, the peel of fresh fruit had higher concentrations of polyphenols when compared to flesh. In addition, the pharmacological activity of apples grown in Washington was evaluated. Apple extracts exhibited dose-dependent anti-cancer, anti-inflammatory, and anti-oxidant activities, which suggests a potential phytoprotective effect of apple consumption in pathological conditions of the gastrointestinal tract. These findings demonstrate the importance of cross-disciplinary studies to further advance our knowledge in the potential health benefits of fruit consumption.

9.2   FUTURE DIRECTIONS

The findings presented in this thesis demonstrated that small structural differences like those observed between the stereoisomers of chiral xenobiotics may produce significant differences in their pharmacokinetic profiles and pharmacodynamic effects. Similarly, differences in the substitution groups found in flavonoids as well as the presence or absence of sugar moieties result in differences in the pharmacological activity. The pharmacokinetic studies of homoeriodictyol, isosakuranetin and taxifolin demonstrated the need to develop assays with increased sensitivity due to the almost negligible amount of compounds detectable in the vascular system after a short period of time.

The lipophilic nature of the chiral compounds studied and poor aqueous solubility demonstrated to be a limiting factor in the assessment of the pharmacological effect of these flavonoids. Future optimization of the formulation of homoeriodictyol, isosakuranetin, and taxifolin may greatly alter the pharmacokinetic and pharmacological activity observed. Previous studies with epigallocatechin gallate (EGCG; MW = 458.37 g/mol, XLogP = 1.2), a polyphenol found in green tea, demonstrated that the use of anhydrous glycerin-based Carbopol gels can increase the stability and incorporation of water-sensitive drugs [219]. The optimization of formulation of lipophilic flavonoids *per se* has not been studied; however, biodegradable nanoparticles have been successfully used in the delivery of oral vaccines with no toxicity reported [220]. This and other approaches can be investigated to improve the delivery of homoeriodictyol, Isosakuranetin, and taxifolin to the target tissue both *in vivo* and *in vitro*.

These studies will then be useful in the investigation of the effect of drugs commonly used in the treatment of GI tract pathologies such as corticosteroids (i.e. prednisone), antibiotics, and immunomodulators (i.e. azathioprine) [221] with homoeriodictyol or taxifolin

i.e. as adjunct drugs. In addition, future studies *in vivo* can be performed based on the results obtained in the *in vitro* exploratory pharmacology in *in vivo* models of cancer, arthritis, and hyperlipidemia.

10 <u>REFERENCES</u>

1. Khosla C and Keasling JD. Metabolic engineering for drug discovery and development. *Nat Rev Drug Discov* 2003; **2**: 1019-1025.

2. Cragg GM, Newman DJ and Snader KM. Natural products in drug discovery and development. *J Nat Prod* 1997; **60**: 52-60.

3. Raskin I and Ripoll C. Can an apple a day keep the doctor away? *Curr Pharm Des* 2004; **10**: 3419-3429.

4. Balandrin MF, Klocke JA, Wurtele ES and Bollinger WH. Natural plant chemicals: sources of industrial and medicinal materials. *Science* 1985; **228**: 1154-1160.

5. Stafford HA. Flavonoid Metabolism, CRC Press, Inc. Boca Raton, 1990, 298.

6. Beecher GR. Overview of dietary flavonoids: nomenclature, occurrence and intake. *J Nutr* 2003; **133**: 3248S-3254S.

7. Yáñez JA, Andrews PK and Davies NM. Methods of analysis and separation of chiral flavonoids. *J Chromatogr B Analyt Technol Biomed Life Sci* 2007; **848**: 159-181.

8. Krause M and Galensa R. Direct enantiomeric separation of racemic flavanones by high-performance liquid chromatography using cellulose triacetate as a chiral stationary phase. *J Chromatogr A* 1988; **441**: 417-422.

9. Krause M and Galensa R. Improved chiral stationary phase based on cellulose triacetate supported on non-macroporous silica gel diol for the high-performance liquid chromatographic separation of racemic flavanones and diastereomeric flavanone glycosides. *J Chromatogr A* 1990; **502**: 287-296.

10. Krause M and Galensa R. Analysis of Enantiomeric Flavanones in Plant extracts by High-Performance Liquid Chromatography on a Cellulose Triacetate Based Chiral Stationary Phase. *Chromatographia* 1991; **32**: 69-72.

11. Stafford HA. *Biosynthesis of Flavanones and 3-Hydroxyflavanones (Dihydroxyflavonols): The "Grid" Pattern of Basic Hydroxylations of the B- and C-rings*, Flavonoid Metabolism. CRC Press, Inc. Boca Raton, 1990; 39-44.

12. Hemingway RW, Foo LY and Porter LJ. Linkage isomerism in trimeric acid polymeric 2,3-*cis* procyanidins. *J Chem Soc Perkin Trans* 1982; **1**: 1209.

13. Mossa JS, Sattar EA, Abou-Shoer M and Galal AM. Free Flavonoids from *Rhus retinorrhoea* Steud ex Olive. *Int J Pharmacog* 1996; **34**: 198-201.

14. Grael CF, Vichnewski W, Souza GE, Lopes JL, Albuquerque S and Cunha WR. A study of the trypanocidal and analgesic properties from Lychnophora granmongolense (Duarte) Semir & Leitao Filho. *Phytother Res* 2000; **14**: 203-206.

15. Ley JP, Krammer G, Reinders G, Gatfield IL and Bertram HJ. Evaluation of bitter masking flavanones from Herba Santa (Eriodictyon californicum (H. and A.) Torr., Hydrophyllaceae). *J Agric Food Chem* 2005; **53**: 6061-6066.

16. Lin JH, Chiou YN and Lin YL. Phenolic glycosides from Viscum angulatum. *J Nat Prod* 2002; **65**: 638-640.

17. Yin J, Han N, Xu X, Liu Z, Zhang B and Kadota S. Inhibitory activity of the ethyl acetate fraction from Viscum coloratum on bone resorption. *Planta Med* 2008; **74**: 120-125.

18. Zhao Y, Wang X, Zhao Y, Gao X, Bi K and Yu Z. HPLC determination and pharmacokinetic study of homoeriodictyol-7-O-beta-D-glucopyranoside in rat plasma and tissues. *Biol Pharm Bull* 2007; **30**: 617-620.

19. Fukunaga T, Kajikawa I, Nishiya K, Takeya K and Itokawa H. Studies on the Constituents of Japanese Mistletoe, *Viscum album* L. var. *coloratum* OHWI Grown on Different Host Trees. *Chem Pharm Bull (Tokyo)* 1989; **37**: 1300-1303.

20. McCormick S. Pigment synthesis in maize aleurone from precursors fed to anthocyanin mutants. *Biochem Genet* 1978; **16**: 777-785.

21. Gil-Izquierdo A, Riquelme MT, Porras I and Ferreres F. Effect of the rootstock and interstock grafted in lemon tree (Citrus limon (L.) Burm.) on the flavonoid content of lemon juice. *J Agric Food Chem* 2004; **52**: 324-331.

22. Smyth EM and FitzGerald GA. *The Eicosanoids, Prostaglandins, Tromboxanes, Leukotrienes and Related Compounds*, Basic and Clinical Pharmacology. Katzung DG. McGraw Hill. New York, 2007; 1179.

23. Ibrahim AR, Galal AM, Ahmed MS and Mossa GS. O-demethylation and sulfation of 7-methoxylated flavanones by Cunninghamella elegans. *Chem Pharm Bull (Tokyo)* 2003; **51**: 203-206.

24. Schröder G, Wehinger E, Lukacin R, Wellmann F, Seefelder W, Schwab W and Schroder J. Flavonoid methylation: a novel 4'-O-methyltransferase from Catharanthus roseus, and evidence that partially methylated flavanones are substrates of four different flavonoid dioxygenases. *Phytochemistry* 2004; **65**: 1085-1094.

25. Wistuba D, Trapp O, Gel-Moreto N, Galensa R and Schurig V. Stereoisomeric separation of flavanones and flavanone-7-O-glycosides by capillary electrophoresis and determination of interconversion barriers. *Anal Chem* 2006; **78**: 3424-3433.

26. Asztemborska M, Miskiewicz M and Sybilska D. Separation of some chiral flavanones by micellar electrokinetic chromatography. *Electrophoresis* 2003; **24**: 2527-2531.

27. Ficarra P, Ficarra R, Bertucci C, Tommasini S, Calabro ML, Costantino D and Carulli M. Direct Enantiomeric Separation of Flavanones by High Performance Liquid Chromatography using Various Chiral Stationary Phases. *Planta Med* 1995; **61**: 171-176.

28. Miyake Y, Sakurai C, Usuda M, Fukumoto S, Hiramitsu M, Sakaida K, Osawa T and Kondo K. Difference in plasma metabolite concentration after ingestion of lemon flavonoids and their aglycones in humans. *J Nutr Sci Vitaminol (Tokyo)* 2006; **52**: 54-60.

29. Matsumoto H, Ikoma Y, Sugiura M, Yano M and Hasegawa Y. Identification and quantification of the conjugated metabolites derived from orally administered hesperidin in rat plasma. *J Agric Food Chem* 2004; **52**: 6653-6659.

30. Miyake Y, Shimoi K, Kumazawa S, Yamamoto K, Kinae N and Osawa T. Identification and antioxidant activity of flavonoid metabolites in plasma and urine of eriocitrin-treated rats. *J Agric Food Chem* 2000; **48**: 3217-3224.

31. Booth AN, Jones FT and De EF. Metabolic fate of hesperidin, eriodictyol, homoeridictyol, and diosmin. *J Biol Chem* 1958; **230**: 661-668.

32. Zhao Y, Yu Z, Zhang L, Zhou D, Chen X and Bi K. Simultaneous determination of homoeriodictyol-7-O-beta-D-Glccopyranoside and its metabolite homoeriodictyol in rat tissues and urine by liquid chromatography-mass spectrometry. *J Pharm Biomed Anal* 2007; **44**: 293-300.

33. Doostdar H, Burke MD and Mayer RT. Bioflavonoids: selective substrates and inhibitors for cytochrome P450 CYP1A and CYP1B1. *Toxicology* 2000; **144**: 31-38.

34. Liu YL, Ho DK, Cassady JM, Cook VM and Baird WM. Isolation of potential cancer chemopreventive agents from Eriodictyon californicum. *J Nat Prod* 1992; **55**: 357-363.

35. Ley JP, Paetz S, Blings M, Hoffmann-Lucke P, Bertram HJ and Krammer GE. Structural Analogues of Homoeriodictyol as Flavor Modifiers. Part III: Short Chain Gingerdione Derivatives. *J Agric Food Chem* 2008;
36. Shimizu K, Ashida H, Matsuura Y and Kanazawa K. Antioxidative bioavailability of artepillin C in Brazilian propolis. *Arch Biochem Biophys* 2004; **424**: 181-188.

37. Simoes LM, Gregorio LE, Da Silva Filho AA, de Souza ML, Azzolini AE, Bastos JK and Lucisano-Valim YM. Effect of Brazilian green propolis on the production of reactive oxygen species by stimulated neutrophils. *J Ethnopharmacol* 2004; **94**: 59-65.

38. Tavares DC, Lira WM, Santini CB, Takahashi CS and Bastos JK. Effects of propolis crude hydroalcoholic extract on chromosomal aberrations induced by Doxorubicin in rats. *Planta Med* 2007; **73**: 1531-1536.

39. de Sousa JP, Bueno PC, Gregorio LE, da Silva Filho AA, Furtado NA, de Sousa ML and Bastos JK. A reliable quantitative method for the analysis of phenolic compounds in Brazilian propolis by reverse phase high performance liquid chromatography. *J Sep Sci* 2007; **30**: 2656-2665.

40. Missima F, da Silva Filho AA, Nunes GA, Bueno PC, de Sousa JP, Bastos JK and Sforcin JM. Effect of Baccharis dracunculifolia D.C. (Asteraceae) extracts and its isolated compounds on macrophage activation. *J Pharm Pharmacol* 2007; **59**: 463-468.

41. Garcez FR, Garcez WS, Santana ALBD, Alves MM, Matos MFC and Scaliante AM. Bioactive flavonoids and triterpenes from Terminalia fagifolia (Combretaceae). *J Braz Chem Soc* 2006; **17**: 1223-1228.

42. Suksamrarn A, Chotipong A, Suavansri T, Boongird S, Timsuksai P, Vimuttipong S and Chuaynugul A. Antimycobacterial activity and cytotoxicity of flavonoids from the flowers of Chromolaena odorata. *Arch Pharm Res* 2004; **27**: 507-511.

43. Metwally AM and Ekejiuba EC. Methoxylated Flavonols and Flavanones from Eupatorium odoratum. *Planta Med* 1981; **42**: 403-405.

44. Vanamala J, Reddivari L, Yoo KS, Pike LM and Patil BS. Variation in the content of bioactive flavonoids in different brands of orange and grapefruit juices. *J Food Comp Anal* 2004; **19**: 157-166.

45. Anagnostopoulou MA, Kefalas P, Kokkalou E, Assimopoulou AN and Papageorgiou VP. Analysis of antioxidant compounds in sweet orange peel by HPLC-diode array detection-electrospray ionization mass spectrometry. *Biomed Chromatogr* 2005; **19**: 138-148.

46. Calabro ML, Galtieri V, Cutroneo P, Tommasini S, Ficarra P and Ficarra R. Study of the extraction procedure by experimental design and validation of a LC method for determination of flavonoids in Citrus bergamia juice. *J Pharm Biomed Anal* 2004; **35**: 349-363.

47. Ross SA, Ziska DS, Zhao K and ElSohly MA. Variance of common flavonoids by brand of grapefruit juice. *Fitoterapia* 2000; **71**: 154-161.

48. Cancalon PF. Analytical monitoring of citrus juices by using capillary electrophoresis. *J AOAC Int* 1999; **82**: 95-106.

49. Avula B, Joshi VC, Weerasooriya A and Khan IA. Liquid chromatography of separation and quantitative determination of adrenergic amines and flavonoids from Poncirus trifoliatus Raf. fruits at different stages of growth. *Chromatographia* 2005; **62**: 379-383.

50. Han AR, Kim JB, Lee J, Nam JW, Lee IS, Shim CK, Lee KT and Seo EK. A new flavanone glycoside from the dried immature fruits of Poncirus trifoliata. *Chem Pharm Bull (Tokyo)* 2007; **55**: 1270-1273.

51. Kim CY, Lee HJ, Lee MK, Ahn MJ and Kim J. One step purification of flavanone glycosides from Poncirus trifoliata by centrifugal partition chromatography. *J Sep Sci* 2007; **30**: 2693-2697.

52. Kim DH, Bae EA and Han MJ. Anti-Helicobacter pylori activity of the metabolites of poncirin from Poncirus trifoliata by human intestinal bacteria. *Biol Pharm Bull* 1999; **22**: 422-424.

53. Kim JB, Han AR, Park EY, Kim JY, Cho W, Lee J, Seo EK and Lee KT. Inhibition of LPS-induced iNOS, COX-2 and cytokines expression by poncirin through the NF-kappaB inactivation in RAW 264.7 macrophage cells. *Biol Pharm Bull* 2007; **30**: 2345-2351.

54. Park SH, Park EK and Kim DH. Passive cutaneous anaphylaxis-inhibitory activity of flavanones from Citrus unshiu and Poncirus trifoliata. *Planta Med* 2005; **71**: 24-27.

55. Horowitz RM and Gentili B. Flavonoid constituents of *Citrus*, The Avi Publishing Company, Inc. Westport, 1977, 529.

56. Kim DH, Kim BG, Lee Y, Ryu JY, Lim Y, Hur HG and Ahn JH. Regiospecific methylation of naringenin to ponciretin by soybean O-methyltransferase expressed in Escherichia coli. *J Biotechnol* 2005; **119**: 155-162.

57. Shimokoriyama M. Interconversion of chalcones and flavanones of a phloroglucinol-type structure. *J Am Chem Soc* 1956; **79**: 4199-4202.

58. Mouly P, Gaydou EM and Auffray A. Simultaneous separation of flavanone glycosides and polymethoxylated flavones in citrus juices using liquid chromatography. *J Chromatogr A* 1998; **800**: 171-179.

59. Gaffield W. Circular dichroism, optical rotatory dispersion and absolute configuration of flavanones, 3-hydroxyflavanones and their glycosides. *Tetrahedron* 1970; **26**: 4093-4108.

60. Park H and Jung S. Separation of some chiral flavonoids by microbial cyclosophoraoses and their sulfated derivatives in micellar electrokinetic chromatography. *Electrophoresis* 2005; **26**: 3833-3838.

61. Wistuba D, Trapp O, Gel-Moreto N, Galensa R and Schurig V. Stereoisomeric separation of flavanones and flavanone-7-O-glycosides by capillary electrophoresis and determination of interconversion barriers. *Anal Chem* 2006; **78**: 3424-3433.

62. Kwon C, Park H and Jung S. Enantioseparation of some chiral flavanones using microbial cyclic beta-(1-->3),(1-->6)-glucans as novel chiral additives in capillary electrophoresis. *Carbohydr Res* 2007; **342**: 762-766.

63. Cancalon PF and Bryan CR. Use of capillary electrophoresis for monitoring citrus juice composition. *J Chromatogr A* 1993; **652**: 555-561.

64. Souza JP, Tacon LA, Correia CC, Bastos JK and Freitas LA. Spray-dried propolis extract, II: prenylated components of green propolis. *Pharmazie* 2007; **62**: 488-492.

65. Silberberg M, Gil-Izquierdo A, Combaret L, Remesy C, Scalbert A and Morand C. Flavanone metabolism in healthy and tumor-bearing rats. *Biomed Pharmacother* 2006; **60**: 529-535.

66. Liu L, Cheng Y and Zhang H. Phytochemical analysis of anti-atherogenic constituents of Xue-Fu-Zhu-Yu-Tang using HPLC-DAD-ESI-MS. *Chem Pharm Bull (Tokyo)* 2004; **52**: 1295-1301.

67. Lee DS, Kim YS, Ko CN, Cho KH, Bae HS, Lee KS, Kim JJ, Park EK and Kim DH. Fecal metabolic activities of herbal components to bioactive compounds. *Arch Pharm Res* 2002; **25**: 165-169.

68. Kim DH, Jung EA, Sohng IS, Han JA, Kim TH and Han MJ. Intestinal bacterial metabolism of flavonoids and its relation to some biological activities. *Arch Pharm Res* 1998; **21**: 17-23.

69. Sacco S and Maffei M. The effect of isosakuranetin (5,7-dihydroxy 4'-methoxy flavanone) on potassium uptake in wheat root segments. *Phytochemistry* 1997; **46**: 245-248.

70. Finotti E and Di Majo D. Influence of solvents on the antioxidant property of flavonoids. *Nahrung* 2003; **47**: 186-187.

71. Furuya H, Shinnoh N, Ohyagi Y, Ikezoe K, Kikuchi H, Osoegawa M, Fukumaki Y, Nakabeppu Y, Hayashi T and Kira J. Some flavonoids and DHEA-S prevent the cis-effect of expanded CTG repeats in a stable PC12 cell transformant. *Biochem Pharmacol* 2005; **69**: 503-516.

72. Bae EA, Han MJ and Kim DH. In vitro anti-Helicobacter pylori activity of some flavonoids and their metabolites. *Planta Med* 1999; **65**: 442-443.

73. Kunizane H, Ueda H and Yamazaki M. Screening of phagocyte activators in plants; enhancement of TNF production by flavonoids. *Yakugaku Zasshi* 1995; **115**: 749-755.

74. Teixeira S, Siquet C, Alves C, Boal I, Marques MP, Borges F, Lima JL and Reis S. Structure-property studies on the antioxidant activity of flavonoids present in diet. *Free Radic Biol Med* 2005; **39**: 1099-1108.

75. Slimestad R, Fossen T and Vagen IM. Onions: a source of unique dietary flavonoids. *J Agric Food Chem* 2007; **55**: 10067-10080.

76. Seidel V, Bailleul F and Waterman PG. Novel oligorhamnosides from the stem bark of Cleistopholis glauca. *J Nat Prod* 2000; **63**: 6-11.

77. Hosoi S, Shimizu E, Ohno K, Yokosawa R, Kuninaga S, Coskun M and Sakushima A. Structural studies of zoospore attractants from Trachelospermum jasminoides var. pubescens: taxifolin 3-O-glycosides. *Phytochem Anal* 2006; **17**: 20-24.

78. Kim NC, Graf TN, Sparacino CM, Wani MC and Wall ME. Complete isolation and characterization of sylbins and isosylbins from milk thistle (*Sylbum marianum*). *Org Biomol Chem* 2003; **1**: 1684-1689.

79. Minakhmetov RA, Onuchak LA, Kurkin VA, Avdeeva EV and Volotsueva AV. Analysis of flavonoids in *Silybum marianum* fruit by HPLC. *Chem Nat Comp* 2001; **37**: 318-321.

80. Kiehlmann E and Slade PW. Methylation of dihydroquercetin acetates: synthesis of 5-O-methyldihydroquercetin. *J Nat Prod* 2003; **66**: 1562-1566.

81. Bais HP, Walker TS, Kennan AJ, Stermitz FR and Vivanco JM. Structure-dependent phytotoxicity of catechins and other flavonoids: flavonoid conversions by cell-free protein extracts of Centaurea maculosa (spotted knapweed) roots. *J Agric Food Chem* 2003; **51**: 897-901.

82. Delporte C, Backhouse N, Erazo S, Negrete R, Vidal P, Silva X, Lopez-Perez JL, Feliciano AS and Munoz O. Analgesic-antiinflammatory properties of Proustia pyrifolia. *J Ethnopharmacol* 2005; **99**: 119-124.

83. Lee EH, Kim HJ, Song YS, Jin C, Lee KT, Cho J and Lee YS. Constituents of the stems and fruits of Opuntia ficus-indica var. saboten. *Arch Pharm Res* 2003; **26**: 1018-1023.

84. Mbafor JT, Fomum ZT, Promsattha R, Sanson DR and Tempesta MS. Isolation and characterization of taxifolin 6-C-glucoside from Garcinia epunctata. *J Nat Prod* 1989; **52**: 417-419.

85. Exarchou V, Fiamegos YC, van Beek TA, Nanos C and Vervoort J. Hyphenated chromatographic techniques for the rapid screening and identification of antioxidants in methanolic extracts of pharmaceutically used plants. *J Chromatogr A* 2006; **1112**: 293-302.

86. Sakushima A, Ohno K, Coskun M, Seki KI and Ohkura K. Separation and identification of taxifolin 3-O-glucoside isomers from *Chamaecyparis obtusa* (Cupressaceae). *Nat Prod Lett* 2002; **16**: 383-387.

87. Nonaka GI, Goto Y, Kinjo JE, Nohara T and Nishioka I. Tannins and related compounds. LII. Studies on the constituents of the leaves of *Thujopsis dolobrata* SIEB. *et* ZUCC. *Chem Pharm Bull* 1987; **35**: 1105-1108.

88. Dai SJ and Yu DQ. [Studies on the flavonoids in stem of Rhododendron anthopogonoide II]. *Zhongguo Zhong Yao Za Zhi* 2005; **30**: 1830-1833.

89. Voirin B, Bayet C, Favre-Bonvin J, Ramachandran Nair AG and Krishnakumary P. Flavonoids from the flowers of Acacia latifolia. *J Nat Prod* 1986; **49**: 943.

90. Pistelli L, Giachi I, Potenza D and Morelli I. A new isoflavone from Genista corsica. *J Nat Prod* 2000; **63**: 504-506.

91. Prati S, Baravelli V, Fabbri D, Schwarzinger C, Brandolini V, Maietti A, Tedeschi P, Benvenuti S, Macchia M, Marotti I, Bonetti A, Catizone P and Dinelli G. Composition and content of seed flavonoids in forage and grain legume crops. *J Sep Sci* 2007; **30**: 491-501.

92. Haraguchi H, Mochida Y, Sakai S, Masuda H, Tamura Y, Mizutani K, Tanaka O and Chou WH. Protection against oxidative damage by dihydroflavonols in Engelhardtia chrysolepis. *Biosci Biotechnol Biochem* 1996; **60**: 945-948.

93. Exarchou V, Godejohann M, van Beek TA, Gerothanassis IP and Vervoort J. LC-UV-solid-phase extraction-NMR-MS combined with a cryogenic flow probe and its application to the identification of compounds present in Greek oregano. *Anal Chem* 2003; **75**: 6288-6294.

94. Dapkevicius A, van Beek TA, Lelyveld GP, van Veldhuizen A, de Groot A, Linssen JP and Venskutonis R. Isolation and structure elucidation of radical scavengers from Thymus vulgaris leaves. *J Nat Prod* 2002; **65**: 892-896.

95. Cai Y, Chen T and Xu Q. Astilbin suppresses collagen-induced arthritis via the dysfunction of lymphocytes. *Inflamm Res* 2003; **52**: 334-340.

96. Chen L, Yin Y, Yi H, Xu Q and Chen T. Simultaneous quantification of five major bioactive flavonoids in rhizoma smilacis glabrae by high-performance liquid chromatography. *J Pharm Biomed Anal* 2007; **43**: 1715-1720.

97. Chen T, Li J, Cao J, Xu Q, Komatsu K and Namba T. A new flavanone isolated from rhizoma smilacis glabrae and the structural requirements of its derivatives for preventing immunological hepatocyte damage. *Planta Med* 1999; **65**: 56-59.

98. Du Q, Li L and Jerz G. Purification of astilbin and isoastilbin in the extract of smilax glabra rhizome by high-speed counter-current chromatography. *J Chromatogr A* 2005; **1077**: 98-101.

99. Li YQ, Yi YH, Tang HF and Xiao K. [Studies on the structure of isoastilbin]. *Yao Xue Xue Bao* 1996; **31**: 761-763.

100. Fukunaga T, Nishiya K, Kajikawa I, Takeya K and Itokawa H. Studies on the constituents of Japanese mistletoes from different host trees, and their antimicrobial and hypotensive properties. *Chem Pharm Bull (Tokyo)* 1989; **37**: 1543-1546.

101. Messanga B, Sondengam B and Bodo B. Calodendroside A: a taxifolin diglucoside from the stem bark of Ochna calodendron. *Can J Chem* 2000; **78**: 487-489.

102. Japón-Luján R and Luque de Castro MD. Static-dynamic superheated liquid extraction of hydroxytyrosol and other biophenols from alperujo (a semisolid residue of the olive oil industry). *J Agric Food Chem* 2007; **55**: 3629-3634.

103. Brignolas F, Lacroix B, Lieutier F, Sauvard D, Drouet A, Claudot AC, Yart A, Berryman AA and Christiansen E. Induced Responses in Phenolic Metabolism in Two Norway Spruce Clones after Wounding and Inoculations with Ophiostoma polonicum, a Bark Beetle-Associated Fungus. *Plant Physiol* 1995; **109**: 821-827.

104. Lundgren LN and Theander O. *Cis-* and *trans*-dihydroquercetin glucosides from needles of *Pinus sylvestris*. *Phytochemistry* 1988; **27**: 829-832.

105. Saleem A, Kivela H and Pihlaja K. Antioxidant activity of pine bark constituents. *Z Naturforsch [C]* 2003; **58**: 351-354.

106. Trebatická J, Kopasová S, Činovský K, Ŝkodáček I, Ŝuba J, Muchová J, Žitňanová I, Waczulídováa I, Rohdewald P and Ďuračková Z. Treatment of ADHD with French maritime pine bark extract, Pycnogenol®. *Eur Child Adolesc Psychiatry* 2006; **15**: 329-335.

107. Ohmura W, Ohara S, Hashida K, Aoyama M and Doi S. Hydrothermolysis of flavonoids in relation to steaming of Japanese larch wood. *Holzforschung* 2002; **56**: 493-497.

108. Willfor SM, Ahotupa MO, Hemming JE, Reunanen MH, Eklund PC, Sjoholm RE, Eckerman CS, Pohjamo SP and Holmbom BR. Antioxidant activity of knotwood extractives and phenolic compounds of selected tree species. *J Agric Food Chem* 2003; **51**: 7600-7606.

109. Tsydendambaev PB, Khyshiktyev BS, Dutov AA, Nikolaev SM and Savin AV. [High-performance liquid chromatographic method for the determination of dihydroquercetin in extracts of medicinal plants]. *Biomed Khim* 2007; **53**: 212-215.

110. Miyazawa M and Tamura N. Inhibitory compound of tyrosinase activity from the sprout of Polygonum hydropiper L. (Benitade). *Biol Pharm Bull* 2007; **30**: 595-597.

111. Morimura K, Gatayama A, Tsukimata R, Matsunami K, Otsuka H, Hirata E, Shinzato T, Aramoto M and Takeda Y. 5-O-glucosyldihydroflavones from the leaves of Helicia cochinchinensis. *Phytochemistry* 2006; **67**: 2681-2685.

112. Shao B, Guo H, Cui Y, Liu A, Yu H, Guo H, Xu M and Guo D. Simultaneous determination of six major stilbenes and flavonoids in *Smilax china* by high performance liquid chromatography. *J Pharm Biomed Anal* 2007; **44**: 737-742.

113. Yi Y, Cao Z, Yang D, Cao Y, Wu Y and Zhao S. Studies on the chemical constituents of Smilax glabra. *Acta Pharm sinica* 1998; **33**: 873-875.

114. Meyer P, Heidman I, Forkman G and Saedler H. A new petunia flower colour generated by transformation of a mutant with a maize gene. *Nature* 1987; **330**: 677-678.

115. Wang Y, Zhou L, Li R and Wang Y. [Studies on the chemical constituents from Ampelopsis grossedentata]. *Zhong Yao Cai* 2002; **25**: 254-256.

116. Souquet JM, Labarbe B, Le Guerneve C, Cheynier V and Moutounet M. Phenolic composition of grape stems. *J Agric Food Chem* 2000; **48**: 1076-1080.

117. Baderschneider B and Winterhalter P. Isolation and characterization of novel benzoates, cinnamates, flavonoids, and lignans from Riesling wine and screening for antioxidant activity. *J Agric Food Chem* 2001; **49**: 2788-2798.

118. Pozo-Bayon MA, Hernandez MT, Martin-Alvarez PJ and Polo MC. Study of low molecular weight phenolic compounds during the aging of sparkling wines manufactured with red and white grape varieties. *J Agric Food Chem* 2003; **51**: 2089-2095.

119. Tiukavkina NA, Rulenko IA and Kolesnik Iu A. [Dihydroquercetin--a new antioxidant and biologically active food additive]. *Vopr Pitan* 1997; 12-15.

120. Towatari K, Yoshida K, Mori N, Shimizu K, Kondo R and Sakai K. Polyphenols from the heartwood of *Cercidiphyllum japonicum* and their effects on proliferation of mouse hair epithelial cells. *Planta Med* 2002; **68**: 995-998.

121. Moriguchi T, Kita M, Ogawa K, Tomono Y, Endo T and Omura M. Flavonol synthase gene expression during citrus fruit development. *Physiol Plant* 2002; **114**: 251-258.

122. Matsuda M, Otsuka Y, Jin S, Wasaki J, Watanabe J, Watanabe T and Osaki M. Biotransformation of (+)-catechin into taxifolin by a two-step oxidation: primary stage of (+)-catechin metabolism by a novel (+)-catechin-degrading bacteria, Burkholderia sp. KTC-1, isolated from tropical peat. *Biochem Biophys Res Commun* 2008; **366**: 414-419.

123. Kiehlmann E and Edmond PML. Isomerization of dihydroquercetin. *J Nat Prod* 1995; **58**: 450-455.

124. Testa B, Carrupt PA and Gal J. The so-called "interconversion" of stereoisomeric drugs: an attempt at clarification. *Chirality* 1993; **5**: 105-111.

125. Geodakyan SV, Voskoboinikova IV, Kolesnik JA, Tjukavkina NA, Litvinenko VI and Glyzin VI. High-performance liquid chromatographic method for the determination of mangiferin, likviritin and dihydroquercetin in rat plasma and urine. *J Chromatogr* 1992; **577**: 371-375.

126. Lepri L, Del Bubba M, Coas V and Cincinelli A. Reversed-Phase Planar Chromatography of Racemic Flavanones. *J Liq Chrom & Rel Technol* 1999; **22**: 105-118.

127. Ng SC, Ong TT, Fu P and Ching CB. Enantiomer separation of flavour and fragrance compounds by liquid chromatography using novel urea-covalent bonded methylated beta-cyclodextrins on silica. *J Chromatogr A* 2002; **968**: 31-40.

128. Schneider H and Blaut M. Anaerobic degradation of flavonoids by Eubacterium ramulus. *Arch Microbiol* 2000; **173**: 71-75.

129. Smolarz HD. Comparative study on the free flavonoid aglycones in herbs of different species of Polygonum L. *Acta Pol Pharm* 2002; **59**: 145-148.

130. Kolesnik YA, Demyanovich VM, Tashlitsky VN, Tikhonov VP, Titova EV and Shmatov DA. The composition of a flavonoid complex from Larix wood (Pinaceae). The stereochemistry of dihydroquercetin. *Planta Med* 2007; **73**: DOI: 10.1055/s-2007-987149.

131. Lepri L, Del Bubba M and Masi F. Reversed-Phase Planar Chromatography of Enantiomeric Compounds on Microcrystalline Cellulose Triacetate (MCTA). *J Planar Chromatogr. Mod. TLC*. 1997; **10**: 108-113.

132. Kolesnikov MP and Gins VK. [Phenolic compounds in medicinal plants]. *Prikl Biokhim Mikrobiol* 2001; **37**: 457-465.

133. Düweler KG and Rohdewald P. Urinary metabolites of French maritime pine bark extract in humans. *Pharmazie* 2000; **55**: 364-368.

134. Grimm T, Skrabala R, Chovanova Z, Muchova J, Sumegova K, Liptakova A, Durackova Z and Hogger P. Single and multiple dose pharmacokinetics of maritime pine bark extract (pycnogenol) after oral administration to healthy volunteers. *BMC Clin Pharmacol* 2006; **6**: 4.

135. Schoefer L, Mohan R, Schwiertz A, Braune A and Blaut M. Anaerobic degradation of flavonoids by Clostridium orbiscindens. *Appl Environ Microbiol* 2003; **69**: 5849-5854.

136. Nielsen SE, Breinholt V, Justesen U, Cornett C and Dragsted LO. *In vitro* biotransformation of flavonoids by rat liver microsomes. *Xenobiotica* 1998; **28**: 389-401.

137. Svobodova A, Walterova D and Psotova J. Influence of silymarin and its flavonolignans on H(2)O(2)-induced oxidative stress in human keratinocytes and mouse fibroblasts. *Burns* 2006; **32**: 973-979.

138. Vitrac X, Monti JP, Vercauteren J, Deffieux G and Merillon JM. Direct liquid chromatographic analysis of resveratrol derivates and flavanonols in wines with absorbance and fluorescence detection. *Anal Chim Acta* 2002; **458**: 103-110.

139. Trouillas P, Fagnère C, Lazzaroni R, Calliste C, Markaf A and Duroux JL. A theorical study of the conformational behavior and electronic structure of taxifolin correlated with the free radical-scavenging activity. *Food Chem* 2004; **88**: 571-582.

140. Theriault A, Wang Q, Van Iderstine SC, Chen B, Franke AA and Adeli K. Modulation of hepatic lipoprotein synthesis and secretion by taxifolin, a plant flavonoid. *J Lipid Res* 2000; **41**: 1969-1979.

141. Braca A, Sortino C, Politi M, Morelli I and Mendez J. Antioxidant activity of flavonoids from Licania licaniaeflora. *J Ethnopharmacol* 2002; **79**: 379-381.

142. Shah VP, Midha KK, Dighe S, McGilveray IJ, Skelly JP, Yacobi A, Layloff T, Viswanathan CT, Cook CE, McDowall RD and et al. Analytical methods validation: bioavailability, bioequivalence and pharmacokinetic studies. Conference report. *Eur J Drug Metab Pharmacokinet* 1991; **16**: 249-255.

143. Hartmann C, Smeyers-Verbeke J, Massart DL and McDowall RD. Validation of bioanalytical chromatographic methods. *J Pharm Biomed Anal* 1998; **17**: 193-218.

144. Slade D, Ferreira D and Marais JP. Circular dichroism, a powerful tool for the assessment of absolute configuration of flavonoids. *Phytochemistry* 2005; **66**: 2177-2215.

145. Vega-Villa KR, Yanez JA, Remsberg CM, Ohgami Y and Davies NM. Stereospecific high-performance liquid chromatographic validation of homoeriodictyol in serum and Yerba Santa (Eriodictyon glutinosum). *J Pharm Biomed Anal* 2008; **46**: 971-974.

146. Roupe K, Halls S and Davies NM. Determination and assay validation of pinosylvin in rat serum: application to drug metabolism and pharmacokinetics. *J Pharm Biomed Anal* 2005; **38**: 148-154.

147. Yáñez JA, Remsberg CM, Miranda ND, Vega-Villa KR, Andrews PK and Davies NM. Pharmacokinetics of selected chiral flavonoids: hesperetin, naringenin and eriodictyol in rats and their content in fruit juices. *Biopharm Drug Dispos* 2007; **29**: 63-82.

148. Li XC, Joshi AS, Tan B, ElSohly HN, Walker LA, Zjawiony JK and Ferreira D. Absolute configuration, conformation, and chiral properties of flavanone (3→8")-flavone biflavonoids from *Rheedia acuminata*. *Tetrahedron* 2002; **58**: 8709-8717.

149. Yang CY, Tsai SY, Chao PDL, Yen HF, Chien TM and Hsiu SL. Determination of Hersperitin and Its Conjugate Metabolites in Serum and Urine. *Journal of Food and Drug Analysis* 2002; **10**: 143-148.

150. Shargel L, Wu-Pong S and Yu ABC. Applied Biopharmaceutics and Pharmacokinetics, The McGraw-Hill Companies, Inc. New York, 2005, 892.

151. Jamali F, Alballa RS, Mehvar R and Lemko CH. Longer plasma half-life for procainamide utilizing a very sensitive high performance liquid chromatography assay. *Ther Drug Monit* 1988; **10**: 91-96.

152. Yanez JA, Remsberg CM, Miranda ND, Vega-Villa KR, Andrews PK and Davies NM. Pharmacokinetics of selected chiral flavonoids: hesperetin, naringenin and eriodictyol in rats and their content in fruit juices. *Biopharm Drug Dispos* 2008; **29**: 63-82.

153. Remsberg CM, Yanez JA, Ohgami Y, Vega-Villa KR, Rimando AM and Davies NM. Pharmacometrics of pterostilbene: preclinical pharmacokinetics and metabolism, anticancer, antiinflammatory, antioxidant and analgesic activity. *Phytother Res* 2008; **22**: 169-179.

154. Takemoto JK, Remsberg CM, Yanez JA, Vega-Villa KR and Davies NM. Stereospecific analysis of sakuranetin by high-performance liquid chromatography: pharmacokinetic and botanical applications. *J Chromatogr B Analyt Technol Biomed Life Sci* 2008; **875**: 136-141.

155. Davies B and Morris T. Physiological parameters in laboratory animals and humans. *Pharm Res* 1993; **10**: 1093-1095.

156. Legg B and Rowland M. Cyclosporin: measurement of fraction unbound in plasma. *J Pharm Pharmacol* 1987; **39**: 599-603.

157. Sodergard R, Backstrom T, Shanbhag V and Carstensen H. Calculation of free and bound fractions of testosterone and estradiol-17 beta to human plasma proteins at body temperature. *J Steroid Biochem* 1982; **16**: 801-810.

158. Zapletal CM, Taut FJH, Martin E, Breitkreutz R, Babylon A, Dröge W and Thies J. Influence of N-acetylcysteine on hepatic amino acid metabolism in patients undergoing orthotopic liver transplantation. *Transplant Int* 2001; **14**: 329 - 333.

159. Rowland M and Tozer TN. Clinical Pharmacokinetics. Concepts and Applications., Williams & Wilkins. Baltimore, 1995, 601.

160. Mortensen RW, Sidelmann UG, Tjornelund J and Hansen SH. Stereospecific pH-dependent degradation kinetics of R- and S-naproxen-beta-l-O-acyl-glucuronide. *Chirality* 2002; **14**: 305-312.

161. Tallarida RJ. Drug synergism and dose-effect data analysis. , Chapman & Hall/Cr. Boca Raton, 2000, 247.

162. Waldeck B. Biological significance of the enantiomeric purity of drugs. *Chirality* 1993; **5**: 350-355.

163. Dey I, Lejeune M and Chadee K. Prostaglandin E2 receptor distribution and function in the gastrointestinal tract. *Br J Pharmacol* 2006; **149**: 611-623.

164. Rosengren JP, Karlsson JG and Nicholls IA. Enantioselective synthetic thalidomide receptors based upon DNA binding motifs. *Org Biomol Chem* 2004; **2**: 3374-3378.

165. Grillo MP and Hua F. Enantioselective formation of ibuprofen-S-acyl-glutathione in vitro in incubations of ibuprofen with rat hepatocytes. *Chem Res Toxicol* 2008; **21**: 1749-1759.

166. Qazzaz HM, El-Masri MA, Stolowich NJ and Valdes R, Jr. Two biologically active isomers of dihydroouabain isolated from a commercial preparation. *Biochim Biophys Acta* 1999; **1472**: 486-497.

167. Sterner O. Chemistry, health and environment, Wiley-VCH. Weinheim, NY., 1999, 345.

168. Andoh A, Fujiyama Y, Sumiyoshi K, Sakumoto H, Okabe H and Bamba T. Tumour necrosis factor-alpha up-regulates decay-accelerating factor gene expression in human intestinal epithelial cells. *Immunology* 1997; **90**: 358-363.

169. Pereira C, Medeiros RM and Dinis-Ribeiro MJ. Cyclooxygenase polymorphisms in gastric and colorectal carcinogenesis: are conclusive results available? *Eur J Gastroenterol Hepatol* 2009; **21**: 76-91.

170. Miller NJ and Rice-Evans CA. Factors influencing the antioxidant activity determined by the ABTS.+ radical cation assay. *Free Radic Res* 1997; **26**: 195-199.

171. Prior RL, Wu X and Schaich K. Standardized methods for the determination of antioxidant capacity and phenolics in foods and dietary supplements. *J Agric Food Chem* 2005; **53**: 4290-4302.

172. Kwon HJ, Kim MS, Kim MJ, Nakajima H and Kim KW. Histone deacetylase inhibitor FK228 inhibits tumor angiogenesis. *Int J Cancer* 2002; **97**: 290-296.

173. Johnstone RW. Histone-deacetylase inhibitors: novel drugs for the treatment of cancer. *Nat Rev Drug Discov* 2002; **1**: 287-299.

174. Zhang F, Zhang T, Teng ZH, Zhang R, Wang JB and Mei QB. Sensitization to gamma-irradiation-induced cell cycle arrest and apoptosis by the histone deacetylase inhibitor trichostatin A in non-small cell lung cancer (NSCLC) cells. *Cancer Biol Ther* 2009; **8**:
175. Tong Q and Hotamisligil GS. Molecular mechanisms of adipocyte differentiation. *Rev Endocr Metab Disord* 2001; **2**: 349-355.

176. TomatoNet. <http://www.tomatonet.org/>. (December 1, 2008)

177. California Tomato Farmers. <http://www.californiatomatofarmers.com/>. (December 1, 2008)

178. Kavanaugh CJ, Trumbo PR and Ellwood KC. The U.S. Food and Drug Administration's evidence-based review for qualified health claims: tomatoes, lycopene, and cancer. *J Natl Cancer Inst* 2007; **99**: 1074-1085.

179. King AB. "An apple a day keeps the doctor away" and other health claims. *Nutrition* 1993; **9**: 280.

180. de Lorgeril M, Salen P, Paillard F, Laporte F, Boucher F and de Leiris J. Mediterranean diet and the French paradox: two distinct biogeographic concepts for one consolidated scientific theory on the role of nutrition in coronary heart disease. *Cardiovasc Res* 2002; **54**: 503-515.

181. de Lorgeril M, Salen P, Martin JL, Monjaud I, Delaye J and Mamelle N. Mediterranean diet, traditional risk factors, and the rate of cardiovascular complications after myocardial infarction: final report of the Lyon Diet Heart Study. *Circulation* 1999; **99**: 779-785.

182. Nicoletti I, De Rossi A, Giovinazzo G and Corradini D. Identification and quantification of stilbenes in fruits of transgenic tomato plants (Lycopersicon esculentum Mill.) by reversed phase HPLC with photodiode array and mass spectrometry detection. *J Agric Food Chem* 2007; **55**: 3304-3311.

183. Torres CA, Andrews PK and Davies NM. Physiological and biochemical responses of fruit exocarp of tomato (Lycopersicon esculentum Mill.) mutants to natural photo-oxidative conditions. *J Exp Bot* 2006; **57**: 1933-1947.

184. Torres CA, Davies NM, Yanez JA and Andrews PK. Disposition of selected flavonoids in fruit tissues of various tomato (lycopersicon esculentum mill.) Genotypes. *J Agric Food Chem* 2005; **53**: 9536-9543.

185. Slimestad R, Fossen T and Verheul MJ. The flavonoids of tomatoes. *J Agric Food Chem* 2008; **56**: 2436-2441.

186. Washington Apple Commission. <http://www.bestapples.com/>. (December 2, 2008)

187. Lata B. Relationship between apple peel and the whole fruit antioxidant content: year and cultivar variation. *J Agric Food Chem* 2007; **55**: 663-671.

188. Gerhauser C. Cancer chemopreventive potential of apples, apple juice, and apple components. *Planta Med* 2008; **74**: 1608-1624.

189. Lamperi L, Chiuminatto U, Cincinelli A, Galvan P, Giordani E, Lepri L and Del Bubba M. Polyphenol levels and free radical scavenging activities of four apple cultivars from integrated and organic farming in different italian areas. *J Agric Food Chem* 2008; **56**: 6536-6546.

190. Tsao R, Yang R, Young JC and Zhu H. Polyphenolic profiles in eight apple cultivars using high-performance liquid chromatography (HPLC). *J Agric Food Chem* 2003; **51**: 6347-6353.

191. Ahmed S, Rahman A, Hasnain A, Lalonde M, Goldberg VM and Haqqi TM. Green tea polyphenol epigallocatechin-3-gallate inhibits the IL-1 beta-induced activity and expression of cyclooxygenase-2 and nitric oxide synthase-2 in human chondrocytes. *Free Radic Biol Med* 2002; **33**: 1097-1105.

192. Wellmann F, Griesser M, Schwab W, Martens S, Eisenreich W, Matern U and Lukacin R. Anthocyanidin synthase from Gerbera hybrida catalyzes the conversion of (+)-catechin to cyanidin and a novel procyanidin. *FEBS Lett* 2006; **580**: 1642-1648.

193. Boyer J and Liu RH. Apple phytochemicals and their health benefits. *Nutr J* 2004; **3**: 5.

194. Ruhmann S, Treutter D, Fritsche S, Briviba K and Szankowski I. Piceid (resveratrol glucoside) synthesis in stilbene synthase transgenic apple fruit. *J Agric Food Chem* 2006; **54**: 4633-4640.

195. Gosch C, Halbwirth H, Kuhn J, Miosic S and Stich K. Biosynthesis of phloridzin in apple (Malus domestica Borkh.). *Plant Science* 2009; **176**: 223-231.

196. Napolitano A, Cascone A, Graziani G, Ferracane R, Scalfi L, Di Vaio C, Ritieni A and Fogliano V. Influence of variety and storage on the polyphenol composition of apple flesh. *J Agric Food Chem* 2004; **52**: 6526-6531.

197. Peck GM, Andrews PK, Reganold JP and Fellman JK. Apple orchard productivity and fruit quality under organic, conventional, and integrated management. *Hort Science* 2006; **41**: 99-107.

198. Updike AA and Schwartz SJ. Thermal processing of vegetables increases cis isomers of lutein and zeaxanthin. *J Agric Food Chem* 2003; **51**: 6184-6190.

199. Guyot S, Marnet N, Sanoner P and Drilleau JF. Variability of the polyphenolic composition of cider apple (Malus domestica) fruits and juices. *J Agric Food Chem* 2003; **51**: 6240-6247.

200. Alonso-Salces RM, Barranco A, Abad B, Berrueta LA, Gallo B and Vicente F. Polyphenolic profiles of Basque cider apple cultivars and their technological properties. *J Agric Food Chem* 2004; **52**: 2938-2952.

201. Cao X, Wang C, Pei H and Sun B. Separation and identification of polyphenols in apple pomace by high-speed counter-current chromatography and high-performance liquid chromatography coupled with mass spectrometry. *J Chromatogr A* 2009;

202. Loots DT, van der Westhuizen FH and Jerling J. Polyphenol composition and antioxidant activity of Kei-apple (Dovyalis caffra) juice. *J Agric Food Chem* 2006; **54**: 1271-1276.

203. Mihalev K, Schieber A, Mollov P and Carle R. Effect of mash maceration on the polyphenolic content and visual quality attributes of cloudy apple juice. *J Agric Food Chem* 2004; **52**: 7306-7310.

204. van der Sluis AA, Dekker M, Skrede G and Jongen WM. Activity and concentration of polyphenolic antioxidants in apple juice. 2. Effect of novel production methods. *J Agric Food Chem* 2004; **52**: 2840-2848.

205. Chen MS, Chen D and Dou QP. Inhibition of proteasome activity by various fruits and vegetables is associated with cancer cell death. *In Vivo* 2004; **18**: 73-80.

206. Fridrich D, Kern M, Pahlke G, Volz N, Will F, Dietrich H and Marko D. Apple polyphenols diminish the phosphorylation of the epidermal growth factor receptor in HT29 colon carcinoma cells. *Mol Nutr Food Res* 2007; **51**: 594-601.

207. He X and Liu RH. Triterpenoids isolated from apple peels have potent antiproliferative activity and may be partially responsible for apple's anticancer activity. *J Agric Food Chem* 2007; **55**: 4366-4370.

208. Pohl C, Will F, Dietrich H and Schrenk D. Cytochrome P450 1A1 expression and activity in Caco-2 cells: modulation by apple juice extract and certain apple polyphenols. *J Agric Food Chem* 2006; **54**: 10262-10268.

209. Lapidot T, Walker MD and Kanner J. Can apple antioxidants inhibit tumor cell proliferation? Generation of H(2)O(2) during interaction of phenolic compounds with cell culture media. *J Agric Food Chem* 2002; **50**: 3156-3160.

210. Liu RH and Sun J. Antiproliferative activity of apples is not due to phenolic-induced hydrogen peroxide formation. *J Agric Food Chem* 2003; **51**: 1718-1723.

211. Davis PA, Polagruto JA, Valacchi G, Phung A, Soucek K, Keen CL and Gershwin ME. Effect of apple extracts on NF-kappaB activation in human umbilical vein endothelial cells. *Exp Biol Med (Maywood)* 2006; **231**: 594-598.

212. Zessner H, Pan L, Will F, Klimo K, Knauft J, Niewohner R, Hummer W, Owen R, Richling E, Frank N, Schreier P, Becker H and Gerhauser C. Fractionation of polyphenol-enriched apple juice extracts to identify constituents with cancer chemopreventive potential. *Mol Nutr Food Res* 2008; **52 Suppl 1**: S28-44.

213. Chrousos GP. *Adrenocrticosteroids and adrenocortical antagonists*, Basic and Clinical Pharmacology. Katzung DG. McGraw Hill. New York, 2007; 1179.

214. Jaffrey SR. *Nitric Oxide*, Basic and Clinical Pharmacology. Katzung DG. McGraw Hill. New York, 2007; 1179.

215. Elsaid KA, Fleming BC, Oksendahl HL, Machan JT, Fadale PD, Hulstyn MJ, Shalvoy R and Jay GD. Decreased lubricin concentrations and markers of joint inflammation in the synovial fluid of patients with anterior cruciate ligament injury. *Arthritis Rheum* 2008; **58**: 1707-1715.

216. Yanez JA, Remsberg CM, Vega-Villa KR, Miranda ND, Navas J, Ohgami Y, McCormick D, Hughes K, Temple C, Martinez S and Davies NM. Pharmacological evaluation of Glycoflex ® III and its constituents on canine chondrocytes. *J Med Sci* 2008; **8**: 1 - 14.

217. Teva Animal Health. <http://www.tevaanimalhealth.com/>. (May 31, 2009)

218. Aprikian O, Duclos V, Guyot S, Besson C, Manach C, Bernalier A, Morand C, Remesy C and Demigne C. Apple pectin and a polyphenol-rich apple concentrate are more effective together than separately on cecal fermentations and plasma lipids in rats. *J Nutr* 2003; **133**: 1860-1865.

219. Proniuk S and Blanchard J. Anhydrous Carbopol polymer gels for the topical delivery of oxygen/water sensitive compounds. *Pharm Dev Technol* 2002; **7**: 249-255.

220. Vega-Villa KR, Takemoto JK, Yanez JA, Remsberg CM, Forrest ML and Davies NM. Clinical toxicities of nanocarrier systems. *Adv Drug Deliv Rev* 2008; **60**: 929-938.

221. Cucchiara S, Escher JC, Hildebrand H, Amil-Dias J, Stronati L and Ruemmele FM. Pediatric inflammatory bowel diseases and the risk of lymphoma: should we revise our treatment strategies? *J Pediatr Gastroenterol Nutr* 2009; **48**: 257-267.